

# 國立交通大學

機械工程學系

博士論文

新渾沌系統之超渾沌、智慧型模糊控制、廣義渾沌同步與陰



Hyperchaos, Intelligent Fuzzy Logic Control, Generalized

Synchronizations of New Chaotic System and *Yin-Yang* Chaos

研究生：李仕宇

指導教授：戈正銘 榮譽教授

中華民國九十九年一月

新渾沌系統之超渾沌，智慧型模糊控制及廣義渾沌同步與陰  
陽渾沌

Hyperchaos, Intelligent Fuzzy Logic Control, Generalized  
Synchronizations of New Chaotic System and *Yin-Yang* Chaos

研 究 生：李仕宇

Student : Shih-Yu Li

指 導 教 授：戈正銘

Advisor : Zheng-Ming Ge

國 立 交 通 大 學  
機 械 工 程 學 系



Submitted to Department of Mechanical Engineering  
College of Engineering  
National Chiao Tung University  
In Partial Fulfillment of the Requirements  
for the Degree of  
Doctor of Philosophy  
in  
Mechanical Engineering  
January 2010  
Hsinchu, Taiwan, Republic of China

中華民國九十九年一月

# 新渾沌系統之超渾沌，智慧型模糊控制及廣義渾沌同步與陰陽渾沌

學生：李仕宇

指導老師：戈正銘 教授

國立交通大學機械工程學系

## 摘要

本論文探討渾沌系統之超渾沌現象，首次提出並研究陰陽渾沌。採用新模糊模型、新模糊控制器、GYC 部份區域穩定理論以及實用漸進穩定理論來達到廣義渾沌同步。主要研究重點如下：

1. 分析經典 Lorenz 系統的陰渾沌，並與其系統的陽渾沌做對比研究。
2. 新 Mathieu-van der Pol 系統超渾沌現象的研究。運用相圖、功率頻譜圖、李亞普諾夫指數以及二維和三維參數圖來分析其渾沌行為。就四狀態變量系統，發現三個正李亞普諾夫指數。
3. 運用 GYC 部份穩定理論以達到系統之渾沌控制和適應性渾沌同步。
4. 提出只須兩個線性子系統即能表達複雜渾沌行為的新模糊模型，並用以達成複雜系統以及不同系統之渾沌同步。
5. 提出常數模糊控制器的簡化概念，運用其完滿達成廣義同步。

# Hyperchaos, Intelligent Fuzzy Logic Control, Generalized Synchronizations of New Chaotic System and *Yin-Yang* Chaos

Student : Shih-Yu Li

Advisor : Zheng-Ming Ge

Department of Mechanical Engineering  
National Chiao Tung University

## Abstract

Hyperchaos of chaotic systems, *Yin-Yang* chaos, new fuzzy model, new fuzzy logic controllers, generalized chaos synchronization via GYC partial region stability theory and pragmatical asymptotically stability theorem are studied in this thesis. The main points in the researches are shown as follow:

1. Analyzing *Yin* chaos of the classical Lorenz system and comparing it with *Yang* chaos.
2. Hyperchaos in a new Mathieu-van der Pol system is identified by phase portraits, power spectrum, Lyapunov exponents and 2-D and 3-D parameters diagrams. Three positive Lyapunov exponents are found for system with four states.
3. Chaotic control and synchronization for a system by GYC partial region theory.
4. New fuzzy model is proposed to simulate the complicated chaotic behaviors via only two linear subsystems and used to carry out synchronization of complicated chaotic systems and different chaotic systems.
5. Simplified fuzzy logic constant controller (FLCC) is presented to achieve generalized synchronization.

## 誌謝

一個人能有多麼的成功，取決於在人生的關鍵點中，是否有貴人提攜，是否有把握住機會，是否有儲備好自己的能量，以及最重要的一是否有滿滿的愛與包容在我們的背後支撐著我們繼續向前邁進。

貴人提攜—首先，我打從心底真誠的、衷心的要向我人生中的貴人，值得尊敬的長輩，同時也是我的博士指導老師—戈正銘榮譽教授，至上最真誠的感謝與敬意。老師是我遇過最學識淵博，智慧超群的學者。我最喜歡這些日子以來，和老師談天文、說古今、聊想法、分享彼此生命中的點滴。在小小的房間裡，聽著老師分享著人生的經歷與智慧，使我向老師學習到看世界的角度、做學問的態度與思考問題的深度。心中對老師萬分的感謝與珍惜，化作簡單而綿密的字句，除了紀錄在字裡行間，也深深的刻畫在心板。謝謝您，我最敬愛的老師。

在交大三年半的日子裡，我很幸運的能夠認識許多很優秀的學長，以及活潑開朗，聰明絕頂的學弟妹們。我要感謝陳獻庚學長，總是能給予我方向以及身為過來人的看法，謝謝學長總是這麼照顧我們。我要感謝張晉銘學長，一路走來，您總是在我身旁幫助我、提點我、聽我訴苦，謝謝學長，您真的很棒。我要感謝95屆的學弟們彥賢、凱銘、俊諺，感謝妳們這麼的出類拔萃，讓我們一起不斷的進步與超越。我還要感謝瑜韓、志銘、育銘、聰文、尚恩、翔平、泳厚以及振賓，謝謝你們這些日子來的陪伴。

最後，我要感謝我的家人，接納這麼一個不完美、不甚體貼、總是忙碌的我。我感謝我親愛的老爸，鼓勵我在成大碩士畢業之後，繼續攻讀交大的博士學位。因為您的堅持，我來到了這裡，認識了很多人、學習到不少新知、長了些許智慧。我要感謝我親愛的媽咪，謝謝您總是能站在我的角度來為我思考，謝謝您支持我、傾聽我、保護我，給我溫暖與滿滿的愛。我要感謝我親愛的老姊，謝謝老姊總是這麼的疼愛我。我愛你們。

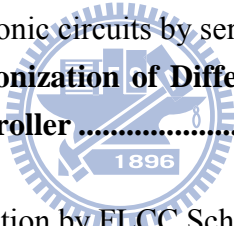
謝謝您們的愛與關懷，謹以此論獻給所有我關心我愛的人。

李仕宇 謹致  
庚寅年 國立交通大學

# CONTENTS

摘要 .....	ii
Abstract .....	ii
Acknowledgement.....	iii
Contents .....	ii
List of Tables.....	vi
List of Figures.....	vii
<b>Chapter 1 Introduction.....</b>	<b>1</b>
<b>Chapter 2 Yin-Yang Chaos.....</b>	<b>7</b>
2.1 Preliminaries	7
2.2 Yang Lorenz system with Yang parameters	7
2.3 Yin Lorenz system with Yin parameters	8
2.4 Comparison between Yin and Yang Lorenz systems	9
2.5 Family of Yin Lorenz system	12
2.6 Pragmatical Adaptive Synchronization Scheme	13
2.7 Adaptive Yin-Yang synchronization of Yin chaos and Yang chaos	14
<b>Chapter 3 Hyperchaos of New Mathieu-van der Pol system with Three Positive Lyapunov Exponents .....</b>	<b>29</b>
3.1 Preliminaries	29
3.2 Differential equations for Mathieu-van der Pol system and phase portraits	29
3.3 Power spectrum	30
3.4 Lyapunov exponents	30
3.5 Parameter diagrams	31
3.6 Phase portraits and its implementation of electronic circuits	31
3.7 Summary	32
<b>Chapter 4 Chaos Control of New Mathieu-van der Pol Systems with New Mathieu -Duffing Systems as Goal System by GYC Partial Region Stability Theory .....</b>	<b>42</b>
4.1 Preliminaries	42
4.2 Chaos Control Scheme	42
4.3 New Chaotic Mathieu- Duffing System	43
4.4 Numerical Simulations	43
<b>Chapter 5 Generalized Chaos Synchronization of New Mathieu-van der Pol Systems with New Duffing-van der Pol systems as Functional system by GYC Partial Region Stability Theory .....</b>	<b>54</b>
5.1 Preliminaries	54

5.2 Generalized Chaos Synchronization Strategy	54
5.3 New Chaotic Duffing-van der Pol System	55
5.4 Numerical Simulations	55
<b>Chapter 6 Pragmatical Adaptive Yin-Yang Synchronization of Chaos by G-Y-C</b>	
<b>Partial Region Stability Theory .....</b>	<b>74</b>
6.1 Preliminaries	74
6.2 GYC Pragmatical Adaptive Synchronization Scheme	74
6.3 Yin and Yang Lorenz system	76
6.4 Adaptive Yin-Yang synchronization by GYC partial region stability theory	77
6.5 Discussion	82
<b>Chapter 7 Fuzzy Modeling and Synchronization of Complicated Nonlinear</b>	
<b>Systems via Novel Fuzzy Model and Its Implementation on Electronic</b>	
<b>Circuits.....</b>	<b>91</b>
7.1 Preliminaries	91
7.2 New fuzzy model theory	92
7.4 Fuzzy synchronization scheme	103
7.5 Simulation results	106
7.6 Implementation of electronic circuits by series expansion method	110
<b>Chapter 8 Generalized Synchronization of Different Chaotic Systems by Fuzzy</b>	
<b>Logic Constant Controller .....</b>	<b>121</b>
8.1 Preliminaries	121
8.2 Generalized Synchronization by FLCC Scheme	121
8.3 Simulation Results	125
<b>Chapter 9 Conclusions.....</b>	<b>139</b>
<b>References.....</b>	<b>141</b>
<b>Paper List .....</b>	<b>147</b>



## List of Tables

Table 2 - 1 Dynamic behaviors of <i>Yin</i> Lorenz system for different signs of .....	8
Table 2 - 2 Range of parameter c of <i>Yang</i> Lorenz system .....	9
Table 2 - 3 Range of parameter c of <i>Yin</i> Lorenz system .....	9
Table 2 - 4 Range of parameter b of <i>Yang</i> Lorenz system .....	10
Table 2 - 5 Range of parameter b of <i>Yin</i> Lorenz system .....	11
Table 2 - 6 Range of parameter a of <i>Yang</i> Lorenz system .....	11
Table 2 - 7 Range of parameter a of <i>Yin</i> Lorenz system .....	11
Table 6 - 1 Comparison between errors data at 19.96s, 19.97s, 19.98s, 19.99s and 20.00s after the action of controllers .....	89
Table 6 - 2 Comparison between parametric errors at 9.96s, 9.97s, 9.98s, 9.99s and 10.00s after the action of controllers .....	90
Table 8 - 1 Rule-table of FLCC .....	124





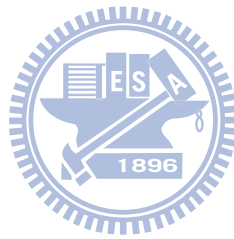
# List of Figures

Fig.2- 1 Projections of phase portrait of chaotic <i>Yang</i> Lorenz system with $\sigma = 10$ , $b=8/3$ and $r=28$ .....	18
Fig.2- 2 Projections of phase portrait of chaotic <i>Yin</i> Lorenz system with <i>Yin</i> parameters $\sigma = -10$ , $b=-8/3$ and $r=-28$ . ....	18
Fig.2- 3 Bifurcation diagram and Lyapunov exponents of chaotic <i>Yang</i> Lorenz system .....	19
Fig.2- 4 Bifurcation diagram and Lyapunov exponents of chaotic <i>Yin</i> Lorenz system with $b=-8/3$ and $\sigma = -10$ . ....	20
Fig.2- 5 Bifurcation and Lyapunov exponents of chaotic <i>Yang</i> Lorenz system with $\sigma = 28$ and $r=10$ .....	21
Fig.2- 6 Bifurcation and Lyapunov exponents of chaotic <i>Yin</i> Lorenz system with $\sigma = -28$ and $r=-10$ . ....	22
Fig.2- 7 Bifurcation and Lyapunov exponents of chaotic <i>Yang</i> Lorenz system .....	23
Fig.2- 8 Bifurcation and Lyapunov exponents of chaotic <i>Yin</i> Lorenz system .....	244
Fig.2- 9 Projections of phase portraits of family of <i>Yin</i> Lorenz system with $\sigma = -6$ , ..	255
Fig.2- 10 Bifurcation diagram and Lyapunov exponents of family of <i>Yin</i> Lorenz system with $\sigma = -6$ , $b=-8/3$ and $r=-28$ . (varied by $\mu$ ) .....	266
Fig.2- 11 Time histories of errors for <i>Yin</i> and <i>Yang</i> Lorenz chaotic systems.....	277
Fig.2- 12 Time histories of parametric errors for <i>Yin</i> and <i>Yang</i> Lorenz chaotic systems. .....	277
Fig.2- 13 Time histories of states of <i>Yin</i> and <i>Yang</i> Lorenz chaotic systems. ....	288
Fig.2- 14 Phase portraits of synchronization of <i>Yin</i> and <i>Yang</i> Lorenz.....	288
Fig.3- 1 Phase portrait projections of four state Mathieu-van der Pol system with $a=91.17$ , $b=5.023$ , $c=-0.001$ , $d=91$ , $e=87.001$ , $f=0.0180$ and $g=9.5072$ .. .....	33
Fig.3- 2 Power spectrum of $x$ for Mathieu-van der Pol system with $a=91.17$ , $b=5.023$ , $c=-0.001$ , $d=91$ , $e=87.001$ , $f=0.018$ and $g=9.5072$ .....	33
Fig.3- 3 Lyapunov exponents of Mathieu-van der Pol system with $b=5.023$ , $c=-0.001$ , $d=91$ , $e=87.001$ , $f=0.018$ and $g=9.5072$ ... ..	34
Fig.3- 4 Lyapunov exponents of Mathieu-van der Pol system with $b=5.023$ , $c=-0.001$ , $d=25$ , $e=87.001$ , $f=0.018$ and $g=9.5072$ .. ..	34
Fig.3- 5 Lyapunov exponents of Mathieu-van der Pol system with $a=96.326680$ , $c=-0.001$ , $d=25$ , $e=87.001$ , $f=0.018$ and $g=9.5072$ .....	35
Fig.3- 6 Lyapunov exponents of Mathieu-van der Pol system with $a=96.326680$ , $b=5.023$ , $c=-0.001$ , $e=87.001$ , $f=0.018$ and $g=9.5072$ ... ..	35
Fig.3- 7 Lyapunov exponents of Mathieu-van der Pol system with $a=96.326680$ ,	

$b=5.023, c=-0.001, e=87.001, f=0.018$ and $g=9.5072$ .....	36
Fig.3- 8 Lyapunov exponents of Mathieu-van der Pol system with $a=96.326680,$ $b=5.023, c=-0.001, d=25, f=0.018$ and $g=9.5072$ .....	36
Fig.3- 9 Parameter diagrams of Mathieu-van der Pol system with $a=96.326680,$ $b=5.023, c=-0.001, e=87.001$ and $f=0.018$ .....	37
Fig.3- 10 2D Parameter diagrams varied with $f. a=96.326680, b=5.023, c=-0.001$ and $e=87.001. Part A$ and $B$ are shown in Fig.7.....	38
Fig.3- 11 2D Parameter diagrams varied with $f. a=96.326680, b=5.023, c=-0.001$ and $e=87.001. Part C$ are shown in Fig. 8.....	38
Fig.3- 12 3D Parameter diagrams of Mathieu-van der Pol system with $a=96.326680,$ $b=5.023, c=-0.001$ and $e=87.001$ .....	39
Fig.3- 13 3D Parameter diagrams of Mathieu-van der Pol system with $a=96.326680,$ $b=5.023, c=-0.001$ and $e=87.001$ .....	39
Fig.3- 14 Parameter diagrams of Mathieu-van der Pol system with $a=96.326680,$ $b=5.023, c=-0.001, e=87.001$ and $g=9.5072$ .....	40
Fig.3- 15 Projection of phase portraits outputs in electronic circuit for Mathieu-van der Pol system.....	40
Fig.3- 16 The configuration of electronic circuit for chaotic Mathieu-van der Pol system.....	41
Fig.4- 1 Chaotic phase portrait projections for new Mathieu-Duffing system.....	49
Fig.4- 2 Phase portrait projections of error dynamics for Case I.....	49
Fig.4- 3 Time histories of errors for Case I.....	50
Fig.4- 4 Phase portrait projections of error dynamics for Case II.....	50
Fig.4- 5 Time histories of errors for Case II.....	51
Fig.4- 6 Time histories of $x_1, x_2, x_3, x_4$ for Case II.....	51
Fig.4- 7 Phase portrait projections of error dynamics for Case III.....	52
Fig.4- 8 Time histories of errors for Case III.....	52
Fig.4- 9 Time histories of $x_1, x_2, x_3, x_4$ and $z_1, z_2, z_3, z_4$ for Case III.....	53
Fig.5- 1 Phase portrait projections of new chaotic Duffing-van der Pol System.....	65
Fig.5- 2 Lyapunov exponents of new chaotic Duffing-van der Pol System.....	65
Fig.5- 3 Phase portrait projections of error dynamics for Case I.....	66
Fig.5- 4 Time histories of errors for Case I.....	66
Fig.5- 5 Time histories of $x_1, x_2, x_3, x_4, y_1, y_2, y_3, y_4$ for Case I.....	67
Fig.5- 6 Phase portrait projections of error dynamics for Case II.....	67
Fig.5- 7 Time histories of errors for Case II.....	68
Fig.5- 8 Time histories of $x_i - y_i + 100$ and $-F \sin \omega t$ for Case II.....	68
Fig.5- 9 Phase portrait projections of error dynamics for Case III.....	69
Fig.5- 10 Time histories of errors for Case III.....	69

Fig.5- 11 Time histories of $x_i - y_i + 100$ and $-Fe^{\sin(\omega t)}$ for Case III.....	70
Fig.5- 12 Phase portrait projections of error dynamics for Case IV.....	70
Fig.5- 13 Time histories of errors for Case IV.....	71
Fig.5- 14 Phase portrait projections of error dynamics for Case V.....	71
Fig.5- 15 Time histories of errors for Case V.....	72
Fig.5- 16 Phase portrait projections of error dynamics for Case VI.....	72
Fig.5- 17 Time histories of errors for Case VI.....	73
Fig.5- 18 Time histories of $x_i - y_i + 100$ and $-z_i$ for Case VI.....	73
Fig.6- 1 Projections of phase portrait of chaotic <i>Yang</i> Lorenz system with $a=10$ , $b=8/3$ and $c=28$ .....	84
Fig.6- 2 Projections of phase portrait of chaotic <i>Yin</i> Lorenz system with <i>Yin</i> parameters $a=-10$ , $b=-8/3$ and $c=-28$ .....	84
Fig.6- 3 Time histories of errors for <i>Yin</i> and <i>Yang</i> Lorenz chaotic systems for Case 1.....	85
Fig.6- 4 Time histories of parametric errors for <i>Yin</i> and <i>Yang</i> Lorenz chaotic systems for Case 1.....	85
Fig.6- 5 Phase portraits of synchronization of <i>Yin</i> and <i>Yang</i> Lorenz chaotic systems for Case 1.....	86
Fig.6- 6 Time histories of errors for <i>Yin</i> and <i>Yang</i> Lorenz chaotic systems for Case 2.....	86
Fig.6- 7 Time histories of parametric errors for <i>Yin</i> and <i>Yang</i> Lorenz chaotic systems for Case 2.....	87
Fig.6- 8 Time histories of errors in 20s for Case 1.....	87
Fig.6- 9 Time histories of errors in 20s for Case 2.....	88
Fig.7- 1 Chaotic behavior of Q-CNN system.....	114
Fig.7- 2 Chaotic behavior of new fuzzy Q-CNN system.....	114
Fig.7- 3 Chaotic behavior of Qi system.....	115
Fig.7- 4 Chaotic behavior of new fuzzy Qi system.....	115
Fig.7- 5 Time history of errors via fuzzy feedback gain.....	116
Fig.7- 6 Time histories of errors for Case I.....	116
Fig.7- 7 Chaotic behavior in <i>Case 1</i> .....	117
Fig.7- 8 Chaotic behavior in <i>Case 2</i> .....	117
Fig.7- 9 Chaotic behavior in <i>Case 3</i> .....	118
Fig.7- 10 Implementation on electronic circuits of Chaotic Q-CNN system.....	119
Fig.7- 11 Configuration of electronic circuits.....	120
Fig.8- 1 The configuration of fuzzy logic controller.....	134
Fig.8- 2 Membership function.....	134

Fig.8- 3 Projections of phase portrait of chaotic Lorenz system with $a=10$ , $b=8/3$ and $c=28$ .....	135
Fig.8- 4 Time histories of error derivatives for master and slave Lorenz chaotic systems without controllers.....	135
Fig.8- 5 Time histories of errors for Example 1- the FLCC is coming into after 30s.....	136
Fig.8- 6 Time histories of states for Example 1- the FLCC is coming into after 30s.....	136
Fig.8- 7 Projections of phase portrait of chaotic Chen-Lee system.....	137
Fig.8- 8 Time histories of error derivatives for master and slave chaotic systems without controllers.....	137
Fig.8- 9 Time histories of errors for Example 2- the FLCC is coming into after 30s.....	138
Fig.8- 10 Time histories of states for Example 2- the FLCC is coming into after 30s.....	138



# Chapter 1

## Introduction

Nonlinear dynamics, commonly called the chaos theory, changes the scientific way of looking at the dynamics of natural and social systems, which has been intensively studied over the past several decades. The phenomenon of chaos has attracted widespread attention amongst mathematicians, physicists and engineers. Chaos has also been extensively studied in many fields, such as chemical reactions, power converters, biological systems, information processing, secure communications, etc. [1-6]. Whilst many researchers analyze complicated, physically motivated configurations, there is also a need to investigate simple equations which may capture the essence of chaos in a less involved setting, thereby aiding the understanding of essential characteristics. The original investigation of an extraordinary three-dimensional nonlinear system by the mathematical meteorologist E.N. Lorenz who discovered chaos in a simple system of three autonomous ordinary differential equations in order to describe the simplified Rayleigh – Benard problem [7] (which is called *Yang Lorenz system* in this paper) is the most popular system for studying.

There are tremendous amount of articles in studying *Yang Lorenz* and other systems [8-12]. Although these systems have been analyzed in detail, there are no articles in looking into these systems, such as Lorenz system with  $x(-t)$ ,  $y(-t)$ ,  $z(-t)$  and  $-t$  (which is called *Yin Lorenz system* in this article). Since Lorenz discovered chaos on 1963, all studies of chaos concentrated when time went forward i.e.  $t : 0 \rightarrow \infty$  in the last 47 years. Physically backward time,  $t : 0 \rightarrow -\infty$ , has not discovered up to now, but mathematically it can be easily performed and must be studied for complete understanding of the property of chaos. In this Chapter, we find

out that there are rich dynamics in such *Yin* Lorenz system.

In Chinese philosophy, *Yin* is the negative, historical or feminine category in nature, while *Yang* is the positive, contemporary or masculine category in nature. *Yin* and *Yan* are two fundamental opposites in Chinese philosophy. In Chapter 2, the *Yin* Lorenz system is introduced and the chaotic behavior with *Yin* parameters is investigated by phase portrait, Lyapunov exponents and bifurcation in the following simulation results. We use positive, i.e. *Yang*, parameters for the *Yang* Lorenz system, and negative, i.e. *Yin*, parameters for the *Yin* Lorenz system.

Chaotic systems are characterized by one positive Lyapunov exponent (PLE) in the Lyapunov spectrum [2-9]. The one PLE just indicates that the dynamics of the underlying chaotic attractor expands only in one direction. If a chaotic attractor is characterized by more than one positive Lyapunov exponent, it is termed hyperchaos. In this case, the dynamics of the chaotic attractor expands in more than one direction giving rise to a “thick” chaotic attractor [10-14]. There are both theoretical and practical interests in hyperchaos. Hyperchaos was first reported from computer simulations of hypothetical ordinary differential equations in [15-17]. The first observation of hyperchaos from a real physical system, a fourth-order electrical circuit, was later reported in [18]. Very few hyperchaos generators have been reported since then [19-22].

As the numerical example, recently developed new Mathieu-van der pol autonomous oscillator with four state variables is used. For this new system four Lyapunov exponents are not zero. Although by traditional theory [23], for four-dimensional continuous-time systems, there must be a zero Lyapunov exponent, however, on the history of science, as said by T. S. Kuhn in his book “The Structure of Scientific Revolution”, the unexpected discovery or anomaly (counterinstance) is not simply factual in its import and the scientist’s world is qualitatively transformed

as well as quantitatively enriched by fundamental novelties of either fact or theory. “Conversion as a feature of revolutions in science” is the conclusion of the book “Revolution in Science” written by I. B. Cohen [24]. One of the patterns of the evolution of science is: current paradigm  $\rightarrow$  normal science  $\rightarrow$  anomaly (counterinstance)  $\rightarrow$  crisis  $\rightarrow$  emergence of scientific theories  $\rightarrow$  new paradigm.

Recently, Ott and Yorke [25] show that the existence of Lyapunov exponents is a subtle question for systems that are not conservative. They describe a simple continuous-time flow such that Lyapunov exponents fail to exist at nearly every point in the phase space. Ge and Yang [26] firstly find out the simulation results of 3PLES in Quantum Cellular Neuro Network autonomous system with four state variables. As a consequence, in Chapter 3, Mathieu-van der pol autonomous system with four state variables is introduced, and the hyperchaos for 3PLEs are investigated by phase portrait, power spectrum, Lyapunov exponents and parameter diagram in the following simulation results.

In our natural world, plenty of chaotic systems describing natural phenomenon are found that they have some states always positive. It means these states are always in the first quadrant. Such as the three species prey-predator system [36], double Mackey-Glass systems [37-38], energy communication system in biological research [39] and virus-immune system [40]. In Chapter 4, a new strategy to achieve chaos control by GYC partial region stability theory is proposed [32-33]. Via using the GYC partial region stability theory, the new Lyapunov function is a simple linear homogeneous function of error states and the lower order controllers are much more simple and introduce less simulation error.

In Chapter 5, a new chaos generalized synchronization strategy by GYC partial region stability theory is proposed [20-21]. It means that there exists a given functional relationship between the states of the master and that of the slave. Via using

the GYC partial region stability theory, the new Lyapunov function is a simple linear homogeneous function of states and the lower order controllers are much more simple and introduce less simulation error.

In current scheme of adaptive synchronization, traditional Lyapunov stability theorem and Barbalat lemma are used to prove that the error vector approaches zero as time approaches infinity, but the question that why those estimated parameters also approach the uncertain values remains no answer. In this article, pragmatical asymptotically stability theorem and an assumption of equal probability for ergodic initial conditions [50-51] are used to prove strictly that those estimated parameters approach the uncertain values. Moreover, traditional adaptive chaos synchronization in general is limited for the same system. Therefore, In Chapter 6, a new adaptive synchronizing strategy - pragmatical adaptive synchronization by GYC partial region stability theory is proposed as well. Via using this new approach, the new Lyapunov function is a simple linear homogeneous function of states and the lower order controllers and parametric update laws are much simpler and introduce less simulation error.

In recent years, some chaos synchronizations based on fuzzy systems have been proposed [41-44]. The fuzzy set theory was initiated by Zadeh [45]. Fuzzy concept has received much attention as a powerful tool for the nonlinear control. Among various kinds of fuzzy methods, Takagi-Sugeno fuzzy system is widely accepted as a tool for design and analysis of fuzzy control system [46]. A well-known approach to control and synchronize chaos via LMI-based fuzzy control system design is suggested in [47-49], where the idea is to use the Takagi-Sugeno (T-S) fuzzy model to represent typical chaotic models and then apply some effective fuzzy techniques.

Although Takagi-Sugeno fuzzy system is widely accepted as a powerful tool for design and analysis of fuzzy control system, its number of fuzzy rules is based on the



number of nonlinear terms. It means that if there are  $N$  nonlinear terms in a chaotic system, there will be  $2^N$  fuzzy rules in its fuzzy model, and then there will be  $2^N$  linear system to simulate only one chaotic system. Therefore when there are lots of nonlinear terms in a chaotic system, the problem is going to be more complicated. Consequently, in Chapters 7, a new fuzzy model is provided to model and synchronize two different and complicated chaotic systems with lots of nonlinear terms. By using this new fuzzy model, it becomes much simpler to synchronize two different, complicated chaotic systems.

On the other hand, the fuzzy logic control (FLC) scheme has been widely developed for almost 40 years and has been successfully applied to many applications [21]. Recently, Yau and Shieh [22] proposed an amazing new idea in designing fuzzy logic controllers - constructing fuzzy rules subject to a common Lyapunov function such that the master-slave chaos systems satisfy stability in the Lyapunov sense. In [22], there are two main controllers in their slave system. One is used in elimination of nonlinear terms and the other is built by fuzzy rules subject to a common Lyapunov function. Therefore, the resulting controllers are nonlinear form. In [22], the regular form is necessary. In order to carry out the new method, the original system must to be transformed into their regular form.

In Chapter 8, we propose a new strategy, fuzzy logic constant controller (FLCC), which is also constructing fuzzy rules subject to a Lyapunov direct method. Error derivatives are used to be upper bound and lower bound. Through this new approach, a simplest controller, i.e. constant controller, can be obtained and the difficulty in realization of complicated controllers in chaos synchronization by Lyapunov direct method can be also coped. Unlike conventional approaches, the resulting control law has less maximum magnitude of the instantaneous control command and it can reduce the actuator saturation phenomenon in real physic system.

The layout of this thesis can be organized as follow: In Chapter 2, the *Yang* Lorenz system is reviewed and the *Yin* Lorenz system is introduced. Three simulation cases of *Yin* and *Yang* Lorenz systems are given for comparing and observation. In Chapter 3, a new system, Mathieu-van der Pol autonomous system, with four state variables will be introduced, and the hyperchaos for 3PLEs is investigated by phase portrait, power spectrum, Lyapunov exponents and parameter diagram in simulation results. In Chapter 4, chaos control scheme by GYC partial region stability theory is proposed and new Mathieu-Van der pol system and new Mathieu -Duffing system are presented. Three simulation examples are given. In Chapter 5, generalized chaos synchronization strategy by GYC partial region stability theory is proposed. Six simulation examples are given. In Chapter 6, a new and high-performance strategy, pragmatical adaptive synchronization by GYC partial region stability theory, on synchronization is proposed. Yin and Yang Lorenz system are introduced and used for simulation as well. In Chapters 7, a new fuzzy model is provided to model and synchronize two different and complicated chaotic systems. Q-CNN and Qi systems are introduced for examples. In Chapter 8, a new controller - fuzzy logic constant controller (FLCC) is given for efficiently synchronizing different chaotic systems. In Chapter 9, conclusions are drawn.

# Chapter 2

## *Yin-Yang* Chaos

### 2.1 Preliminaries

The *Yang* and *Yin* parameters of Lorenz system are firstly presented in this Chapter. When the transformation from  $(x(t), y(t), z(t), t)$  to  $(x(-t), y(-t), z(-t), -t)$  is made, simulation results show that chaos of the new Lorenz system (which is called *Yin* Lorenz system in this article) can be generated via using “*Yin*” parameters, i.e.  $(\sigma, r, b)$  to  $(-\sigma, -r, -b)$ . To our best knowledge, most characters of Lorenz system are studied in detail, but there are no articles in making a thorough inquiry about the yin Lorenz system. As a result, this *Yin* Lorenz system with “*Yin* parameters” and its one-parameter family are introduced in this paper, and various kinds of phenomena in such systems are investigated by Lyapunov exponents, phase portraits and bifurcation diagrams. An adaptive *Yin-Yang* synchronization from *Yin* to *Yang* Lorenz chaos are achieved by using pragmatism asymptotically stability theorem.

### 2.2 *Yang* Lorenz system with *Yang* parameters

Before introducing the *Yin* Lorenz equation, the *Yang* Lorenz system with *Yang* parameters [7] can be recalled as follows:

$$\begin{cases} \frac{dx}{dt} = \sigma(y - x) \\ \frac{dy}{dt} = rx - xz - y \\ \frac{dz}{dt} = xy - bz \end{cases} \quad (2-2-1)$$

When initial condition  $(x_0, y_0, z_0) = (-0.1, 0.2, 0.3)$  and *Yang* parameters  $\sigma = 10$ ,  $b=8/3$  and  $r=28$ , chaos of the Lorenz system in Eq. (2-2-1) appears. The chaotic

behavior is shown in Fig 2-1.

### 2.3 Yin Lorenz system with Yin parameters

Replacing  $(x(t), y(t), z(t), t)$  via  $(x(-t), y(-t), z(-t), -t)$  in system (2-2-1), a new Lorenz system can be obtained as follows:

$$\begin{cases} \frac{dx(-t)}{d(-t)} = \sigma(y - x) \\ \frac{dy(-t)}{d(-t)} = rx - xz - y \\ \frac{dz(-t)}{d(-t)} = xy - bz \end{cases} \quad (2-3-1)$$

It is clear that in the left hand sides of Eq. (2-3-1), the derivative are taken with the back-time. It means Eq. (2-3-1) aims to find out the behavior of the Yin Lorenz system and to comprehend the relation between systems (2-2-1) and (2-3-1). The simulation results are arranged in Table 2-1.

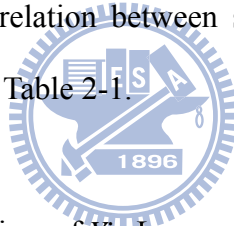


Table 2 - 1 Dynamic behaviors of Yin Lorenz system for different signs of parameters

$\sigma$	$b$	$r$	states
-	+	+	Approach to infinite
+	-	+	Approach to infinite
+	+	-	periodic
-	-	+	Approach to infinite
-	+	-	Approach to infinite
-	-	-	Chaos and periodic

Table 2-1 shows the dynamic behaviors of Yin Lorenz system for different signs of parameters. An awe-inspiring phenomenon is discovered. For initial

condition  $(x_0, y_0, z_0) = (-0.1, 0.2, 0.3)$  and parameters  $\sigma = -10$ ,  $b = -8/3$  and  $r = -28$ , chaos of the *Yin* Lorenz system appears. Therefore, we call these parameters *Yin* parameters. In Chinese philosophy, *Yin* is the negative, past or feminine category in nature, while *Yang* is the positive, present or masculine category in nature. *Yin* and *Yang* are two fundamental opposites in Chinese philosophy. Consequently, the positive value of parameters,  $\sigma = 10$ ,  $b = 8/3$  and  $r = 28$ , in *Yang* Lorenz system can be called *Yang* parameters. The chaotic behavior of Eq. (2-3-1) is shown in Fig 2-2.

As a consequence, system (2-3-1) can be regarded as being carried over into system (2-2-1) by the transformation as follows:

$$(x(t), y(t), z(t), t, \sigma, r, b) \rightarrow (x(-t), y(-t), z(-t), -t, -\sigma, -r, -b) \quad (2-3-2)$$

## 2.4 Comparison between *Yin* and *Yang* Lorenz systems

In order to study the difference and similarity between *Yang* and *Yin* Lorenz system, the bifurcation and Lyapunov exponents are used. The simulation results are divided into three parts:

*Part1:* Parameter  $r$  is varied and  $\sigma$ ,  $b$  are fixed, the simulation results are shown in Fig 2-3 and Fig 2-4, Table 2-2 and Table 2-3.

Table 2 - 2 Range of parameter  $r$  of *Yang* Lorenz system

20.0~24.1	Converges to a fixed point
24.1~70.0	Chaos

Table 2 - 3 Range of parameter  $r$  of *Yin* Lorenz system

-20.0~-46.8	Chaos
-46.8~-47.7	Periodic trajectory

-47.7~-51.3	Chaos
-51.3~-52.4	Periodic trajectory
-52.4~-59.5	Chaos
-59.5~-59.8	Periodic trajectory
-59.8~-68.3	Chaos
-68.3~-69.6	Periodic trajectory
After -69.6	Chaos

Table 2-2 and Table 2-3 show the different dynamics between *Yang* and *Yin* Lorenz systems with different ranges of parameter  $r$ . In Table 2-2, the behaviors of *Yang* Lorenz system are varied with parameter  $c$ . It becomes either chaos or converges to a fixed point. When  $20.0 \leq r \leq 24.1$ , *Yang* Lorenz system is going to converge to a fixed point. When  $24.1 \leq r$ , chaos appears. Table 2-3 shows that when parameter  $c$  takes  $-20.0 \sim -46.8$ ,  $-47.7 \sim -51.3$ ,  $-52.4 \sim -59.5$ ,  $-59.8 \sim -68.3$  and  $-69.6 \leq$ , the chaotic behavior is shown in *Yin* Lorenz system. When parameter  $r$  takes  $-46.8 \sim -47.7$ ,  $-51.3 \sim -52.4$ ,  $-59.5 \sim -59.8$  and  $-68.3 \sim -69.6$ , the behaviors of *Yin* Lorenz system are periodic trajectories. Comparing Table 2-2 and 2-3, it can be found out that there are only two cases, chaos and fixed point, in *Yang* Lorenz system for parameter  $r$  in range 20 to 70, but there exist chaotic behavior and periodic trajectory in *Yin* Lorenz system with parameter  $c$  in range 20 to 70.

*Part2:* Parameter  $b$  is varied and  $\sigma$ ,  $r$  are fixed, the simulation results are shown in

Fig 2-5 and Fig 2-6, Table 2-4 and Table 2-5.

Table 2 - 4 Range of parameter  $b$  of *Yang* Lorenz system

Before 0.592	Converges to a fixed point
0.592~0.648	Chaos

0.648~0.720	Periodic trajectory
0.720~3.448	Chaos
After 3.448	Converge to a fixed point

Table 2 - 5 Range of parameter  $b$  of *Yin* Lorenz system

Before -0.568	Converges to a fixed point
-0.568~-0.728	Chaos
-0.728~-0.792	Periodic trajectory
-0.792~-4.000	Chaos

Table 2-4 and Table 2-5 show that the behaviors of *Yang* and *Yin* Lorenz systems are similar but not the same.

*Part3:* Parameter  $\sigma$  is varied and  $b, r$  are fixed, the simulation results are shown in Fig 2-7 and Fig 2-8, Table 2-6 and Table 2-7.

Table 2 - 6 Range of parameter  $\sigma$  of *Yang* Lorenz system

5.000~5.760	Converges to a fixed point
5.760~18.368	Chaos
18.368~20.000	Converges to a fixed point

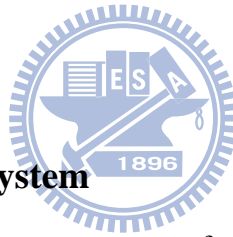
Table 2 - 7 Range of parameter  $\sigma$  of *Yin* Lorenz system

-5.00~-5.45	Periodic trajectory (one attractor or two attractors)
-5.45~-5.60	Chaos
-5.60~-6.05	Periodic trajectory
-6.05~-6.17	Chaos

-6.17~-6.35	Periodic trajectory
-6.35~-7.58	Chaos
-7.58~-7.76	Periodic trajectory
-7.76~-20	Chaos

In Table 2-6 and Table 2-7, the behaviors of *Yang* and *Yin* Lorenz system are very different. In Table 2-6, chaotic behavior only exists in *Yang* Lorenz system in range of  $5.760 \leq \sigma \leq 18.368$ . In Table 2-7, chaos and periodic trajectory appear alternatively in *Yin* Lorenz system for different  $a$ .

By numerical evidence, all trajectories of system (2-3-1) enter a fixed ball (the same ball for trajectories) and remain there. This implies already the existence of compact global attractor.



## 2.5 Family of *Yin* Lorenz system

In this Section, furthermore, one-parameter family of system (2-3-1) is presented as well and can be described as follows:

$$\begin{cases} \frac{dx(-t)}{d(-t)} = \sigma(y - x) \\ \frac{dy(-t)}{d(-t)} = rx - xz - \mu y \\ \frac{dz(-t)}{d(-t)} = xy - bz \end{cases} \quad (2-5-1)$$

where  $\mu \in [-1,1]$ . We choose initial condition  $(x_0, y_0, z_0) = (-0.1, 0.2, 0.3)$  and *Yin* parameters  $\sigma = -6$ ,  $b = -8/3$  and  $r = -28$ , the projection of phase portraits, bifurcation diagrams and Lyapunov exponents with  $\mu \in [-1,1]$  are shown in Figs 2-9 and 2-10. By observation of Figs 2-5 and 2-6, it is clear that there are periodic and chaotic motions in such a family system when  $\mu$  is varying.



## 2.6 Pragmatical Adaptive Synchronization Scheme

There are two identical nonlinear dynamical systems, and the master system controls the slave system. The master system is given by

$$\dot{x} = Ax + f(x, B) \quad (2-6-1)$$

where  $x = [x_1, x_2, \dots, x_n]^T \in R^n$  denotes a state vector,  $A$  is an  $n \times n$  uncertain constant coefficient matrix,  $f$  is a nonlinear vector function, and  $B$  is a vector of uncertain constant coefficients in  $f$ .

The slave system is given by

$$\dot{y} = \hat{A}y + f(y, \hat{B}) + u(t) \quad (2-6-2)$$

where  $y = [y_1, y_2, \dots, y_n]^T \in R^n$  denotes a state vector,  $\hat{A}$  is an  $n \times n$  estimated coefficient matrix,  $\hat{B}$  is a vector of estimated coefficients in  $f$ , and  $u(t) = [u_1(t), u_2(t), \dots, u_n(t)]^T \in R^n$  is a control input vector.

Our goal is to design a controller  $u(t)$  so that the state vector of the chaotic system (2-6-1) asymptotically approaches the state vector of the master system (2-6-2).

The chaos synchronization can be accomplished in the sense that the limit of the error vector  $e(t) = [e_1, e_2, \dots, e_n]^T$  approaches zero:

$$\lim_{t \rightarrow \infty} e = 0 \quad (2-6-3)$$

where

$$e = x - y \quad (2-6-4)$$

From Eq. (2-6-4) we have

$$\dot{e} = \dot{x} - \dot{y} \quad (2-6-5)$$

$$\dot{e} = Ax - \hat{A}y + f(x, B) - f(y, \hat{B}) - u(t) \quad (2-6-6)$$

A Lyapunov function  $V(e, \tilde{A}_c, \tilde{B}_c)$  is chosen as a positive definite function

$$V(e, \tilde{A}, \tilde{B}) = \frac{1}{2} e^T e + \frac{1}{2} \tilde{A}^T \tilde{A} + \frac{1}{2} \tilde{B}^T \tilde{B} \quad (2-6-7)$$

where  $\tilde{A} = A - \hat{A}$ ,  $\tilde{B} = B - \hat{B}$ ,  $\tilde{A}_c$  and  $\tilde{B}_c$  are two column matrices whose elements are all the elements of matrix  $\hat{A}$  and of matrix  $\hat{B}$ , respectively.

Its derivative along any solution of the differential equation system consisting of Eq. (2-6-6) and update parameter differential equations for  $\tilde{A}_c$  and  $\tilde{B}_c$  is

$$\dot{V}(e, \tilde{A}_c, \tilde{B}_c) = e^t \left[ Ax - \hat{A}y + Bf(x) - \hat{B}f(y) - u(t) \right] + \tilde{A}_c \dot{\tilde{A}}_c + \tilde{B}_c \dot{\tilde{B}}_c \quad (2-6-8)$$

where  $u(t)$ ,  $\dot{\tilde{A}}_c$ , and  $\dot{\tilde{B}}_c$  are chosen so that  $\dot{V} = e^T C e$ ,  $C$  is a diagonal negative definite matrix, and  $\dot{V}$  is a negative semi-definite function of  $e$  and parameter differences  $\tilde{A}_c$  and  $\tilde{B}_c$ . In current scheme of adaptive control of chaotic motion [18-20], traditional Lyapunov stability theorem and Babalat lemma are used to prove that the error vector approaches zero, as time approaches infinity. But the question, why the estimated or given parameters also approach to the uncertain or goal parameters, remains no answer. By pragmatistical asymptotical stability theorem [50-51], the question can be answered strictly.

## 2.7 Adaptive Yin-Yang synchronization of Yin chaos and Yang chaos

In this Section, adaptive synchronization from *Yin* Lorenz chaos to *Yang* Lorenz chaos is proposed. The *Yin* Lorenz system is consider as slave system and the *Yang* Lorenz system is regarded as master system. These two equations are shown below:

Master system- *Yang* Lorenz system:

$$\begin{cases} \frac{dx_1(t)}{dt} = a(x_2(t) - x_1(t)) \\ \frac{dx_2(t)}{dt} = cx_1(t) - x_1(t)x_3(t) - x_2(t) \\ \frac{dx_3(t)}{dt} = x_1(t)x_2(t) - bx_3(t) \end{cases} \quad (2-7-1)$$

Slave system- *Yin* Lorenz system:

$$\begin{cases} \frac{dy_1(-t)}{d(t)} = -\hat{a}(y_2(-t) - y_1(-t)) + u_1 \\ \frac{dy_2(-t)}{d(t)} = -(\hat{c}y_1(-t) - y_1(-t)y_3(-t) - y_2(-t)) + u_2 \\ \frac{dy_3(-t)}{d(t)} = -(y_1(-t)y_2(-t) - \hat{b}y_3(-t)) + u_3 \end{cases} \quad (2-7-2)$$

where  $x_i(t)$  stands for states variables of the master system and  $y_i(-t)$  that of the slave system, respectively. Parameters,  $a$ ,  $b$  and  $c$  are uncertain parameters of master system.

$\hat{a}$ ,  $\hat{b}$  and  $\hat{c}$  are estimated parameters.  $u_1$ ,  $u_2$  and  $u_3$  are nonlinear controller to synchronize the slave Lorenz system to master one, i.e.,

$$\lim_{t \rightarrow \infty} \mathbf{e} = 0 \quad (2-7-3)$$

where the error vector  $\mathbf{e} = [e_1(t) \ e_2(t) \ e_3(t)]$  and

$$\begin{cases} e_1(t) = x_1(t) - y_1(-t) \\ e_2(t) = x_2(t) - y_2(-t) \\ e_3(t) = x_3(t) - y_3(-t) \end{cases} \quad (2-7-4)$$

From Eq. (2-7-4), we have the following error dynamics:

$$\begin{cases} \frac{de_1(t)}{dt} = \frac{dx_1(t)}{dt} - \frac{dy_1(-t)}{d(-t)} = \frac{dx_1(t)}{dt} + \frac{dy_1(-t)}{d(-t)} \\ \frac{de_2(t)}{dt} = \frac{dx_2(t)}{dt} - \frac{dy_2(-t)}{d(-t)} = \frac{dx_2(t)}{dt} + \frac{dy_2(-t)}{d(-t)} \\ \frac{de_3(t)}{dt} = \frac{dx_3(t)}{dt} - \frac{dy_3(-t)}{d(-t)} = \frac{dx_3(t)}{dt} + \frac{dy_3(-t)}{d(-t)} \end{cases}$$

$$\begin{aligned} \dot{e}_1 &= a(x_2 - x_1) + (-\hat{a}(y_2 - y_1) + u_1) \\ \dot{e}_2 &= cx_1 - x_1x_3 - x_2 + (-\hat{c}y_1 - y_1y_3 - y_2) + u_2 \\ \dot{e}_3 &= x_1x_2 - bx_3 + (-y_1y_2 - \hat{b}y_3) + u_3 \end{aligned} \quad (2-7-5)$$

These two systems will be synchronized for any initial condition by appropriate controllers and update laws for those estimated parameters. As a result, the following controllers and update laws are designed by pragmatistical asymptotical stability theorem as follows:

Choosing Lyapunov function as:

$$V = \frac{1}{2}(e_1^2 + e_2^2 + e_3^2 + \tilde{a}^2 + \tilde{b}^2 + \tilde{c}^2) \quad (2-7-6)$$

where  $\tilde{a} = a - \hat{a}$ ,  $\tilde{b} = b - \hat{b}$  and  $\tilde{c} = c - \hat{c}$ .

Its time derivative is:

$$\begin{aligned} \dot{V} &= e_1 \dot{e}_1 + e_2 \dot{e}_2 + e_3 \dot{e}_3 + \tilde{a} \dot{\tilde{a}} + \tilde{b} \dot{\tilde{b}} + \tilde{c} \dot{\tilde{c}} \\ &= e_1 (a(x_2 - x_1) + (-\hat{a}(y_2 - y_1) + u_1)) \\ &\quad + e_2 (cx_1 - x_1x_3 - x_2 + (-\hat{c}y_1 - y_1y_3 - y_2) + u_2)) \\ &\quad + e_3 (x_1x_2 - bx_3 + (-y_1y_2 - \hat{b}y_3) + u_3)) \\ &\quad + \tilde{a}(a - \hat{a}) + \tilde{b}(b - \hat{b}) + \tilde{c}(c - \hat{c}) \end{aligned} \quad (2-7-7)$$

We choose the update laws for those uncertain parameters as:

$$\begin{cases} \dot{\tilde{a}} = -\dot{\hat{a}} = -(x_2 - x_1)e_1 + \tilde{a}e_1 \\ \dot{\tilde{c}} = -\dot{\hat{c}} = -(x_1)e_2 + \tilde{c}e_2 \\ \dot{\tilde{b}} = -\dot{\hat{b}} = (x_3)e_3 + \tilde{b}e_3 \end{cases} \quad (2-7-8)$$

Through Eqs. (2-7-8) and (2-7-9), the appropriate controllers can be designed as:

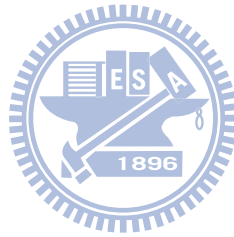
$$\begin{cases} u_1 = -\hat{a}(x_2 - x_1 - y_2 + y_1) - \tilde{a}^2 - e_1 \\ u_2 = -\hat{c}(x_1 - y_1) + x_1x_3 + x_2 + y_1y_3 + y_2 - \tilde{c}^2 - e_2 \\ u_3 = \hat{b}(x_3 - y_3) - x_1x_2 - y_1y_2 - \tilde{b}^2 - e_3 \end{cases} \quad (2-7-9)$$

We obtain

$$\dot{V} = -e_1^2 - e_2^2 - e_3^2 < 0 \quad (2-7-10)$$

which is negative semi-definite function of  $e_1, e_2, e_3, \tilde{a}, \tilde{b}$  and  $\tilde{c}$ . The Lyapunov asymptotical stability theorem is not satisfied. We cannot obtain that common origin of error dynamics (2-7-5) and parameter dynamics (2-7-8) is asymptotically stable. By

pragmatical asymptotically stability theorem,  $D$  is a 6-manifold,  $n = 6$  and the number of error state variables  $p = 3$ . When  $e_1 = e_2 = e_3 = 0$  and  $\tilde{a}$ ,  $\tilde{b}$ ,  $\tilde{c}$  take arbitrary values,  $\dot{V} = 0$ , so  $X$  is of 3 dimensions,  $m = n - p = 6 - 3 = 3$ ,  $m + 1 < n$  is satisfied. According to the pragmatical asymptotically stability theorem, error vector  $e$  approaches zero and the estimated parameters also approach the uncertain parameters. The equilibrium point is pragmatically asymptotically stable. Under the assumption of equal probability, it is actually asymptotically stable. The simulation results are shown in Figs. 2-11~ 2-14.



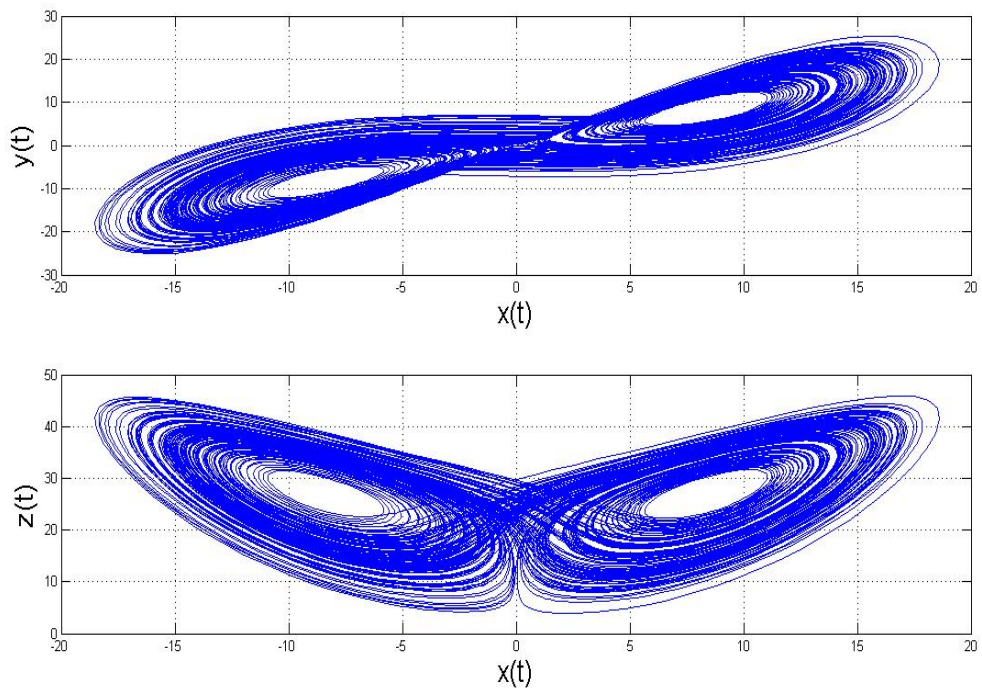


Fig.2- 1 Projections of phase portrait of chaotic *Yang* Lorenz system with  $\sigma = 10$ ,  $b = 8/3$  and  $r = 28$

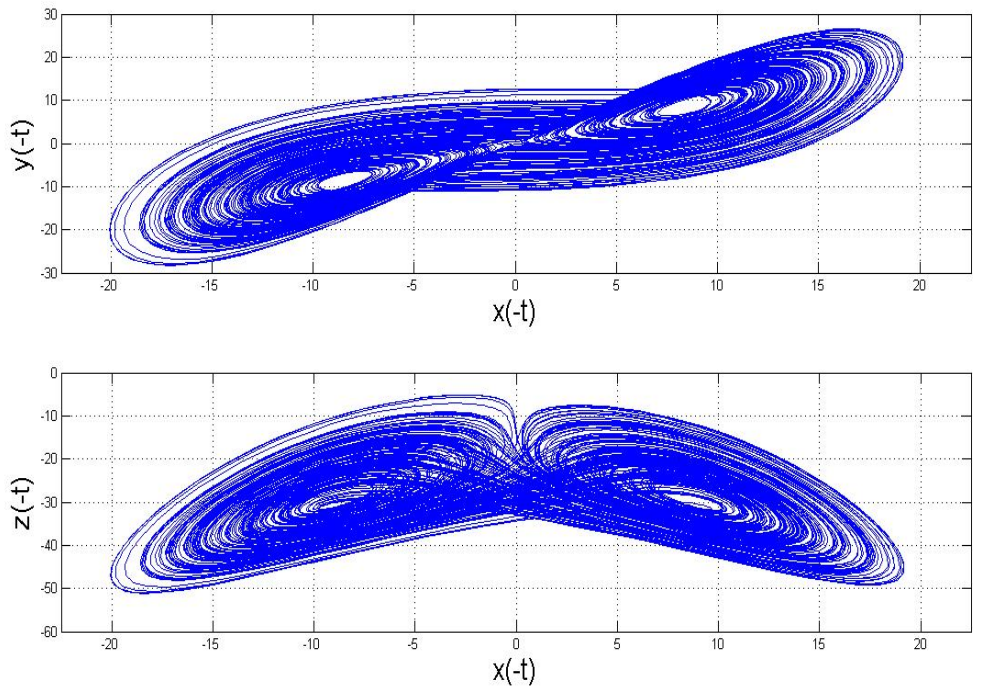


Fig.2- 2 Projections of phase portrait of chaotic *Yin* Lorenz system with Yin parameters  $\sigma = -10$ ,  $b = -8/3$  and  $r = -28$ .

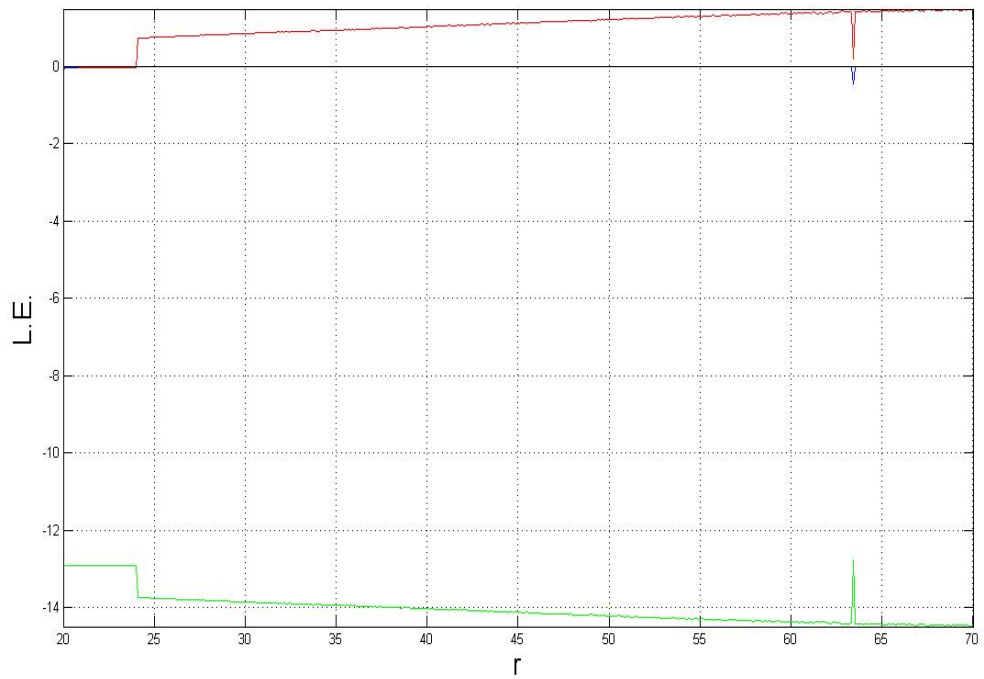
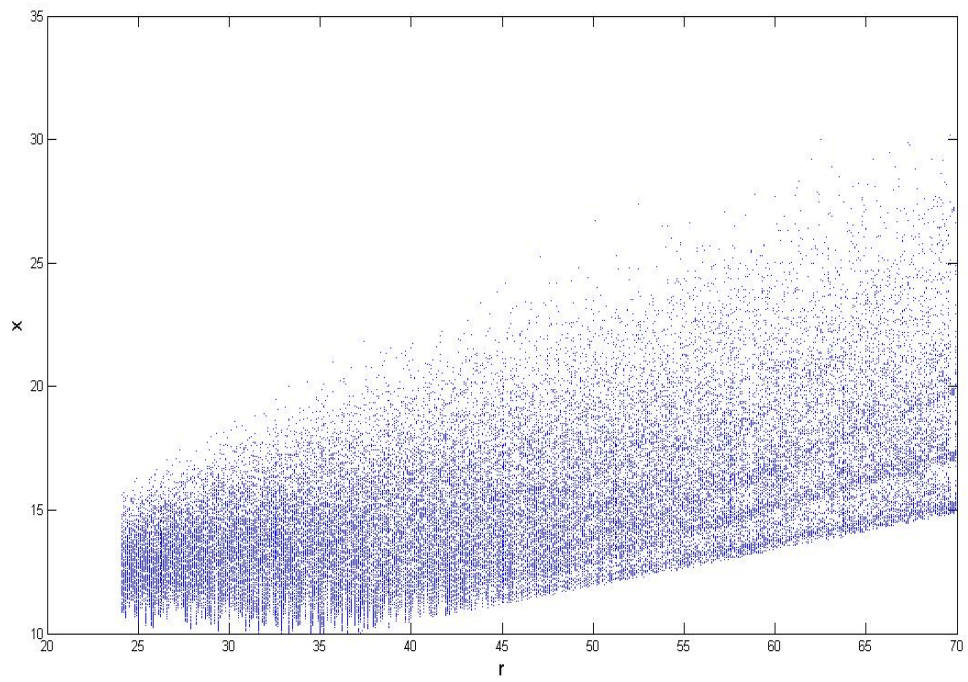


Fig.2- 3 Bifurcation diagram and Lyapunov exponents of chaotic *Yang Lorenz* system with  $b=8/3$  and  $\sigma=10$ .

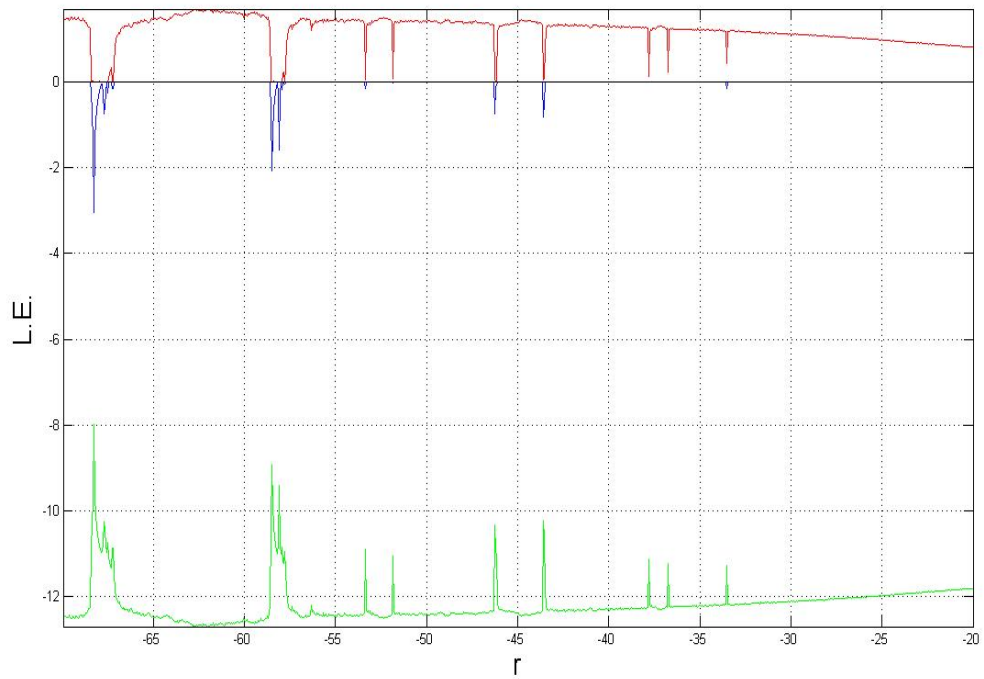
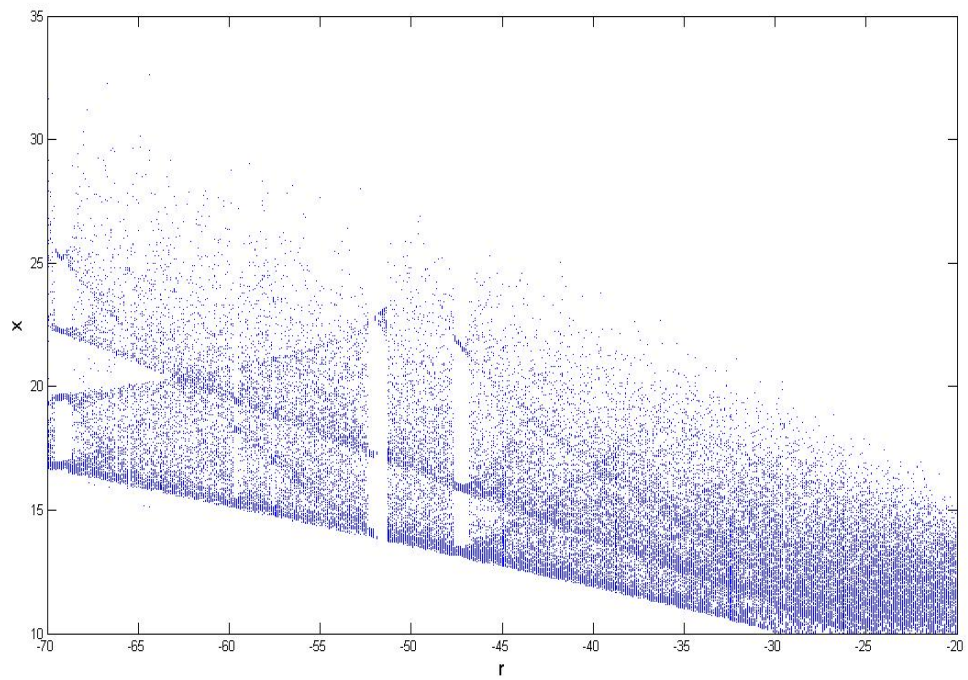


Fig.2- 4 Bifurcation diagram and Lyapunov exponents of chaotic *Yin* Lorenz system with  $b=-8/3$  and  $\sigma=-10$ .



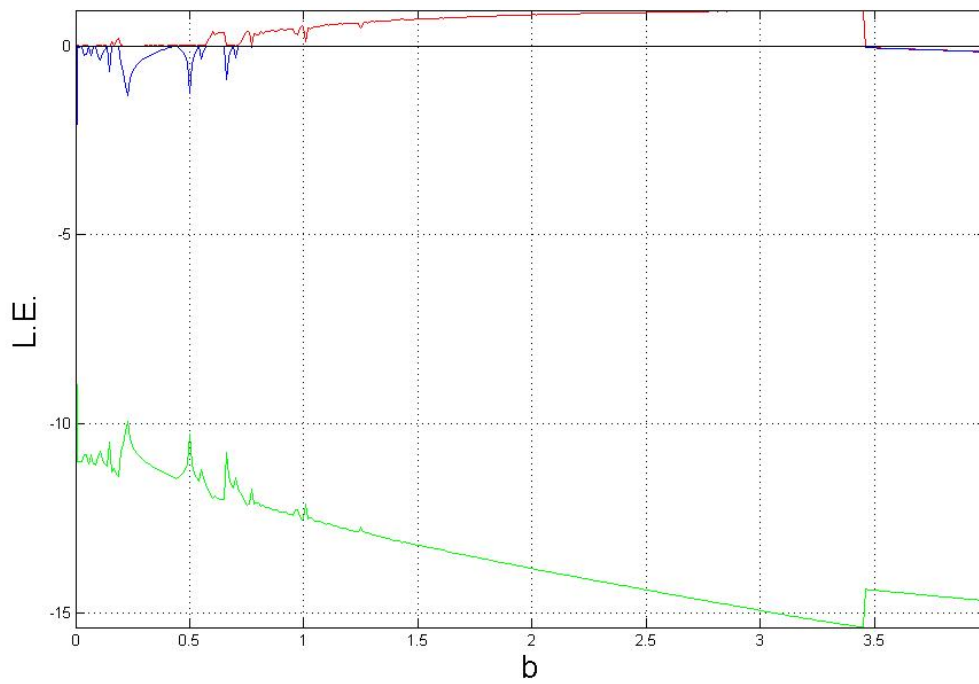
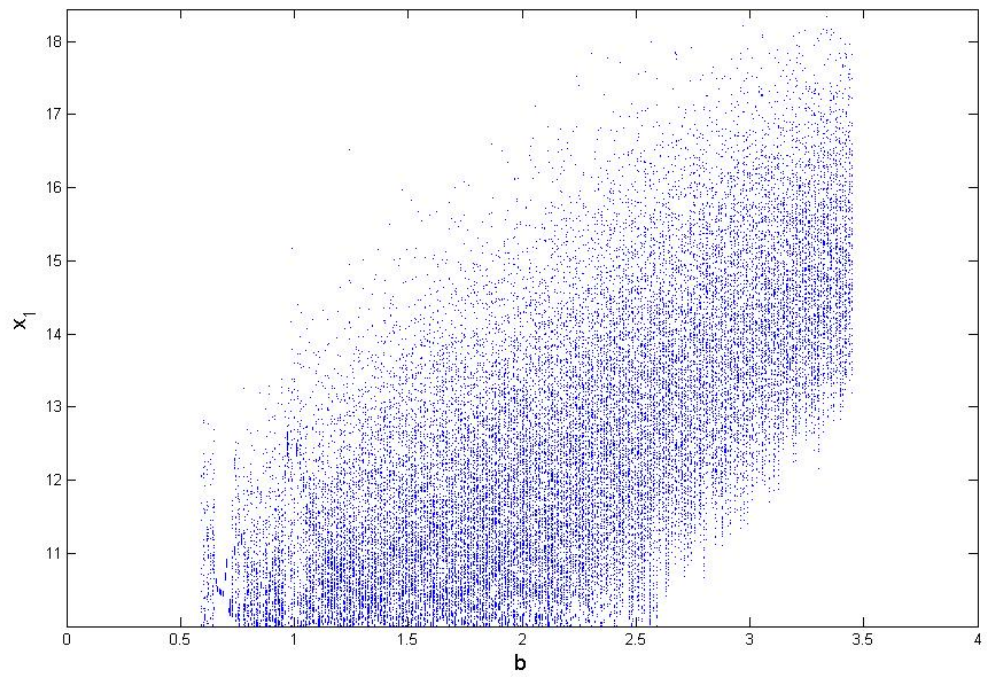


Fig.2- 5 Bifurcation and Lyapunov exponents of chaotic *Yang* Lorenz system with  $\sigma = 28$  and  $r = 10$ .

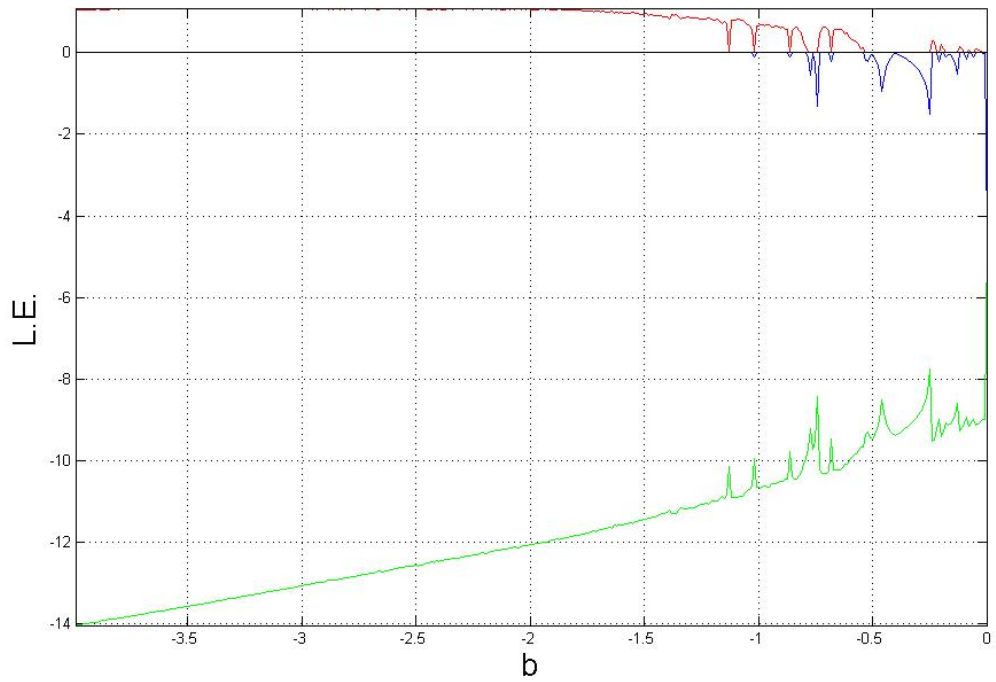
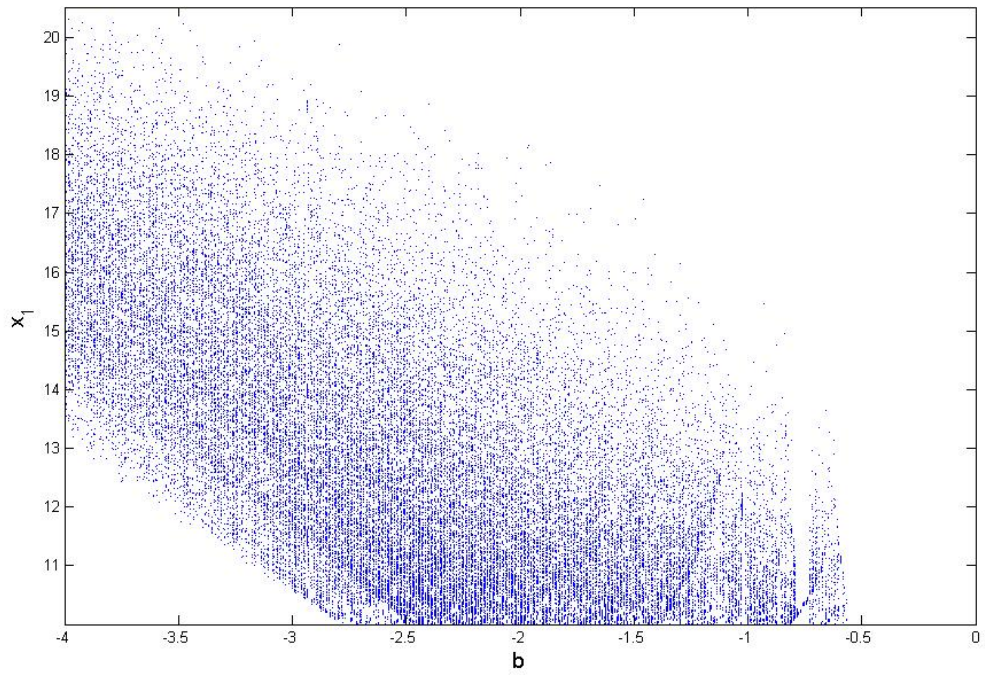


Fig.2- 6 Bifurcation and Lyapunov exponents of chaotic *Yin* Lorenz system with  $\sigma = -28$  and  $r = -10$ .

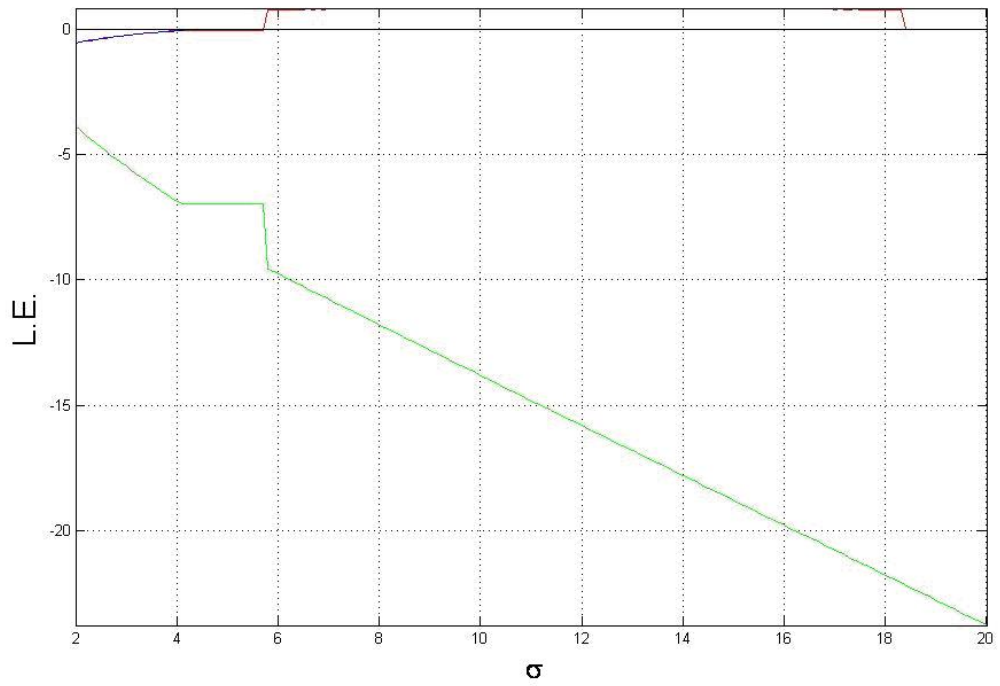
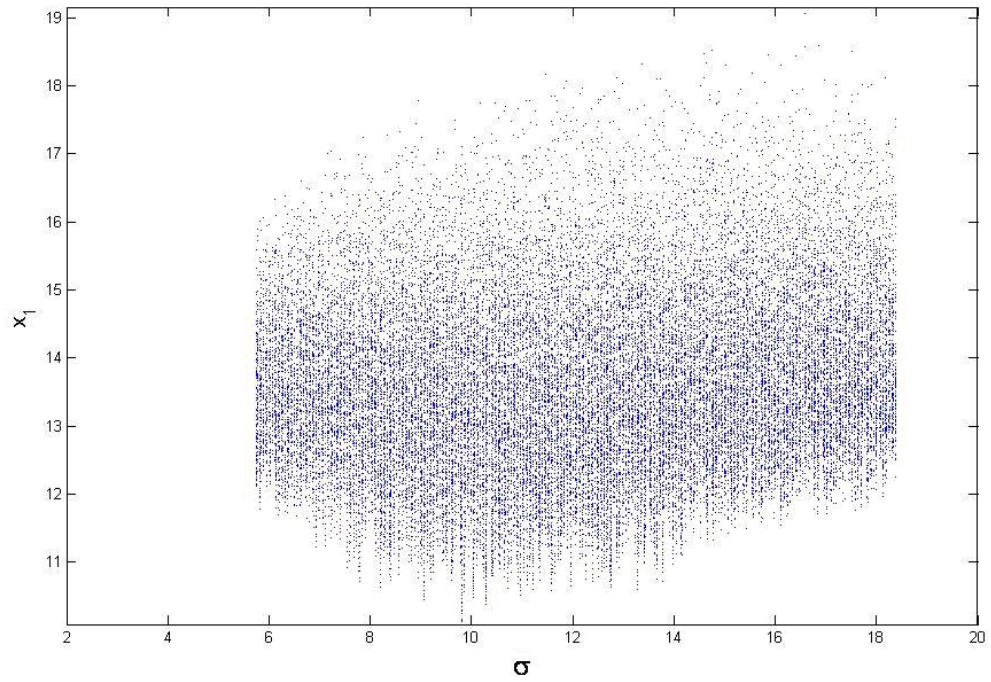


Fig.2- 7 Bifurcation and Lyapunov exponents of chaotic *Yang* Lorenz system with  $b=8/3$  and  $r=28$ .

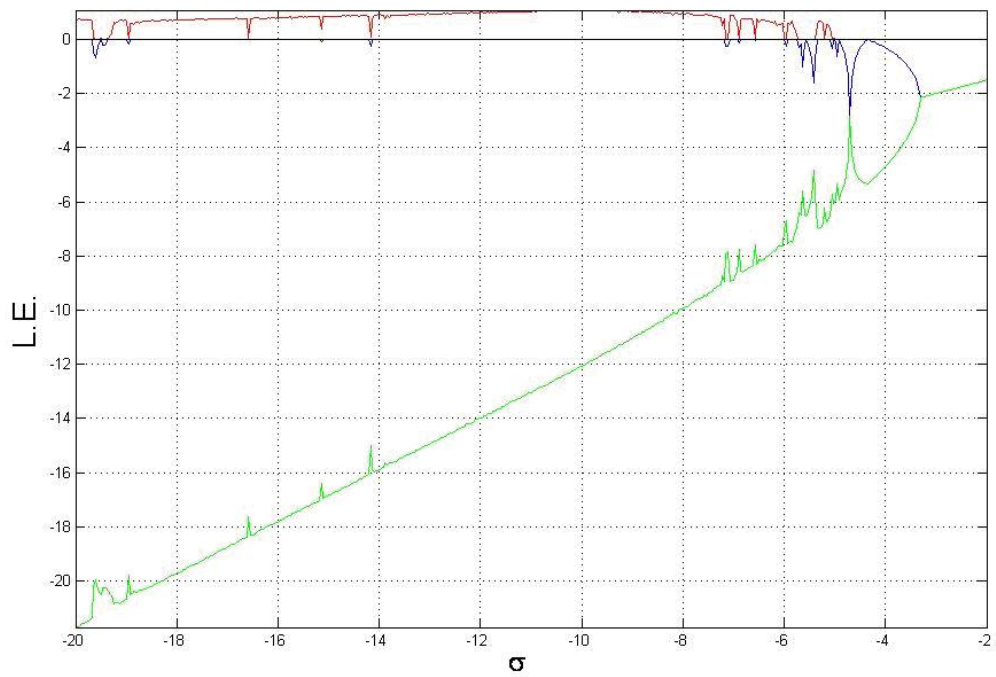
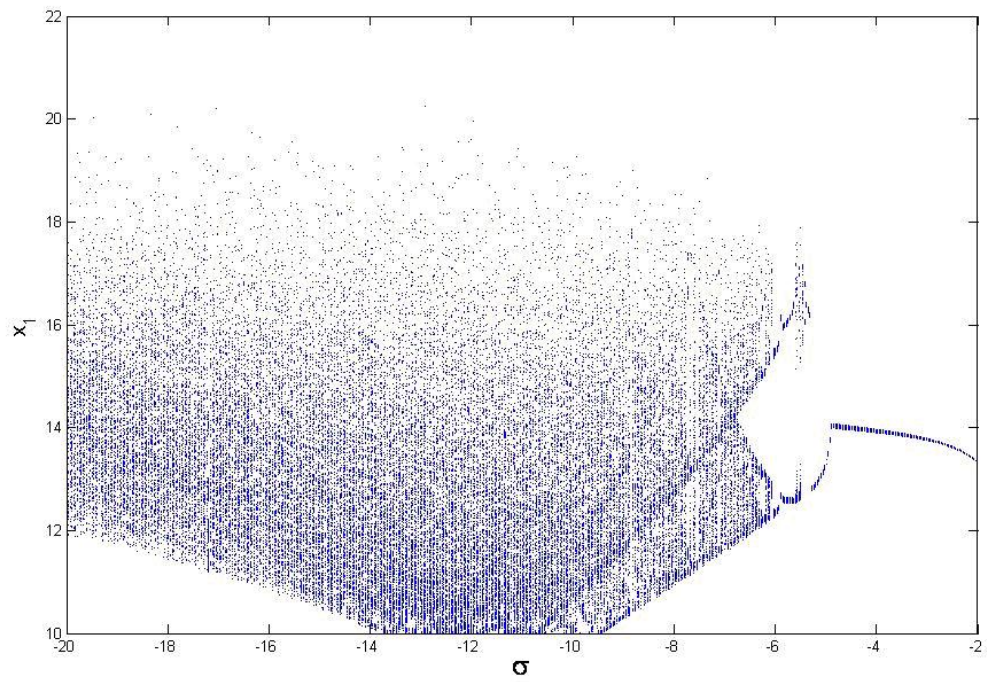
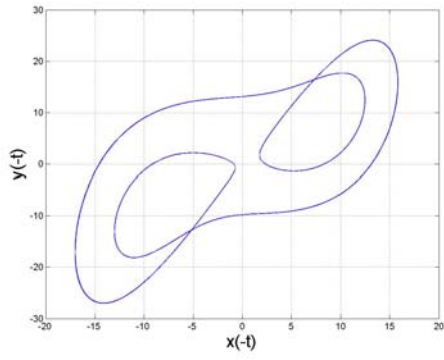
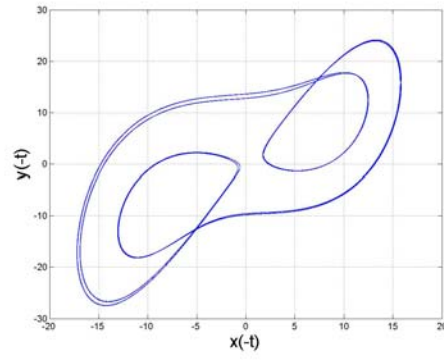


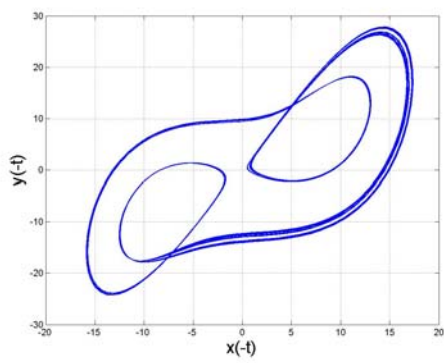
Fig.2- 8 Bifurcation and Lyapunov exponents of chaotic *Yin* Lorenz system with  $b=-8/3$  and  $c=-28$ .



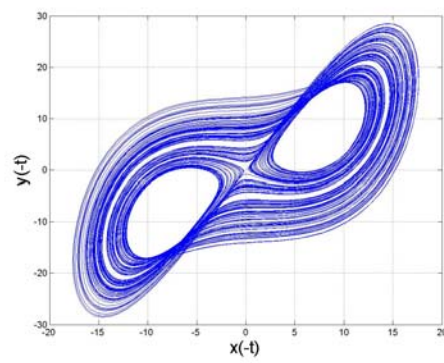
$\mu = 1$



$\mu = 0.99$



$\mu = 0.98$



$\mu = 0.7$



Fig.2- 9 Projections of phase portraits of family of *Yin* Lorenz system with  $\sigma = -6$ ,  $b = -8/3$  and  $r = -28$ .

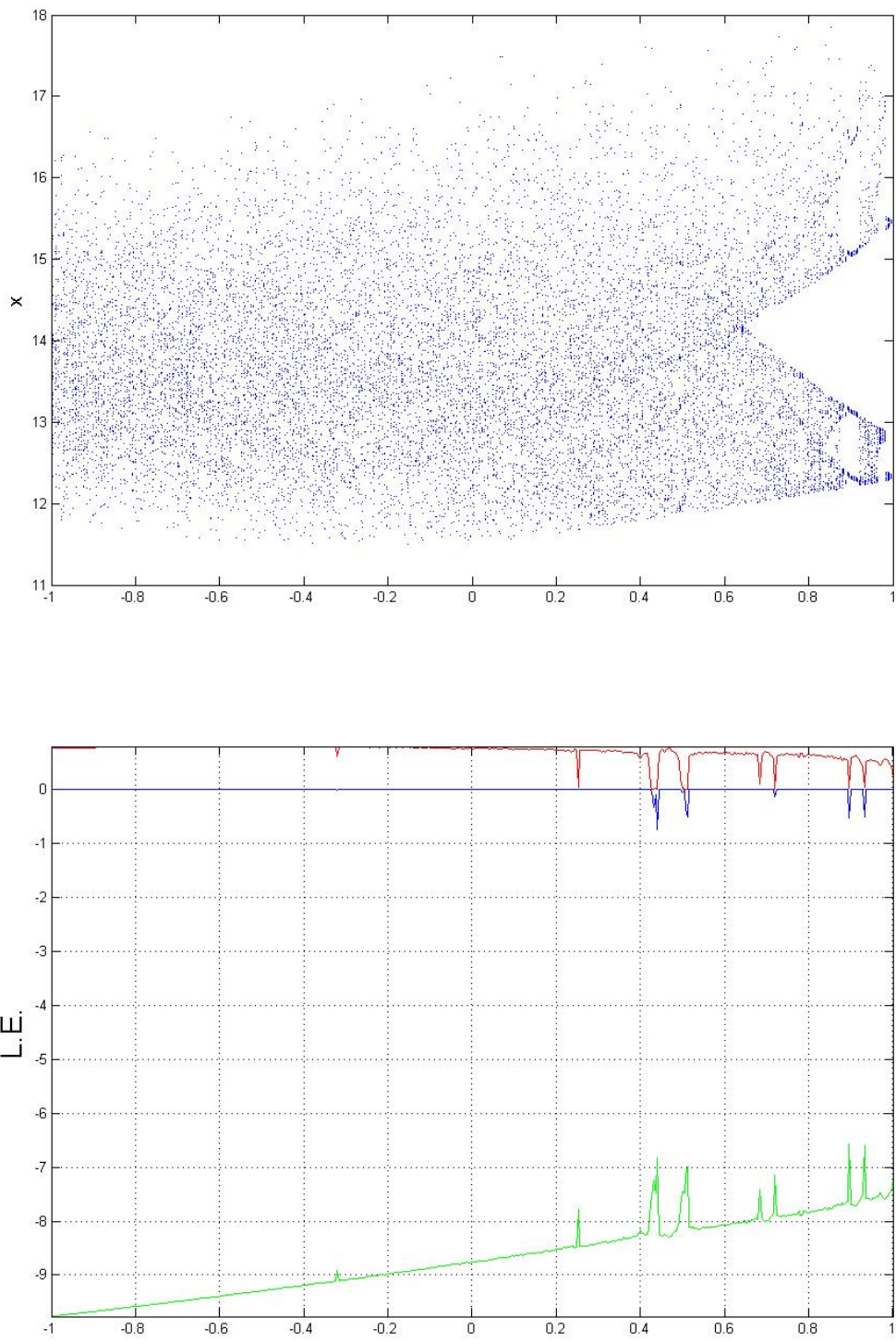


Fig.2- 10 Bifurcation diagram and Lyapunov exponents of family of *Yin* Lorenz system with  $\sigma = -6$ ,  $b = -8/3$  and  $r = -28$ . (varied by  $\mu$ )

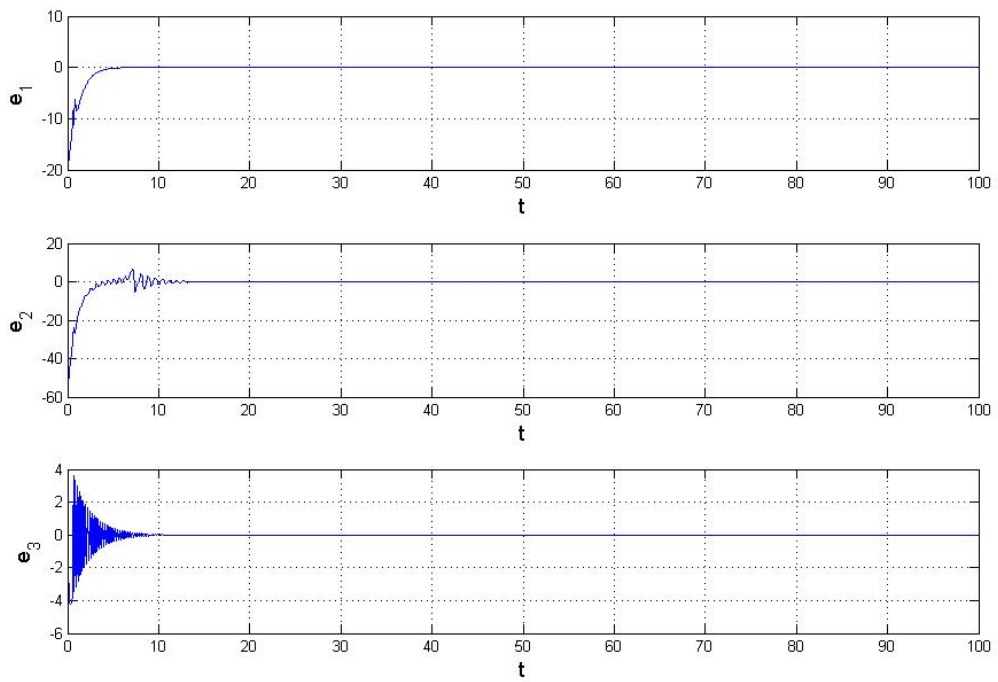


Fig.2- 11 Time histories of errors for *Yin* and *Yang* Lorenz chaotic systems.

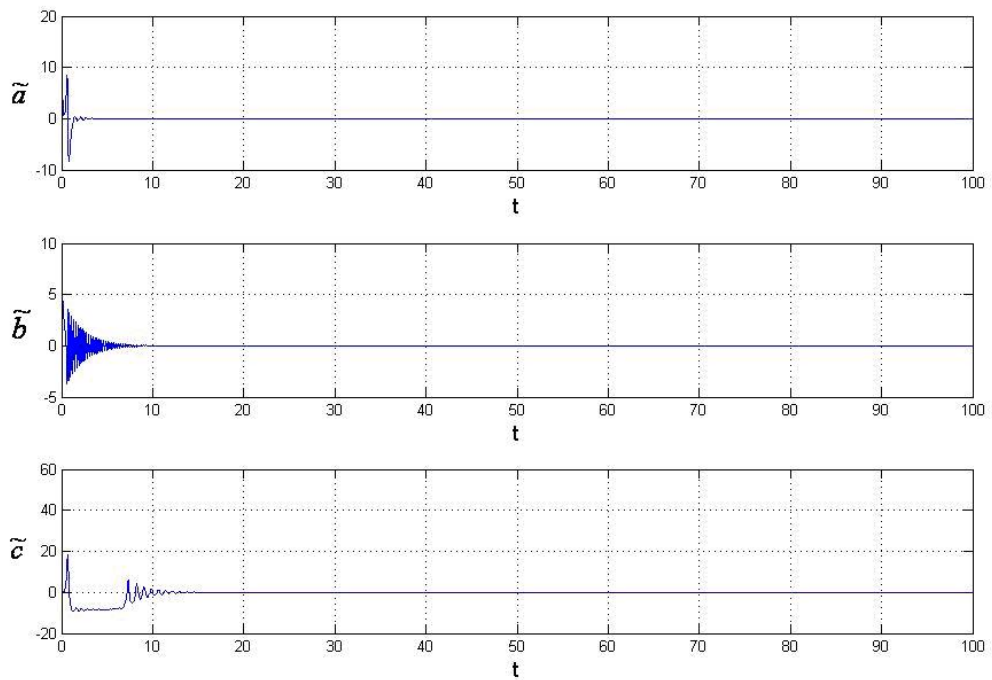


Fig.2- 12 Time histories of parametric errors for *Yin* and *Yang* Lorenz chaotic systems.

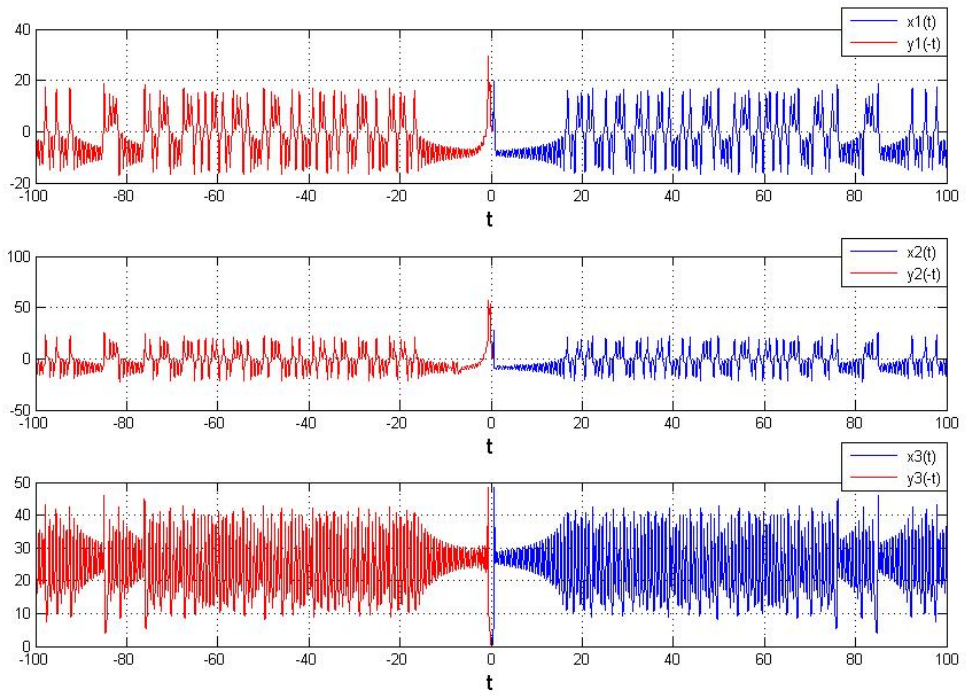


Fig.2- 13 Time histories of states of *Yin* and *Yang* Lorenz chaotic systems.

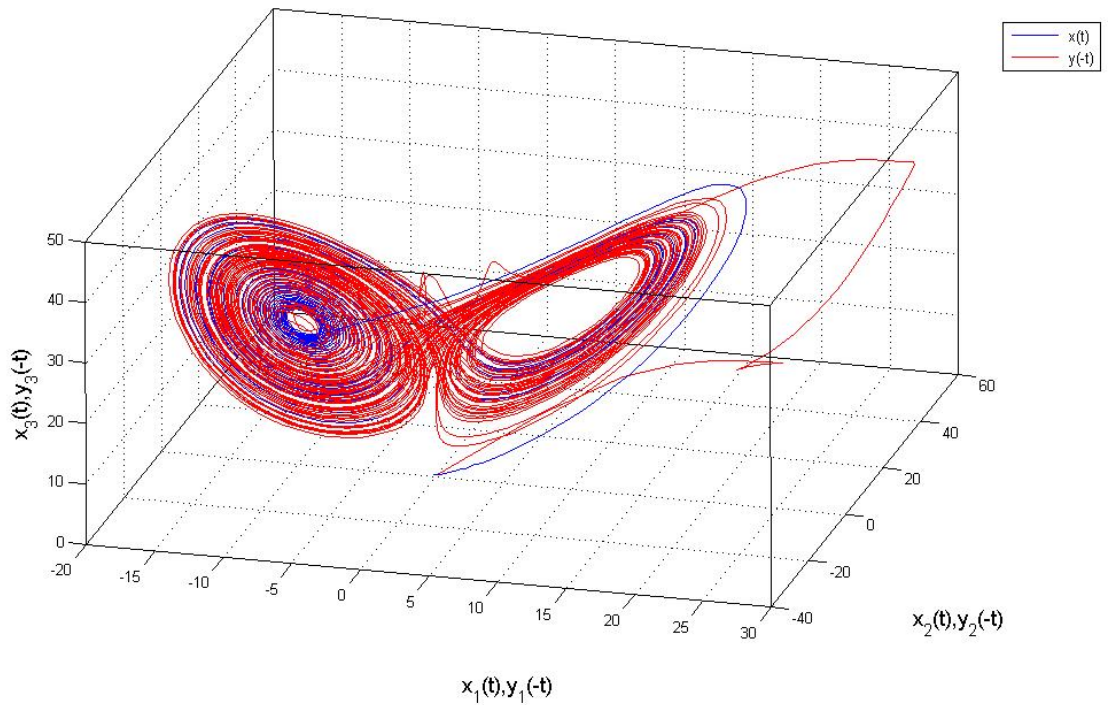


Fig.2- 14 Phase portraits of synchronization of *Yin* and *Yang* Lorenz chaotic systems.



# Chapter 3

## Hyperchaos of New Mathieu-van der Pol system with Three Positive Lyapunov Exponents

### 3.1 Preliminaries

This Chapter gives another illustration of three positive Lyapunov exponents (3PLES) in numerical simulations of a new system, Mathieu-van der pol autonomous system, with four state variables. As we know, two positive Lyapunov exponents confirm hyperchaotic nature of its dynamics and means that system can present more complicated behavior than ordinary chaos. We further generate three positive Lyapunov exponents in a new coupled nonlinear system and anticipate the advanced application in secure communication. Not only a new chaotic system with three Lyapunov exponents is proposed, but also its implementation of electronic circuit is putting into practice in this article. The phase portrait, electronic circuit, power spectrum, Lyapunov exponents and 2-D and 3-D parameter diagram with three positive Lyapunov exponents of the new system will be showed in this Chapter.

### 3.2 Differential equations for Mathieu-van der Pol system and phase portraits

Mathieu equation and van der Pol equation are two typical nonlinear non-autonomous systems:

$$\begin{cases} \dot{x}_1 = x_2 \\ \dot{x}_2 = -(a + b \sin \omega t)x_1 - (a + b \sin \omega t)x_1^3 - cx_2 + d \sin \omega t \end{cases} \quad (3-2-1)$$

$$\begin{cases} \dot{x}_3 = x_4 \\ \dot{x}_4 = -ex_3 + f(1 - x_3^2)x_4 + g \sin \omega t \end{cases} \quad (3-2-2)$$

Exchanging  $\sin\omega t$  in Eq. (3-2-1) by  $x_3$  and  $\sin\omega t$  in Eq. (3-2-2) by  $x_1$ , we obtain the autonomous new Mathieu -van der Pol system:

$$\begin{cases} \dot{x}_1 = x_2 \\ \dot{x}_2 = -(a + bx_3)x_1 - (a + bx_3)x_1^3 - cx_2 + dx_3 \\ \dot{x}_3 = x_4 \\ \dot{x}_4 = -ex_3 + f(1 - x_3^2)x_4 + gx_1 \end{cases} \quad (3-2-3)$$

where  $x, y, z$  and  $w$  are four states of the system,  $a, b, c, d, e, f$  and  $g$  are parameters of the Mathieu-van der Pol system.

It is well-known that the phase portrait presents the evolution of a set of trajectories emanating from various initial conditions. When the solution becomes stable, the asymptotic behaviors of the phase trajectories are particularly interested and the transient behaviors in the system are neglected. As a result, the phase portrait projections of the Mathieu-van der Pol system, Eq. (3-2-3), is plotted in Fig. 3-1. In this numerical studies, the parametric values are taken to be  $a=91.7$ ,  $b=5.023$ ,  $c=-0.001$ ,  $d=91$ ,  $e=87.001$ ,  $f=0.0180$  and  $g=9.5072$  for plotting the hyperchaotic phase portrait projections.

### 3.3 Power spectrum

The power spectrum analysis of the nonlinear dynamical system, Eq. (3-2-3) is shown in Fig. 3-2. The noise-like spectrum is the characteristics of chaotic dynamical system.

### 3.4 Lyapunov exponents

The Lyapunov exponents of Mathieu-van der Pol system with 3PLEs are plotted in Figs. 3-3~3-8. These figures show that there exists at least one PLE in the Lyapunov spectrum for our new system, and the Lyapunov exponents of Mathieu-van der Pol

system are varied with parameters  $a$ ,  $b$ ,  $d$  and  $e$ .

### 3.5 Parameter diagrams

A system with more than one positive Lyapunov exponent can be classified as a hyperchaotic system. In this study, the parameter values,  $b$ ,  $d$ ,  $g$ , and  $f$ , are varied to observe the regions of chaos of our new system. The enriched information of chaotic behaviors of the system can be obtained from the Figs 3-9~3-14.

In Figs 3-9~3-14, the regions of 3PLEs are yellow, 2PLEs green and 1PLEs purple. It can be realized that the Mathieu-van der pol system is chaotic in several different region, especially hyperchaos with 3 PLEs are found in many regions between hyperchaos with 2 PLE and chaos with 1 PLE.

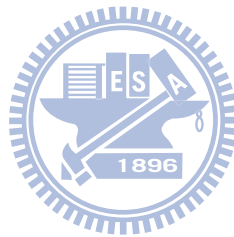
### 3.6 Phase portraits and its implementation of electronic circuits

It is well-known that the phase space can present the evolution of a set of trajectories emanating from various initial conditions. When the solution becomes stable, the asymptotic behaviors of the phase trajectories are particularly interested and the transient behaviors in the system are neglected. As a result, the phase portrait of the Mathieu-van der pol system, equation (3-1-1), is plotted in Fig. 3-1. In this numerical studies, the parametric values are taken to be  $a=91.7$ ,  $b=5.023$ ,  $c=0.01$ ,  $d=91$ ,  $e=87.001$ ,  $f=0.0180$  and  $g=9.5072$  for plotting the tri-chaotic phase portrait. The new system can be represented as an electronic oscillator circuit and projection of phase portraits outputs shown in Figs. 3-15~16. We have implemented it using an electronics simulation package Multisim (previously called Electronic Workbench, EWB) and the approximated nonlinear electronic circuits are presented to realize the disordered behavior in the new chaotic system. The voltage outputs have been normalized to 1 V and the operational amplifiers are considered to be ideal. The phase

diagrams are plotted within the time interval 500 s. The time step is 0.001 s. Due to the limit of the scope of implementation of electronic circuits, the phase portraits can be only shown in two dimensions. In Fig. 3, the configuration of electronic circuits is also given.

### 3.7 Summary

In this Chapter, we have shown that the autonomous continuous-time Mathieu-van der pol autonomous system with four state variables as described by Eq. (3-2-3) can exhibit hyperchaos with three positive Lyapunov exponents. The simulation results have been investigated in phase portraits, power spectrum, parameter diagrams and Lyapunov exponents.



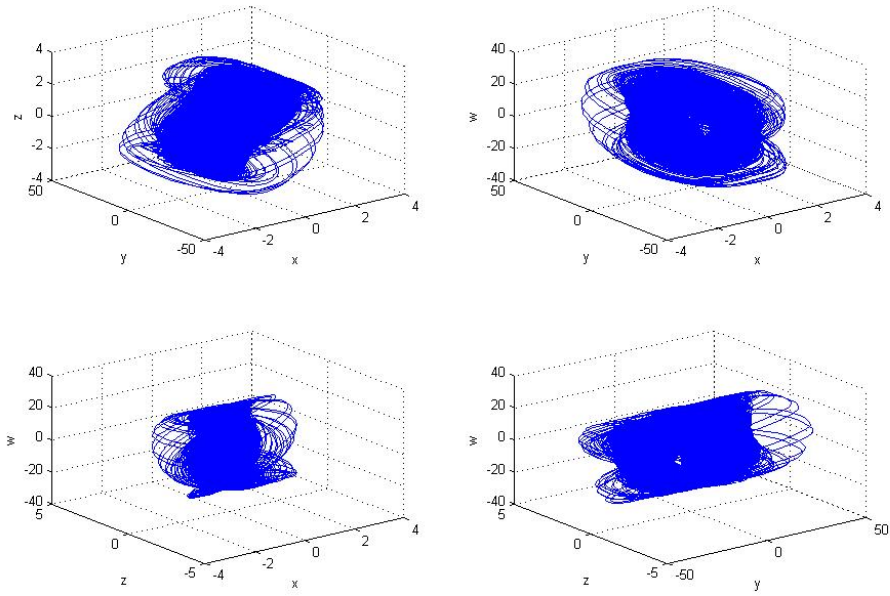


Fig.3- 1 Phase portrait projections of four state Mathieu-van der Pol system with  $a=91.17$ ,  $b=5.023$ ,  $c=-0.001$ ,  $d=91$ ,  $e=87.001$ ,  $f=0.0180$  and  $g=9.5072$ .

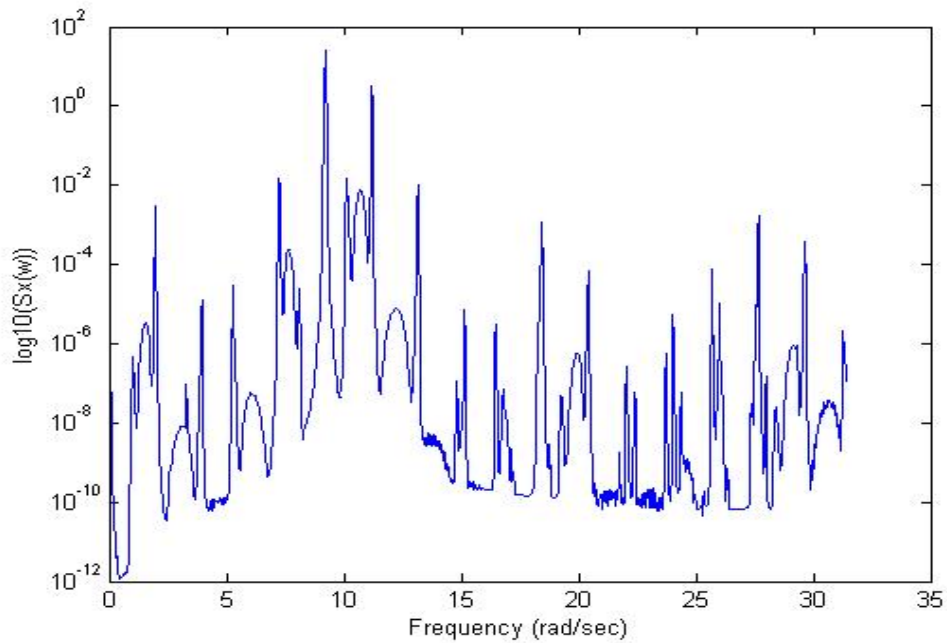
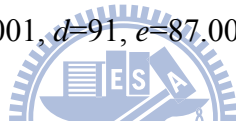


Fig.3- 2 Power spectrum of  $x$  for Mathieu-van der Pol system with  $a=91.17$ ,  $b=5.023$ ,  $c=-0.001$ ,  $d=91$ ,  $e=87.001$ ,  $f=0.018$  and  $g=9.5072$ .

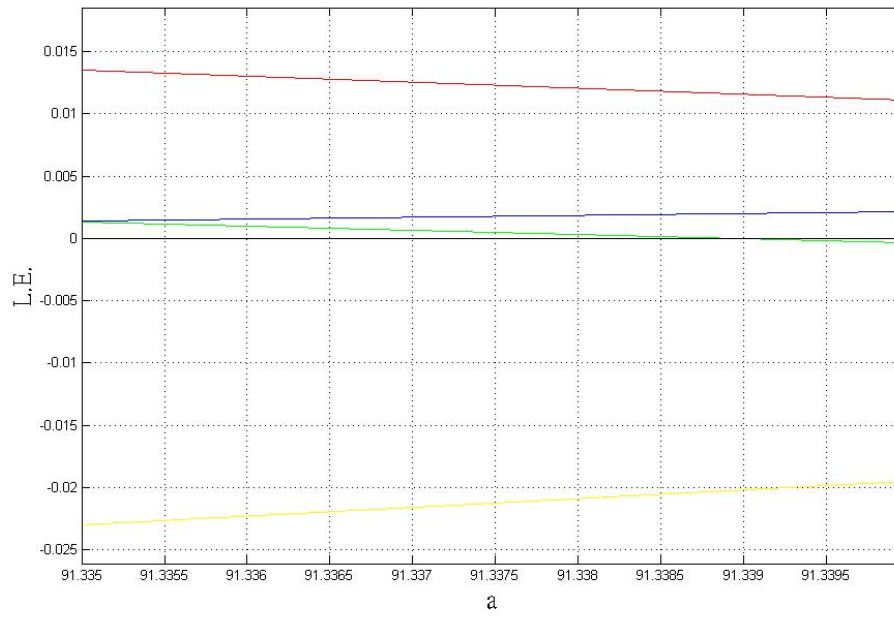


Fig.3- 3 Lyapunov exponents of Mathieu-van der Pol system with  $b=5.023$ ,  $c=-0.001$ ,  $d=91$ ,  $e=87.001$ ,  $f=0.018$  and  $g=9.5072$ .

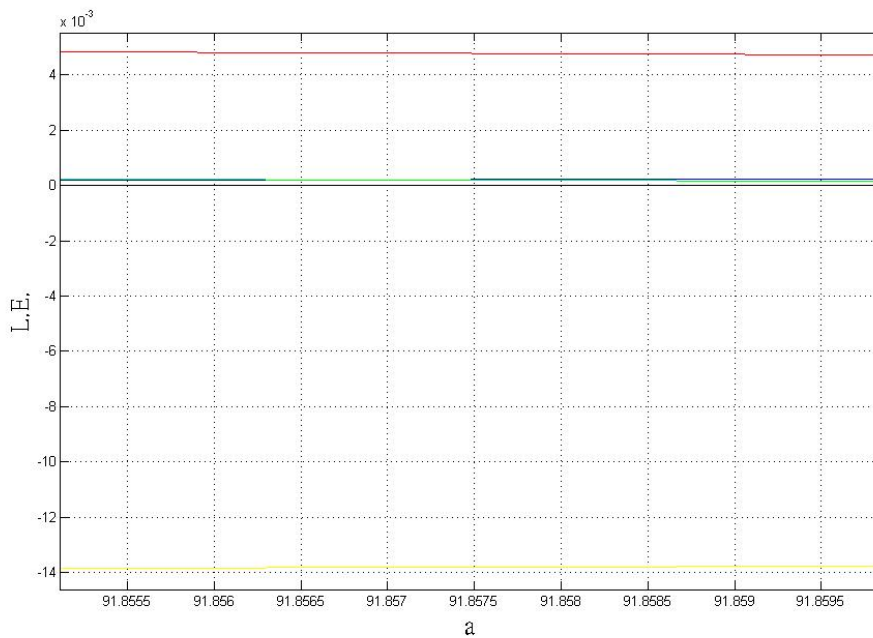


Fig.3- 4 Lyapunov exponents of Mathieu-van der Pol system with  $b=5.023$ ,  $c=-0.001$ ,  $d=25$ ,  $e=87.001$ ,  $f=0.018$  and  $g=9.5072$ .

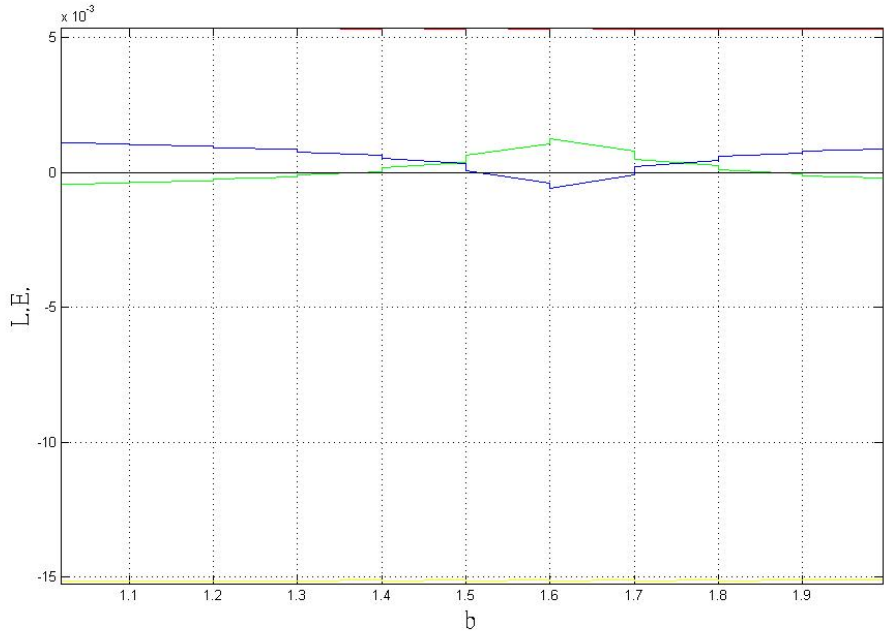


Fig.3- 5 Lyapunov exponents of Mathieu-van der Pol system with  $a=96.326680$ ,  $c=-0.001$ ,  $d=25$ ,  $e=87.001$ ,  $f=0.018$  and  $g=9.5072$ .

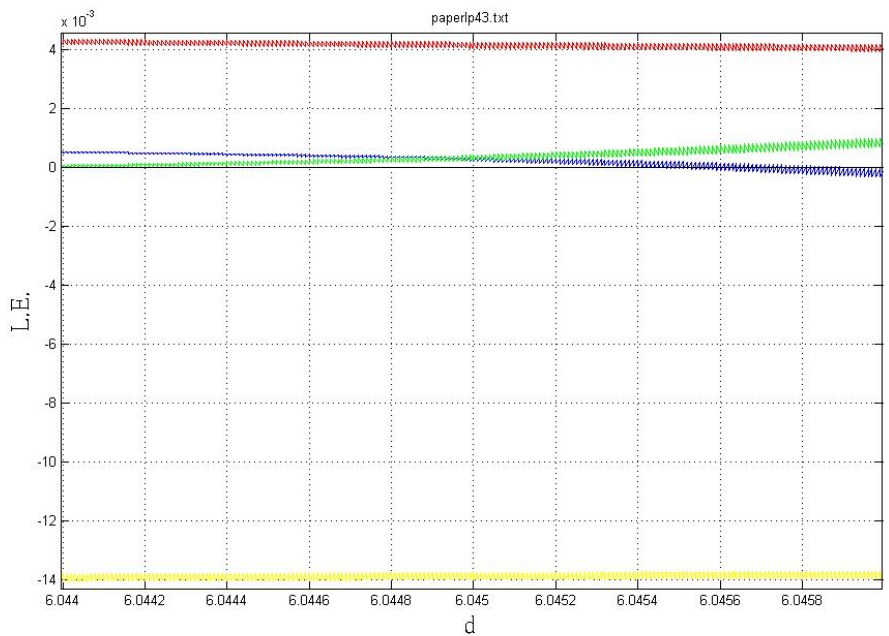


Fig.3- 6 Lyapunov exponents of Mathieu-van der Pol system with  $a=96.326680$ ,  $b=5.023$ ,  $c=-0.001$ ,  $e=87.001$ ,  $f=0.018$  and  $g=9.5072$ .

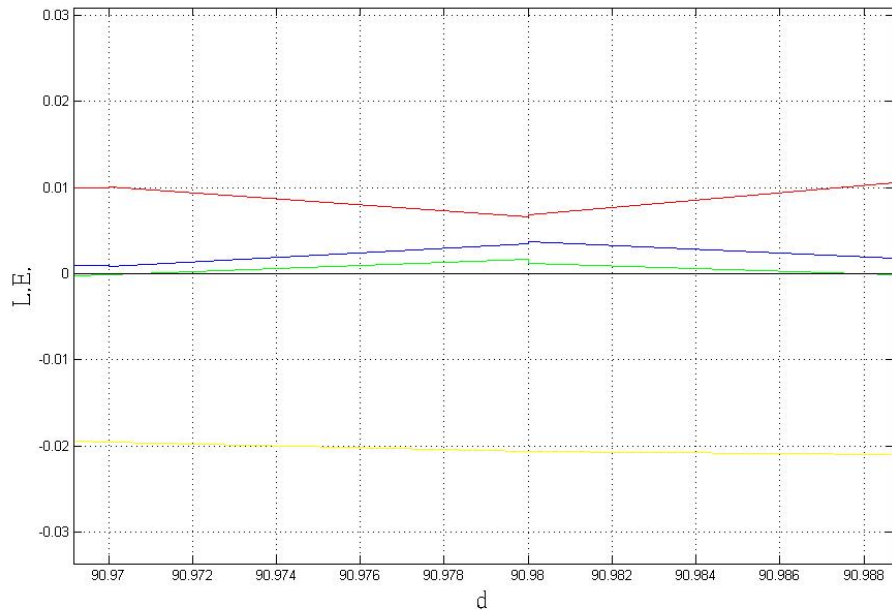


Fig.3- 7 Lyapunov exponents of Mathieu-van der Pol system with  $a=96.326680$ ,  $b=5.023$ ,  $c=-0.001$ ,  $e=87.001$ ,  $f=0.018$  and  $g=9.5072$ .

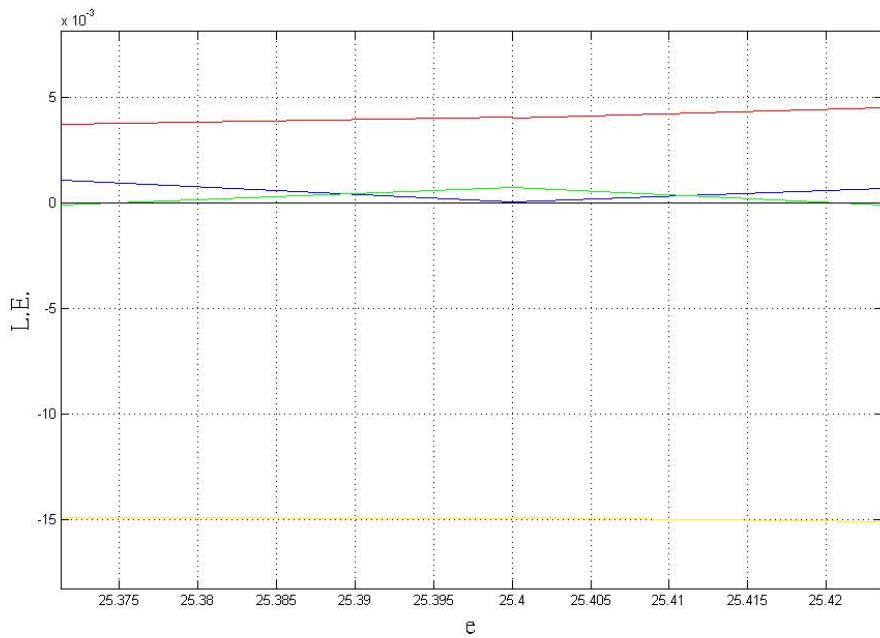


Fig.3- 8 Lyapunov exponents of Mathieu-van der Pol system with  $a=96.326680$ ,  $b=5.023$ ,  $c=-0.001$ ,  $d=25$ ,  $f=0.018$  and  $g=9.5072$ .



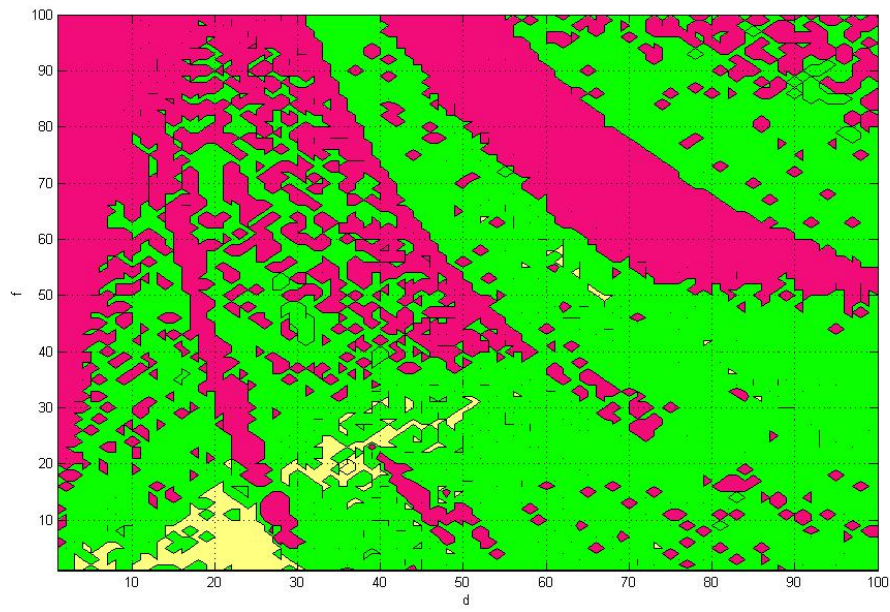
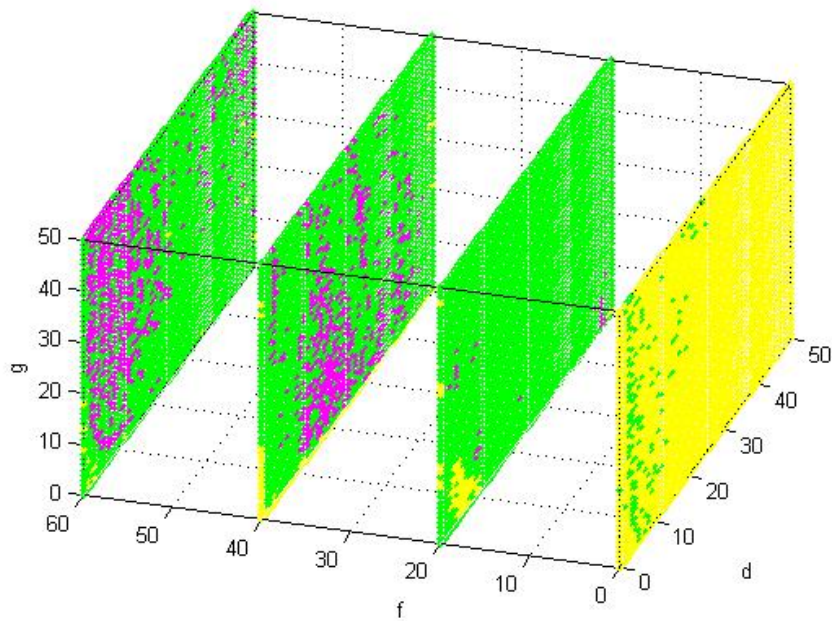
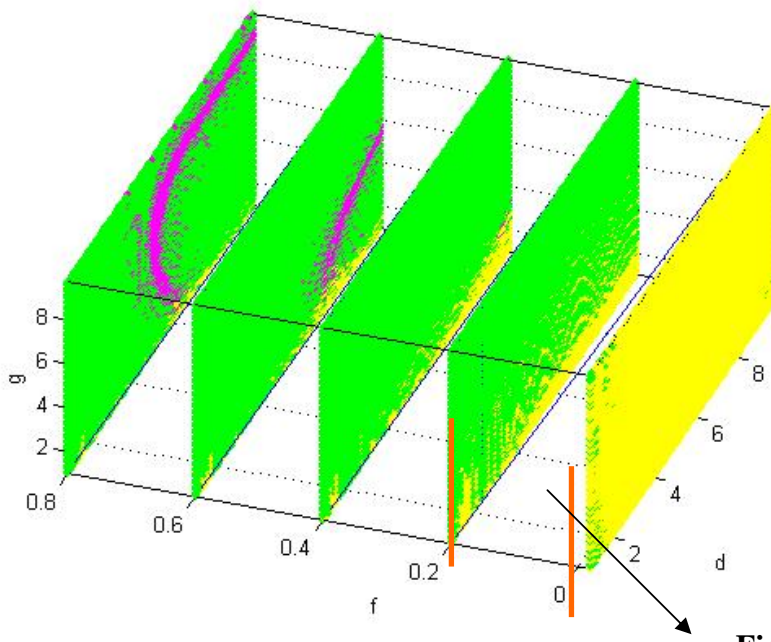


Fig.3- 9 Parameter diagrams of Mathieu-van der Pol system with  $a=96.326680$ ,  $b=5.023$ ,  $c=-0.001$ ,  $e=87.001$  and  $f=0.018$ .





**Fig. 3-11**

Fig.3- 10 2D Parameter diagrams varied with  $f$ .  $a=96.326680$ ,  $b=5.023$ ,  $c=-0.001$  and  $e=87.001$ . Part A and B are shown in Fig.7.

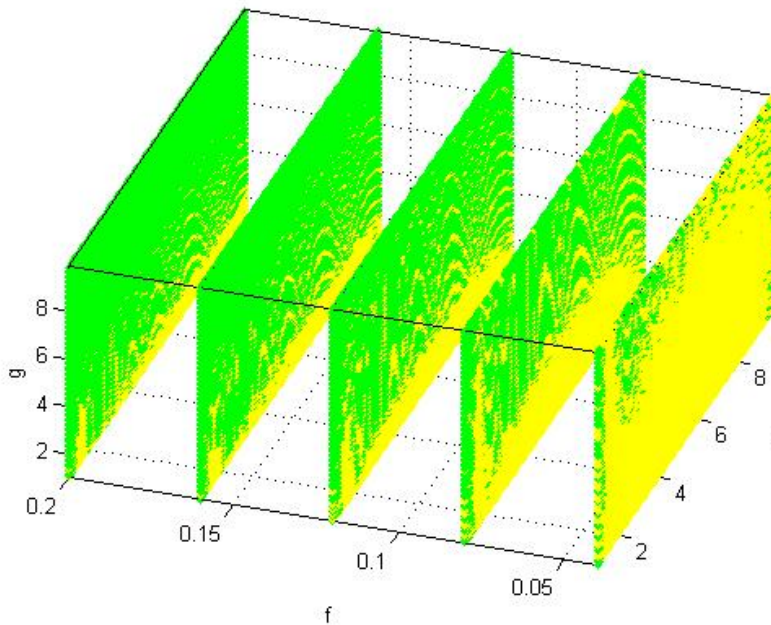


Fig.3- 11 2D Parameter diagrams varied with  $f$ .  $a=96.326680$ ,  $b=5.023$ ,  $c=-0.001$  and  $e=87.001$ . Part C are shown in Fig. 8.

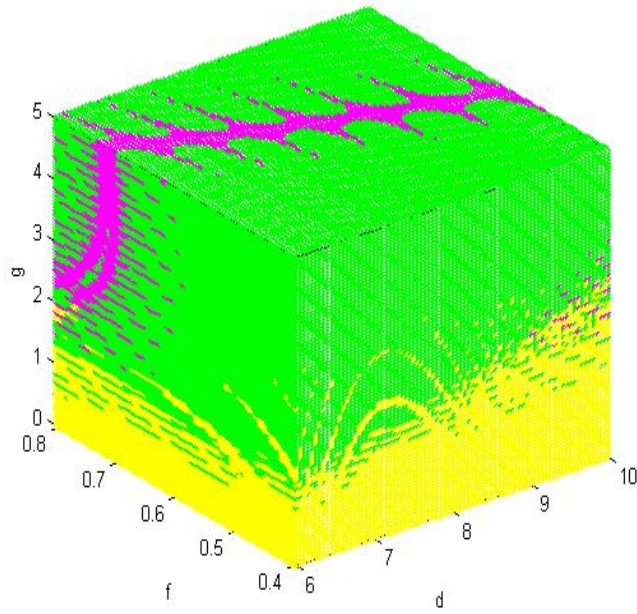


Fig.3- 12 3D Parameter diagrams of Mathieu-van der Pol system with  $a=96.326680$ ,  $b=5.023$ ,  $c=-0.001$  and  $e=87.001$ .

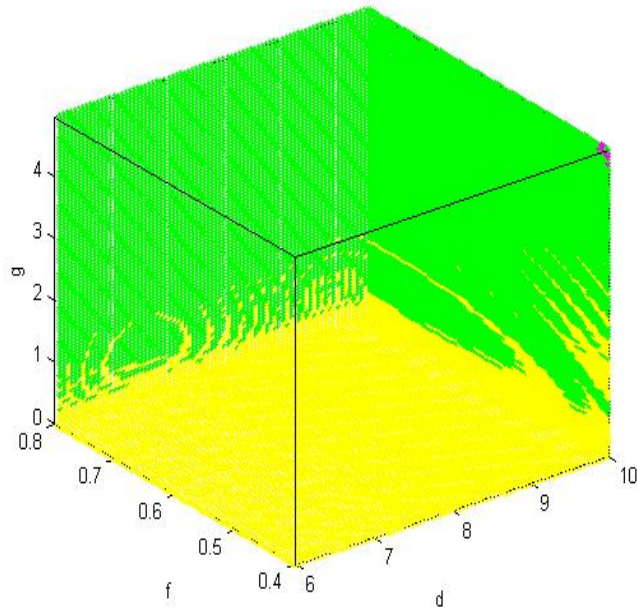


Fig.3- 13 3D Parameter diagrams of Mathieu-van der Pol system with  $a=96.326680$ ,  $b=5.023$ ,  $c=-0.001$  and  $e=87.001$ .

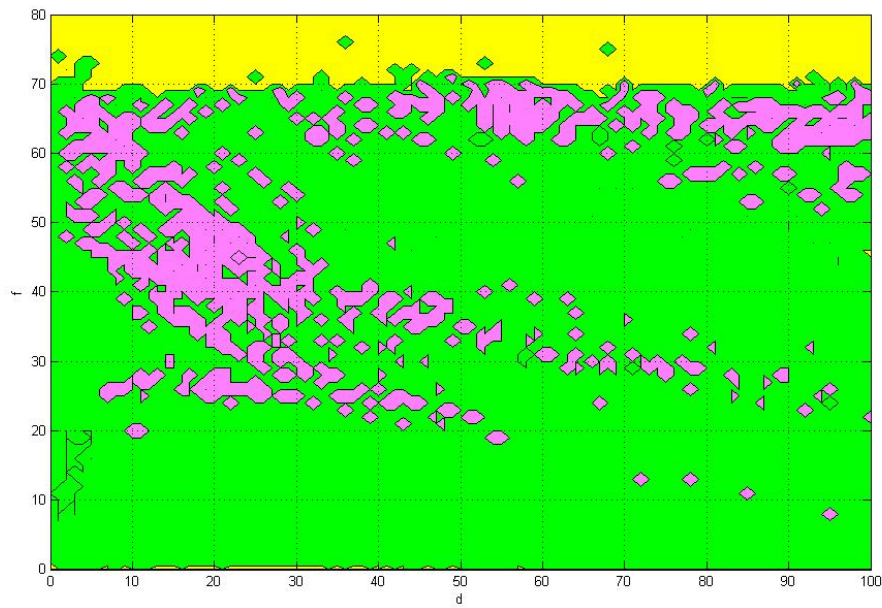


Fig.3- 14 Parameter diagrams of Mathieu-van der Pol system with  $a=96.326680$ ,  $b=5.023$ ,  $c=-0.001$ ,  $e=87.001$  and  $g=9.5072$ .

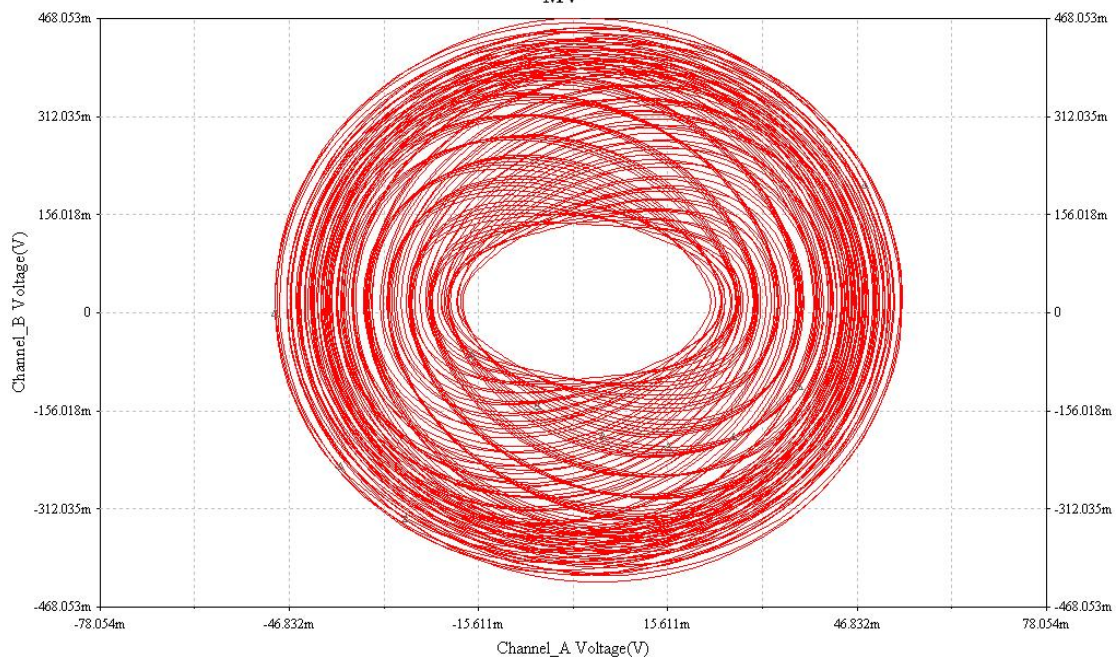


Fig.3- 15 Projection of phase portraits outputs in electronic circuit for Mathieu-van der Pol system.

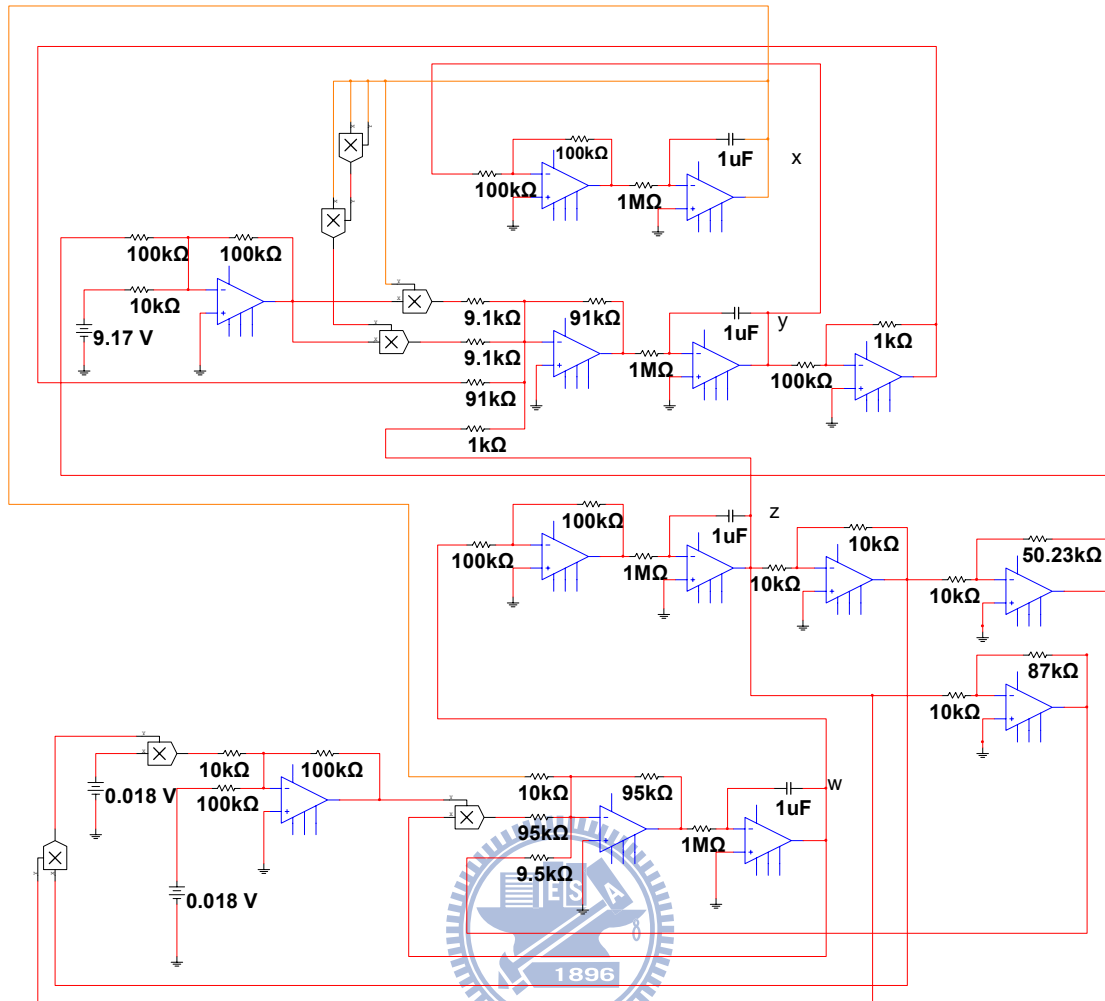


Fig.3- 16 The configuration of electronic circuit for chaotic Mathieu-van der Pol system.

# Chapter 4

## Chaos Control of New Mathieu-van der Pol Systems with New Mathieu -Duffing Systems as Goal System by GYC Partial Region Stability Theory

### 4.1 Preliminaries

In this Chapter, a new strategy by using GYC partial region stability theory is proposed to achieve chaos control. Via using the GYC partial region stability theory, the new Lyapunov function used is a simple linear homogeneous function of error states and the lower order controllers are much simpler and introduce less simulation error. Numerical simulations are given for new Mathieu-van der Pol system and new Mathieu-Duffing system to show the effectiveness of this strategy.



### 4.2 Chaos Control Scheme

Consider the following chaotic system

$$\dot{\mathbf{x}} = \mathbf{f}(t, \mathbf{x}) \quad (4-2-1)$$

where  $\mathbf{x} = [x_1, x_2, \dots, x_n]^T \in R^n$  is a the state vector,  $\mathbf{f} : R_+ \times R^n \rightarrow R^n$  is a vector function.

The goal system which can be either chaotic or regular, is

$$\dot{\mathbf{y}} = \mathbf{g}(t, \mathbf{y}) \quad (4-2-2)$$

where  $\mathbf{y} = [y_1, y_2, \dots, y_n]^T \in R^n$  is a state vector,  $\mathbf{g} : R_+ \times R^n \rightarrow R^n$  is a vector function.

In order to make the chaos state  $\mathbf{x}$  approaching the goal state  $\mathbf{y}$ , define  $\mathbf{e} = \mathbf{x} - \mathbf{y}$  as the state error. The chaos control is accomplished in the sense that

[13-22]:

$$\lim_{t \rightarrow \infty} \mathbf{e} = \lim_{t \rightarrow \infty} (\mathbf{x} - \mathbf{y}) = 0 \quad (4-2-3)$$

In this Chapter, we will use examples in which the error dynamics always happens in the first quadrant of coordinate system and use GYC partial region stability theory [43-44]. The Lyapunov function is a simple linear homogeneous function of error states and the controllers are simpler because they are in lower order than that of traditional controllers

### 4.3 New Chaotic Mathieu- Duffing System

Mathieu equation and Duffing equation are two typical nonlinear non-autonomous systems:

$$\begin{cases} \dot{z}_1 = z_2 \\ \dot{z}_2 = -(a_1 + b_1 \sin \omega t)z_1 - (a_1 + b_1 \sin \omega t)z_1^3 - c_1 z_2 + d_1 \sin \omega t \end{cases} \quad (4-3-1)$$

$$\begin{cases} \dot{z}_3 = z_4 \\ \dot{z}_4 = -z_3 - z_3^3 - e_1 z_4 + f_1 \sin \omega t \end{cases} \quad (4-3-2)$$

Exchanging  $\sin \omega t$  in Eq. (4-3-1) by  $z_3$  and  $\sin \omega t$  in Eq. (4-3-2) by  $z_1$ , we obtain the autonomous master new Mathieu-Duffing system:

$$\begin{cases} \dot{z}_1 = z_2 \\ \dot{z}_2 = -(a_1 + b_1 z_3)z_1 - (a_1 + b_1 z_3)z_1^3 - c_1 z_2 + d_1 z_3 \\ \dot{z}_3 = z_4 \\ \dot{z}_4 = -z_3 - z_3^3 - e_1 z_4 + f_1 z_1 \end{cases} \quad (4-3-3)$$

where  $a_1$ ,  $b_1$ ,  $c_1$ ,  $d_1$ ,  $e_1$  and  $f_1$  are uncertain parameters. This system exhibits chaos when the parameters of system are  $a_1 = 20.30$ ,  $b_1 = 0.5970$ ,  $c_1 = 0.005$ ,  $d_1 = -24.441$ ,  $e_1 = 0.002$ ,  $f_1 = 14.63$  and initial states is  $(-2, 10, -2, 10)$ . Its phase portraits are shown in Fig. 4-1.

### 4.4 Numerical Simulations

The following chaotic system

$$\begin{cases} \dot{x}_1 = x_2 - 200 \\ \dot{x}_2 = -(a + b(x_3 - 200))(x_1 - 200) - (a + b(x_3 - 200))(x_1 - 200)^3 \\ \quad - c(x_2 - 200) + d(x_3 - 200) \\ \dot{x}_3 = (x_4 - 200) \\ \dot{x}_4 = -e(x_3 - 200) + f(1 - (x_3 - 200)^2)(x_4 - 200) + g(x_1 - 200) \end{cases} \quad (4-4-1)$$

is the new Mathieu-van der Pol system of which the old origin is translated to  $(x_1, x_2, x_3, x_4) = (200, 200, 200, 200)$  in order that the error dynamics happens always in the first quadrant of error state coordinate system. This translated new Mathieu-van der Pol system presents chaotic motion when initial conditions is  $(x_{10}, x_{20}, x_{30}, x_{40}) = (210.1, 209.5, 210.1, 209.5)$  and the parameters are  $a = 10$ ,  $b = 3$ ,  $c = 0.4$ ,  $d = 70$ ,  $e = 1$ ,  $f = 5$ ,  $g = 0.1$ .

In order to lead  $(x_1, x_2, x_3, x_4)$  to the goal, we add control terms  $u_1, u_2, u_3$  and  $u_4$  to each equation of Eq. (4-4-1), respectively.

$$\begin{cases} \dot{x}_1 = x_2 - 200 + u_1 \\ \dot{x}_2 = -(a + b(x_3 - 200))(x_1 - 200) - (a + b(x_3 - 200))(x_1 - 200)^3 \\ \quad - c(x_2 - 200) + d(x_3 - 200) + u_2 \\ \dot{x}_3 = (x_4 - 200) + u_3 \\ \dot{x}_4 = -e(x_3 - 200) + f(1 - (x_3 - 200)^2)(x_4 - 200) + g(x_1 - 200) + u_4 \end{cases} \quad (4-4-2)$$

**CASE I.** Control the chaotic motion to zero.

In this case we will control the chaotic motion of the new Mathieu-van der Pol system (4-4-1) to zero. The goal is  $y = 0$ . The state error is  $e_i = x_i - y_i = x_i$ , ( $i=1, 2, 3, 4$ ) and error dynamics becomes

$$\begin{cases} \dot{e}_1 = \dot{x}_1 = x_2 - 200 + u_1 \\ \dot{e}_2 = \dot{x}_2 = -(a + b(x_3 - 200))(x_1 - 200) - (a + b(x_3 - 200))(x_1 - 200)^3 \\ \quad - c(x_2 - 200) + d(x_3 - 200) + u_2 \\ \dot{e}_3 = \dot{x}_3 = (x_4 - 200) + u_3 \\ \dot{e}_4 = \dot{x}_4 = -e(x_3 - 200) + f(1 - (x_3 - 200)^2)(x_4 - 200) + g(x_1 - 200) + u_4 \end{cases} \quad (4-4-3)$$



In Fig. 4-2, we can see that the error dynamics always exists in first quadrant.

By GYC partial region asymptotical stability theorem, one can easily choose a Lyapunov function in the form of a positive definite function in first quadrant as:

$$V = e_1 + e_2 + e_3 + e_4 \quad (4-4-4)$$

Its time derivative through error dynamics (4-4-3) is

$$\begin{aligned} \dot{V} &= \dot{e}_1 + \dot{e}_2 + \dot{e}_3 + \dot{e}_4 \\ &= (x_2 - 200 + u_1) + (-(a + b(x_3 - 200))(x_1 - 200) \\ &\quad - (a + b(x_3 - 200))(x_1 - 200)^3 - c(x_2 - 200) + d(x_3 - 200) + u_2) \\ &\quad + (x_4 - 200 + u_3) + (-e(x_3 - 200) + f(1 - (x_3 - 200)^2)(x_4 - 200) \\ &\quad + g(x_1 - 200) + u_4) \end{aligned} \quad (4-4-5)$$

Choose

$$\begin{aligned} u_1 &= -(x_2 - 200) - e_1 \\ u_2 &= (-(a + b(x_3 - 200))(x_1 - 200) - (a + b(x_3 - 200))(x_1 - 200)^3 \\ &\quad - c(x_2 - 200) + d(x_3 - 200)) - e_2 \\ u_3 &= -(x_4 - 200) - e_3 \\ u_4 &= (-e(x_3 - 200) + f(1 - (x_3 - 200)^2)(x_4 - 200) \\ &\quad + g(x_1 - 200)) - e_4 \end{aligned} \quad (4-4-6)$$

We obtain

$$\dot{V} = -e_1 - e_2 - e_3 - e_4 < 0$$

which is negative definite function in first quadrant. The numerical results are shown in Fig.4-3. After 10 sec, the error trajectories approach the origin.

*CASE II.* Control the chaotic motion to a regular function.

In this case we will control the chaotic motion of the new Mathieu-van der Pol system (4-4-1) to regular function of time. The goal is  $y_i = F_i e^{\sin \omega t}$ , ( $i=1, 2, 3, 4$ ). The error equation

$$e_i = x_i - y_i = x_i - F_i e^{\sin \omega t}, \quad (i=1, 2, 3, 4) \quad (4-4-7)$$

$$\lim_{t \rightarrow \infty} e_i = \lim_{t \rightarrow \infty} (x_i - F_i e^{\sin \omega t}) = 0, \quad (i=1, 2, 3, 4)$$

where  $F_1 = F_2 = F_3 = F_4 = F = 10$  and  $\omega = 0.5$

The error dynamics is

$$\begin{cases} \dot{e}_1 = x_2 - 200 + u_1 - F_1 \omega e^{\sin \omega t} (\cos \omega t) \\ \dot{e}_2 = -(a + b(x_3 - 200))(x_1 - 200) - (a + b(x_3 - 200))(x_1 - 200)^3 \\ \quad - c(x_2 - 200) + d(x_3 - 200) + u_2 - F_2 \omega e^{\sin \omega t} (\cos \omega t) \\ \dot{e}_3 = (x_4 - 200) + u_3 - F_3 \omega e^{\sin \omega t} (\cos \omega t) \\ \dot{e}_4 = -e(x_3 - 200) + f(1 - (x_3 - 200)^2)(x_4 - 200) + g(x_1 - 200) \\ \quad + u_4 - F_4 \omega e^{\sin \omega t} (\cos \omega t) \end{cases} \quad (4-4-8)$$

In Fig. 4-4, the error dynamics always exists in first quadrant.

By GYC partial region asymptotical stability theorem, one can easily choose a Lyapunov function in the form of a positive definite function in first quadrant as:

$$V = e_1 + e_2 + e_3 + e_4$$

Its time derivative is

$$\begin{aligned} \dot{V} = \dot{e}_1 + \dot{e}_2 + \dot{e}_3 + \dot{e}_4 = & (x_2 - 200 + u_1 - F_1 \omega e^{\sin \omega t} (\cos \omega t)) \\ & + (-(a + b(x_3 - 200))(x_1 - 200) - (a + b(x_3 - 200))(x_1 - 200)^3 \\ & - c(x_2 - 200) + d(x_3 - 200) + u_2 - F_2 \omega e^{\sin \omega t} (\cos \omega t)) \\ & + ((x_4 - 200) + u_3 - F_3 \omega e^{\sin \omega t} (\cos \omega t)) \\ & + (-e(x_3 - 200) + f(1 - (x_3 - 200)^2)(x_4 - 200) + g(x_1 - 200) \\ & + u_4 - F_4 \omega e^{\sin \omega t} (\cos \omega t)) \end{aligned} \quad (4-4-9)$$

Choose

$$\begin{aligned} u_1 = & -(x_2 - 200 - F_1 \omega e^{\sin \omega t} (\cos \omega t)) - e_1 \\ u_2 = & -(-(a + b(x_3 - 200))(x_1 - 200) - (a + b(x_3 - 200))(x_1 - 200)^3 \\ & - c(x_2 - 200) + d(x_3 - 200) - F_2 \omega e^{\sin \omega t} (\cos \omega t)) - e_2 \\ u_3 = & -((x_4 - 200) - F_3 \omega e^{\sin \omega t} (\cos \omega t)) - e_3 \\ u_4 = & -(-e(x_3 - 200) + f(1 - (x_3 - 200)^2)(x_4 - 200) + g(x_1 - 200) \\ & - F_4 \omega e^{\sin \omega t} (\cos \omega t)) - e_4 \end{aligned} \quad (4-4-10)$$

We obtain

$$\dot{V} = -e_1 - e_2 - e_3 - e_4 < 0$$

which is a negative definite function in first quadrant. The numerical results are

shown in Fig.4-5 and Fig. 4-6. After 10 sec., the errors approach zero and the chaotic trajectories approach to regular motion.

*CASE III.* Control the chaotic motion of the new Mathieu-van der Pol system to chaotic motion of the new Mathieu-Duffing system.

In this case we will control chaotic motion of the new Mathieu-van der Pol system (4-4-1) to that of following goal system, i.e. the new chaotic Mathieu-Duffing system with initial states  $(-2, 10, -2, 10)$ , system parameters  $a_1 = 20.30$ ,  $b_1 = 0.5970$ ,  $c_1 = 0.005$ ,  $d_1 = -24.441$ ,  $e_1 = 0.002$  and  $f_1 = 14.63$ .

$$\begin{cases} \dot{z}_1 = z_2 \\ \dot{z}_2 = -(a_1 + b_1 z_3)z_1 - (a_1 + b_1 z_3)z_1^3 - c_1 z_2 + d_1 z_3 \\ \dot{z}_3 = z_4 \\ \dot{z}_4 = -z_3 - z_3^3 - e_1 z_4 + f_1 z_1 \end{cases} \quad (4-4-11)$$

The error equation is  $e_i = x_i - z_i$ , ( $i=1, 2, 3, 4$ ). Our aim is  $\lim_{t \rightarrow \infty} e_i = 0$  ( $i=1, 2, 3, 4$ ).

The error dynamics becomes

$$\begin{cases} \dot{e}_1 = \dot{x}_1 - \dot{z}_1 = (x_2 - 200 - z_2) + u_1 \\ \dot{e}_2 = \dot{x}_2 - \dot{z}_2 = -(a + b(x_3 - 200))(x_1 - 200) - (a + b(x_3 - 200))(x_1 - 200)^3 \\ \quad - c(x_2 - 200) + d(x_3 - 200) - (-(a_1 + b_1 z_3)z_1 - (a_1 + b_1 z_3)z_1^3 \\ \quad - c_1 z_2 + d_1 z_3)) + u_2 \\ \dot{e}_3 = \dot{x}_3 - \dot{z}_3 = (x_4 - 200 - z_4) + u_3 \\ \dot{e}_4 = \dot{x}_4 - \dot{z}_4 = (-e(x_3 - 200) + f(1 - (x_3 - 200)^2))(x_4 - 200) + g(x_1 - 200) \\ \quad - (-z_3 - z_3^3 - e_1 z_4 + f_1 z_1)) + u_4 \end{cases} \quad (4-4-12)$$

In Fig. 4-7, the error dynamics always exists in first quadrant.

By GYC partial region asymptotical stability theorem, one can easily choose a Lyapunov function in the form of a positive definite function in first quadrant as:

$$V = e_1 + e_2 + e_3 + e_4$$

Its time derivative is

$$\begin{aligned}
\dot{V} = \dot{e}_1 + \dot{e}_2 + \dot{e}_3 + \dot{e}_4 = & ((x_2 - 200 - z_2) + u_1) \\
& + ((-(a + b(x_3 - 200))(x_1 - 200) - (a + b(x_3 - 200))(x_1 - 200))^3 \\
& - c(x_2 - 200) + d(x_3 - 200) - (-(a_1 + b_1 z_3)z_1 - (a_1 + b_1 z_3)z_1^3 \\
& - c_1 z_2 + d_1 z_3)) + u_2) + ((x_4 - 200 - z_4) + u_3) \\
& + ((-e(x_3 - 200) + f(1 - (x_3 - 200)^2)(x_4 - 200) + g(x_1 - 200) \\
& - (-z_3 - z_3^3 - e_1 z_4 + f_1 z_1)) + u_4)
\end{aligned} \tag{4-4-13}$$

Choose

$$\begin{aligned}
u_1 = & -(x_2 - 200 - z_2) - e_1 \\
u_2 = & -(-(a + b(x_3 - 200))(x_1 - 200) - (a + b(x_3 - 200))(x_1 - 200))^3 \\
& - c(x_2 - 200) + d(x_3 - 200) - (-(a_1 + b_1 z_3)z_1 - (a_1 + b_1 z_3)z_1^3 \\
& - c_1 z_2 + d_1 z_3)) - e_2 \\
u_3 = & -(x_4 - 200 - z_4) - e_3 \\
u_4 = & -(-e(x_3 - 200) + f(1 - (x_3 - 200)^2)(x_4 - 200) + g(x_1 - 200) \\
& - (-z_3 - z_3^3 - e_1 z_4 + f_1 z_1)) - e_4
\end{aligned} \tag{4-4-14}$$

We obtain

$$\dot{V} = -e_1 - e_2 - e_3 - e_4 < 0$$

which is negative definite function in first quadrant. The numerical results are shown in Fig.4-8 and Fig. 4-9. After 10 sec., the errors approach zero and the chaotic trajectories of the new Mathieu-van der Pol system approach to that of the new Mathieu-Duffing system.

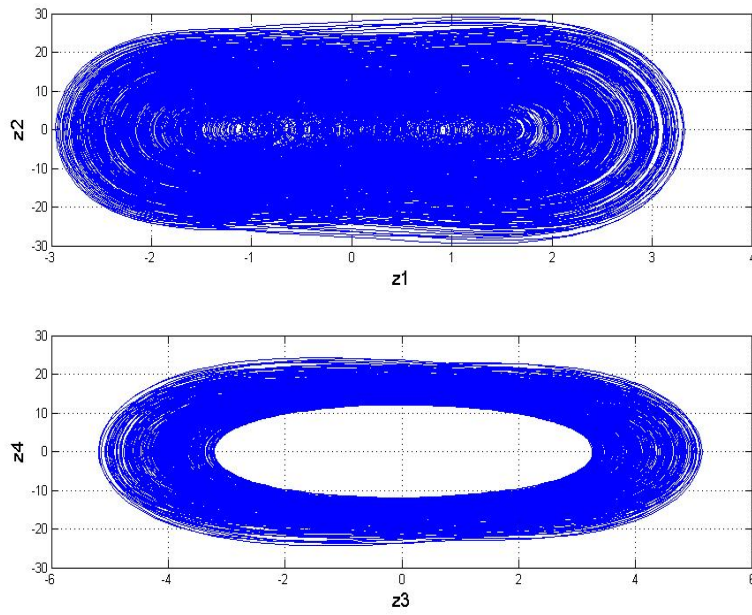


Fig. 4-1 Chaotic phase portrait projections for new Mathieu-Duffing system.

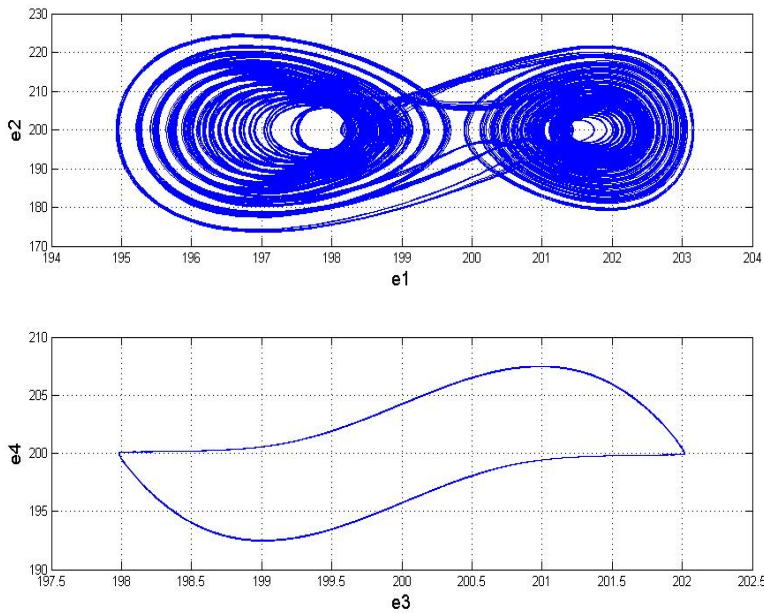


Fig. 4-2 Phase portrait projections of error dynamics for Case I.

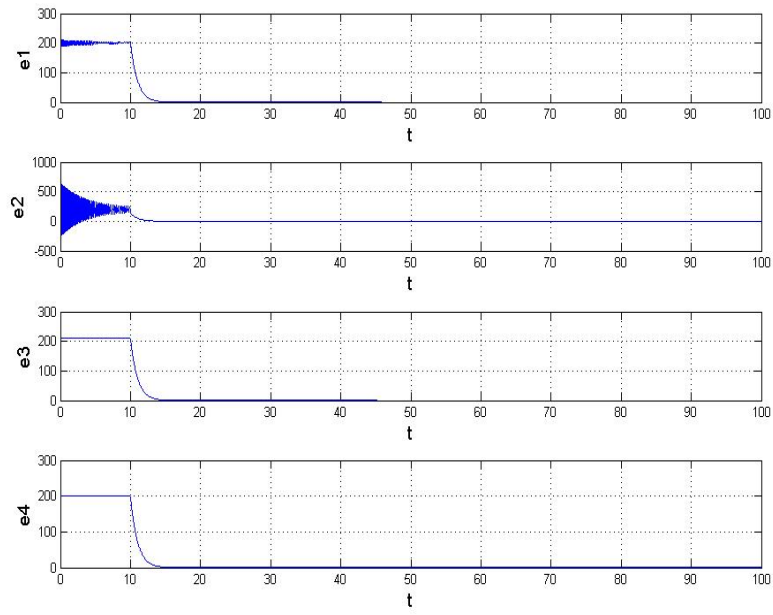


Fig. 4-3 Time histories of errors for Case I.

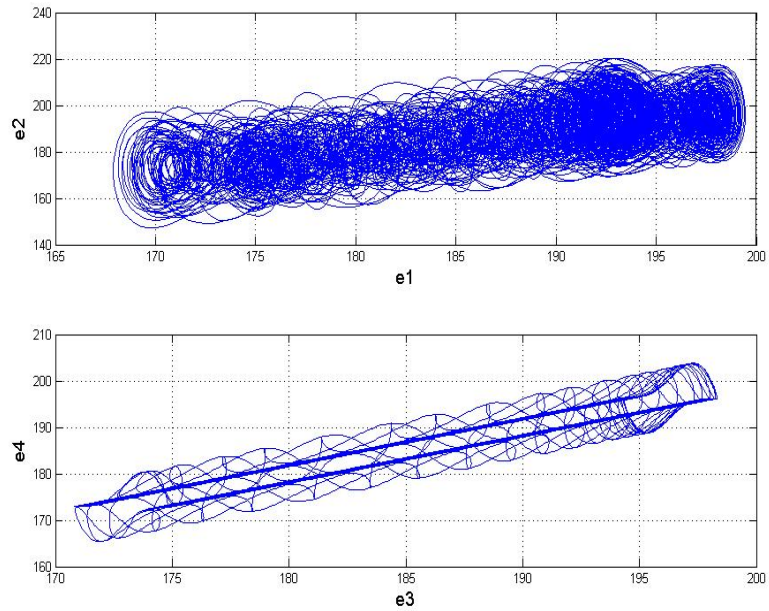


Fig. 4-4 Phase portrait projections of error dynamics for Case II.

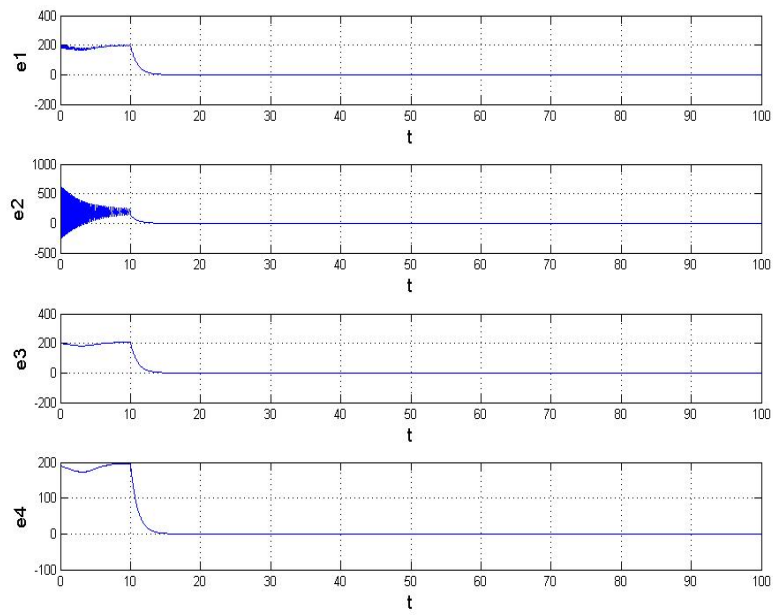


Fig. 4-5 Time histories of errors for Case II.

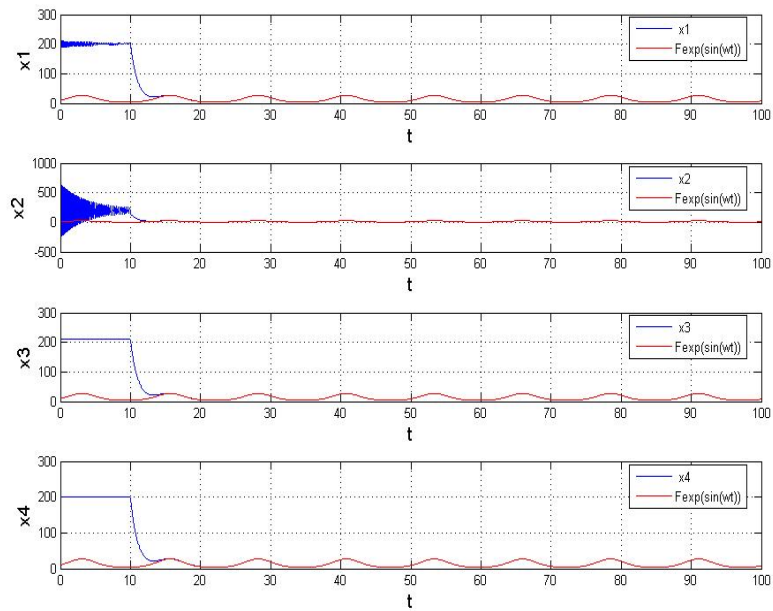


Fig. 4-6 Time histories of  $x_1$ ,  $x_2$ ,  $x_3$ ,  $x_4$  for Case II.

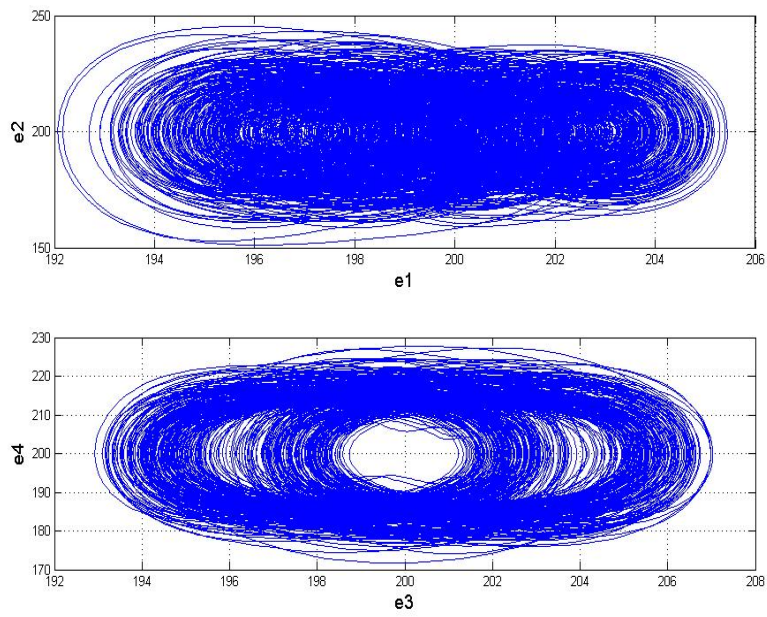


Fig. 4-7 Phase portrait projections of error dynamics for Case III.

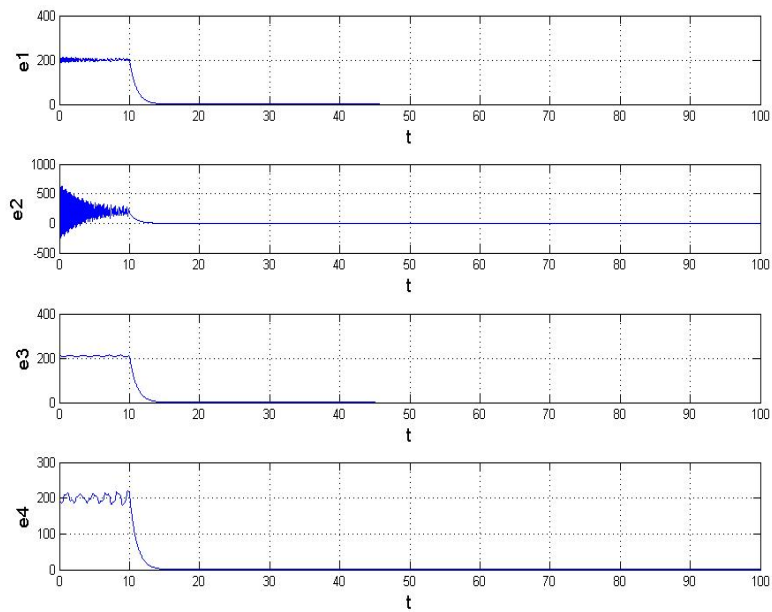
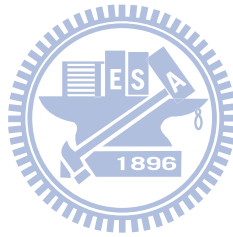


Fig. 4-8 Time histories of errors for Case III.



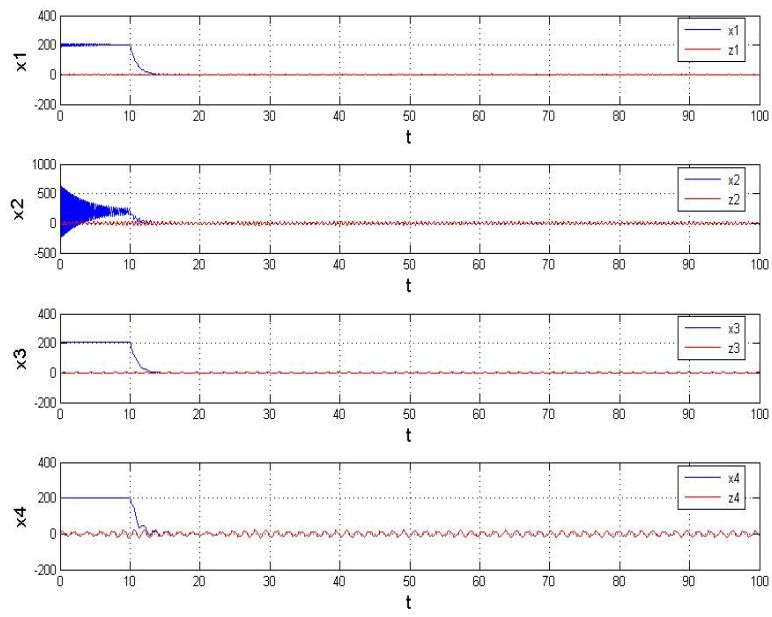
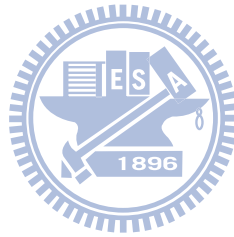


Fig. 4-9 Time histories of  $x_1$ ,  $x_2$ ,  $x_3$ ,  $x_4$  and  $z_1$ ,  $z_2$ ,  $z_3$ ,  $z_4$  for Case III.



# Chapter 5

## Generalized Chaos Synchronization of New Mathieu-van der Pol Systems with New Duffing-van der Pol systems as Functional system by GYC Partial Region Stability Theory

### 5.1 Preliminaries

In this Chapter, a new strategy by using GYC partial region stability theory is proposed to achieve generalized chaos synchronization. Via using the GYC partial region stability theory, the new Lyapunov function used is a simple linear homogeneous function of states and the lower order controllers are much more simple and introduce less simulation error. Numerical simulations are given for new Mathieu-van der Pol system and new Duffing-van der Pol system to show the effectiveness of this strategy.



### 5.2 Generalized Chaos Synchronization Strategy

Consider the following unidirectional coupled chaotic systems

$$\begin{aligned}\dot{\mathbf{x}} &= \mathbf{f}(t, \mathbf{x}) \\ \dot{\mathbf{y}} &= \mathbf{h}(t, \mathbf{y}) + \mathbf{u}\end{aligned}\tag{5-2-1}$$

where  $\mathbf{x} = [x_1, x_2, \dots, x_n]^T \in R^n$ ,  $\mathbf{y} = [y_1, y_2, \dots, y_n]^T \in R^n$  denote the master state vector and slave state vector respectively,  $\mathbf{f}$  and  $\mathbf{h}$  are nonlinear vector functions, and  $\mathbf{u} = [u_1, u_2, \dots, u_n]^T \in R^n$  is a control input vector.

The generalized synchronization can be accomplished when  $t \rightarrow \infty$ , the limit of the error vector  $\mathbf{e} = [e_1, e_2, \dots, e_n]^T$  approaches zero:

$$\lim_{t \rightarrow \infty} \mathbf{e} = 0\tag{5-2-2}$$

where

$$\mathbf{e} = \mathbf{G}(\mathbf{x}) - \mathbf{y} \quad (5-2-3)$$

$\mathbf{G}(\mathbf{x})$  is a given function of  $\mathbf{x}$ .

By using the partial region stability theory [50-51], the Lyapunov function is easier to find, since the linear homogenous terms of the entries of  $\mathbf{e}$  can be used to construct the definite Lyapunov function and the controllers can be designed in lower order.

### 5.3 New Chaotic Duffing-van der Pol System

Duffing equation and van der Pol equation are two typical nonlinear non-autonomous systems:

$$\begin{cases} \dot{z}_1 = z_2 \\ \dot{z}_2 = -z_1 - z_1^3 - hz_2 + i \sin \omega t \end{cases} \quad (5-3-1)$$

$$\begin{cases} \dot{z}_3 = z_4 \\ \dot{z}_4 = -jz_3 - k(1 - z_3^2)z_4 + l \sin \omega t \end{cases} \quad (5-3-2)$$

Exchanging  $\sin \omega t$  in Eq. (5-3-1) by  $z_3$  and  $\sin \omega t$  in Eq. (5-3-2) by  $z_1$ , we obtain the autonomous master new Duffing-van der Pol system:

$$\begin{cases} \dot{z}_1 = z_2 \\ \dot{z}_2 = -z_1 - z_1^3 - hz_2 + iz_3 \\ \dot{z}_3 = z_4 \\ \dot{z}_4 = -jz_3 + k(1 - z_3^2)z_4 + lz_1 \end{cases} \quad (5-3-3)$$

where  $h, i, j, k, l$  are uncertain parameter. This system exhibits chaos when the parameters of system are  $h = 0.0006, j = 1, k = 5, i = 0.67$  and  $l = 0.05$  and initial states is  $(2, 2.4, 5, 6)$ , its phase portraits projections and Lyapunov exponents as shown in Fig. 5-1 and 5-2.

### 5.4 Numerical Simulations

The two unidirectional coupled new chaotic Mathieu-van der pol systems are

shown as follows:

$$\begin{aligned}
\dot{x}_1 &= x_2 \\
\dot{x}_2 &= -(a + bx_3)x_1 - (a + bx_3)x_1^3 - cx_2 + dx_3 \\
\dot{x}_3 &= x_4 \\
\dot{x}_4 &= -ex_3 + f(1 - x_3^2)x_4 + gx_1 \\
\dot{y}_1 &= y_2 + u_1 \\
\dot{y}_2 &= -(a + by_3)y_1 - (a + by_3)y_1^3 - cy_2 + dy_3 + u_2 \\
\dot{y}_3 &= y_4 + u_3 \\
\dot{y}_4 &= -ey_3 + f(1 - y_3^2)y_4 + gy_1 + u_4
\end{aligned} \tag{5-4-1}$$

*CASE I.* The generalized synchronization error function is  $e_i = (x_i - y_i + 100)$ , ( $i=1, 2, 3, 4$ ).

The addition of 100 makes the error dynamics always happens in first quadrant.

Our goal is  $y_i = x_i + 100$ , i.e.

$$\lim_{t \rightarrow \infty} e_i = \lim_{t \rightarrow \infty} (x_i - y_i + 100) = 0 \quad (i=1, 2, 3, 4) \tag{5-4-2}$$

The error dynamics becomes:

$$\begin{aligned}
\dot{e}_1 &= \dot{x}_1 - \dot{y}_1 = x_2 - y_2 - u_1 \\
\dot{e}_2 &= \dot{x}_2 - \dot{y}_2 = -((a + bx_3)x_1 - (a + by_3)y_1) - ((a + bx_3)x_1^3 - (a + by_3)y_1^3) \\
&\quad - c(x_2 - y_2) + d(x_3 - y_3) - u_2 \\
\dot{e}_3 &= \dot{x}_3 - \dot{y}_3 = x_4 - y_4 - u_3 \\
\dot{e}_4 &= \dot{x}_4 - \dot{y}_4 = -e(x_3 - y_3) + f((1 - x_3^2)x_4 - (1 - y_3^2)y_4) + g(x_1 - y_1) - u_4
\end{aligned} \tag{5-4-3}$$

System parameters are chosen as  $a = 10$ ,  $b = 3$ ,  $c = 0.4$ ,  $d = 70$ ,  $e = 1$ ,  $f = 5$ ,  $g = 0.1$  and initial states are  $(x_{10}, x_{20}, x_{30}, x_{40}) = (0.1, -0.5, 0.1, -0.5)$ ,  $(y_{10}, y_{20}, y_{30}, y_{40}) = (0.3, -0.1, 0.3, -0.1)$ . Before control action, the error dynamics always happens in first quadrant as shown in Fig. 5-3. By GYC partial region stability, one can choose a Lyapunov function in the form of a positive definite function in first quadrant:

$$V = e_1 + e_2 + e_3 + e_4 \tag{5-4-4}$$

Its time derivative through Eq. (5-4-2) is

$$\begin{aligned}\dot{V} &= \dot{e}_1 + \dot{e}_2 + \dot{e}_3 + \dot{e}_4 \\ &= (x_2 - y_2 - u_1) + (-((a + bx_3)x_1 - (a + by_3)y_1) - ((a + bx_3)x_1^3 \\ &\quad - (a + by_3)y_1^3) - c(x_2 - y_2) + d(x_3 - y_3) - u_2) + (x_4 - y_4 - u_3) \\ &\quad + (-e(x_3 - y_3) + f((1 - x_3^2)x_4 - (1 - y_3^2)y_4) + g(x_1 - y_1) - u_4)\end{aligned}\quad (5-4-5)$$

Choose

$$\begin{aligned}u_1 &= (x_2 - y_2) + e_1 \\ u_2 &= (-((a + bx_3)x_1 - (a + by_3)y_1) - ((a + bx_3)x_1^3 - (a + by_3)y_1^3) \\ &\quad - c(x_2 - y_2) + d(x_3 - y_3)) + e_2 \\ u_3 &= (x_4 - y_4) + e_3 \\ u_4 &= (-e(x_3 - y_3) + f((1 - x_3^2)x_4 - (1 - y_3^2)y_4) + g(x_1 - y_1)) + e_4\end{aligned}\quad (5-4-6)$$

We obtain

$$\dot{V} = -e_1 - e_2 - e_3 - e_4 < 0 \quad (5-4-7)$$

which is negative definite function in the first quadrant. Four state errors versus time and time histories of states are shown in Fig. 5-4 and Fig. 5-5.

*CASE II.* The generalized synchronization error function is  $e_i = (x_i - y_i + F_i \sin \omega t + 100)$ , ( $i=1, 2, 3, 4$ ).

The addition of 100 makes the error dynamics always happens in first quadrant.

Our goal is  $y_i = x_i + F_i \sin \omega t + 100$ , i.e.

$$\lim_{t \rightarrow \infty} e_i = \lim_{t \rightarrow \infty} (x_i - y_i + F_i \sin \omega t + 100) = 0 \quad (i=1, 2, 3, 4). \quad (5-4-8)$$

where  $F_1 = F_2 = F_3 = F_4 = F = 10$ ,  $\omega = 0.5$ .

The error dynamics becomes

$$\begin{aligned}\dot{e}_1 &= x_2 - y_2 - u_1 + F \sin \omega t \\ \dot{e}_2 &= (-((a + bx_3)x_1 - (a + by_3)y_1) - ((a + bx_3)x_1^3 - (a + by_3)y_1^3) \\ &\quad - c(x_2 - y_2) + d(x_3 - y_3) - u_2 + F \sin \omega t \\ \dot{e}_3 &= x_4 - y_4 - u_3 + F \sin \omega t \\ \dot{e}_4 &= -e(x_3 - y_3) + f((1 - x_3^2)x_4 - (1 - y_3^2)y_4) + g(x_1 - y_1) - u_4 + F \sin \omega t\end{aligned}\quad (5-4-9)$$

System parameters are chosen as  $a = 10$ ,  $b = 3$ ,  $c = 0.4$ ,  $d = 70$ ,  $e = 1$ ,  $f = 5$ ,

$g = 0.1$  and initial states are  $(x_{10}, x_{20}, x_{30}, x_{40}) = (0.1, -0.5, 0.1, -0.5)$ ,  $(y_{10}, y_{20}, y_{30}, y_{40}) = (0.3, -0.1, 0.3, -0.1)$ . Before control action, the error dynamics always happens in first quadrant as shown in Fig. 5-6. By GYC partial region stability, one can choose a Lyapunov function in the form of a positive definite function in first quadrant:

$$V = e_1 + e_2 + e_3 + e_4 \quad (5-4-10)$$

Its time derivative through Eq. (5-4-8) is

$$\begin{aligned} \dot{V} &= \dot{e}_1 + \dot{e}_2 + \dot{e}_3 + \dot{e}_4 \\ &= (x_2 - y_2 - u_1 + F\omega \cos \omega t) + (-((a + bx_3)x_1 - (a + by_3)y_1) - ((a + bx_3)x_1^3 \\ &\quad - (a + by_3)y_1^3) - c(x_2 - y_2) + d(x_3 - y_3) - u_2 + F\omega \cos \omega t) + (x_4 - y_4 - u_3 \\ &\quad + F\omega \cos \omega t) + (-e(x_3 - y_3) + f((1 - x_3^2)x_4 - (1 - y_3^2)y_4) + g(x_1 - y_1) \\ &\quad - u_4 + F\omega \cos \omega t) \end{aligned} \quad (5-4-11)$$

Choose

$$\begin{aligned} u_1 &= (x_2 - y_2) + F\omega \cos \omega t + e_1 \\ u_2 &= (-((a + bx_3)x_1 - (a + by_3)y_1) - ((a + bx_3)x_1^3 - (a + by_3)y_1^3) \\ &\quad - c(x_2 - y_2) + d(x_3 - y_3)) + F\omega \cos \omega t + e_2 \\ u_3 &= (x_4 - y_4) + F\omega \cos \omega t + e_3 \\ u_4 &= (-e(x_3 - y_3) + f((1 - x_3^2)x_4 - (1 - y_3^2)y_4) + g(x_1 - y_1)) + F\omega \cos \omega t + e_4 \end{aligned} \quad (5-4-12)$$

We obtain

$$\dot{V} = -e_1 - e_2 - e_3 - e_4 < 0 \quad (5-4-13)$$

which is a negative definite function in the first quadrant. Four state errors versus time and time histories of  $x_i - y_i + 100$  and  $-F_i \sin \omega t$  are shown in Fig. 5-7 and Fig. 5-8.

*CASE III.* The generalized synchronization error function is

$$e_i = x_i - y_i + F_i e^{\sin \omega t} + 100, \quad (i=1, 2, 3, 4).$$

The addition of 100 makes the error dynamics always happens in first quadrant.

Our goal is  $y_i = x_i + F_i e^{\sin \omega t} + 100$ , i.e.

$$\lim_{t \rightarrow \infty} e_i = \lim_{t \rightarrow \infty} (x_i - y_i + F_i e^{\sin \omega t} + 100) = 0 \quad (i=1, 2, 3, 4). \quad (5-4-14)$$

The error dynamics becomes

$$\begin{aligned} \dot{e}_1 &= x_2 - y_2 - u_1 + F e^{\sin \omega t} \\ \dot{e}_2 &= -((a + bx_3)x_1 - (a + by_3)y_1) - ((a + bx_3)x_1^3 - (a + by_3)y_1^3) \\ &\quad - c(x_2 - y_2) + d(x_3 - y_3) - u_2 + F e^{\sin \omega t} \\ \dot{e}_3 &= x_4 - y_4 - u_3 + F e^{\sin \omega t} \\ \dot{e}_4 &= -e(x_3 - y_3) + f((1 - x_3^2)x_4 - (1 - y_3^2)y_4) + g(x_1 - y_1) - u_4 + F e^{\sin \omega t} \end{aligned} \quad (5-4-15)$$

System parameters are chosen as  $a = 10$ ,  $b = 3$ ,  $c = 0.4$ ,  $d = 70$ ,  $e = 1$ ,  $f = 5$ ,  $g = 0.1$ ,  $F_1 = F_2 = F_3 = F_4 = F = 10$ ,  $\omega = 0.5$  and initial states are  $(x_{10}, x_{20}, x_{30}, x_{40}) = (0.1, -0.5, 0.1, -0.5)$ ,  $(y_{10}, y_{20}, y_{30}, y_{40}) = (0.3, -0.1, 0.3, -0.1)$ .

Before control action, the error dynamics always happens in first quadrant as shown in Fig. 5-9. By GYC partial region stability, one can choose a Lyapunov function in the form of a positive definite function in first quadrant:

$$V = e_1 + e_2 + e_3 + e_4 \quad (5-4-16)$$

Its time derivative through Eq. (5-4-14) is

$$\begin{aligned} \dot{V} &= \dot{e}_1 + \dot{e}_2 + \dot{e}_3 + \dot{e}_4 \\ &= (x_2 - y_2 - u_1 + F \omega e^{\sin \omega t} \cos \omega t) + (-((a + bx_3)x_1 - (a + by_3)y_1) - ((a + bx_3)x_1^3 \\ &\quad - (a + by_3)y_1^3) - c(x_2 - y_2) + d(x_3 - y_3) - u_2 + F \omega e^{\sin \omega t} \cos \omega t) + (x_4 - y_4 - u_3 \\ &\quad + F \omega e^{\sin \omega t} \cos \omega t) + (-e(x_3 - y_3) + f((1 - x_3^2)x_4 - (1 - y_3^2)y_4) + g(x_1 - y_1) \\ &\quad - u_4 + F \omega e^{\sin \omega t} \cos \omega t) \end{aligned} \quad (5-4-17)$$

Choose

$$\begin{aligned}
u_1 &= (x_2 - y_2) + F\omega e^{\sin \omega t} \cos \omega t + e_1 \\
u_2 &= -((a + bx_3)x_1 - (a + by_3)y_1) - ((a + bx_3)x_1^3 - (a + by_3)y_1^3) \\
&\quad - c(x_2 - y_2) + d(x_3 - y_3) + F\omega e^{\sin \omega t} \cos \omega t + e_2 \\
u_3 &= (x_4 - y_4) + F\omega e^{\sin \omega t} \cos \omega t + e_3 \\
u_4 &= (-e(x_3 - y_3) + f((1 - x_3^2)x_4 - (1 - y_3^2)y_4) + g(x_1 - y_1)) + F\omega e^{\sin \omega t} \cos \omega t + e_4
\end{aligned} \tag{5-4-18}$$

We obtain

$$\dot{V} = -e_1 - e_2 - e_3 - e_4 < 0 \tag{5-4-19}$$

which is a negative definite function in the first quadrant. Four state errors versus time and time histories of  $x_i - y_i + 100$  and  $-F_i e^{\sin \omega t}$  are shown in Fig. 5-10 and Fig. 5-11.

*CASE IV.* The generalized synchronization error function is  $e_i = \frac{1}{2}x_i^2 - y_i + 100$ , ( $i=1, 2, 3, 4$ ).

The addition of 100 makes the error dynamics always happens in first quadrant.

Our goal is  $y_i = \frac{1}{2}x_i^2 + 100$ , i.e.

$$\lim_{t \rightarrow \infty} e_i = \lim_{t \rightarrow \infty} \left( \frac{1}{2}x_i^2 - y_i + 100 \right) \quad (i=1, 2, 3, 4) \tag{5-4-20}$$

The error dynamics becomes

$$\begin{aligned}
\dot{e}_1 &= x_1 \dot{x}_1 - \dot{y}_1 = x_1 x_2 - y_2 - u_1 \\
\dot{e}_2 &= x_2 \dot{x}_2 - \dot{y}_2 = -((a + bx_3)x_2 x_1 - (a + by_3)y_1) - ((a + bx_3)x_2 x_1^3 - (a + by_3)y_1^3) \\
&\quad - c(x_2^2 - y_2) + d(x_2 x_3 - y_3) - u_2 \\
\dot{e}_3 &= x_3 \dot{x}_3 - \dot{y}_3 = x_3 x_4 - y_4 - u_3 \\
\dot{e}_4 &= x_4 \dot{x}_4 - \dot{y}_4 = -e(x_4 x_3 - y_3) + f((1 - x_3^2)x_4^2 - (1 - y_3^2)y_4) + g(x_4 x_1 - y_1) - u_4
\end{aligned} \tag{5-4-21}$$

System parameters are chosen as  $a = 10$ ,  $b = 3$ ,  $c = 0.4$ ,  $d = 70$ ,  $e = 1$ ,  $f = 5$ ,  $g = 0.1$  and initial states are  $(x_{10}, x_{20}, x_{30}, x_{40}) = (0.1, -0.5, 0.1, -0.5)$ ,  $(y_{10}, y_{20}, y_{30}, y_{40}) = (0.3, -0.1, 0.3, -0.1)$ . Before control action, the error dynamics



always happens in first quadrant as shown in Fig. 5-12. By GYC partial region stability, one can choose a Lyapunov function in the form of a positive definite function in first quadrant:

$$V = e_1 + e_2 + e_3 + e_4 \quad (5-4-22)$$

Its time derivative through Eq. (5-4-20) is

$$\begin{aligned} \dot{V} &= \dot{e}_1 + \dot{e}_2 + \dot{e}_3 + \dot{e}_4 \\ &= (x_1x_2 - y_2 - u_1) + (-((a + bx_3)x_2x_1 - (a + by_3)y_1) - ((a + bx_3)x_2x_1^3 \\ &\quad - (a + by_3)y_1^3) - c(x_2^2 - y_2) + d(x_2x_3 - y_3) - u_2) + (x_3x_4 - y_4 - u_3) \\ &\quad + (-e(x_4x_3 - y_3) + f((1 - x_3^2)x_4^2 - (1 - y_3^2)y_4) + g(x_4x_1 - y_1) - u_4) \end{aligned} \quad (5-4-23)$$

Choose

$$\begin{aligned} u_1 &= x_1x_2 - y_2 + e_1 \\ u_2 &= -((a + bx_3)x_2x_1 - (a + by_3)y_1) - ((a + bx_3)x_2x_1^3 - (a + by_3)y_1^3) \\ &\quad - c(x_2^2 - y_2) + d(x_2x_3 - y_3) + e_2 \\ u_3 &= x_3x_4 - y_4 + e_3 \\ u_4 &= -e(x_4x_3 - y_3) + f((1 - x_3^2)x_4^2 - (1 - y_3^2)y_4) + g(x_4x_1 - y_1) + e_4 \end{aligned} \quad (5-4-24)$$

We obtain

$$\dot{V} = -e_1 - e_2 - e_3 - e_4 < 0 \quad (5-4-25)$$

which is a negative definite function in the first quadrant. Three state errors versus time is shown in Fig. 5-13.

*CASE V.* The generalized synchronization error function is  $e_i = \frac{1}{3}x_i^3 - y_i + 10000$  ( $i=1, 2, 3, 4$ ).

The addition of 10000 makes the error dynamics always happens in first quadrant.

Our goal is  $y_i = \frac{1}{3}x_i^3 + 10000$ , i.e.

$$\lim_{t \rightarrow \infty} e_i = \lim_{t \rightarrow \infty} \left( \frac{1}{3}x_i^3 - y_i + 10000 \right) \quad (i=1, 2, 3, 4) \quad (5-4-26)$$

The error dynamics becomes

$$\begin{aligned}
\dot{e}_1 &= x_1^2 \dot{x}_1 - \dot{y}_1 = x_1^2 x_2 - y_2 - u_1 \\
\dot{e}_2 &= x_2^2 \dot{x}_2 - \dot{y}_2 = -((a + bx_3)x_2^2 x_1 - (a + by_3)y_1) - ((a + bx_3)x_2^2 x_1^3 - (a + by_3)y_1^3) \\
&\quad - c(x_2^3 - y_2) + d(x_2^2 x_3 - y_3) - u_2 \\
\dot{e}_3 &= x_3^2 \dot{x}_3 - \dot{y}_3 = x_3^2 x_4 - y_4 - u_3 \\
\dot{e}_4 &= x_4^2 \dot{x}_4 - \dot{y}_4 = -e(x_4^2 x_3 - y_3) + f((1 - x_3^2)x_4^3 - (1 - y_3^2)y_4) + g(x_4^2 x_1 - y_1) - u_4
\end{aligned} \tag{5-4-27}$$

System parameters are chosen as  $a=10$ ,  $b=3$ ,  $c=0.4$ ,  $d=70$ ,  $e=1$ ,  $f=5$ ,  $g=0.1$  and initial states are  $(x_{10}, x_{20}, x_{30}, x_{40}) = (0.1, -0.5, 0.1, -0.5)$ ,  $(y_{10}, y_{20}, y_{30}, y_{40}) = (0.3, -0.1, 0.3, -0.1)$ . Before control action, the error dynamics always happens in first quadrant as shown in Fig. 5-14. By GYC partial region stability, one can choose a Lyapunov function in the form of a positive definite function in first quadrant:

$$V = e_1 + e_2 + e_3 + e_4 \tag{5-4-28}$$

Its time derivative through Eq. (5-4-26) is

$$\begin{aligned}
\dot{V} &= \dot{e}_1 + \dot{e}_2 + \dot{e}_3 + \dot{e}_4 \\
&= (x_1^2 x_2 - y_2 - u_1) + (-((a + bx_3)x_2^2 x_1 - (a + by_3)y_1) - ((a + bx_3)x_2^2 x_1^3 \\
&\quad - (a + by_3)y_1^3) - c(x_2^3 - y_2) + d(x_2^2 x_3 - y_3) - u_2) + (x_3^2 x_4 - y_4 - u_3) \\
&\quad + (-e(x_4^2 x_3 - y_3) + f((1 - x_3^2)x_4^3 - (1 - y_3^2)y_4) + g(x_4^2 x_1 - y_1) - u_4)
\end{aligned} \tag{5-4-29}$$

Choose

$$\begin{aligned}
u_1 &= x_1^2 x_2 - y_2 + e_1 \\
u_2 &= -((a + bx_3)x_2^2 x_1 - (a + by_3)y_1) - ((a + bx_3)x_2^2 x_1^3 - (a + by_3)y_1^3) \\
&\quad - c(x_2^3 - y_2) + d(x_2^2 x_3 - y_3) + e_2 \\
u_3 &= x_3^2 x_4 - y_4 + e_3 \\
u_4 &= -e(x_4^2 x_3 - y_3) + f((1 - x_3^2)x_4^3 - (1 - y_3^2)y_4) + g(x_4^2 x_1 - y_1) + e_4
\end{aligned} \tag{5-4-30}$$

We obtain

$$\dot{V} = -e_1 - e_2 - e_3 - e_4 < 0 \tag{5-4-31}$$

which is a negative definite function in the first quadrant. Three state errors versus

time is shown in Fig. 5-15.

*CASE VI.* The generalized synchronization error function is  $e_i = x_i - y_i + z_i + 100$ ,  $z_i$  ( $i=1, 2, 3, 4$ ) is the states of new chaotic Duffing-van der Pol system.

The functional system for synchronization is a new Duffing-van der pol system and initial states is (2, 2.4, 5, 6), system parameters  $h = 0.0006$ ,  $j = 1$ ,  $k = 5$ ,  $i = 0.67$  and  $l = 0.05$ .

$$\begin{aligned}\dot{z}_1 &= z_2 \\ \dot{z}_2 &= -z_1 - z_1^3 - hz_2 + iz_3 \\ \dot{z}_3 &= z_4 \\ \dot{z}_4 &= -jz_3 + k(1 - z_3^2)z_4 + lz_1\end{aligned}\tag{5-4-32}$$

$$\text{We have } \lim_{t \rightarrow \infty} e = \lim_{t \rightarrow \infty} (x_i - y_i + z_i + 100) = 0 \quad (i=1, 2, 3, 4)\tag{5-4-33}$$

The error dynamics becomes

$$\begin{aligned}\dot{e}_1 &= \dot{x}_1 - \dot{y}_1 = x_2 + z_2 - y_2 - u_1 \\ \dot{e}_2 &= \dot{x}_2 - \dot{y}_2 = -((a + bx_3)x_1 - (a + by_3)y_1) - ((a + bx_3)x_1^3 - (a + by_3)y_1^3) \\ &\quad - c(x_2 - y_2) + d(x_3 - y_3) + (-z_1 - z_1^3 - hz_2 + iz_3) - u_2 \\ \dot{e}_3 &= \dot{x}_3 - \dot{y}_3 = x_4 + z_4 - y_4 - u_3 \\ \dot{e}_4 &= \dot{x}_4 - \dot{y}_4 = -e(x_3 - y_3) + f((1 - x_3^2)x_4 - (1 - y_3^2)y_4) + g(x_1 - y_1) - u_4 \\ &\quad + (-jz_3 + k(1 - z_3^2)z_4 + lz_1)\end{aligned}\tag{5-4-34}$$

System parameters are chosen as  $a = 10$ ,  $b = 3$ ,  $c = 0.4$ ,  $d = 70$ ,  $e = 1$ ,  $f = 5$ ,  $g = 0.1$  and initial states are  $(x_{10}, x_{20}, x_{30}, x_{40}) = (0.1, -0.5, 0.1, -0.5)$ ,  $(y_{10}, y_{20}, y_{30}, y_{40}) = (0.3, -0.1, 0.3, -0.1)$ . Before control action, the error dynamics always happens in first quadrant as shown in Fig. 5-16. By GYC partial region stability, one can choose a Lyapunov function in the form of a positive definite function in first quadrant:

$$V = e_1 + e_2 + e_3 + e_4\tag{5-4-35}$$

Its time derivative through Eq. (5-4-33) is

$$\begin{aligned}
\dot{V} &= \dot{e}_1 + \dot{e}_2 + \dot{e}_3 + \dot{e}_4 \\
&= (x_2 + z_2 - y_2 - u_1) + (-((a + bx_3)x_1 - (a + by_3)y_1) - ((a + bx_3)x_1^3 \\
&\quad - (a + by_3)y_1^3) - c(x_2 - y_2) + d(x_3 - y_3) + (-z_1 - z_1^3 - hz_2 + iz_3) \\
&\quad - u_2) + (x_4 + z_4 - y_4 - u_3) + (-e(x_3 - y_3) + f((1 - x_3^2)x_4 - (1 - y_3^2)y_4) \\
&\quad + g(x_1 - y_1) - u_4 + (-jz_3 + k(1 - z_3^2)z_4 + lz_1))
\end{aligned} \tag{5-4-36}$$

Choose

$$\begin{aligned}
u_1 &= x_2 + z_2 - y_2 + e_1 \\
u_2 &= -((a + bx_3)x_1 - (a + by_3)y_1) - ((a + bx_3)x_1^3 - (a + by_3)y_1^3) \\
&\quad - c(x_2 - y_2) + d(x_3 - y_3) + (-z_1 - z_1^3 - hz_2 + iz_3) + e_2 \\
u_3 &= x_4 + z_4 - y_4 + e_3 \\
u_4 &= -e(x_3 - y_3) + f((1 - x_3^2)x_4 - (1 - y_3^2)y_4) + g(x_1 - y_1) + e_4 \\
&\quad + (-jz_3 + k(1 - z_3^2)z_4 + lz_1)
\end{aligned} \tag{5-4-37}$$

We obtain

$$\dot{V} = -e_1 - e_2 - e_3 - e_4 \leq 0 \tag{5-4-38}$$

which is a negative definite function in the first quadrant. Four state errors versus time and time histories of  $x_i - y_i + 100$  and  $-z_i$  are shown in Fig. 5-17 and Fig. 5-18.

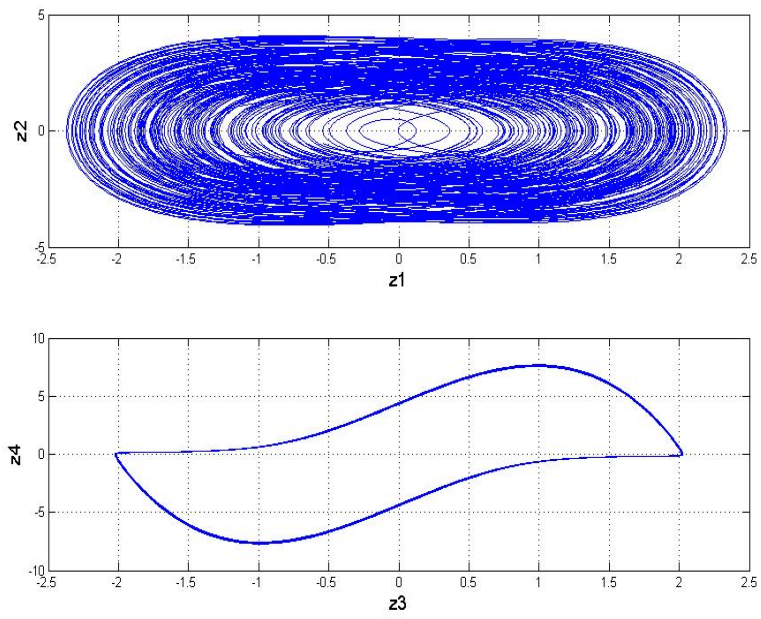


Fig. 5-1 Phase portrait projections of new chaotic Duffing-van der Pol System.

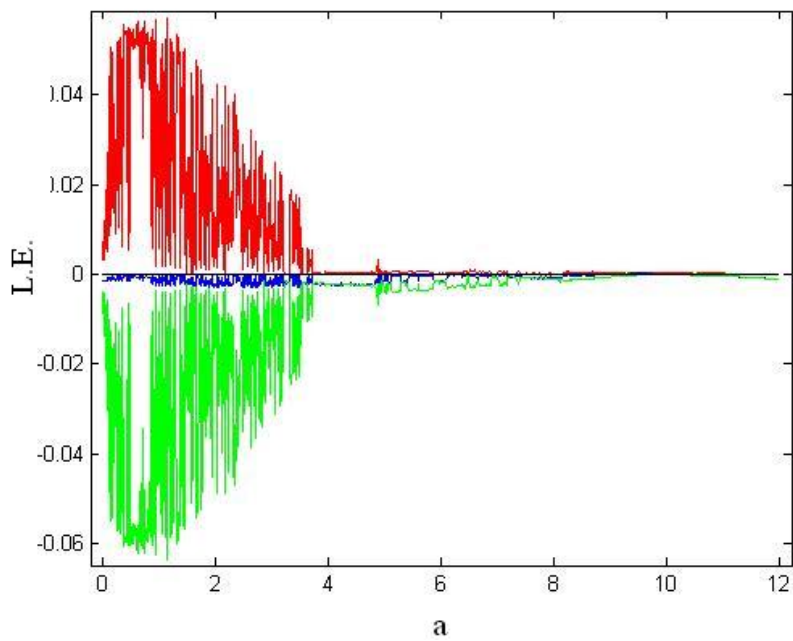
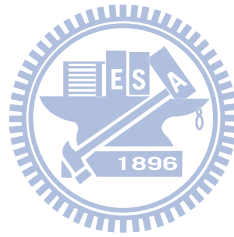


Fig. 5-2 Lyapunov exponents of new chaotic Duffing-van der Pol System.

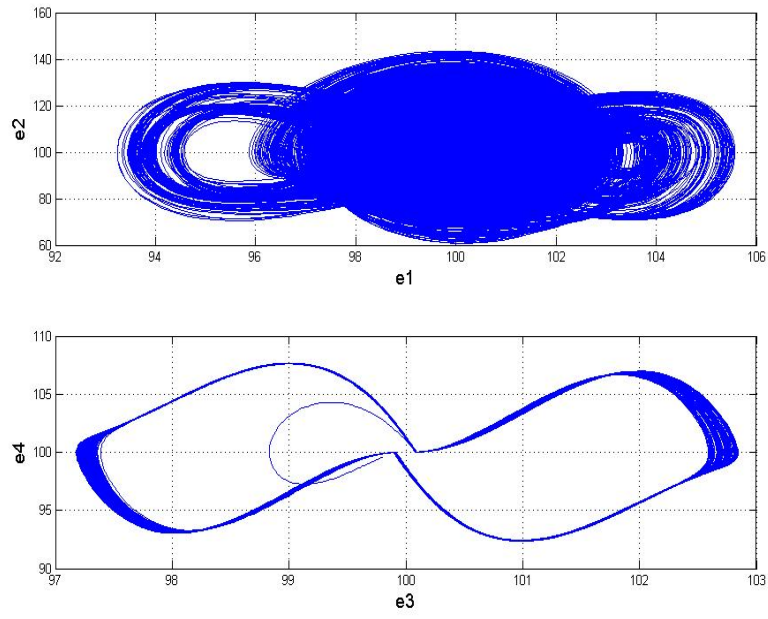


Fig. 5-3 Phase portrait projections of error dynamics for Case I.

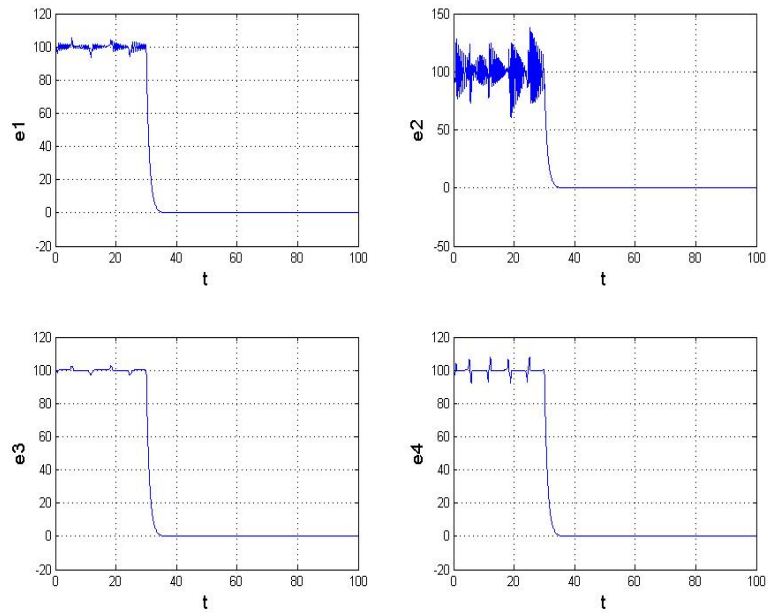


Fig. 5-4 Time histories of errors for Case I.

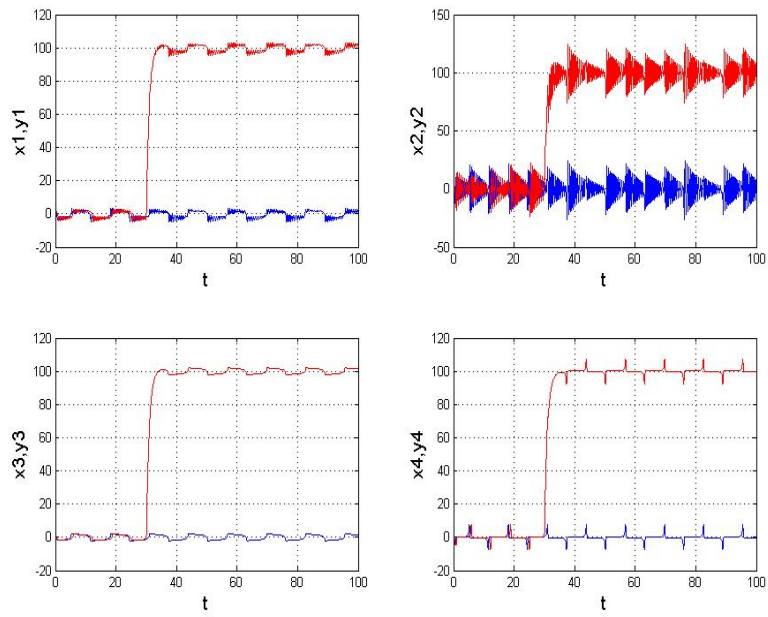


Fig. 5-5 Time histories of  $x_1, x_2, x_3, x_4, y_1, y_2, y_3, y_4$  for Case I.

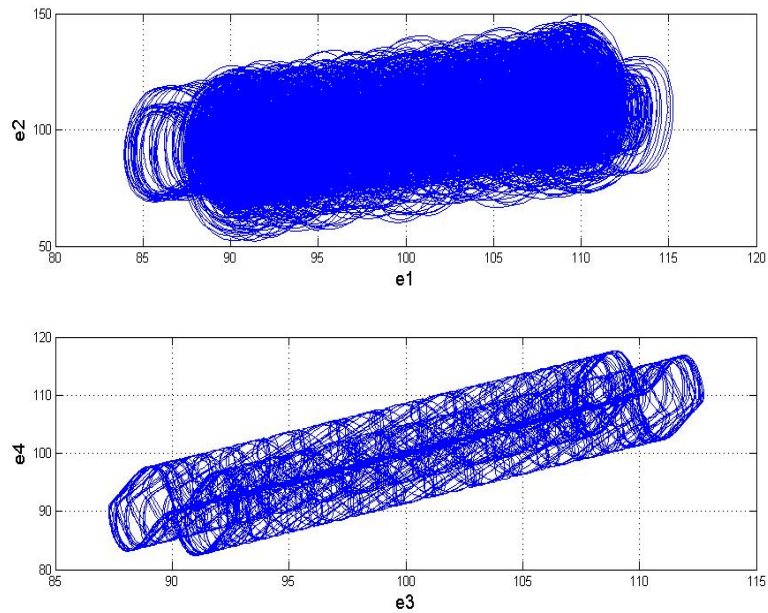


Fig. 5-6 Phase portrait projections of error dynamics for Case II.

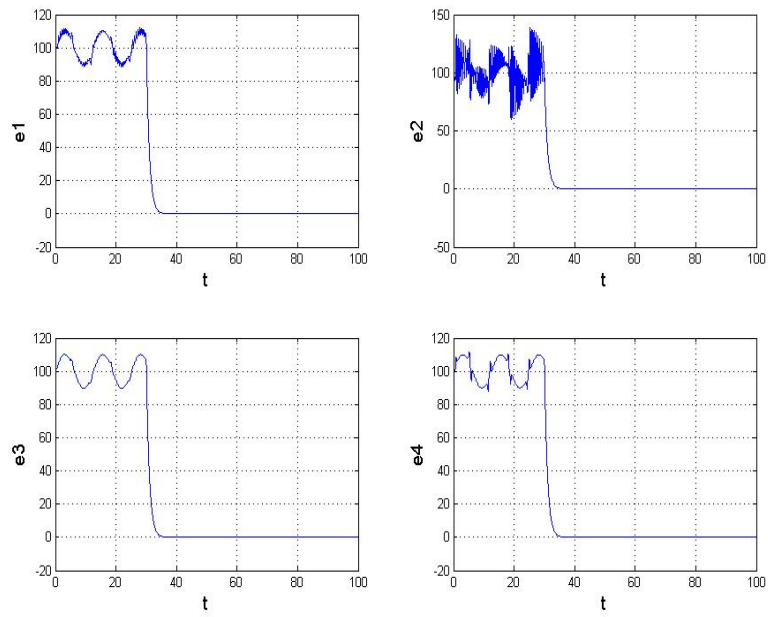


Fig. 5-7 Time histories of errors for Case II.

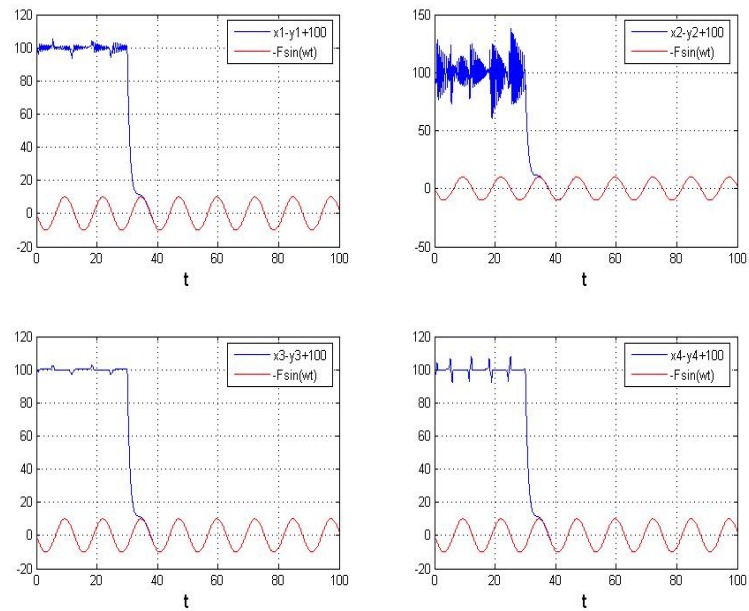


Fig. 5-8 Time histories of  $x_i - y_i + 100$  and  $-F \sin \omega t$  for Case II.



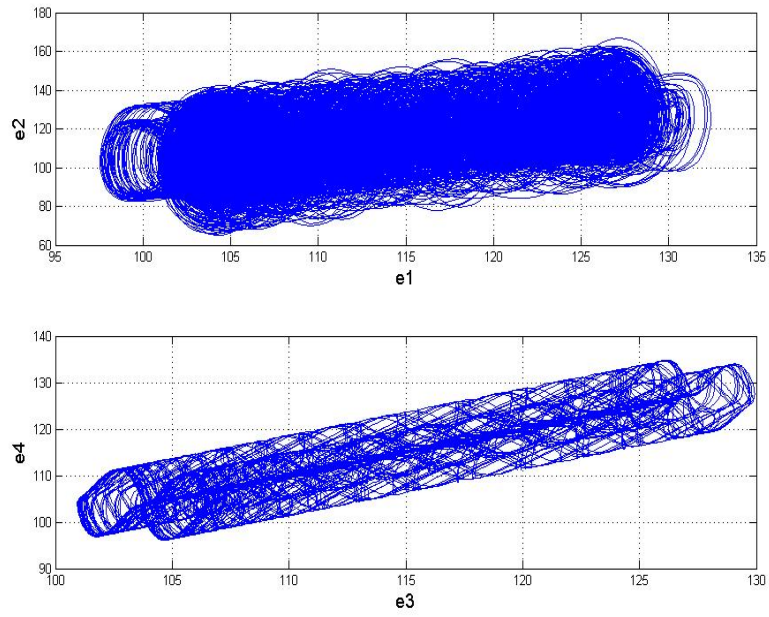


Fig. 5-9 Phase portrait projections of error dynamics for Case III.

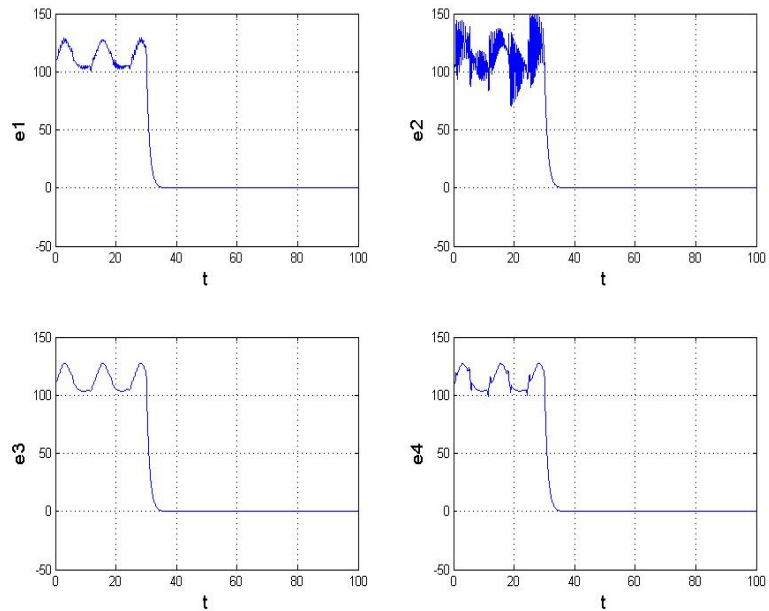


Fig. 5-10 Time histories of errors for Case III.

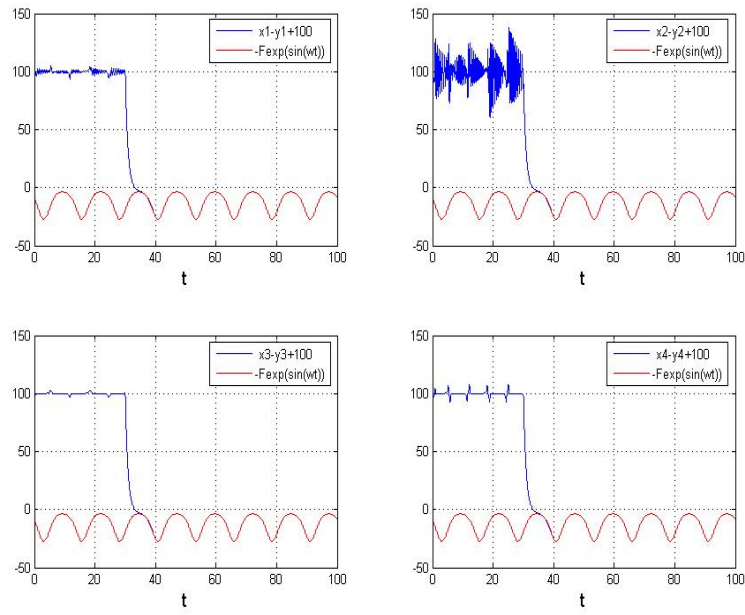


Fig. 5-11 Time histories of  $x_i - y_i + 100$  and  $-F e^{\sin(\omega t)}$  for Case III.

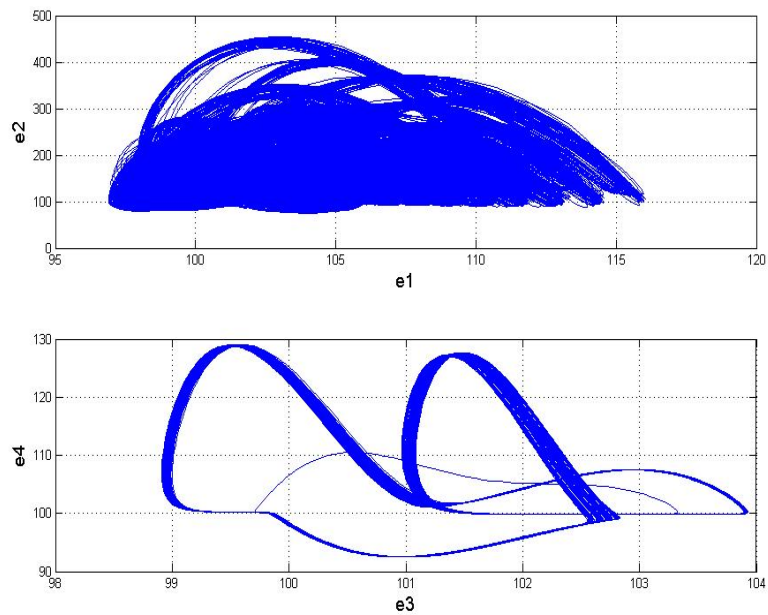
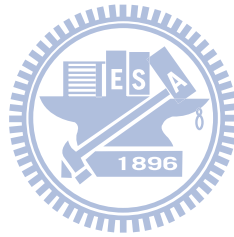


Fig. 5-12 Phase portrait projections of error dynamics for Case IV.

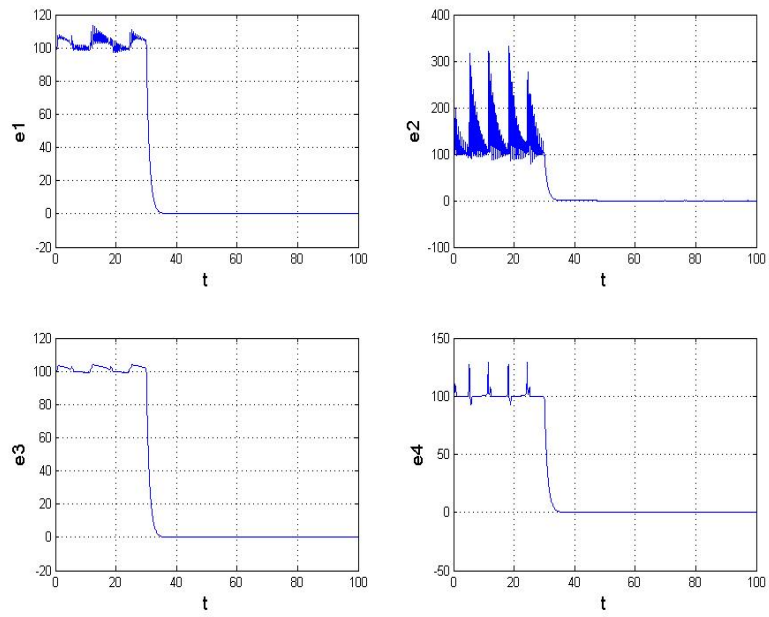


Fig. 5-13 Time histories of errors for Case IV.

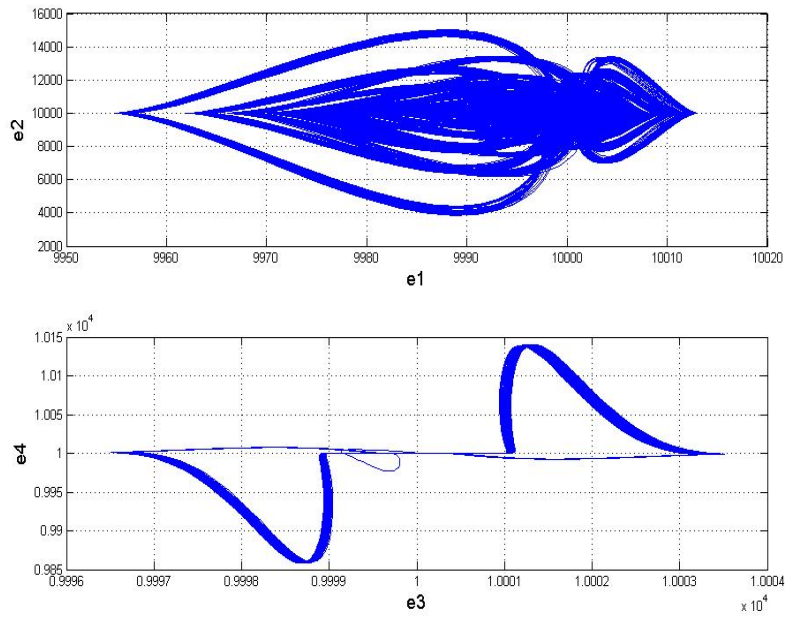


Fig. 5-14 Phase portrait projections of error dynamics for Case V.

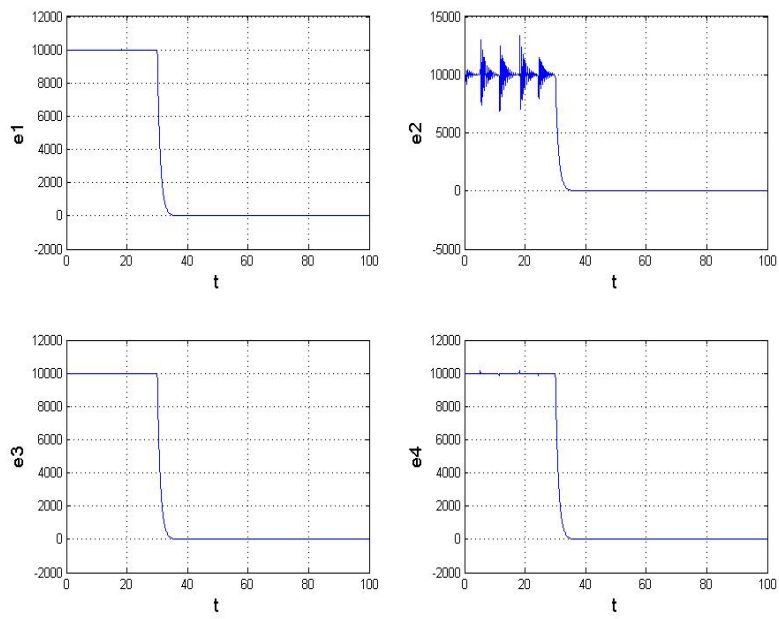


Fig. 5-15 Time histories of errors for Case V.

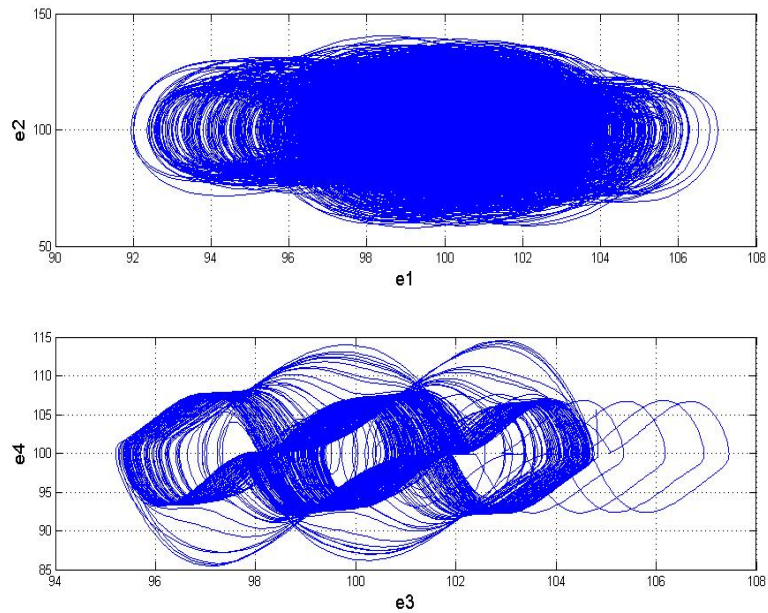


Fig. 5-16 Phase portrait projections of error dynamics for Case VI.

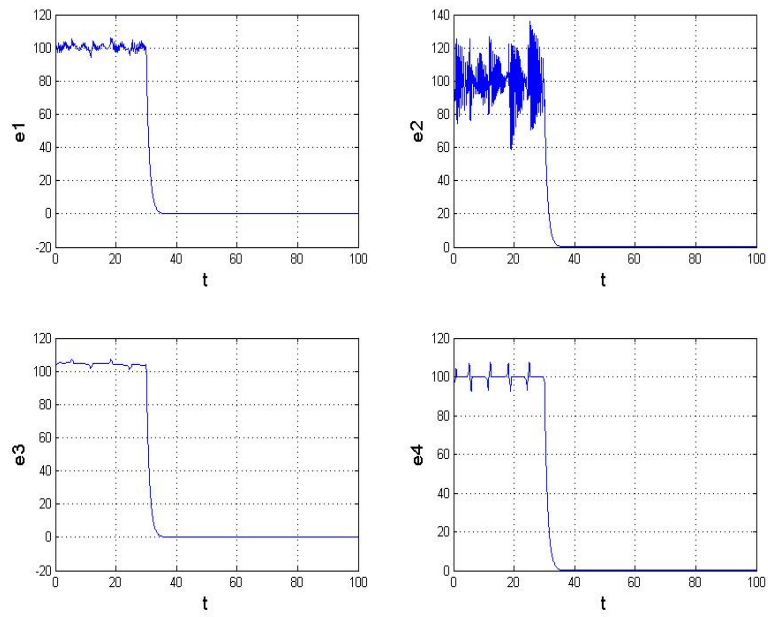


Fig. 5-17 Time histories of errors for Case VI.

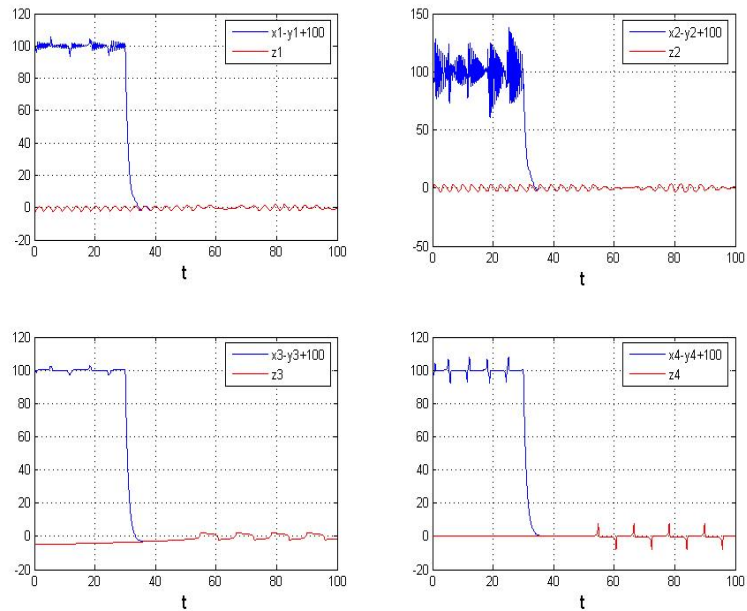


Fig. 5-18 Time histories of  $x_i - y_i + 100$  and  $-z_i$  for Case VI.

# Chapter 6

## Pragmatical Adaptive *Yin-Yang* Synchronization of Chaos by G-Y-C Partial Region Stability Theory

### 6.1 Preliminaries

The *Yin* and *Yang* Lorenz systems are used in this Chapter. A new effective approach to achieve pragmatical adaptive *Yin-Yang* synchronization is proposed. Via using Ge-Yao-Chen (GYC) partial region stability theory, in the numerical simulation results, the states errors and parametric errors approach zero much more exactly and efficiently. In this Chapter, two cases are presented in pragmatical adaptive *Yin-Yang* synchronization and the simulation results are listed in table for comparison.

### 6.2 GYC Pragmatical Adaptive Synchronization Scheme

There are two identical nonlinear dynamical systems, and the master system controls the slave system. The master system is given by

$$\dot{x} = Ax + f(x, B) \quad (6-2-1)$$

where  $x = [x_1, x_2, \dots, x_n]^T \in R^n$  denotes a state vector,  $A$  is an  $n \times n$  uncertain constant coefficient matrix,  $f$  is a nonlinear vector function, and  $B$  is a vector of uncertain constant coefficients in  $f$ .

The slave system is given by

$$\dot{y} = \hat{A}y + f(y, \hat{B}) + u(t) \quad (6-2-2)$$

where  $y = [y_1, y_2, \dots, y_n]^T \in R^n$  denotes a state vector,  $\hat{A}$  is an  $n \times n$  estimated coefficient matrix,  $\hat{B}$  is a vector of estimated coefficients in  $f$ , and  $u(t) = [u_1(t), u_2(t), \dots, u_n(t)]^T \in R^n$  is a control input vector.

Our goal is to design a controller  $u(t)$  so that the state vector of the chaotic system (6-2-1) asymptotically approaches the state vector of the master system (6-2-2).

The chaos synchronization can be accomplished in the sense that the limit of the error vector  $e(t) = [e_1, e_2, \dots, e_n]^T$  approaches zero:

$$\lim_{t \rightarrow \infty} e = 0 \quad (6-2-3)$$

where

$$e = x - y + K \quad (6-2-4)$$

where  $K$  is a positive constant by which the error dynamics occurs in the first quadrant of state space of  $e$ .

From Eq. (6-2-4) we have

$$\dot{e} = \dot{x} - \dot{y} \quad (6-2-5)$$

$$\dot{e} = Ax - \hat{A}y + f(x, B) - f(y, \hat{B}) - u(t) \quad (6-2-6)$$

A Lyapunov function  $V(e, \tilde{A}, \tilde{B})$  is chosen as a positive definite function in first quadrant of state space of  $e, \tilde{A}, \tilde{B}$ .

We have

$$\dot{V}(e, \tilde{A}, \tilde{B}) = e + \tilde{A} + \tilde{B} \quad (6-2-7)$$

where  $\tilde{A} = A - \hat{A}$ ,  $\tilde{B} = B - \hat{B}$ ,  $\tilde{A}$  and  $\tilde{B}$  are two column matrices whose elements are all the elements of matrix  $\hat{A}$  and of matrix  $\hat{B}$ , respectively.

Its derivative along any solution of the differential equation system consisting of Eq. (6-2-6) and update parameter differential equations for  $\tilde{A}$  and  $\tilde{B}$  is

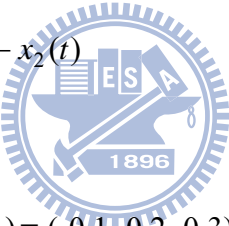
$$\dot{V}(e, \tilde{A}, \tilde{B}) = [Ax - \hat{A}y + Bf(x) - \hat{B}f(y) - u(t)] + \dot{\tilde{A}} + \dot{\tilde{B}} \quad (6-2-8)$$

where  $u(t)$ ,  $\dot{\tilde{A}}$ , and  $\dot{\tilde{B}}$  are chosen so that  $\dot{V} = Ce$ ,  $C$  is a diagonal negative definite

matrix, and  $\dot{V}$  is a negative semi-definite function of  $e$  and parameter differences  $\tilde{A}$  and  $\tilde{B}$ . In current scheme of adaptive control of chaotic motion [22-24], traditional Lyapunov stability theorem and Babalat lemma are used to prove the error vector approaches zero, as time approaches infinity. But the question, why the estimated or given parameters also approach to the uncertain or goal parameters, remains no answer. By pragmatcal asymptotical stability theorem, the question can be answered strictly.

### 6.3 Yin and Yang Lorenz system

The *Yang* Lorenz system [10] can be recalled firstly as follow:

$$\begin{cases} \frac{dx_1(t)}{dt} = a(x_2(t) - x_1(t)) \\ \frac{dx_2(t)}{dt} = cx_1(t) - x_1(t)x_3(t) - x_2(t) \\ \frac{dx_3(t)}{dt} = x_1(t)x_2(t) - bx_3(t) \end{cases} \quad (6-3-1)$$


when initial condition  $(x_{10}, x_{20}, x_{30}) = (-0.1, 0.2, 0.3)$  and parameters  $a=10$ ,  $b=8/3$  and  $c=28$ , chaos of the *Yang* Lorenz system appears. The chaotic behavior of Eq. (6-3-1) is shown in Fig 6-1.

*Yin* Lorenz equations are:

$$\begin{cases} \frac{dx_1(-t)}{d(-t)} = a(x_2(-t) - x_1(-t)) \\ \frac{dx_2(-t)}{d(-t)} = cx_1(-t) - x_1(-t)x_3(-t) - x_2(-t) \\ \frac{dx_3(-t)}{d(-t)} = x_1(-t)x_2(-t) - bx_3(-t) \end{cases} \quad (6-3-2)$$

It is clear that in the left hand sides of Eq. (6-3-2), the derivative are taken with the back-time. When initial condition  $(x_{10}, x_{20}, x_{30}) = (-0.1, 0.2, 0.3)$  and parameters  $a=-10$ ,  $b=-8/3$  and  $c=-28$ , the chaotic behavior of Eq. (6-3-2) is shown in Fig 6-2.



## 6.4 Adaptive *Yin-Yang* synchronization by GYC partial region stability theory

In this section, there are two Cases in simulation results. In Case 1, originally adaptive synchronization from *Yin* Lorenz chaos to *Yang* Lorenz chaos is proposed. In Case 2, adaptive synchronization by GYC partial region stability theory is presented to synchronize the *Yin* and *Yang* Lorenz chaos. The *Yin* Lorenz system is considered as slave system and the *Yang* Lorenz system is regarded as master system. These two equations are shown below:

Master system- *Yang* Lorenz system:

$$\begin{cases} \frac{dx_1(t)}{dt} = a(x_2(t) - x_1(t)) \\ \frac{dx_2(t)}{dt} = cx_1(t) - x_1(t)x_3(t) - x_2(t) \\ \frac{dx_3(t)}{dt} = x_1(t)x_2(t) - bx_3(t) \end{cases} \quad (6-4-1)$$

Slave system- *Yin* Lorenz system:

$$\begin{cases} \frac{dy_1(-t)}{d(t)} = -\hat{a}(y_2(-t) - y_1(-t)) + u_1 \\ \frac{dy_2(-t)}{d(t)} = -(\hat{c}y_1(-t) - y_1(-t)y_3(-t) - y_2(-t)) + u_2 \\ \frac{dy_3(-t)}{d(t)} = -(y_1(-t)y_2(-t) - \hat{b}y_3(-t)) + u_3 \end{cases} \quad (6-4-2)$$

where  $x_i(t)$  stands for states variables of the master system and  $y_i(-t)$  the slave system, respectively. Parameters,  $a$ ,  $b$  and  $c$  are positive uncertain parameters of master system.  $\hat{a}$ ,  $\hat{b}$  and  $\hat{c}$  are estimated parameters.  $u_1$ ,  $u_2$  and  $u_3$  are nonlinear controller to synchronize the slave Lorenz system to master one, i.e.,

$$\lim_{t \rightarrow \infty} \mathbf{e} = 0 \quad (6-4-3)$$

where the error vector  $\mathbf{e} = [e_1(t) \ e_2(t) \ e_3(t)]$ .

CASE I: Adaptive synchronization from Yin to Yang Lorenz chaos.

The error vector  $e = [e_1(t) \ e_2(t) \ e_3(t)]$  and

$$\begin{cases} e_1(t) = x_1(t) - y_1(-t) \\ e_2(t) = x_2(t) - y_2(-t) \\ e_3(t) = x_3(t) - y_3(-t) \end{cases} \quad (6-4-4)$$

From Eq. (6-4-4), we have the following error dynamics:

$$\begin{cases} \frac{de_1(t)}{dt} = \frac{dx_1(t)}{dt} - \frac{dy_1(-t)}{dt} = \frac{dx_1(t)}{dt} + \frac{dy_1(-t)}{d(-t)} \\ \frac{de_2(t)}{dt} = \frac{dx_2(t)}{dt} - \frac{dy_2(-t)}{dt} = \frac{dx_2(t)}{dt} + \frac{dy_2(-t)}{d(-t)} \\ \frac{de_3(t)}{dt} = \frac{dx_3(t)}{dt} - \frac{dy_3(-t)}{dt} = \frac{dx_3(t)}{dt} + \frac{dy_3(-t)}{d(-t)} \end{cases}$$

$$\begin{aligned} \dot{e}_1 &= a(x_2 - x_1) + (-\hat{a}(y_2 - y_1) + u_1) \\ \dot{e}_2 &= cx_1 - x_1x_3 - x_2 + (-\hat{c}y_1 - y_1y_3 - y_2) + u_2 \\ \dot{e}_3 &= x_1x_2 - bx_3 + (-(y_1y_2 - \hat{b}y_3) + u_3) \end{aligned} \quad (6-4-5)$$

The two systems will be synchronized for any initial condition by appropriate controllers and update laws for those estimated parameters. As a result, the following controllers and update laws are designed by pragmatistical asymptotical stability theorem as follows:

Choosing Lyapunov function as:

$$V = \frac{1}{2}(e_1^2 + e_2^2 + e_3^2 + \tilde{a}^2 + \tilde{b}^2 + \tilde{c}^2) \quad (6-4-6)$$

where  $\tilde{a} = a - \hat{a}$ ,  $\tilde{b} = b - \hat{b}$  and  $\tilde{c} = c - \hat{c}$ .

Its time derivative is:

$$\begin{aligned} \dot{V} &= e_1\dot{e}_1 + e_2\dot{e}_2 + e_3\dot{e}_3 + \tilde{a}\dot{\tilde{a}} + \tilde{b}\dot{\tilde{b}} + \tilde{c}\dot{\tilde{c}} \\ &= e_1(a(x_2 - x_1) + (-\hat{a}(y_2 - y_1) + u_1)) \\ &\quad + e_2(cx_1 - x_1x_3 - x_2 + (-\hat{c}y_1 - y_1y_3 - y_2) + u_2) \\ &\quad + e_3(x_1x_2 - bx_3 + (-(y_1y_2 - \hat{b}y_3) + u_3)) \\ &\quad + \dot{\tilde{a}}(a - \hat{a}) + \dot{\tilde{b}}(b - \hat{b}) + \dot{\tilde{c}}(c - \hat{c}) \end{aligned} \quad (6-4-7)$$

We choose the update laws for those uncertain parameters as:

$$\begin{cases} \dot{\tilde{a}} = -\hat{a} = -(x_2 - x_1)e_1 + \tilde{a}e_1 \\ \dot{\tilde{c}} = -\hat{c} = -(x_1)e_2 + \tilde{c}e_2 \\ \dot{\tilde{b}} = -\hat{b} = (x_3)e_3 + \tilde{b}e_3 \end{cases} \quad (6-4-8)$$

Through Eqs. (6-4-7) and (6-4-8), the appropriate controllers can be designed as:

$$\begin{cases} u_1 = -\hat{a}(x_2 - x_1 - y_2 + y_1) - \tilde{a}^2 - e_1 \\ u_2 = -\hat{c}(x_1 - y_1) + x_1x_3 + x_2 + y_1y_3 + y_2 - \tilde{c}^2 - e_2 \\ u_3 = \hat{b}(x_3 - y_3) - x_1x_2 - y_1y_2 - \tilde{b}^2 - e_3 \end{cases} \quad (6-4-9)$$

We obtain

$$\dot{V} = -e_1^2 - e_2^2 - e_3^2 < 0 \quad (6-4-10)$$

which is negative semi-definite function of  $e_1, e_2, e_3, \hat{a}, \hat{b}$  and  $\hat{c}$ . The Lyapunov asymptotical stability theorem is not satisfied. We cannot obtain that common origin of error dynamics (6-4-5) and parameter dynamics (6-4-8) is asymptotically stable. By pragmatical asymptotically stability theorem (see Appendix A),  $D$  is a 6-manifold,  $n = 6$  and the number of error state variables  $p = 3$ . When  $e_1 = e_2 = e_3 = 0$  and  $\hat{a}, \hat{b}, \hat{c}$  take arbitrary values,  $\dot{V} = 0$ , so  $X$  is of 3 dimensions,  $m = n - p = 6 - 3 = 3$ ,  $m + 1 < n$  is satisfied. According to the pragmatical asymptotically stability theorem, error vector  $e$  approaches zero and the estimated parameters also approach the uncertain parameters. The equilibrium point is pragmatically asymptotically stable. Under the assumption of equal probability, it is actually asymptotically stable. The simulation results are shown in Figs. 6-3, 6-4 and 6-5.

**CASE 2: Adaptive synchronization from *Yin* to *Yang* Lorenz chaos by GYC partial region stability theory.**

In order to obtain more simple controllers and achieve high efficiency in adaptive synchronization, GYC partial region stability theory is used here

We choose error vector  $e = [e_1(t) \ e_2(t) \ e_3(t)]$  and

$$\begin{cases} e_1(t) = x_1(t) - y_1(-t) + K \\ e_2(t) = x_2(t) - y_2(-t) + K \\ e_3(t) = x_3(t) - y_3(-t) + K \end{cases} \quad (6-4-11)$$

where  $K$  is a constant and choose as 200 so that the error dynamics occurs in the first quadrant of state space of  $e$ . From Eq. (6-4-11), we have the following error dynamics:

$$\begin{cases} \frac{de_1(t)}{dt} = \frac{dx_1(t)}{dt} - \frac{dy_1(-t)}{dt} = \frac{dx_1(t)}{dt} + \frac{dy_1(-t)}{d(-t)} \\ \frac{de_2(t)}{dt} = \frac{dx_2(t)}{dt} - \frac{dy_2(-t)}{dt} = \frac{dx_2(t)}{dt} + \frac{dy_2(-t)}{d(-t)} \\ \frac{de_3(t)}{dt} = \frac{dx_3(t)}{dt} - \frac{dy_3(-t)}{dt} = \frac{dx_3(t)}{dt} + \frac{dy_3(-t)}{d(-t)} \end{cases}$$

$$\begin{aligned} \dot{e}_1 &= a(x_2 - x_1) + (-\hat{a}(y_2 - y_1) + u_1) \\ \dot{e}_2 &= cx_1 - x_1x_3 - x_2 + (-\hat{c}y_1 - y_1y_3 - y_2) + u_2 \\ \dot{e}_3 &= x_1x_2 - bx_3 + (-y_1y_2 - \hat{b}y_3) + u_3 \end{aligned} \quad (6-4-12)$$

The two systems will be synchronized for any initial condition by appropriate controllers and update laws for those estimated parameters. As a result, the following controllers and update laws are designed by pragmatistical asymptotical stability theorem and GYC partial region stability theory as follows:

Choosing Lyapunov function as:

$$V = e_1 + e_2 + e_3 + \tilde{a} + \tilde{b} + \tilde{c} \quad (6-4-13)$$

where  $\tilde{a} = a - \hat{a}$ ,  $\tilde{b} = b - \hat{b}$  and  $\tilde{c} = c - \hat{c}$ .  $a$ ,  $b$  and  $c$  are positive uncertain parameters and  $\hat{a}$ ,  $\hat{b}$  and  $\hat{c}$  are estimated parameters in negative initial values.  $V$  is a positive definite function in the first of the state space of  $e_1, e_2, e_3, \tilde{a}, \tilde{b}$  and  $\tilde{c}$ .

Its time derivative is:

$$\begin{aligned}
\dot{V} &= \dot{e}_1 + \dot{e}_2 + \dot{e}_3 + \dot{\tilde{a}} + \dot{\tilde{b}} + \dot{\tilde{c}} \\
&= (a(x_2 - x_1) + (-\hat{a}(y_2 - y_1) + u_1)) \\
&\quad + (cx_1 - x_1x_3 - x_2 + (-\hat{c}y_1 - y_1y_3 - y_2) + u_2) \\
&\quad + (x_1x_2 - bx_3 + (-y_1y_2 - \hat{b}y_3) + u_3) \\
&\quad + (a - \hat{a}) + (b - \hat{b}) + (c - \hat{c})
\end{aligned} \tag{6-4-14}$$

We choose the update laws for those uncertain parameters as:

$$\begin{cases}
\dot{\tilde{a}} = -\dot{\hat{a}} = -(x_2 - x_1)\tilde{a} - \tilde{a}e_1 \\
\dot{\tilde{c}} = -\dot{\hat{c}} = -(x_1)\tilde{c} - \tilde{c}e_2 \\
\dot{\tilde{b}} = -\dot{\hat{b}} = (x_3)\tilde{b} - \tilde{b}e_3
\end{cases} \tag{6-4-15}$$

Through Eqs. (6-4-14) and (6-4-15), the appropriate controllers can be designed as:

$$\begin{cases}
u_1 = \hat{a}(x_2 - x_1 + y_2 - y_1) + e_1 \\
u_2 = \hat{c}(x_1 + y_1) - x_1x_3 - x_2 - y_1y_3 - y_2 + e_2 \\
u_3 = x_1x_2 + y_1y_2 - \hat{b}(x_3 + y_3) + e_3
\end{cases} \tag{6-4-16}$$

We obtain

$$\dot{V} = -e_1 - e_2 - e_3 < 0 \tag{6-4-17}$$



which is negative semi-definite function of  $e_1, e_2, e_3, \tilde{a}, \tilde{b}$  and  $\tilde{c}$  in the first quadrant of state space of  $e_1, e_2, e_3, \tilde{a}, \tilde{b}$  and  $\tilde{c}$ . The Lyapunov asymptotical stability theorem is not satisfied. We cannot obtain that common origin of error dynamics (6-4-12) and parameter dynamics (6-4-15) is asymptotically stable. By pragmatcal asymptotically stability theorem (see Appendix A),  $D$  is a 6-manifold,  $n = 6$  and the number of error state variables  $p = 3$ . When  $e_1 = e_2 = e_3 = 0$  and  $\hat{a}, \hat{b}, \hat{c}$  take arbitrary values,  $\dot{V} = 0$ , so  $X$  is of 3 dimensions,  $m = n - p = 6 - 3 = 3$ ,  $m + 1 < n$  is satisfied. According to the pragmatcal asymptotically stability theorem, error vector  $e$  approaches zero and the estimated parameters also approach the uncertain parameters. The equilibrium point is pragmatcally asymptotically stable. Under the assumption of equal probability, it is actually asymptotically stable. The simulation results are shown

in Figs. 6-6 and 6-7.

## 6.5 Discussion

In this Section, we are going to show the efficiency and effectiveness of our new approach via comparing Figs and numerical data. There are two main topics here: (1) Errors of states, (2) Errors of parameters.

### (1). Errors of states:

The simulation results in Fig. 6-3 and Fig. 6-6 can be clearly found out that the errors in Case 2 (in Fig. 6-6) are reaching original point much faster than the errors in Case 1 (in Fig. 6-3). Further, the data of numerical results in Case 1 and Case 2 are also provided for comparing, which are listed in Table 6-2.

Table 6-2 shows that the errors in Case 2 are faster converging to original point than the errors in Case 1. When time is going to achieve 20s, the data of errors in Case 2 are approaching to  $4.1 \times 10^{-7}$  and are greatly less than the data of errors in Case 1,  $e_1 \approx 8.1 \times 10^{-5}$ ,  $e_2 \approx 1.3 \times 10^{-3}$  and  $e_3 \approx 1.8 \times 10^{-4}$ .

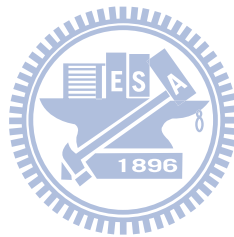
### (2). Errors of parameters:

In Fig. 6-4 (Case 1), the time of achieving parametric terminal value is about 16s. In Fig. 6-7 (Case 2), the time of achieving parametric terminal value is only about 0.1s. It can be found out when GYC partial region stability theory is used in pragmatical adaptive synchronization, the efficiency of parametric synchronization can be hugely raised up.

On the other hand, the numerical data of parametric errors in Case 1 and 2 are listed in Table 6-3. In Table 6-3, the parametric errors for Case 2 are completely converging to the original point before 10.00s. Through our new strategy, the *Yin*-parameters of *Yin* Lorenz system can exactly approach to the *Yang*-parameters of

*Yang* Lorenz system via pragmatical asymptotically stability theorem. The numerical results are marvelously satisfactory.

Through the comparison of figures and tables in simulation results, our new approach – pragmatical adaptive synchronization via GYC partial region stability theory is demonstrated as an effective and powerful tool. It is not only increasing the converging speed to our goal enormously (for errors of states and errors of parameters, the goal is original point), but also reducing the simulation errors.



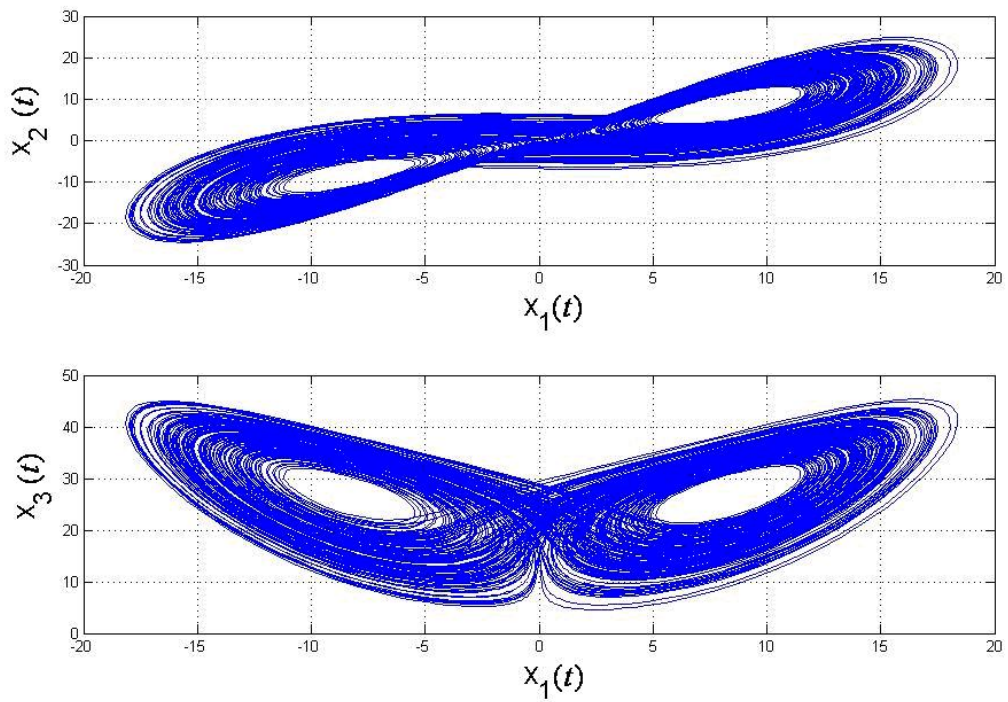


Fig. 6-1. Projections of phase portrait of chaotic *Yang* Lorenz system with  $a=10$ ,

$b=8/3$  and  $c=28$ .

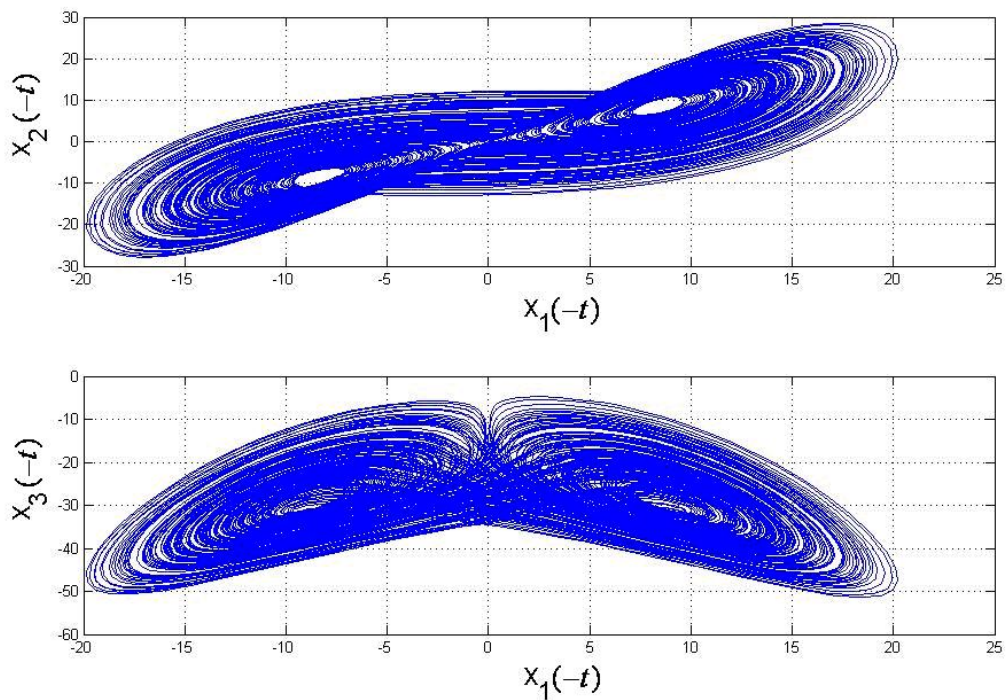


Fig. 6-2. Projections of phase portrait of chaotic *Yin* Lorenz system with Yin

parameters  $a=-10$ ,  $b=-8/3$  and  $c=-28$ .



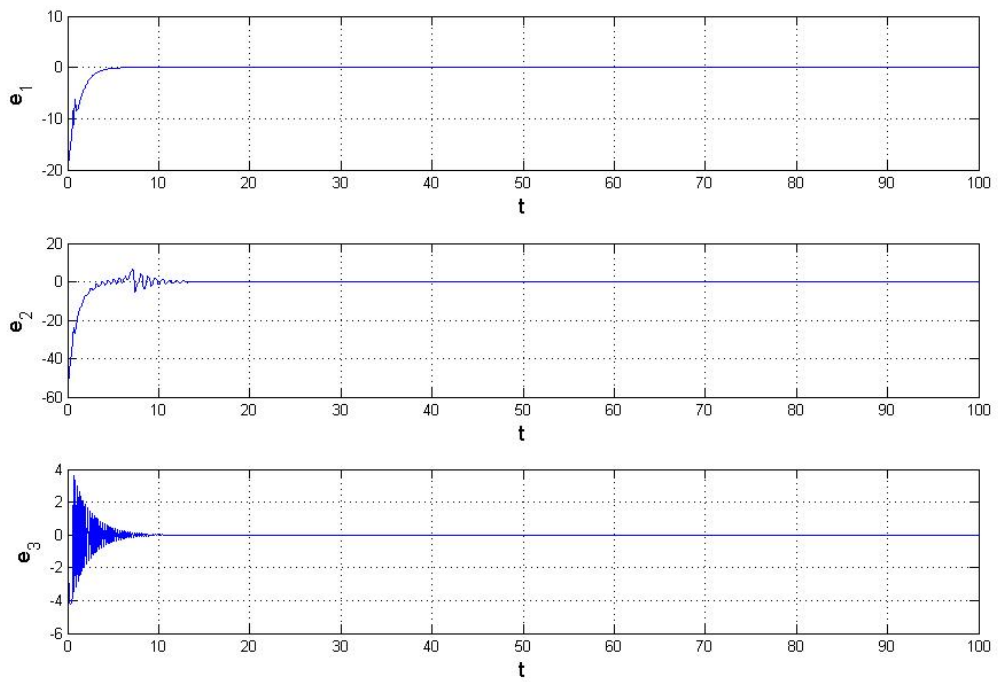


Fig. 6-3. Time histories of errors for *Yin* and *Yang* Lorenz chaotic systems for Case 1

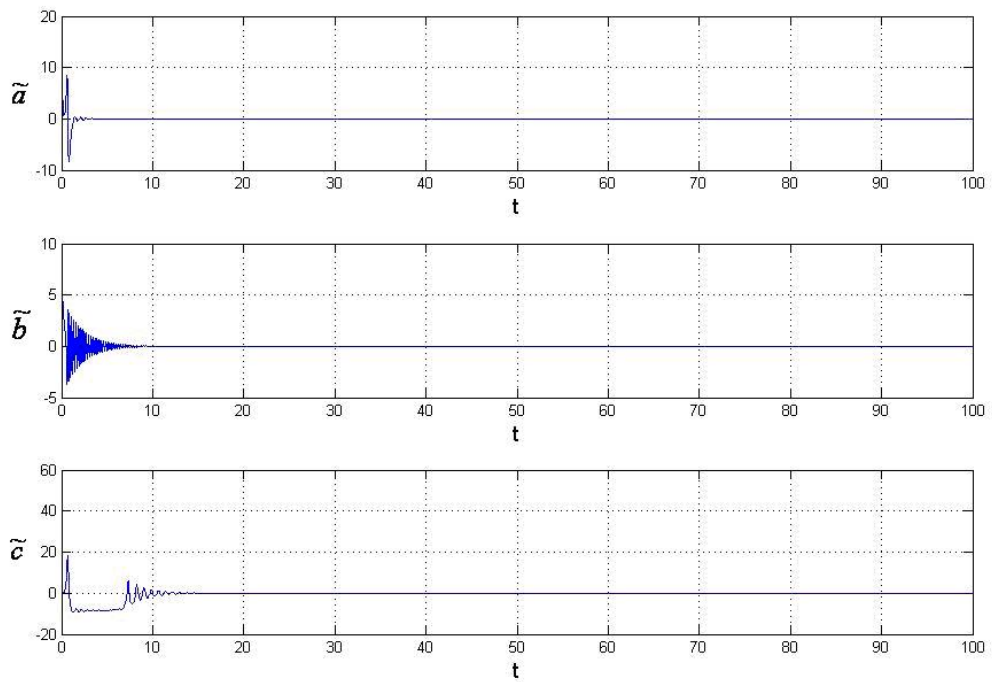


Fig. 6-4. Time histories of parametric errors for *Yin* and *Yang* Lorenz chaotic systems for Case 1

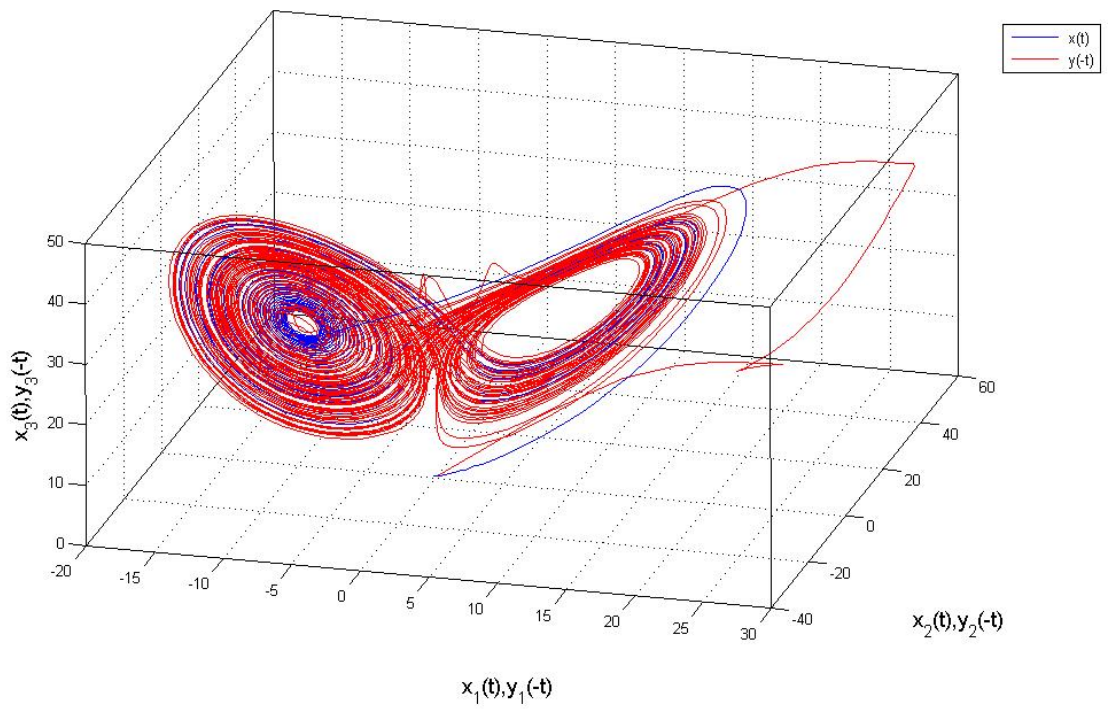


Fig. 6-5. Phase portraits of synchronization of *Yin* and *Yang* Lorenz chaotic systems for



Case 1

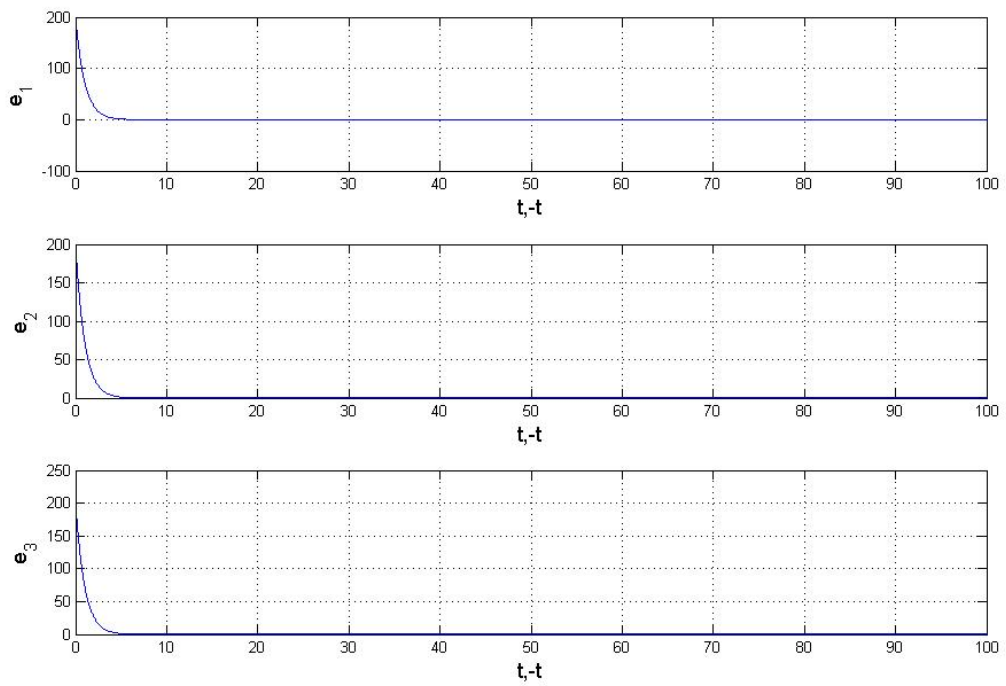


Fig. 6-6. Time histories of errors for *Yin* and *Yang* Lorenz chaotic systems for Case 2

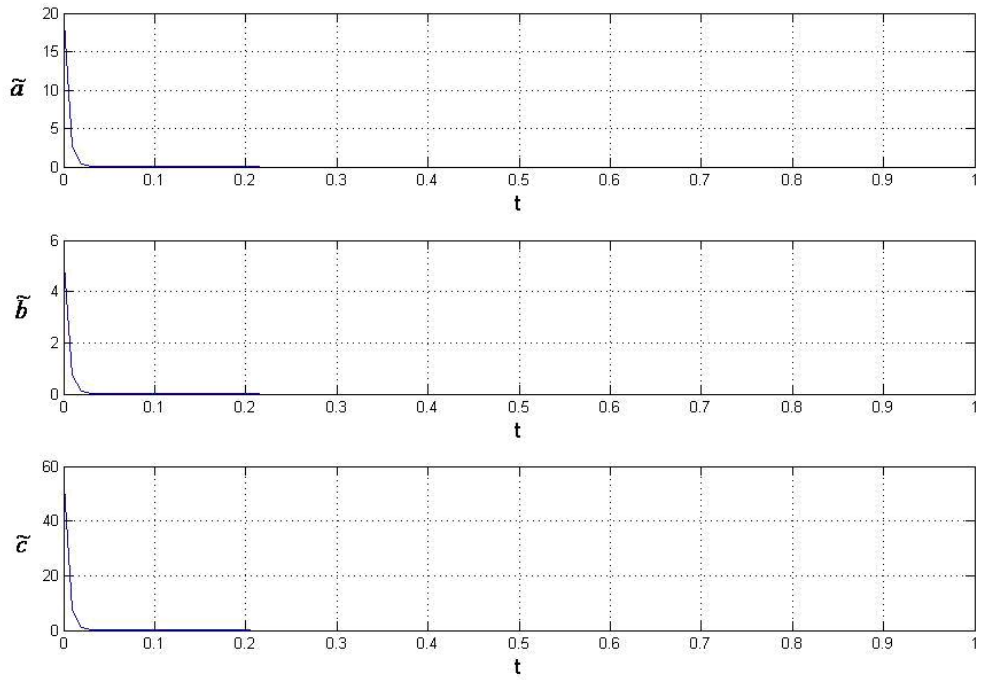


Fig. 6-7. Time histories of parametric errors for *Yin* and *Yang* Lorenz chaotic systems

for Case 2

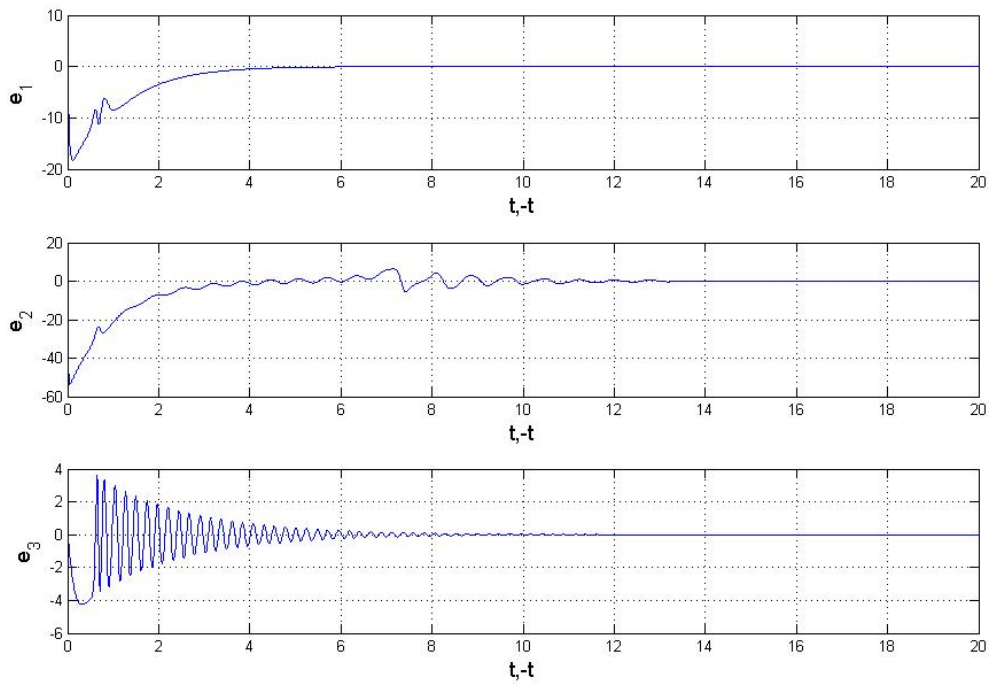
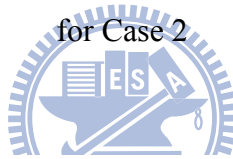


Fig. 6-8. Time histories of errors in 20s for Case 1

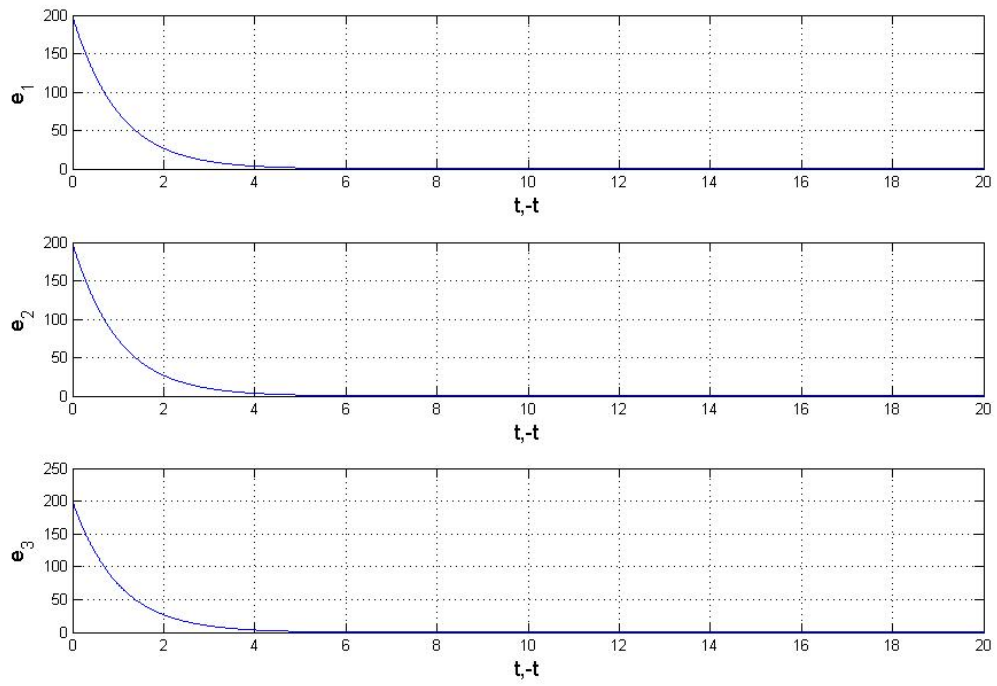


Fig. 6-9 Time histories of errors in 20s for Case 2

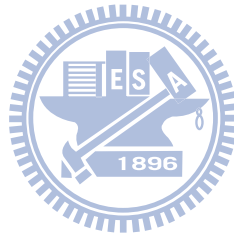
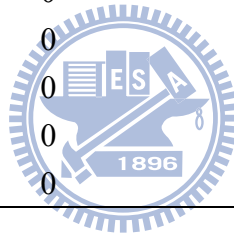


Table 6-1 Comparison between errors data at 19.96s, 19.97s, 19.98s, 19.99s and 20.00s after the action of controllers

Time	Errors for Case 2	Errors for Case 1
	$e_1$	$e_1$
19.96s	0.00000043256	0.00011282000
19.97s	0.00000042826	0.00010565000
19.98s	0.00000042399	0.00009795500
19.99s	0.00000041978	0.00008996100
20.00s	0.00000041560	0.00008187800
	$e_2$	$e_2$
19.96s	0.00000043266	-0.00210000000
19.97s	0.00000042836	-0.00110000000
19.98s	0.00000042410	-0.00020560000
19.99s	0.00000041988	0.00061179000
20.00s	0.00000041570	0.00130000000
	$e_3$	$e_3$
19.96s	0.00000043378	0.00009716000
19.97s	0.00000042947	0.00001637300
19.98s	0.00000042519	-0.00006358000
19.99s	0.00000042096	-0.00013330000
20.00s	0.00000041677	-0.00018590000

Table 6-2 Comparison between parametric errors at 9.96s, 9.97s, 9.98s, 9.99s and 10.00s after the action of controllers

Time	Errors for Case 2	Errors for Case 1
	$\tilde{a}$	$\tilde{a}$
9.96s	0	0.00075110
9.97s	0	0.00075450
9.98s	0	0.00076372
9.99s	0	0.00077850
10.00s	0	0.00079843
	$\tilde{b}$	$\tilde{b}$
9.96s	0	-0.01620000
9.97s	0	-0.00630000
9.98s	0	0.00430000
9.99s	0	0.01440000
10.00s	0	0.02310000
	$\tilde{c}$	$\tilde{c}$
9.96s	0	1.10510000
9.97s	0	0.93560000
9.98s	0	0.75750000
9.99s	0	0.57490000
10.00s	0	0.39130000



# Chapter 7

## Fuzzy Modeling and Synchronization of Complicated Nonlinear Systems via Novel Fuzzy Model and Its Implementation on Electronic Circuits

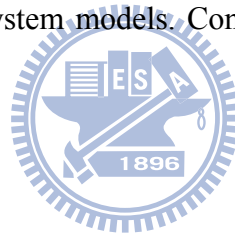
### 7.1 Preliminaries

In this Chapter, a new fuzzy model is presented to simulate complicated nonlinear systems, such as Quantum cellular neural networks nano system (called Quantum-CNN system) and Qi system. Quantum-CNN system is a complicated nonlinear system. There are too more nonlinear terms in its mathematical equations, such as radical terms, square terms, sin and cos terms, etc. If the traditional T-S fuzzy model is used here, there will be 16 fuzzy rules and even 64 linear equations for modeling such a complex system. It is definitely an inefficient work. As a result, by using the new fuzzy model, the numbers of fuzzy rules can be reduced from  $2^N$  to  $2 \times N$  (where  $N$  is the number of nonlinear terms) and only two subsystems will be existed. The fuzzy equations become much simpler. Moreover, the LMI-based fuzzy synchronization of two identical or totally different fuzzy chaotic systems, Q-CNN and Qi systems, and its related new theorem are proposed as well. Via using the new fuzzy model, only two feedback gains are needed in the fuzzy controllers. There are two examples in numerical simulation results to show the effectiveness and feasibility of our new model. Finally, via using Taylor's expansion, the complicated nonlinear terms can be expanded to series form, and then the simplified Q-CNN system can be implemented on electronic circuits for secure communication. Simulation results in MATLAB and implementation of electronic circuits are given to show the effectiveness and feasibility of the new fuzzy model and the new

approaches.

## 7.2 New fuzzy model theory

In system analysis and design, it is important to select an appropriate model representing a real system. As an expression model of a real plant, the fuzzy implications and the fuzzy reasoning method suggested by Takagi and Sugeno are traditionally used. The new fuzzy model is also described by fuzzy IF-THEN rules. The core of the new fuzzy model is to express each nonlinear equation in two linear sub-equations by fuzzy IF-THEN rules and then take all the first linear sub-equations to form one linear subsystem and all the second linear sub-equations to form another linear subsystem. The overall fuzzy model of the system is achieved by fuzzy blending of this two linear subsystem models. Consider a continuous-time nonlinear dynamic system as follows:



Equation i:

rule 1:

IF  $z_i(t)$  is  $M_{i1}$   
 THEN  $\dot{x}_i(t) = A_{i1}x(t) + B_{i1}u(t)$ ,

rule 2:

IF  $z_i(t)$  is  $M_{i2}$   
 THEN  $\dot{x}_i(t) = A_{i2}x(t) + B_{i2}u(t)$ , (7-2-1)

where

$$x(t) = [x_1(t), x_2(t), \dots, x_n(t)]^T,$$

$$u(t) = [u_1(t), u_2(t), \dots, u_n(t)]^T,$$

$i = 1, 2, \dots, n$  ( $n$  is the number of nonlinear terms).  $M_{i1}, M_{i2}$  are fuzzy sets,  $A_i, B_i$  are column vectors and  $\dot{x}_i(t) = A_{ij}x(t) + B_{ij}u(t)$ ,  $j = 1, 2$ , is the output from the first and



the second IF-THEN rules. Given a pair of  $(x(t), u(t))$  and take all the first linear sub-equations to form one linear subsystem and all the second linear sub-equations to form another linear subsystem, the final output of the fuzzy system is inferred as follows:

$$\dot{x}(t) = M_1 \begin{bmatrix} A_{11}x(t) + B_{11}u(t) \\ A_{21}x(t) + B_{21}u(t) \\ \vdots \\ A_{i1}x(t) + B_{i1}u(t) \end{bmatrix} + M_2 \begin{bmatrix} A_{12}x(t) + B_{12}u(t) \\ A_{22}x(t) + B_{22}u(t) \\ \vdots \\ A_{i2}x(t) + B_{i2}u(t) \end{bmatrix} \quad (7-2-2)$$

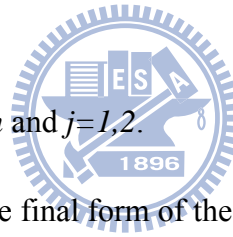
where  $M_1$  and  $M_2$  are diagonal matrices as following:

$$\text{dia}(M_1) = [M_{11} \quad M_{21} \quad \dots \quad M_{i1}], \quad \text{dia}(M_2) = [M_{12} \quad M_{22} \quad \dots \quad M_{i2}]$$

Note that for each equation i:

$$\sum_{j=1}^2 M_{ij}(z_i(t)) = 1,$$

$$M_{ij}(z_i(t)) \geq 0, \quad i = 1, 2, \dots, n \text{ and } j=1, 2.$$



Via the new fuzzy model, the final form of the fuzzy model becomes very simple.

The new model provides a much more convenient approach for fuzzy model research and fuzzy application. The simulation results of complicated chaotic systems are discussed in next Section.

### 7.3 New Fuzzy model of complicated chaotic systems

In this section, the new fuzzy models of two different chaotic systems, two-cell Quantum-CNN system and Qi system, are shown in Model 1 and Model 2. In order to investigate the convenience and effectiveness of the new fuzzy model, original T-S fuzzy model is given for comparison.

#### *Model 1: New fuzzy model of Quantum-CNN system*

For a two-cell Quantum-CNN, the following differential equations are obtained

[26]:

$$\begin{cases} \dot{x}_1 = -2a_1\sqrt{1-x_1^2} \sin x_2 \\ \dot{x}_2 = -w_1(x_1 - x_3) + 2a_1 \frac{x_1}{\sqrt{1-x_1^2}} \cos x_2 \\ \dot{x}_3 = -2a_2\sqrt{1-x_3^2} \sin x_4 \\ \dot{x}_4 = -w_2(x_3 - x_1) + 2a_2 \frac{x_3}{\sqrt{1-x_3^2}} \cos x_4 \end{cases} \quad (7-3-1)$$

where  $x_1$  and  $x_3$  are polarizations,  $x_2$  and  $x_4$  are quantum phase displacements,  $a_1$  and  $a_2$  are proportional to the inter-dot energy inside each cell and  $w_1$  and  $w_2$  are parameters that weigh effects on the cell of the difference of the polarization of neighboring cells, like the cloning templates in traditional CNNs. When  $a_1 = -0.83$ ,  $a_2 = -0.53$ ,  $w_1 = 0.5$  and  $w_2 = 0.5$  (assume two balanced cells) and initial states chosen as  $(0.001, 0.005, 0.001, 0.005)$ , the nano system is chaotic which is shown in Fig. 7-1.

If T-S fuzzy model is used for representing local linear models of Quantum-CNN nano system, there are going to be 16 fuzzy rules, 16 linear subsystems and 64 equations. The process of modeling is shown as follow:

*T-S fuzzy model:*

Assume that:

- (1)  $\sqrt{1-x_1^2} \sin x_2 \in [-Z_1, Z_1]$  and  $Z_1 > 0$ ,
- (2)  $\cos x_2 / \sqrt{1-x_1^2} \in [1+Z_2, 1-Z_2]$  and  $Z_2 > 0$ ,
- (3)  $\sqrt{1-x_3^2} \sin x_4 \in [-Z_3, Z_3]$  and  $Z_3 > 0$ ,
- (4)  $\cos x_4 / \sqrt{1-x_3^2} \in [1+Z_4, 1-Z_4]$  and  $Z_4 > 0$

Then we have the following T-S fuzzy rules:

Rule 1: IF  $\sqrt{1-x_1^2} \sin x_2$  is  $M_{11}$ ,  $\cos x_2 / \sqrt{1-x_1^2}$  is  $M_{21}$ ,  $\sqrt{1-x_3^2} \sin x_4$  is  $M_{31}$  and

$$\cos x_4 / \sqrt{1-x_3^2} \text{ is } M_{41}, \text{ THEN } \dot{X} = A_1 X.$$

Rule 2: IF  $\sqrt{1-x_1^2} \sin x_2$  is  $M_{11}$ ,  $\cos x_2 / \sqrt{1-x_1^2}$  is  $M_{21}$ ,  $\sqrt{1-x_3^2} \sin x_4$  is  $M_{31}$  and

$$\cos x_4 / \sqrt{1-x_3^2} \text{ is } M_{42}, \text{ THEN } \dot{X} = A_2 X.$$

Rule 3: IF  $\sqrt{1-x_1^2} \sin x_2$  is  $M_{11}$ ,  $\cos x_2 / \sqrt{1-x_1^2}$  is  $M_{21}$ ,  $\sqrt{1-x_3^2} \sin x_4$  is  $M_{32}$  and

$$\cos x_4 / \sqrt{1-x_3^2} \text{ is } M_{41}, \text{ THEN } \dot{X} = A_3 X.$$

Rule 4: IF  $\sqrt{1-x_1^2} \sin x_2$  is  $M_{11}$ ,  $\cos x_2 / \sqrt{1-x_1^2}$  is  $M_{21}$ ,  $\sqrt{1-x_3^2} \sin x_4$  is  $M_{32}$  and

$$\cos x_4 / \sqrt{1-x_3^2} \text{ is } M_{42}, \text{ THEN } \dot{X} = A_4 X.$$

Rule 5: IF  $\sqrt{1-x_1^2} \sin x_2$  is  $M_{11}$ ,  $\cos x_2 / \sqrt{1-x_1^2}$  is  $M_{22}$ ,  $\sqrt{1-x_3^2} \sin x_4$  is  $M_{31}$  and

$$\cos x_4 / \sqrt{1-x_3^2} \text{ is } M_{41}, \text{ THEN } \dot{X} = A_5 X.$$

Rule 6: IF  $\sqrt{1-x_1^2} \sin x_2$  is  $M_{11}$ ,  $\cos x_2 / \sqrt{1-x_1^2}$  is  $M_{22}$ ,  $\sqrt{1-x_3^2} \sin x_4$  is  $M_{31}$  and

$$\cos x_4 / \sqrt{1-x_3^2} \text{ is } M_{42}, \text{ THEN } \dot{X} = A_6 X.$$

Rule 7: IF  $\sqrt{1-x_1^2} \sin x_2$  is  $M_{11}$ ,  $\cos x_2 / \sqrt{1-x_1^2}$  is  $M_{22}$ ,  $\sqrt{1-x_3^2} \sin x_4$  is  $M_{32}$  and

$$\cos x_4 / \sqrt{1-x_3^2} \text{ is } M_{41}, \text{ THEN } \dot{X} = A_7 X.$$

Rule 8: IF  $\sqrt{1-x_1^2} \sin x_2$  is  $M_{11}$ ,  $\cos x_2 / \sqrt{1-x_1^2}$  is  $M_{22}$ ,  $\sqrt{1-x_3^2} \sin x_4$  is  $M_{32}$  and

$$\cos x_4 / \sqrt{1-x_3^2} \text{ is } M_{42}, \text{ THEN } \dot{X} = A_8 X.$$

Rule 9: IF  $\sqrt{1-x_1^2} \sin x_2$  is  $M_{12}$ ,  $\cos x_2 / \sqrt{1-x_1^2}$  is  $M_{21}$ ,  $\sqrt{1-x_3^2} \sin x_4$  is  $M_{31}$  and

$$\cos x_4 / \sqrt{1-x_3^2} \text{ is } M_{41}, \text{ THEN } \dot{X} = A_9 X.$$

Rule 10: IF  $\sqrt{1-x_1^2} \sin x_2$  is  $M_{12}$ ,  $\cos x_2 / \sqrt{1-x_1^2}$  is  $M_{21}$ ,  $\sqrt{1-x_3^2} \sin x_4$  is  $M_{31}$  and

$$\cos x_4 / \sqrt{1-x_3^2} \text{ is } M_{42}, \text{ THEN } \dot{X} = A_{10} X.$$

Rule 11: IF  $\sqrt{1-x_1^2} \sin x_2$  is  $M_{12}$ ,  $\cos x_2 / \sqrt{1-x_1^2}$  is  $M_{21}$ ,  $\sqrt{1-x_3^2} \sin x_4$  is  $M_{32}$  and  $\cos x_4 / \sqrt{1-x_3^2}$  is  $M_{41}$ , THEN  $\dot{X} = A_{11}X$ .

Rule 12: IF  $\sqrt{1-x_1^2} \sin x_2$  is  $M_{12}$ ,  $\cos x_2 / \sqrt{1-x_1^2}$  is  $M_{21}$ ,  $\sqrt{1-x_3^2} \sin x_4$  is  $M_{32}$  and  $\cos x_4 / \sqrt{1-x_3^2}$  is  $M_{42}$ , THEN  $\dot{X} = A_{12}X$ .

Rule 13: IF  $\sqrt{1-x_1^2} \sin x_2$  is  $M_{12}$ ,  $\cos x_2 / \sqrt{1-x_1^2}$  is  $M_{22}$ ,  $\sqrt{1-x_3^2} \sin x_4$  is  $M_{31}$  and  $\cos x_4 / \sqrt{1-x_3^2}$  is  $M_{41}$ , THEN  $\dot{X} = A_{13}X$ .

Rule 14: IF  $\sqrt{1-x_1^2} \sin x_2$  is  $M_{12}$ ,  $\cos x_2 / \sqrt{1-x_1^2}$  is  $M_{22}$ ,  $\sqrt{1-x_3^2} \sin x_4$  is  $M_{31}$  and  $\cos x_4 / \sqrt{1-x_3^2}$  is  $M_{42}$ , THEN  $\dot{X} = A_{14}X$ .

Rule 15: IF  $\sqrt{1-x_1^2} \sin x_2$  is  $M_{12}$ ,  $\cos x_2 / \sqrt{1-x_1^2}$  is  $M_{22}$ ,  $\sqrt{1-x_3^2} \sin x_4$  is  $M_{32}$  and  $\cos x_4 / \sqrt{1-x_3^2}$  is  $M_{41}$ , THEN  $\dot{X} = A_{15}X$ .

Rule 16: IF  $\sqrt{1-x_1^2} \sin x_2$  is  $M_{12}$ ,  $\cos x_2 / \sqrt{1-x_1^2}$  is  $M_{22}$ ,  $\sqrt{1-x_3^2} \sin x_4$  is  $M_{32}$  and  $\cos x_4 / \sqrt{1-x_3^2}$  is  $M_{42}$ , THEN  $\dot{X} = A_{16}X$ .

Then the final output of the two cells Quantum-CNN system can be composed by fuzzy linear subsystems mentioned above. It is obviously an inefficient and complicated work.

*New fuzzy model:*

By using the new fuzzy model, Quantum-CNN system can be linearized as simple linear equations. The steps of fuzzy modeling are shown as follow:

*Step of fuzzy modeling:*

*Step 1:*

Assume that  $\sqrt{1-x_1^2} \sin x_2 \in [-Z_1, Z_1]$  and  $Z_1 > 0$ , then the first equation of (7-3-1) can be exactly represented by new fuzzy model as following:

$$\text{Rule 1: IF } \sqrt{1-x_1^2} \sin x_2 \text{ is } M_{11}, \text{ THEN } \dot{x}_1 = -2a_1 Z_1, \quad (7-3-2)$$

$$\text{Rule 2: IF } \sqrt{1-x_1^2} \sin x_2 \text{ is } M_{12}, \text{ THEN } \dot{x}_1 = 2a_1 Z_1 \quad (7-3-3)$$

where

$$M_{11} = \frac{1}{2} \left( 1 + \frac{\sqrt{1-x_1^2} \sin x_2}{Z_1} \right), \quad M_{12} = \frac{1}{2} \left( 1 - \frac{\sqrt{1-x_1^2} \sin x_2}{Z_1} \right),$$

and  $Z_1 = 0.01$ .  $M_{11}$  and  $M_{12}$  are fuzzy sets of the first equation of (7-3-1) and  $M_{11} + M_{12} = 1$ .

*Step 2:*

Assume that  $\cos x_2 / \sqrt{1-x_1^2} \in [1-Z_2, 1+Z_2]$  and  $Z_2 > 0$ , then the second equation of (8-3-1) can be exactly represented by new fuzzy model as following:

$$\text{Rule 1: IF } \cos x_2 / \sqrt{1-x_1^2} \text{ is } M_{21}, \text{ THEN} \quad (7-3-4)$$

$$\dot{x}_2 = -w_1(x_1 - x_3) + 2a_1 x_1 Z_2$$

$$\text{Rule 2: IF } \cos x_2 / \sqrt{1-x_1^2} \text{ is } M_{22}, \text{ THEN} \quad (7-3-5)$$

$$\dot{x}_2 = -w_1(x_1 - x_3) - 2a_1 x_1 Z_2$$

where

$$M_{21} = \frac{1}{2} \left( 1 + \frac{\cos x_2 / \sqrt{1-x_1^2}}{Z_2} \right), \quad M_{22} = \frac{1}{2} \left( 1 - \frac{\cos x_2 / \sqrt{1-x_1^2}}{Z_2} \right),$$

and  $Z_2 = 0.01$ .  $M_{21}$  and  $M_{22}$  are fuzzy sets of the second equation of (8-3-1) and  $M_{21} + M_{22} = 1$ .

*Step 3:*

Assume that  $\sqrt{1-x_3^2} \sin x_4 \in [-Z_3, Z_3]$  and  $Z_3 > 0$ , then the third equation of

(7-3-1) can be exactly represented by new fuzzy model as following:

$$\text{Rule 1: IF } \sqrt{1-x_3^2} \sin x_4 \text{ is } M_{31}, \text{ THEN } \dot{x}_3 = -2a_2 Z_3, \quad (7-3-6)$$

$$\text{Rule 2: IF } \sqrt{1-x_3^2} \sin x_4 \text{ is } M_{32}, \text{ THEN } \dot{x}_3 = 2a_2 Z_3 \quad (7-3-7)$$

where

$$M_{31} = \frac{1}{2} \left( 1 + \frac{\sqrt{1-x_3^2} \sin x_4}{Z_3} \right), \quad M_{32} = \frac{1}{2} \left( 1 - \frac{\sqrt{1-x_3^2} \sin x_4}{Z_3} \right),$$

and  $Z_3 = 0.01$ .  $M_{31}$  and  $M_{32}$  are fuzzy sets of the third equation of (7-3-1) and  $M_{31} + M_{32} = 1$ .

*Step 4:*

Assume that  $\cos x_4 / \sqrt{1-x_3^2} \in [1-Z_4, 1+Z_4]$  and  $Z_4 > 0$ , then the fourth equation of (7-3-1) can be exactly represented by new fuzzy model as following:

$$\text{Rule 1: IF } \cos x_4 / \sqrt{1-x_3^2} \text{ is } M_{41}, \text{ THEN} \quad (7-3-8)$$

$$\dot{x}_4 = -w_2(x_3 - x_1) + 2a_2 x_3 Z_4$$

$$\text{Rule 2: IF } \cos x_4 / \sqrt{1-x_3^2} \text{ is } M_{42}, \text{ THEN} \quad (7-3-9)$$

$$\dot{x}_4 = -w_2(x_3 - x_1) - 2a_2 x_3 Z_4$$

where

$$M_{41} = \frac{1}{2} \left( 1 + \frac{\cos x_4 / \sqrt{1-x_3^2}}{Z_4} \right), \quad M_{42} = \frac{1}{2} \left( 1 - \frac{\cos x_4 / \sqrt{1-x_3^2}}{Z_4} \right),$$

and  $Z_4 = 0.01$ .  $M_{41}$  and  $M_{42}$  are fuzzy sets of the fourth equation of (7-3-1) and  $M_{41} + M_{42} = 1$ .

Here, we call (7-3-2), (7-3-4), (7-3-6) and (7-3-8) the first liner subsystem under the fuzzy rules and (7-3-3), (7-3-5), (7-3-7) and (7-3-9) the second liner subsystem under the fuzzy rules.

The first linear subsystem is

$$\begin{cases} \dot{x}_1 = -2a_1 Z_1 \\ \dot{x}_2 = -w_1(x_1 - x_3) + 2a_1 x_1 Z_2 \\ \dot{x}_3 = -2a_2 Z_3 \\ \dot{x}_4 = -w_2(x_3 - x_1) + 2a_2 x_3 Z_4 \end{cases} \quad (7-3-10)$$

The second linear subsystem is

$$\begin{cases} \dot{x}_1 = 2a_1 Z_1 \\ \dot{x}_2 = -w_1(x_1 - x_3) - 2a_1 x_1 Z_2 \\ \dot{x}_3 = 2a_2 Z_3 \\ \dot{x}_4 = -w_2(x_3 - x_1) - 2a_2 x_3 Z_4 \end{cases} \quad (7-3-11)$$

The final output of the fuzzy Quantum-CNN system is inferred as follows and the chaotic behavior of fuzzy system is shown in Fig. 7-2.

$$\begin{aligned} \begin{bmatrix} \dot{x}_1 \\ \dot{x}_2 \\ \dot{x}_3 \\ \dot{x}_4 \end{bmatrix} &= \begin{bmatrix} M_{11} & 0 & 0 & 0 \\ 0 & M_{21} & 0 & 0 \\ 0 & 0 & M_{31} & 0 \\ 0 & 0 & 0 & M_{41} \end{bmatrix} \begin{bmatrix} -2a_1 Z_1 \\ -w_1(x_1 - x_3) + 2a_1 x_1 Z_2 \\ -2a_2 Z_3 \\ -w_2(x_3 - x_1) + 2a_2 x_3 Z_4 \end{bmatrix} \\ &+ \begin{bmatrix} M_{12} & 0 & 0 & 0 \\ 0 & M_{22} & 0 & 0 \\ 0 & 0 & M_{32} & 0 \\ 0 & 0 & 0 & M_{42} \end{bmatrix} \begin{bmatrix} 2a_1 Z_1 \\ -w_1(x_1 - x_3) - 2a_1 x_1 Z_2 \\ 2a_2 Z_3 \\ -w_2(x_3 - x_1) - 2a_2 x_3 Z_4 \end{bmatrix} \end{aligned} \quad (7-3-12)$$

Eq. (7-3-12) can be rewritten as a simple mathematical expression:

$$\dot{X}(t) = \sum_{i=1}^2 \Psi_i (A_i X(t) + b_i) \quad (7-3-13)$$

where  $\Psi_i$  are diagonal matrices as follows:

$$\text{dia}(\Psi_1) = [M_{11} \quad M_{21} \quad M_{31} \quad M_{41}], \quad \text{dia}(\Psi_2) = [M_{12} \quad M_{22} \quad M_{32} \quad M_{42}]$$

$$A_1 = \begin{bmatrix} 0 & 0 & 0 & 0 \\ -w_1 + 2a_1 Z_2 & 0 & w_1 & 0 \\ 0 & 0 & 0 & 0 \\ w_2 & 0 & -w_2 + 2a_2 Z_4 & 0 \end{bmatrix}, \quad b_1 = \begin{bmatrix} -2a_1 Z_1 \\ 0 \\ -2a_2 Z_3 \\ 0 \end{bmatrix}$$

$$A_2 = \begin{bmatrix} 0 & 0 & 0 & 0 \\ -w_1 - 2a_1Z_2 & 0 & w_1 & 0 \\ 0 & 0 & 0 & 0 \\ w_2 & 0 & -w_2 - 2a_2Z_4 & 0 \end{bmatrix}, \quad b_2 = \begin{bmatrix} 2a_1Z_1 \\ 0 \\ 2a_2Z_3 \\ 0 \end{bmatrix}$$

Via using new fuzzy model, the number of fuzzy rules in fuzzy Quantum-CNN system can be reduced from  $2^4$  to  $2 \times 4$  and only two subsystems can express such complex chaotic behaviors. The simulation results are perfectly the same to the original chaotic behavior of the Quantum-CNN system.

### ***Model 2: New fuzzy model of Qi system***

The four-order autonomous Qi system:

$$\begin{cases} \dot{y}_1 = a_3(y_2 - y_1) + y_2y_3y_4 \\ \dot{y}_2 = b_3(y_1 + y_2) - y_1y_3y_4 \\ \dot{y}_3 = -c_3y_3 + y_1y_2y_4 \\ \dot{y}_4 = -d_3y_4 + y_1y_2y_3 \end{cases} \quad (7-3-14)$$

where  $y_1, y_2, y_3$  and  $y_4$  are the state variables of the system and  $a_3, b_3, c_3$  and  $d_3$  are all positive real parameters. This Qi system in Eq. (7-3-14) was recently introduced by Qi et al. [20] and it has been shown complex dynamical behavior including the familiar period-doubling route to chaos as well as Hopf bifurcations. For the system parameters:  $a_3=35, b_3=10, c_3=1, d_3=10$  and initial conditions  $(y_{10}, y_{20}, y_{30}, y_{40}) = (2, 5, 2, 5)$ , the Qi model exhibits chaotic motion which is shown in Fig. 7-3

First of all, T-S fuzzy model is used for representing local linear models of Qi system. The process of modeling is shown as follow:

*T-S fuzzy model:*

Assume that:

- (1)  $y_3y_4 \in [-Z_5, Z_5]$  and  $Z_5 > 0$ ,
- (2)  $y_1y_2 \in [-Z_6, Z_6]$  and  $Z_6 > 0$ ,



Then we have the following T-S fuzzy rules:

Rule 1: IF  $y_3y_4$  is  $N_{11}$  and  $y_1y_2$  is  $N_{21}$ , THEN  $\dot{Y} = C_1Y$ .

Rule 2: IF  $y_3y_4$  is  $N_{11}$  and  $y_1y_2$  is  $N_{22}$ , THEN  $\dot{Y} = C_2Y$ .

Rule 3: IF  $y_3y_4$  is  $N_{12}$  and  $y_1y_2$  is  $N_{21}$ , THEN  $\dot{Y} = C_3Y$ .

Rule 4: IF  $y_3y_4$  is  $N_{12}$  and  $y_1y_2$  is  $N_{22}$ , THEN  $\dot{Y} = C_4Y$ .

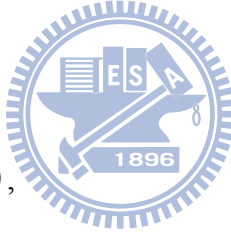
Then the final output of the Qi system can be composed by fuzzy linear subsystems mentioned above. There are 4 linear subsystems and 16 equations in this T-S fuzzy Qi system.

*Novel fuzzy model:*

Assume that:

(1)  $y_3y_4 \in [-Z_5, Z_5]$  and  $Z_5 > 0$ ,

(2)  $y_1y_2 \in [-Z_6, Z_6]$  and  $Z_6 > 0$ ,



then we have the following T-S fuzzy rules:

Rule 1: IF  $y_3y_4$  is  $N_{11}$ , THEN 
$$\begin{aligned} \dot{y}_1 &= a_3(y_2 - y_1) + (c + Z_5)y_2 \\ \dot{y}_2 &= b_3(y_1 + y_2) - (c + Z_5)y_1 \end{aligned} \quad (7-3-15)$$

Rule 2: IF  $y_3y_4$  is  $N_{12}$ , THEN 
$$\begin{aligned} \dot{y}_1 &= a_3(y_2 - y_1) + (c - Z_5)Z_5y_2 \\ \dot{y}_2 &= b_3(y_1 + y_2) - (c - Z_5)y_1 \end{aligned} \quad (7-3-16)$$

where

$$N_{11} = \frac{1}{2} \left( 1 + \frac{y_3y_4 - c}{Z_5} \right), \quad N_{12} = \frac{1}{2} \left( 1 - \frac{y_3y_4 - c}{Z_5} \right) \quad \text{and} \quad c = 20$$

and

Rule 1: IF  $y_1y_2$  is  $N_{21}$ , THEN 
$$\begin{aligned} \dot{y}_3 &= -c_3y_3 + Z_6y_4 \\ \dot{y}_4 &= -d_3y_4 + Z_6y_3 \end{aligned} \quad (7-3-17)$$

Rule 2: IF  $y_1y_2$  is  $N_{22}$ , THEN 
$$\begin{aligned} \dot{y}_3 &= -c_3y_3 - Z_6y_4 \\ \dot{y}_4 &= -d_3y_4 - Z_6y_3 \end{aligned} \quad (7-3-18)$$

where

$$N_{21} = \frac{1}{2} \left(1 + \frac{y_1 y_2}{Z_6}\right), \quad N_{22} = \frac{1}{2} \left(1 - \frac{y_1 y_2}{Z_6}\right).$$

in Eqs. (7-3-15) ~ (7-3-18),  $Z_5 = 80$  and  $Z_6 = 50$ .  $N_{11}, N_{12}, N_{21}$  and  $N_{22}$  are fuzzy sets and  $N_{11} + N_{12} = 1, N_{21} + N_{22} = 1$ .

Here, we call (7-3-15) and (7-3-17) the first liner subsystem under the fuzzy rules and (7-3-16) and (7-3-18) the second liner subsystem under the fuzzy rules.

The first linear subsystem is

$$\begin{cases} \dot{y}_1 = a_3(y_2 - y_1) + (c + Z_5)y_2 \\ \dot{y}_2 = b_3(y_1 + y_2) - (c + Z_5)y_1 \\ \dot{y}_3 = -c_3y_3 + Z_6y_4 \\ \dot{y}_4 = -d_3y_4 + Z_6y_3 \end{cases} \quad (7-3-19)$$

The second linear subsystem is

$$\begin{cases} \dot{y}_1 = a_3(y_2 - y_1) + (c - Z_5)y_2 \\ \dot{y}_2 = b_3(y_1 + y_2) - (c - Z_5)y_1 \\ \dot{y}_3 = -c_3y_3 - Z_6y_4 \\ \dot{y}_4 = -d_3y_4 - Z_6y_3 \end{cases} \quad (7-3-20)$$



The final output of the fuzzy Qi system is inferred as follows and the chaotic behavior of fuzzy system is shown in Fig. 7-4.

$$\begin{aligned} \begin{bmatrix} \dot{y}_1 \\ \dot{y}_2 \\ \dot{y}_3 \\ \dot{y}_4 \end{bmatrix} &= \begin{bmatrix} N_{11} & 0 & 0 & 0 \\ 0 & N_{11} & 0 & 0 \\ 0 & 0 & N_{21} & 0 \\ 0 & 0 & 0 & N_{21} \end{bmatrix}^T \begin{bmatrix} a_3(y_2 - y_1) + (c + Z_5)y_2 \\ b_3(y_1 + y_2) - (c + Z_5)y_1 \\ -c_3y_3 + Z_6y_4 \\ -d_3y_4 + Z_6y_3 \end{bmatrix} \\ &+ \begin{bmatrix} N_{12} & 0 & 0 & 0 \\ 0 & N_{12} & 0 & 0 \\ 0 & 0 & N_{22} & 0 \\ 0 & 0 & 0 & N_{22} \end{bmatrix}^T \begin{bmatrix} a_3(y_2 - y_1) + (c - Z_5)Z_5y_2 \\ b_3(y_1 + y_2) - (c - Z_5)y_1 \\ -c_3y_3 - Z_6y_4 \\ -d_3y_4 - Z_6y_3 \end{bmatrix} \end{aligned} \quad (7-3-21)$$

Eq. (7-3-21) can be rewritten as a simple mathematical expression:

$$\dot{Y}(t) = \sum_{i=1}^2 \Gamma_i (C_i Y(t) + \tilde{c}_i) \quad (7-3-22)$$

where

$$\text{dia}(\Gamma_1) = [N_{11} \quad N_{11} \quad N_{21} \quad N_{21}], \quad \text{dia}(\Gamma_2) = [N_{12} \quad N_{12} \quad N_{22} \quad N_{22}]$$

$$C_1 = \begin{bmatrix} -a_3 & c + Z_5 + a_3 & 0 & 0 \\ -c - Z_5 + b_3 & b_3 & 0 & 0 \\ 0 & 0 & -c_3 & Z_6 \\ 0 & 0 & Z_6 & -d_3 \end{bmatrix}, \quad \tilde{c}_1 = \begin{bmatrix} 0 \\ 0 \\ 0 \\ 0 \end{bmatrix}$$

$$C_2 = \begin{bmatrix} -a_3 & c - Z_5 + a_3 & 0 & 0 \\ -c + Z_5 + b_3 & b_3 & 0 & 0 \\ 0 & 0 & -c_3 & -Z_6 \\ 0 & 0 & -Z_6 & -d_3 \end{bmatrix}, \quad \tilde{c}_2 = \begin{bmatrix} 0 \\ 0 \\ 0 \\ 0 \end{bmatrix}$$

Via using new fuzzy model, two linear subsystems are enough to express such complex chaotic behaviors. The simulation results are perfectly the same to the original chaotic behavior of the Qi system.

## 7.4 Fuzzy synchronization scheme

In this Section, we are going to derive the new fuzzy synchronization scheme for two identical and totally different chaotic systems based on our new fuzzy model.

***For two identical chaotic systems:***

Given the following fuzzy systems as the master and slave systems,

master system:

$$\dot{X}(t) = \sum_{i=1}^2 \Psi_i(A_i X(t) + \tilde{b}_i) \quad (7-4-1)$$

slave system:

$$\dot{Y}(t) = \sum_{i=1}^2 \tilde{\Psi}_i(A_i Y(t) + b_i) + BU(t) \quad (7-4-2)$$

Eq. (7-4-1) and Eq. 7-4-2) represent the same chaotic Quantum-CNN systems with different initial conditions, and Eq. (7-4-2) has control input  $U(t)$ . Define the error signal as  $e(t) = X(t) - Y(t)$ , we have:

$$\dot{e}(t) = \dot{X}(t) - \dot{Y}(t) = \sum_{i=1}^2 \Psi_i(A_i X(t) + b_i) - \sum_{i=1}^2 \tilde{\Psi}_i(A_i Y(t) + b_i) - BU(t) \quad (7-4-3)$$

The fuzzy controllers are designed as follow:

$$U(t) = u_1(t) + u_2(t) \quad (7-4-4)$$

Where

$$u_1(t) = \sum_{i=1}^2 \Psi_i F_i X(t) - \sum_{i=1}^2 \tilde{\Psi}_i F_i Y(t)$$

$$u_2(t) = \sum_{i=1}^2 E_i(\Psi_i, \tilde{\Psi}_i) b_i, \quad E_i(\Psi_i, \tilde{\Psi}_i) = \Psi_i - \tilde{\Psi}_i$$

such that  $\|e(t)\| \rightarrow 0$  as  $t \rightarrow \infty$ . The design is to determine the feedback gains  $F_i$ . By substituting  $U(t)$  into (7-4-3), we obtain:

$$\dot{e}(t) = \sum_{i=1}^2 \Psi_i \{(A_i - BF_i)X(t)\} - \sum_{i=1}^2 \tilde{\Psi}_i \{(A_i - BF_i)Y(t)\} \quad (7-4-5)$$

**Theorem 7-1:** The error system in Eq. (7-4-5) is asymptotically stable and the slave system in Eq. (7-4-2) can synchronize the master system in Eq. (7-4-1) under the fuzzy controller in Eq. (7-4-4) if the following conditions can be satisfied:

$$H = (A_i - BF_i) = (A_i - BF_i) < 0, \quad i=1-2. \quad (7-4-6)$$

*Proof:*

The errors in Eq. (7-4-5) can be exactly linearized via the fuzzy controllers in Eq. (7-4-4) if there exist the feedback gains  $F_i$  such that

$$(A_i - BF_i) = (A_2 - BF_2) < 0. \quad (7-4-7)$$

Then the overall control system is linearized as

$$\dot{e}(t) = Ge(t), \quad (7-4-8)$$

where  $G = (A_i - BF_i) = (A_2 - BF_2) < 0$ .

As a consequence, the error system (7-4-5) via the fuzzy controller (7-4-4) can be asymptotically stable.

***For two totally different chaotic systems:***

Given the following fuzzy systems as the master and slave systems,  
master system:

$$\dot{X}(t) = \sum_{i=1}^2 \Psi_i (A_i X(t) + \tilde{b}_i) \quad (7-4-9)$$

slave system:

$$\dot{Y}(t) = \sum_{i=1}^2 \Gamma_i (C_i Y(t) + \tilde{c}_i) + BU(t) \quad (7-4-10)$$

Eq. (7-4-9) and Eq. (7-4-10) represent the two different chaotic systems, and Eq. (7-4-10) has control input  $U(t)$ . Define the error signal as  $e(t) = X(t) - Y(t)$ , we have:

$$\dot{e}(t) = \dot{X}(t) - \dot{Y}(t) = \sum_{i=1}^2 \Psi_i (A_i X(t) + \tilde{b}_i) - \sum_{i=1}^2 \Gamma_i (C_i Y(t) + \tilde{c}_i) - BU(t) \quad (7-4-11)$$

The fuzzy controllers are designed as follow:

$$U(t) = u_1(t) + u_2(t) \quad (7-4-12)$$

Where

$$u_1(t) = \sum_{i=1}^2 \Psi_i F_i X(t) - \sum_{i=1}^2 \Gamma_i P_i Y(t),$$

$$u_2(t) = \sum_{i=1}^2 \Psi_i \tilde{b}_i - \sum_{i=1}^2 \Gamma_i \tilde{c}_i$$

such that  $\|e(t)\| \rightarrow 0$  as  $t \rightarrow \infty$ . The design is to determine the feedback gains  $F_i$  and  $P_i$ .

By substituting  $U(t)$  into (7-4-11), we obtain:

$$\dot{e}(t) = \sum_{i=1}^2 \Psi_i \{(A_i - BF_i)X(t)\} - \sum_{i=1}^2 \Gamma_i \{(C_i - BP_i)Y(t)\} \quad (7-4-13)$$

**Theorem 7-2:** The error system in Eq. (7-4-13) is asymptotically stable and the slave system in Eq. (7-4-10) can synchronize the master system in Eq. (7-4-9) under the fuzzy controller in Eq. (7-4-12) if the following conditions below can be satisfied:

$$G = (A_1 - BF_1) = (A_2 - BF_2) = (C_1 - BP_1) < 0, \quad i=1 \sim 2. \quad (7-4-14)$$

*Proof:*

The errors in Eq. (9-3-5) can be exactly linearized via the fuzzy controllers in Eq. (7-4-12) if there exist the feedback gains  $F_i$  such that

$$(A_1 - BF_1) = (A_2 - BF_2) = (C_1 - BP_1) = (C_2 - BP_2) < 0. \quad (7-4-15)$$

Then the overall control system is linearized as

$$\dot{e}(t) = Ge(t), \quad (7-4-16)$$

where  $G = (A_1 - BF_1) = (A_2 - BF_2) = (C_1 - BP_1) = (C_2 - BP_2) < 0$ .

As a consequence, the error system (7-4-13) linearized via the fuzzy controller (7-4-12) can be asymptotically stable.

## 7.5 Simulation results

In this section, we are going to achieve fuzzy synchronization of two chaotic Quantum-CNN systems and two totally different chaotic system, Quantum-CNN and Qi systems, via using the new scheme which is given in section 7.4.

*For two identical chaotic systems:*

Eq. (7-3-13) is chosen as the master system and the following fuzzy controlled Quantum-CNN system is the slave system with different initial conditions (1, 5, 1, 5).

$$\dot{Y}(t) = \sum_{i=1}^2 \tilde{\Psi}_i (A_i Y(t) + b_i) + BU(t) \quad (7-5-1)$$

where  $\tilde{\Psi}_i$  are diagonal matrices as follows:

$$\text{dia}(\tilde{\Psi}_1) = [\tilde{M}_{11} \quad \tilde{M}_{21} \quad \tilde{M}_{31} \quad \tilde{M}_{41}], \quad \text{dia}(\tilde{\Psi}_2) = [\tilde{M}_{12} \quad \tilde{M}_{22} \quad \tilde{M}_{32} \quad \tilde{M}_{42}]$$

$$A_1 = \begin{bmatrix} 0 & 0 & 0 & 0 \\ -w_1 + 2a_1 Z_2 & 0 & w_1 & 0 \\ 0 & 0 & 0 & 0 \\ w_2 & 0 & -w_2 + 2a_2 Z_4 & 0 \end{bmatrix}, \quad b_1 = \begin{bmatrix} -2a_1 Z_1 \\ 0 \\ -2a_2 Z_3 \\ 0 \end{bmatrix}$$

$$A_2 = \begin{bmatrix} 0 & 0 & 0 & 0 \\ -w_1 - 2a_1 Z_2 & 0 & w_1 & 0 \\ 0 & 0 & 0 & 0 \\ w_2 & 0 & -w_2 - 2a_2 Z_4 & 0 \end{bmatrix}, \quad b_2 = \begin{bmatrix} 2a_1 Z_1 \\ 0 \\ 2a_2 Z_3 \\ 0 \end{bmatrix}$$

The error and error dynamics are:

$$\begin{bmatrix} e_1 \\ e_2 \\ e_3 \\ e_4 \end{bmatrix} = \begin{bmatrix} x_1 - y_1 \\ x_2 - y_2 \\ x_3 - y_3 \\ x_4 - y_4 \end{bmatrix},$$

$$\begin{bmatrix} \dot{e}_1 \\ \dot{e}_2 \\ \dot{e}_3 \\ \dot{e}_4 \end{bmatrix} = \begin{bmatrix} \dot{x}_1 - \dot{y}_1 \\ \dot{x}_2 - \dot{y}_2 \\ \dot{x}_3 - \dot{y}_3 \\ \dot{x}_4 - \dot{y}_4 \end{bmatrix} = \sum_{i=1}^2 \Psi_i (A_i X(t) + b_i) - \sum_{i=1}^2 \tilde{\Psi}_i (A_i Y(t) + b_i) - BU(t) \quad (7-5-2)$$

B is chosen as identity matrix and the fuzzy controllers in Eq. (7-4-4) are used:

$$\begin{bmatrix} \dot{e}_1 \\ \dot{e}_2 \\ \dot{e}_3 \\ \dot{e}_4 \end{bmatrix} = \Psi_1 [A_1 - BF_1]_{4 \times 4} \begin{bmatrix} x_1 \\ x_2 \\ x_3 \\ x_4 \end{bmatrix} + \Psi_2 [A_2 - BF_2]_{4 \times 4} \begin{bmatrix} x_1 \\ x_2 \\ x_3 \\ x_4 \end{bmatrix} - \tilde{\Psi}_1 [A_1 - BF_1]_{4 \times 4} \begin{bmatrix} y_1 \\ y_2 \\ y_3 \\ y_4 \end{bmatrix} - \tilde{\Psi}_2 [A_2 - BF_2]_{4 \times 4} \begin{bmatrix} y_1 \\ y_2 \\ y_3 \\ y_4 \end{bmatrix} \quad (7-5-3)$$

According to Theorem 1, we have  $H = [A_1 - BF_1] = [A_2 - BF_2] < 0$ . H is chosen as:

$$H = \begin{bmatrix} -1 & 0 & 0 & 0 \\ 0 & -1 & 0 & 0 \\ 0 & 0 & -1 & 0 \\ 0 & 0 & 0 & -1 \end{bmatrix} \quad (7-5-4)$$

Thus, the feedback gains  $F_1$  and  $F_2$  can be determined by the following equation:

$$F_1 = B^{-1} [A_1 - H] = \begin{bmatrix} 1.0000 & 0 & 0 & 0 \\ -0.5166 & 1.0000 & 0.5000 & 0 \\ 0 & 0 & 1.0000 & 0 \\ 0.5000 & 0 & -0.5106 & 1.0000 \end{bmatrix}$$

$$F_2 = B^{-1} [A_2 - H] = \begin{bmatrix} 1.0000 & 0 & 0 & 0 \\ -0.4834 & 1.0000 & 0.5000 & 0 \\ 0 & 0 & 1.0000 & 0 \\ 0.5000 & 0 & -0.4894 & 1.0000 \end{bmatrix} \quad (7-5-5)$$

The synchronization errors are shown in Fig. 7-5. It is clear that the error dynamics system has already achieved asymptotically stable.

***For two totally different chaotic systems:***

Via T-S fuzzy model, different chaotic systems may be transformed into different fuzzy chaotic systems with different number of subsystems. However, when it comes to synchronization of two totally different chaotic systems, the traditional method - employing the idea of PDC to design the fuzzy control law for stabilization of the error dynamics is not work. This is due to different number of subsystems. As a result, through the new fuzzy model, there are only two subsystems in fuzzy Qi system and fuzzy Quantum-CNN system and the idea of PDC and LMI-based synchronization can be applied to. .

The fuzzy Quantum-CNN system in Eq. (7-3-13) is chosen as the master system and the fuzzy slave system, Qi system, with fuzzy controllers is as follow:

$$\dot{Y}(t) = \sum_{i=1}^2 \Gamma_i C_i Y(t) + BU(t) \quad (7-5-6)$$

where  $\Gamma_i$  are diagonal matrices

$$\text{dia}(\Gamma_1) = [N_{11} \quad N_{11} \quad N_{21} \quad N_{21}], \quad \text{dia}(\Gamma_2) = [N_{12} \quad N_{12} \quad N_{22} \quad N_{22}]$$

and

$$C_1 = \begin{bmatrix} -a_3 & c + Z_5 + a_3 & 0 & 0 \\ -c - Z_5 + b_3 & b_3 & 0 & 0 \\ 0 & 0 & -c_3 & Z_6 \\ 0 & 0 & Z_6 & -d_3 \end{bmatrix},$$

$$C_2 = \begin{bmatrix} -a_3 & c - Z_5 + a_3 & 0 & 0 \\ -c + Z_5 + b_3 & b_3 & 0 & 0 \\ 0 & 0 & -c_3 & -Z_6 \\ 0 & 0 & -Z_6 & -d_3 \end{bmatrix}.$$

Therefore, the error and error dynamics are:



$$\begin{bmatrix} e_1 \\ e_2 \\ e_3 \\ e_4 \end{bmatrix} = \begin{bmatrix} x_1 - y_1 \\ x_2 - y_2 \\ x_3 - y_3 \\ x_4 - y_4 \end{bmatrix},$$

$$\begin{bmatrix} \dot{e}_1 \\ \dot{e}_2 \\ \dot{e}_3 \\ \dot{e}_4 \end{bmatrix} = \begin{bmatrix} \dot{x}_1 - \dot{y}_1 \\ \dot{x}_2 - \dot{y}_2 \\ \dot{x}_3 - \dot{y}_3 \\ \dot{x}_4 - \dot{y}_4 \end{bmatrix} = \sum_{i=1}^2 \Psi_i (A_i X(t) + \tilde{b}_i) - \sum_{i=1}^2 \Gamma_i C_i Y(t) - BU(t) \quad (7-5-7)$$

B is chosen as identity matrix and the fuzzy controllers in Eq. (7-4-12) are used:

$$\begin{bmatrix} \dot{e}_1 \\ \dot{e}_2 \\ \dot{e}_3 \\ \dot{e}_4 \end{bmatrix} = \Psi_1 [A_1 - BF_1]_{4 \times 4} \begin{bmatrix} x_1 \\ x_2 \\ x_3 \\ x_4 \end{bmatrix} + \Psi_2 [A_2 - BF_2]_{4 \times 4} \begin{bmatrix} x_1 \\ x_2 \\ x_3 \\ x_4 \end{bmatrix} - \Gamma_1 [C_1 - BF_1]_{4 \times 4} \begin{bmatrix} y_1 \\ y_2 \\ y_3 \\ y_4 \end{bmatrix} - \Gamma_2 [C_2 - BF_2]_{4 \times 4} \begin{bmatrix} y_1 \\ y_2 \\ y_3 \\ y_4 \end{bmatrix} \quad (7-5-8)$$

According to Theorem 1, we have  $G = [A_1 - BF_1] = [A_2 - BF_2] = [C_1 - BF_1] = [C_2 - BF_2] < 0$ . G is chosen as:

$$G = \begin{bmatrix} -1 & 0 & 0 & 0 \\ 0 & -1 & 0 & 0 \\ 0 & 0 & -1 & 0 \\ 0 & 0 & 0 & -1 \end{bmatrix} \quad (7-5-9)$$

Thus, the feedback gains  $F_1$ ,  $F_2$ ,  $P_1$  and  $P_2$  can be determined by the following equation:

$$F_1 = B^{-1} [A_1 - G] = \begin{bmatrix} 1.0000 & 0 & 0 & 0 \\ 22.500 & 1.0000 & 4.7000 & 0 \\ 0 & 0 & 1.0000 & 0 \\ 3.9000 & 0 & 9.0000 & 1.0000 \end{bmatrix}$$

$$\begin{aligned}
F_2 = B^{-1}[A_2 - G] &= \begin{bmatrix} 1.0000 & 0 & 0 & 0 \\ -31.90 & 1.0000 & 4.7000 & 0 \\ 0 & 0 & 1.0000 & 0 \\ 3.9 & 0 & -16.80 & 1.0000 \end{bmatrix} \\
P_1 = B^{-1}[C_1 - G] &= \begin{bmatrix} -34 & 135 & 0 & 0 \\ -90 & 11 & 0 & 0 \\ 0 & 0 & 0 & 50 \\ 0 & 0 & 50 & -9 \end{bmatrix} \\
P_2 = B^{-1}[C_2 - G] &= \begin{bmatrix} -34 & 25 & 0 & 0 \\ 70 & 11 & 0 & 0 \\ 0 & 0 & 0 & -50 \\ 0 & 0 & -50 & -9 \end{bmatrix}
\end{aligned} \tag{7-5-10}$$

The synchronization errors are shown in Fig. 7-6. It is clear that the error dynamics system has already achieved asymptotically stable.

## 7.6 Implementation of electronic circuits by series expansion method

In this section, the implementations of chaotic Quantum-CNN systems on electronic circuits are presented. While Quantum-CNN system is a complicated nonlinear system, there are too more nonlinear terms in its mathematical equations, such as radical terms, square terms, sin and cos terms, etc. Implementing such a complicated system in electronic circuits without any simplified process is really impossible. The Quantum-CNN system is definitely simplified to a simpler form via our new fuzzy model, but there are still some nonlinear terms, especially the radical terms, contained in the membership functions (The same problems are also existed in T-S fuzzy model). As a result, a new approach (which is called *series expansion form*) is given in this section to approximately implement the Quantum-CNN systems on electronic circuits.

Eq. (7-3-1) is rewritten as:

$$\begin{cases} \dot{x}_1 = -2a_1 m_1 \\ \dot{x}_2 = -w_1(x_1 - x_3) + 2a_1 x_1 m_2 \\ \dot{x}_3 = -2a_2 m_1 \\ \dot{x}_4 = -w_2(x_3 - x_1) + 2a_2 x_3 m_4 \end{cases} \quad (7-6-1)$$

where  $m_1, m_2, m_3$  and  $m_4$  are the nonlinear terms in Q-CNN system which are shown in Eq. (7-6-2) as follow:

$$\begin{bmatrix} m_1 \\ m_2 \\ m_3 \\ m_4 \end{bmatrix} = \begin{bmatrix} \sqrt{1-x_1^2} \sin x_2 \\ \cos x_2 / \sqrt{1-x_1^2} \\ \sqrt{1-x_3^2} \sin x_4 \\ \cos x_4 / \sqrt{1-x_3^2} \end{bmatrix} \quad (7-6-2)$$

In order to approximately simulate the complicated Quantum-CNN system, we expand the right-hand sides of Eq. (7-6-2) into power series:

$$\begin{bmatrix} m_1 \\ m_2 \\ m_3 \\ m_4 \end{bmatrix} = \begin{bmatrix} -\frac{1}{2}x_1^2 x_2 + \frac{1}{12}x_1^2 x_2^3 - \frac{1}{8}x_1^4 x_2 + x_2 - \frac{1}{6}x_2^3 + \frac{1}{120}x_2^5 + \dots \\ x_1 - \frac{1}{2}x_1 x_2^2 + \frac{1}{24}x_1 x_2^4 + \frac{1}{2}x_1^3 - \frac{1}{4}x_1^3 x_2^2 + \frac{5}{8}x_1^5 + \dots \\ -\frac{1}{2}x_3^2 x_4 + \frac{1}{12}x_3^2 x_4^3 - \frac{1}{8}x_3^4 x_4 + x_4 - \frac{1}{6}x_4^3 + \frac{1}{120}x_4^5 + \dots \\ x_3 - \frac{1}{2}x_3 x_4^2 + \frac{1}{24}x_3 x_4^4 + \frac{1}{2}x_3^3 - \frac{1}{4}x_3^3 x_4^2 + \frac{5}{8}x_3^5 + \dots \end{bmatrix} \quad (7-6-3)$$

It is well-known [27] that necessary and sufficient condition for the convergence of the infinite series:

$$u_1 + u_2 + \dots + u_n + \dots \quad (7-6-4)$$

is that for any previously assigned positive  $\varepsilon$ , there exists an  $N$  such that, for any  $n > N$  and for positive  $p$ ,

$$|u_{n+1} + u_{n+2} + \dots + u_{n+p}| < \varepsilon \quad (7-6-5)$$

From Fig. 1, we know that

$$|x_i| < 1, \quad i=1 \sim 4, \quad (7-6-6)$$

therefore, series in Eq. (7-6-3) which satisfy condition in Eq. 7-6-5), are convergent and has a bounded sum.

Due to the values of the states in Quantum-CNN nano systems and the behaviors of nonlinear terms are smaller than 1, the high order terms can be ignored reasonably. In order to show the feasibility of the series expansion form with neglecting high order terms, three cases are proposed to investigate the accuracy of our method.

*Case 1:* Considering the order of the term  $\leq 6$ . Then the nonlinear terms are:

$$\begin{bmatrix} m_1 \\ m_2 \\ m_3 \\ m_4 \end{bmatrix} = \begin{bmatrix} -\frac{1}{2}x_1^2x_2 + \frac{1}{12}x_1^2x_2^3 - \frac{1}{8}x_1^4x_2 + x_2 - \frac{1}{6}x_2^3 + \frac{1}{120}x_2^5 \\ x_1 - \frac{1}{2}x_1x_2^2 + \frac{1}{24}x_1x_2^4 + \frac{1}{2}x_1^3 - \frac{1}{4}x_1^3x_2^2 + \frac{5}{8}x_1^5 \\ -\frac{1}{2}x_3^2x_4 + \frac{1}{12}x_3^2x_4^3 - \frac{1}{8}x_3^4x_4 + x_4 - \frac{1}{6}x_4^3 + \frac{1}{120}x_4^5 \\ x_3 - \frac{1}{2}x_3x_4^2 + \frac{1}{24}x_3x_4^4 + \frac{1}{2}x_3^3 - \frac{1}{4}x_3^3x_4^2 + \frac{5}{8}x_3^5 \end{bmatrix} \quad (7-6-7)$$

By Substituting Eq. (7-6-7) into Eq. (7-6-1), an approximate series expansion form of chaotic Quantum-CNN system is obtained. The simulation results in MATLAB are shown in Fig. 7-7. Fig. 7-7 gives the projections of phase portraits of Quantum-CNN system in Case 1.



*Case 2:* Considering the order of the term  $\leq 3$ . Then the nonlinear terms are:

$$\begin{bmatrix} m_1 \\ m_2 \\ m_3 \\ m_4 \end{bmatrix} = \begin{bmatrix} -\frac{1}{2}x_1^2x_2 + x_2 - \frac{1}{6}x_2^3 \\ x_1 - \frac{1}{2}x_1x_2^2 + \frac{1}{2}x_1^3 \\ -\frac{1}{2}x_3^2x_4 + x_4 - \frac{1}{6}x_4^3 \\ x_3 - \frac{1}{2}x_3x_4^2 + \frac{1}{2}x_3^3 \end{bmatrix} \quad (7-6-8)$$

By Substituting Eq. (7-6-8) into Eq. (7-6-1), an approximate series expansion form of chaotic Quantum-CNN system is obtained. The simulation results in MATLAB are shown in Fig. 7-8. Fig. 7-8 gives the projections of phase portraits of Quantum-CNN system in Case 2.

*Case 3:* Considering the order of the term  $\leq 1$ . Then the nonlinear terms are:

$$\begin{bmatrix} \mathbf{m}_1 \\ \mathbf{m}_2 \\ \mathbf{m}_3 \\ \mathbf{m}_4 \end{bmatrix} = \begin{bmatrix} x_2 \\ x_1 \\ x_4 \\ x_3 \end{bmatrix} \quad (7-6-9)$$

By Substituting Eq. (7-6-9) into Eq. (7-6-1), an approximate series expansion form of chaotic Quantum-CNN system is obtained. The simulation results in MATLAB are shown in Fig. 7-9. Fig. 7-9 gives the projections of phase portraits of Quantum-CNN system in Case 3.

Through observing Case 1, Case 2 and Case 3, it is clear that using the series expansion form can approximately realize the original chaotic motion of Quantum-CNN nano system with acceptable errors via ignoring the order of the terms  $> 1$  as well. As a consequence, the model in Case 3 is decided to use for implementation of electronic circuits of chaotic Quantum-CNN nano system. The chaotic motion of Quantum-CNN system and the configuration of electronic circuits are shown in Fig. 7-10 and Fig. 7-11.

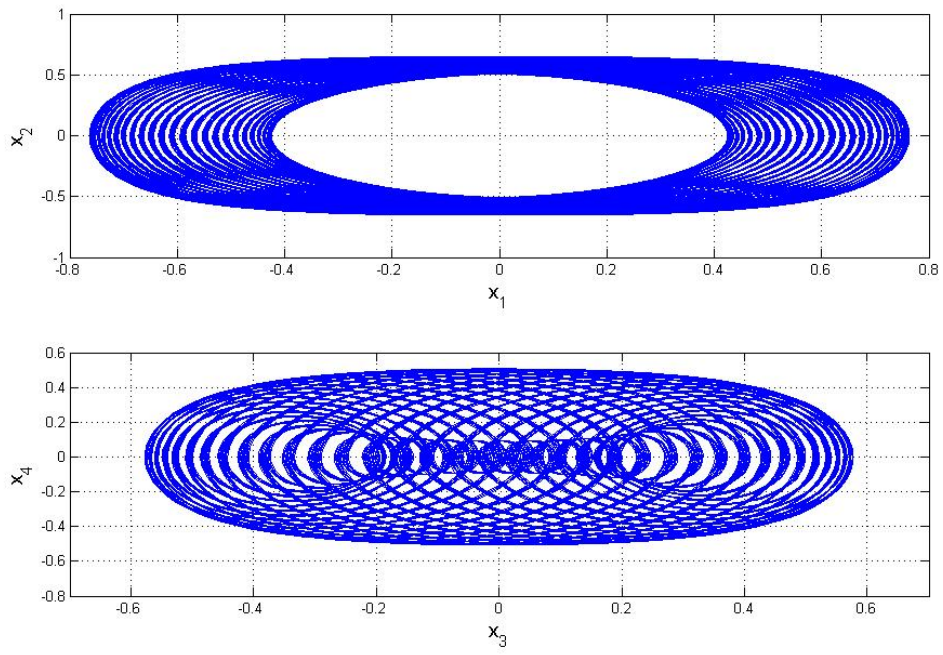


Fig. 7-1. Chaotic behavior of Q-CNN system.

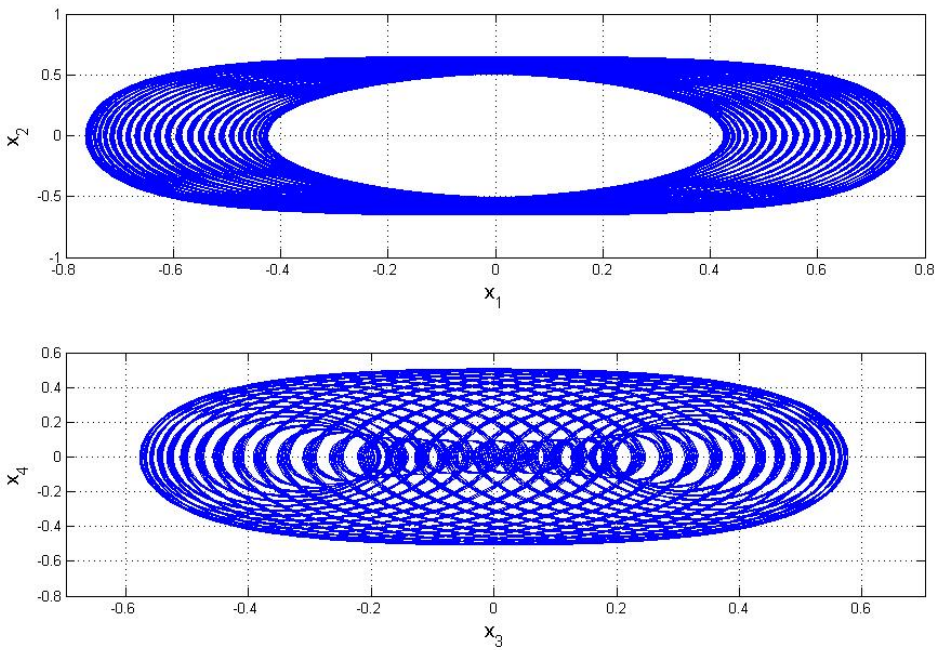


Fig. 7-2. Chaotic behavior of new fuzzy Q-CNN system.

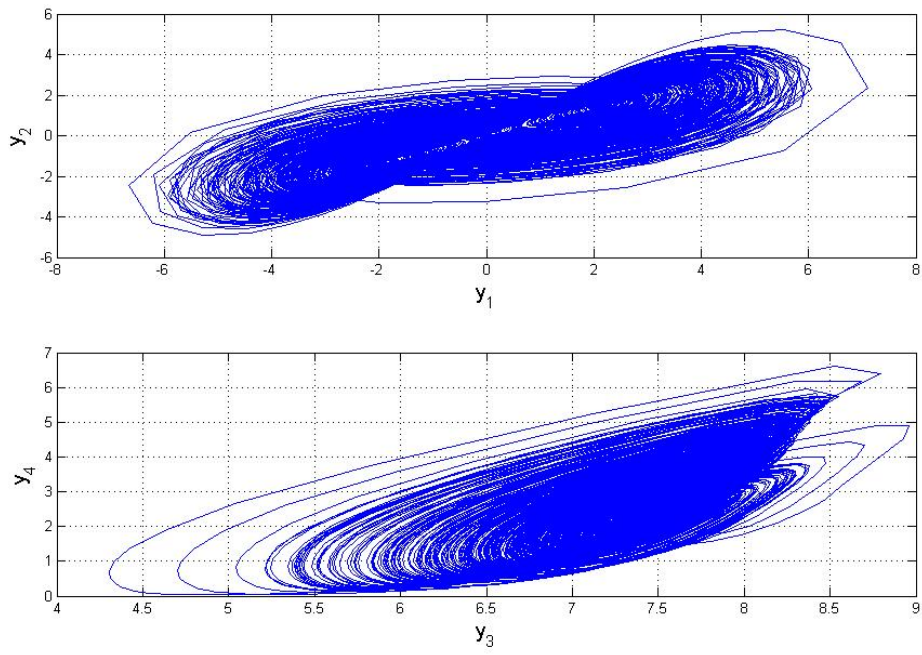


Fig. 7-3. Chaotic behavior of Qi system.

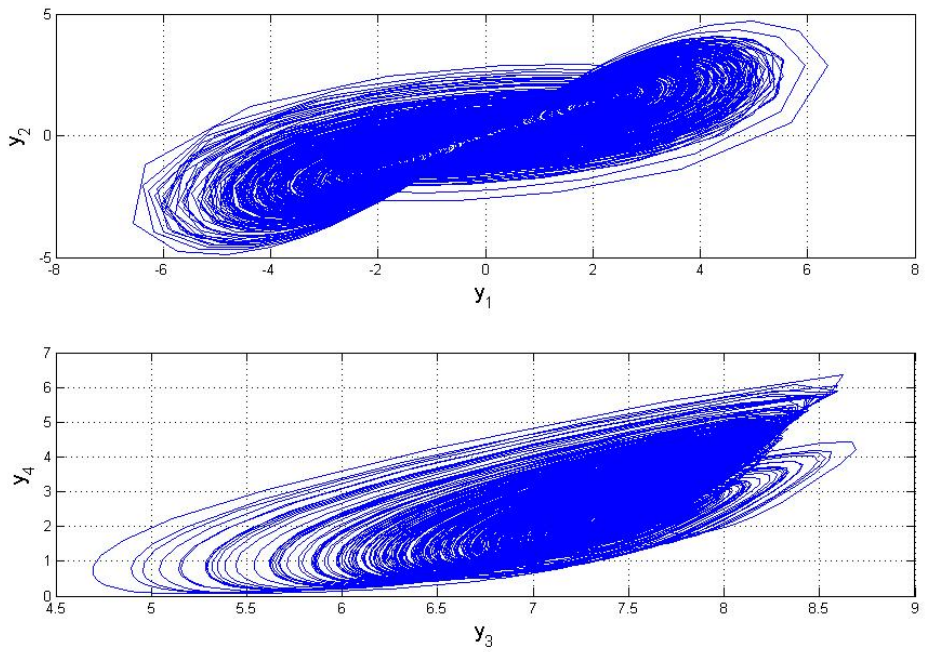


Fig. 7-4. Chaotic behavior of new fuzzy Qi system.

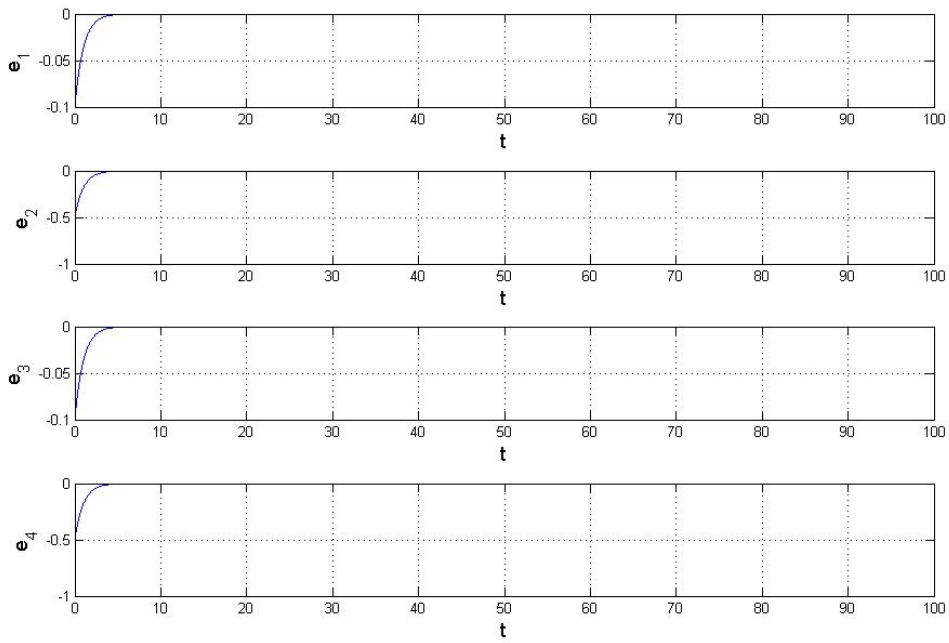


Fig. 7-5 Time history of errors via fuzzy feedback gain.

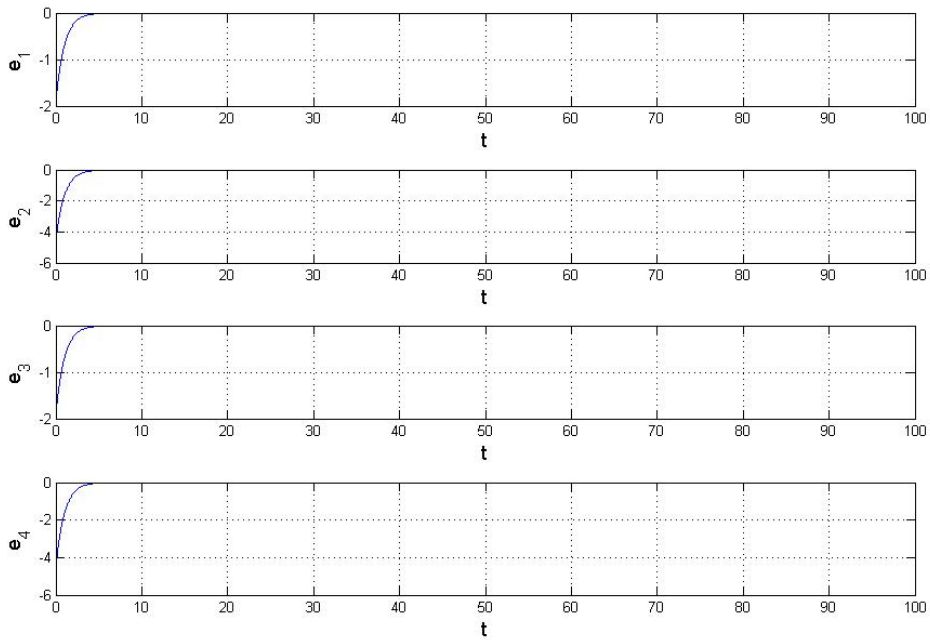


Fig. 7-6. Time histories of errors for Case I.



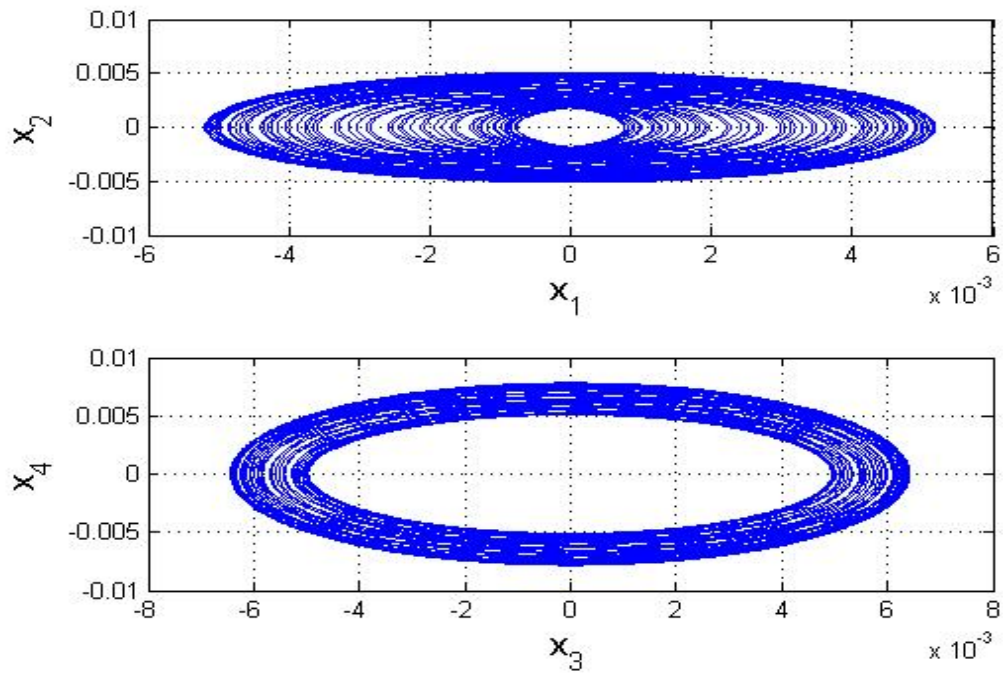


Fig. 7-7 Chaotic behavior in *Case 1*.

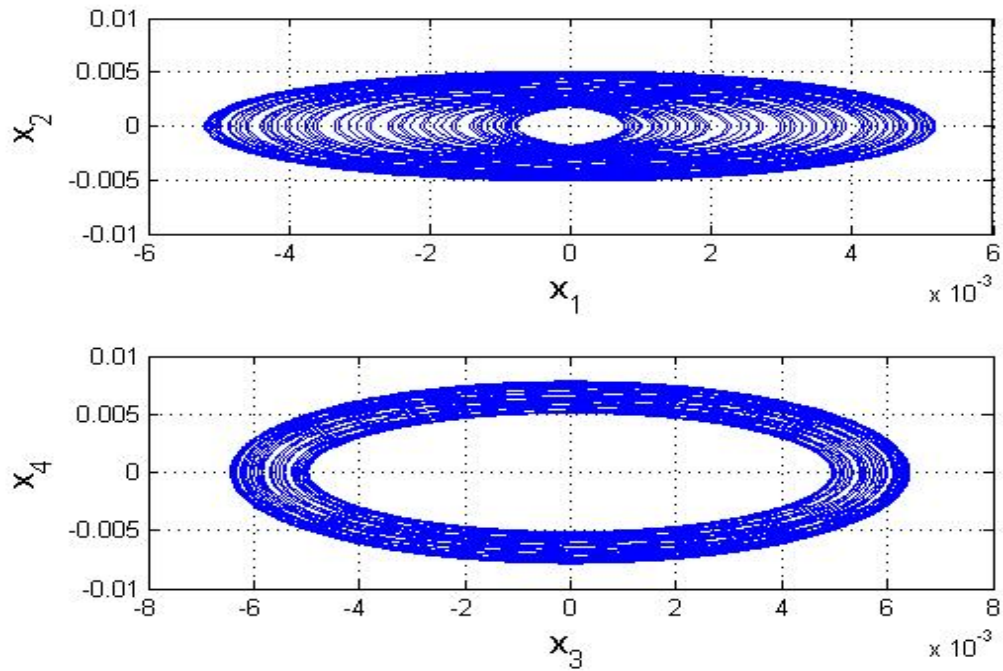


Fig. 7-8 Chaotic behavior in *Case 2*.

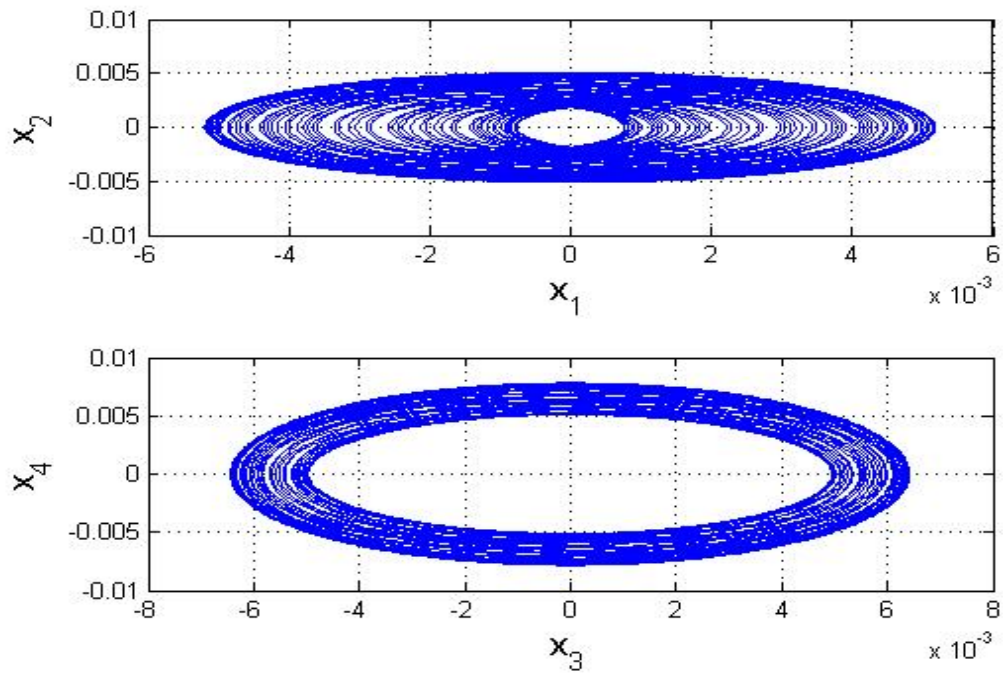
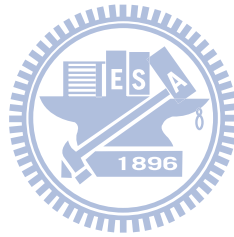


Fig. 7-9 Chaotic behavior in *Case 3*.



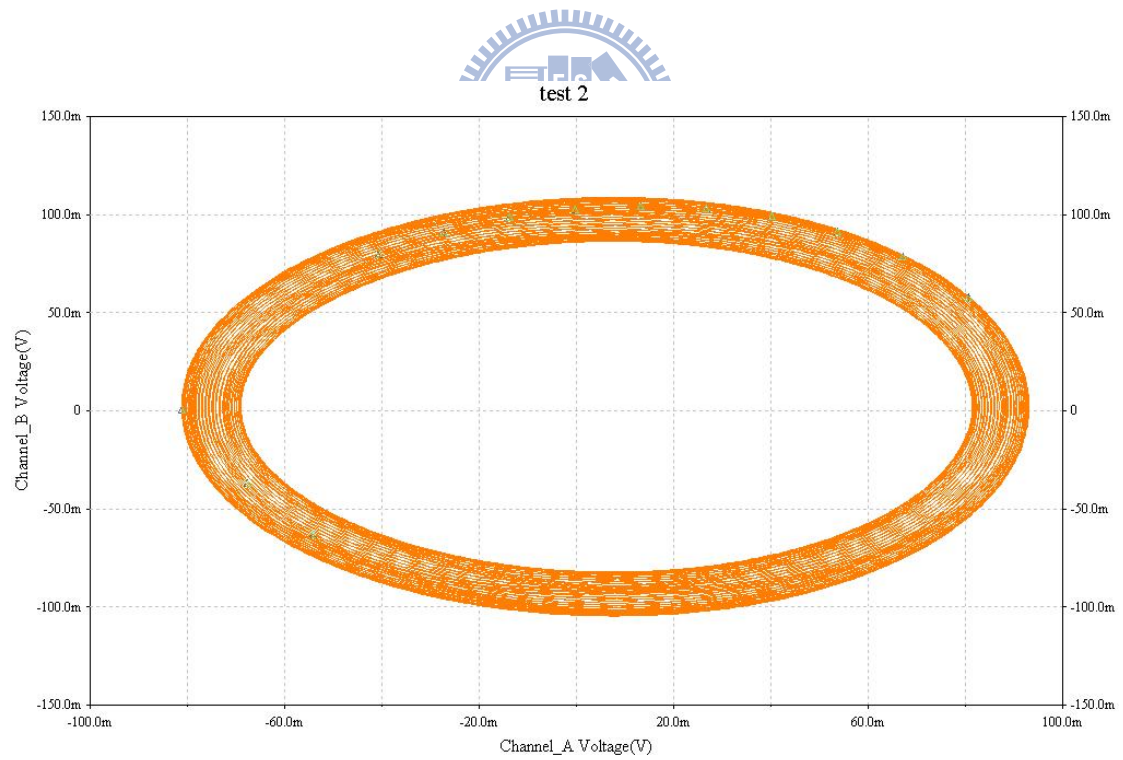
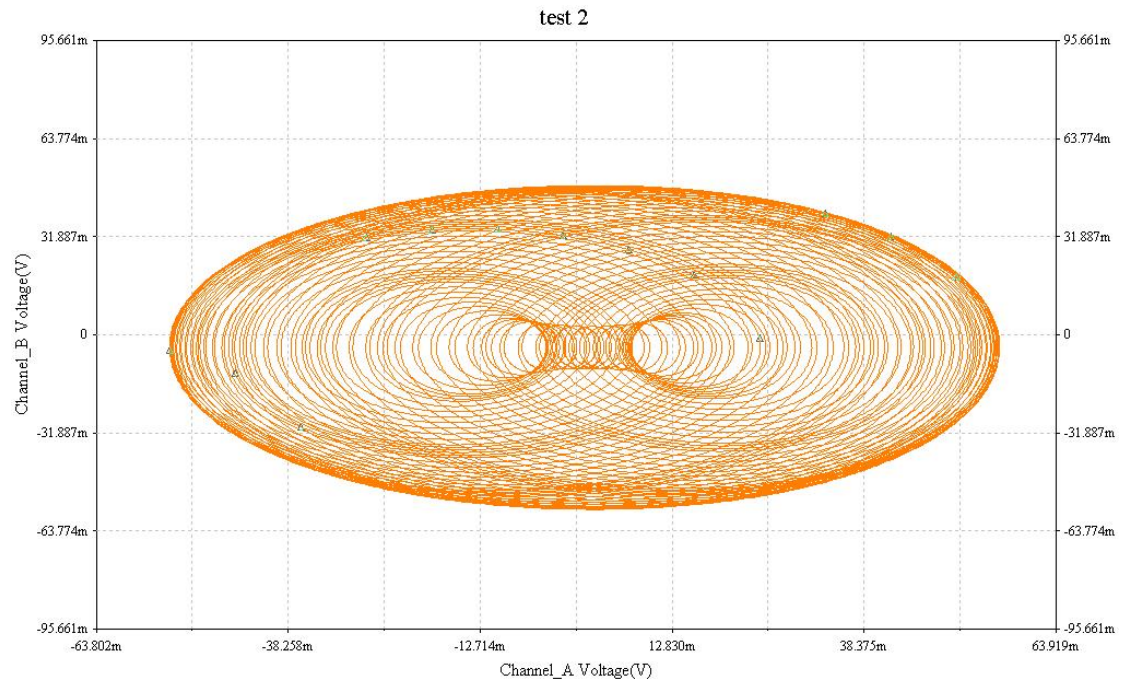


Fig. 7-10 Implementation on electronic circuits of Chaotic Q-CNN system.

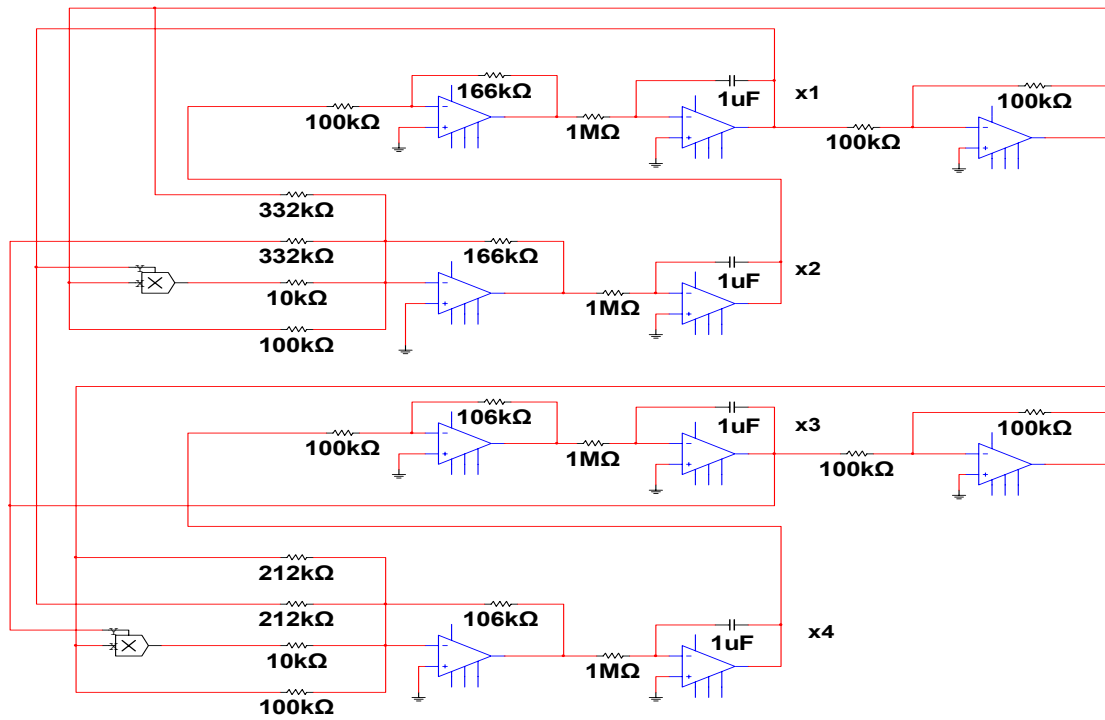
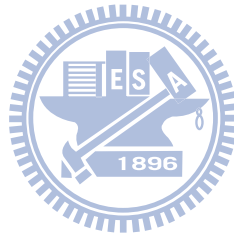


Fig. 7-11 Configuration of electronic circuits.



# Chapter 8

## Generalized Synchronization of Different Chaotic Systems by Fuzzy Logic Constant Controller

### 8.1 Preliminaries

The fuzzy logic constant controller (FLCC) is introduced in this Chapter. Unlike traditional method, a simplest controller is proposed via fuzzy logic design and Lyapunov direct method. Controllers in traditional method by Lyapunov direct method are always complicated or the functions of errors. We propose a new idea to design constant numbers as controllers, while the constant numbers are decided by the upper bound and the lower bound of the error derivatives. Via fuzzy logic rules, the strength of controllers in our new approach can be adjusted according to the error derivatives. Consequently, the slave system becomes exactly and efficiently synchronized to the trajectory of master system through FLCC. Two examples, Lorenz system and four order Chen-Lee system, are presented to illustrate the effectiveness of the new controllers in chaos generalized synchronization.

### 8.2 Generalized Synchronization by FLCC Scheme

#### 8.2.1 Generalized Synchronization Scheme

There are two nonlinear dynamical systems, while the master system controls the slave system. The master system is given by

$$\dot{x} = Ax + f(x) \tag{8-2-1}$$

where  $x = [x_1, x_2, \dots, x_n]^T \in R^n$  denotes a state vector,  $A$  is an  $n \times n$  constant coefficient matrix and  $f$  is a nonlinear vector function.

The slave system is given by

$$\dot{y} = By + g(y) + u \quad (8-2-2)$$

where  $y = [y_1, y_2, \dots, y_n]^T \in R^n$  denotes a state vector,  $B$  is an  $n \times n$  constant coefficient matrix,  $g$  is a nonlinear vector function., and  $u = [u_1, u_2, \dots, u_n]^T \in R^n$  is a constant control input vector.

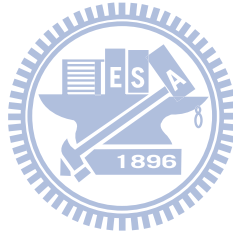
Our goal is to design appropriate fuzzy rules and corresponding constant controllers  $u$  so that the state vector of the chaotic system (8-2-1) asymptotically approaches the state vector of the master system (8-2-2).

The generalized chaos synchronization can be accomplished in the sense that the limit of the error vector  $e(t) = [e_1, e_2, \dots, e_n]^T$  approaches zero:

$$\lim_{t \rightarrow \infty} e = 0 \quad (8-2-3)$$

where

$$e = H(x) - y \quad (8-2-4)$$



where  $H(x)$  is a given vector function of  $x$ . From Eq. (8-2-4) we have

$$\dot{e} = \frac{\partial H(x)}{\partial x} \dot{x} - \dot{y} \quad (8-2-5)$$

$$\dot{e} = \frac{\partial H(x)}{\partial x} [Ax + f(x)] - By - G(y) - u \quad (8-2-6)$$

A Lyapunov function  $V(e)$  is chosen as a positive definite function

$$V(e) = \frac{1}{2} e^T e \quad (8-2-7)$$

Its derivative along any solution of the differential equation system consisting of Eq. (8-2-6) is

$$\dot{V}(e) = e^T \left[ \left( \frac{\partial H(x)}{\partial x} (Ax + f(x)) - By - g(y) - u \right) \right] \quad (8-2-8)$$

If fuzzy constant controllers  $u$  can be appropriately chosen so that  $\dot{V} = Ce^T e$ ,  $C$  is a diagonal negative definite matrix, and  $\dot{V}$  is a negative definite function of  $e$ . By

Lyapunov theorem of asymptotical stability:

$$\lim_{t \rightarrow \infty} e = 0 \quad (8-2-9)$$

The generalized synchronization is obtained. The design process of FLCC is introduced in the following section.

### 8.2.2 Fuzzy logic constant controller design process

The basic configuration of the fuzzy logic system is shown in Fig. 8-1. It is composed of five function blocks [23]:

1. A rule base contains a number of fuzzy if-then rules.
2. A database defines the membership functions of the fuzzy sets used in fuzzy rules.
3. A decision-making unit performs the inference operations on the rules.
4. A fuzzification interface transforms the crisp inputs into degrees of match with linguistic value.
5. A defuzzification interface transforms the fuzzy results of the inference into a crisp output.



The fuzzy rules base consists of collection of fuzzy if-then rules expressed as the form if a is A then b is B, where a and b denote linguistic variables, A and B represent linguistic values which are characterized by membership functions. All of the fuzzy rules can be used to construct the fuzzy associated memory.

We use two signals,  $e(t) = [e_1, e_2 \cdots e_m, \cdots e_n]^T$  in Eq. (8-2-4) and  $\dot{e}(t) = [\dot{e}_1, \dot{e}_2 \cdots \dot{e}_m, \cdots \dot{e}_n]^T$  in Eq. (8-2-5), as the antecedent part of the proposed FLCC to design the control input  $u$  in Eq. (8-2-8) that will be used in the consequent part of the proposed FLCC as follows:

$$u = [u_1, u_2 \cdots u_m, \cdots u_n]^T \quad (8-2-10)$$

where  $u$  is a constant column vector and the FLCC accomplishes the objective to

stabilize the error dynamics (8-2-6). In this Section, we are not going to use the original fuzzy rule base, but using it in each error dynamics separately. In order to obtain the simplest controllers, the  $i$ th if-then rule of the fuzzy rule base of the FLCC is of the following form:

$$\text{Rule } i : \text{ if } e_m \text{ is } X_i \text{ then } \dot{e}_m \text{ is } Y_i \text{ and } u_{mi} = \text{constant} \quad (8-2-11)$$

where  $X_i$  is the input fuzzy sets of  $e_m$ ,  $m=1 \sim n$ ,  $Y_i$  is the output fuzzy sets of  $\dot{e}_m$  and  $u_{mi}$  is the  $i$ -rd output of  $\dot{e}_m$  which is a constant controller. For given input sign of the process variables  $e_m$ , then the output sign of  $\dot{e}_m$  would be decided and its degree of membership  $\mu_{X_i}$ ,  $i=1 \sim 3$  called rule-antecedent weights are calculated. The centroid defuzzifier evaluates the output of all rules as follows:

$$u_m = \frac{\sum_{i=1}^3 \mu_{X_i} \times u_{mi}}{\sum_{i=1}^3 \mu_{X_i}} \quad (8-2-12)$$

The fuzzy rule base is listed in Table 8-1, in which the input variables in the antecedent part of the rules are  $e_m$  and the output variable  $\dot{e}_m$  in the consequent part are  $\dot{e}_m$  and  $u_{mi}$ .

Table 8-1 Rule-table of FLCC

Rule	Antecedent	Consequent Part 1	Consequent Part 2
	$e_m$	$\dot{e}_m$	$u_{mi}$
1	Positive (P)	Negative (N)	$u_{m1}$
2	Negative (N)	Positive (P)	$u_{m2}$
3	Zero (Z)	Zero (Z)	$u_{m3}$

The membership function is obtained via the method shown in Fig. 8-2. After designing appropriate fuzzy logic constant controllers, a negative definite of  $\dot{V}$  in Eq. (8-2-9) can be obtained and the asymptotically stability of Lyapunov theorem can be achieved.



## 8.3 Simulation Results

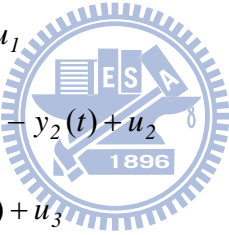
### 10.3.1 Example 1-Synchronization of Master and Slave Lorenz system

The master Lorenz system [24] is:

$$\begin{cases} \frac{dx_1(t)}{dt} = a(x_2(t) - x_1(t)) \\ \frac{dx_2(t)}{dt} = cx_1(t) - x_1(t)x_3(t) - x_2(t) \\ \frac{dx_3(t)}{dt} = x_1(t)x_2(t) - bx_3(t) \end{cases} \quad (8-3-1)$$

When initial condition  $(x_{10}, x_{20}, x_{30}) = (-0.1, 0.2, 0.3)$  and parameters  $a=10$ ,  $b=8/3$  and  $c=28$ , chaos of the Lorenz system appears. The chaotic behavior of Eq. (8-3-1) is shown in Fig 8-3.

The slave Lorenz system is:

$$\begin{cases} \frac{dy_1(t)}{dt} = a(y_2(t) - y_1(t)) + u_1 \\ \frac{dy_2(t)}{dt} = cy_1(t) - y_1(t)y_3(t) - y_2(t) + u_2 \\ \frac{dy_3(t)}{dt} = y_1(t)y_2(t) - by_3(t) + u_3 \end{cases} \quad (8-3-2)$$


When initial condition  $(y_{10}, y_{20}, y_{30}) = (0.5, 0.7, 1.5)$  and parameters are the same as that of Eq. (8-3-1), chaos of the slave Lorenz system appears as well.  $u_1, u_2$  and  $u_3$  are FLCC to synchronize the slave Lorenz system to master one, i.e.,

$$\lim_{t \rightarrow \infty} \mathbf{e} = 0 \quad (8-3-3)$$

where the error vector

$$\mathbf{e} = \begin{bmatrix} e_1(t) \\ e_2(t) \\ e_3(t) \end{bmatrix} = \begin{bmatrix} x_1(t) - y_1(t) \\ x_2(t) - y_2(t) \\ x_3(t) - y_3(t) \end{bmatrix} \quad (8-3-4)$$

From Eq. (8-3-4), we have the following error dynamics:

$$\begin{cases} \dot{e}_1 = a(x_2 - x_1) - (a(y_2 - y_1) + u_1) \\ \dot{e}_2 = cx_1 - x_1x_3 - x_2 - ((cy_1 - y_1y_3 - y_2) + u_2) \\ \dot{e}_3 = x_1x_2 - bx_3 - ((y_1y_2 - by_3) + u_3) \end{cases} \quad (8-3-5)$$

Choosing Lyapunov function as:

$$V = \frac{1}{2}(e_1^2 + e_2^2 + e_3^2) \quad (8-3-6)$$

Its time derivative is:

$$\begin{aligned} \dot{V} &= e_1\dot{e}_1 + e_2\dot{e}_2 + e_3\dot{e}_3 \\ &= e_1(a(x_2 - x_1) - (a(y_2 - y_1) + u_1)) \\ &\quad + e_2(cx_1 - x_1x_3 - x_2 - ((cy_1 - y_1y_3 - y_2) + u_2)) \\ &\quad + e_3(x_1x_2 - bx_3 - ((y_1y_2 - by_3) + u_3)) \end{aligned} \quad (8-3-7)$$

In order to design FLCC, we divide Eq. (8-3-7) into three parts as follows:

Assume  $V = \frac{1}{2}(e_1^2 + e_2^2 + e_3^2) = V_1 + V_2 + V_3$ , then  $\dot{V} = e_1\dot{e}_1 + e_2\dot{e}_2 + e_3\dot{e}_3 = \dot{V}_1 + \dot{V}_2 + \dot{V}_3$ ,

where  $V_1 = \frac{1}{2}e_1^2$ ,  $V_2 = \frac{1}{2}e_2^2$  and  $V_3 = \frac{1}{2}e_3^2$ .

$$\text{Part 1: } \dot{V}_1 = e_1\dot{e}_1 = e_1(a(x_2 - x_1) - (a(y_2 - y_1) + u_1))$$

$$\text{Part 2: } \dot{V}_2 = e_2\dot{e}_2 = e_2(cx_1 - x_1x_3 - x_2 - ((cy_1 - y_1y_3 - y_2) + u_2))$$

$$\text{Part 3: } \dot{V}_3 = e_3\dot{e}_3 = e_3(x_1x_2 - bx_3 - ((y_1y_2 - by_3) + u_3))$$

*Part 1:*

FLCC in *Part 1* can be obtained via the fuzzy rules in Table 8-1 and Table 8-2 as follows and the maxima value and minima value of  $\dot{e}_1$  (without any controller) can be observed in time history of error derivatives drawn in Fig 8-4. We choose  $f_1$  to be the upper bound value and  $g_1$  to be the lower bound value of  $\dot{e}_1$  (without any controller), they are satisfied with  $f_1 < \dot{e}_1$  (without any controller)  $< g_1$  and  $f_1, g_1$  are all constants.

*Rule 1: if  $e_1$  is P, then  $\dot{e}_1$  is N and we take  $u_{11} = f_1$*

*Rule 2: if  $e_1$  is N, then  $\dot{e}_1$  is P and we take  $u_{12} = g_1$*

*Rule 3: if  $e_1$  is Z, then  $\dot{e}_1$  is Z and we take  $u_{13}=0=e_1$*

where  $f_1=-g_1= \text{constant}=400$  and we choose  $u_{13}=0=e_1$  when  $e_1$  approaches to zero.

We take *Rule 1-3* in Part 1,  $\dot{V}_1 = e_1\dot{e}_1$ , for explaining:

*Rule 1: if  $e_1$  is P, then  $\dot{e}_1$  is N and we take  $u_{11}=-f_1$ .*

$$\dot{V}_1 = e_1\dot{e}_1 = e_1(a(x_2 - x_1) - a(y_2 - y_1) - f_1)$$

where  $e_1 > 0$  and  $(a(x_2 - x_1) - a(y_2 - y_1) - f_1) = (\dot{e}_1(\text{without controller}) - f_1) < 0$ .

Therefore,  $\dot{V}_1 = e_1\dot{e}_1 = e_1(a(x_2 - x_1) - a(y_2 - y_1) - f_1) < 0$  and is going to approach asymptotically stable.

*Rule 2: if  $e_1$  is N, then  $\dot{e}_1$  is P and we take  $u_{12} = g_1$*

$$\dot{V}_1 = e_1\dot{e}_1 = e_1(a(x_2 - x_1) - a(y_2 - y_1) - g_1)$$

where  $e_1 < 0$  and  $(a(x_2 - x_1) - a(y_2 - y_1) - g_1) = (\dot{e}_1(\text{without controller}) - g_1) > 0$ .

Therefore,  $\dot{V}_1 = e_1\dot{e}_1 = e_1(a(x_2 - x_1) - a(y_2 - y_1) - g_1) < 0$  and is going to approach asymptotically stable.

*Rule 3: if  $e_1$  is Z, then  $\dot{e}_1$  is Z and we take  $u_{13}=0=e_1$*

$$\dot{V}_1 = e_1\dot{e}_1 = e_1(a(x_2 - x_1) - a(y_2 - y_1) - e_1)$$

where  $e_1 = 0$  and we don't need any controller now. Therefore,  $\dot{V}_1 = e_1\dot{e}_1 = 0$  and achieve asymptotically stable.

As a results, FLCC in *Part 1* can be obtained from *Rule 1,2 and 3*:

$$u_1 = \frac{\mu_P \times u_{11} + \mu_N \times u_{12} + \mu_Z \times u_{13}}{\mu_P + \mu_N + \mu_Z} \quad (8-3-8)$$

*Part 2:*

FLCC in *Part 2* can be obtained via the fuzzy rules in Table 8-1 and Table 8-2 as follows and the maxima value and minima value of  $\dot{e}_2$  (without any controller) can be observed in time history of error derivatives drawn in Fig 8-4. We choose  $f_2$  to be the upper bound value and  $g_2$  to be the lower bound value of  $\dot{e}_2$  (without any controller), they are satisfied with  $f_2 < \dot{e}_2(\text{without any controller}) < g_2$  and  $f_2, g_2$  are all constants.

Rule 1: if  $e_1$  is P, then  $\dot{e}_1$  is N and we take  $u_{11} = f_1$

Rule 1: if  $e_2$  is P, then  $\dot{e}_2$  is N and  $u_{21} = f_2$

Rule 2: if  $e_2$  is N, then  $\dot{e}_2$  is P and  $u_{22} = g_2$

Rule 3: if  $e_2$  is Z, then  $\dot{e}_2$  is Z and  $u_{23} = 0 = e_2$

where  $f_2 = -g_2 = \text{constant} = 500$  and we choose  $u_{23} = 0 = e_2$  when  $e_2$  approaches to zero.

The process of FLCC designing is the same as *Part 1*, as a results, FLCC in *Part 2*

can be obtained from *Rule 1,2 and 3* and are going to take  $\dot{V}_2 = e_2 \dot{e}_2 < 0$  :

$$u_2 = \frac{\mu_P \times u_{21} + \mu_N \times u_{22} + \mu_Z \times u_{23}}{\mu_P + \mu_N + \mu_Z} \quad (8-3-9)$$

*Part 3*:

FLCC in *Part 3* can be obtained via the fuzzy rules in Table 8-1 and Table 8-2 as follows and the maxima value and minima value of  $\dot{e}_3$  (without any controller) can be observed in time history of error derivatives drawn in Fig 8-4. We choose  $f_3$  to be the upper bound value and  $g_3$  to be the lower bound value of  $\dot{e}_3$  (without any controller), they are satisfied with  $f_3 < \dot{e}_3$  (without any controller)  $< g_3$  and  $f_3, g_3$  are all constants.

Rule 1: if  $e_3$  is P, then  $\dot{e}_3$  is N and  $u_{31} = f_3$

Rule 2: if  $e_3$  is N, then  $\dot{e}_3$  is P and  $u_{32} = g_3$

Rule 3: if  $e_3$  is Z, then  $\dot{e}_3$  is Z and  $u_{33} = 0 = e_3$

where  $f_3 = -g_3 = \text{constant} = 500$  and we choose  $u_{33} = 0 = e_3$  when  $e_3$  approaches to zero.

The process of FLCC designing is the same as *Part 1*, as a results, FLCC in *Part 3*

can be obtained from *Rule 1,2 and 3* and are going to take  $\dot{V}_3 = e_3 \dot{e}_3 < 0$  :

$$u_3 = \frac{\mu_P \times u_{31} + \mu_N \times u_{32} + \mu_Z \times u_{33}}{\mu_P + \mu_N + \mu_Z} \quad (8-3-10)$$

FLCC are proposed in *Part 1,2 and 3* and are going to take  $\dot{V}_1 = e_1 \dot{e}_1 < 0, \dot{V}_2 = e_2 \dot{e}_2 < 0$  and  $\dot{V}_3 = e_3 \dot{e}_3 < 0$ . Hence, we have  $\dot{V} = \dot{V}_1 + \dot{V}_2 + \dot{V}_3 < 0$ .

It is clear that all of the rules in our FLC can lead the Lyapunov function to approach

asymptotically stable and the simulation results are shown in Fig. 8-5 and 8-6.

### 8.3.2 Example 2-Generalized Synchronization of different order chaotic system-Lorenz and New Chen-Lee system

Chen and Lee gave a new chaotic system [25] in 2004, which is now called the Chen-Lee system [26]. The system is described by the following nonlinear differential equations and is denoted as system (8-3-11):

$$\begin{cases} \frac{dz_1(t)}{dt} = -z_2(t)z_3(t) + a_1z_1(t) \\ \frac{dz_2(t)}{dt} = z_1(t)z_3(t) + b_1z_2(t) \\ \frac{dz_3(t)}{dt} = \frac{1}{3}z_1(t)z_2(t) + cz_3(t) \end{cases} \quad (8-3-11)$$

where  $z_1$ ,  $z_2$  and  $z_3$  are state variables, and  $a_1$ ,  $b_1$ , and  $c_1$  are three system parameters. When  $(a_1, b_1, c_1) = (5, -10, -3.8)$ , system (8-3-11) is a chaotic attractor. The positive Lyapunov exponent of this attractor is  $\lambda_1 = 0.88$ , while the other ones are  $\lambda_2 = 0$  and  $\lambda_3 = -13.57$ , respectively. It is clear that the Chen-Lee system is a regular chaotic system. For more-detailed dynamics of the Chen-Lee system, see Ref. [25].

It is known that in order to obtain hyper-chaos, there are two important requisites: (1) the minimal dimension of the phase space that embeds a hyper-chaotic attractor should be at least four, which requires a minimum of four couple first-order autonomous ordinary differential equations; and (2) the number of terms in the couple equations giving rise to instability should be at least two, of which at least one should be a nonlinear function. In [27], Chen and Lee introduce a nonlinear feedback controller to the third equation of system (8-3-11), the following dynamic system can be obtained:

$$\begin{cases} \frac{dz_1(t)}{dt} = -z_2(t)z_3(t) + a_1z_1(t) \\ \frac{dz_2(t)}{dt} = z_1(t)z_3(t) + b_1z_2(t) \\ \frac{dz_3(t)}{dt} = \frac{1}{3}z_1(t)z_2(t) + c_1z_3(t) + \frac{1}{5}z_4(t) \\ \frac{dz_4(t)}{dt} = d_1z_1(t) + \frac{1}{2}z_2(t)z_3(t) + \frac{1}{20}z_4(t) \end{cases} \quad (8-3-12)$$

where  $d$  is a constant, determining the dynamic behaviors of the system (8-3-12) and  $a_1$ ,  $b_1$ , and  $c_1$  are three system parameters. Thus, controller  $z_4$  causes chaotic system (8-3-11) to become a four-dimensional system, which has four Lyapunov exponents. This may lead to a hyper-chaotic system. When  $(a_1, b_1, c_1) = (5, -10, -3.8)$  and we choose  $d=1.3$ , system (8-3-12) is a hyper-chaotic attractor. The projection of phase portraits of system (8-3-12) with hyper-chaotic behaviors is shown in Fig. 8-7.

Eq. (8-3-12) is chosen as slave system to be synchronized with the master system (8-3-12). Our goal is  $[e] = [e_1(t), e_2(t), e_3(t)] = [z_1(t) - y_1(t), z_3(t) - y_2(t), z_4(t) - y_3(t)]$ . As a result, we get the following error dynamics:

$$\begin{cases} \dot{e}_1 = -z_2z_3 + a_1z_1 - (a(y_2 - y_1) + u_1) \\ \dot{e}_2 = \frac{1}{3}z_1z_2 + c_1z_3 - ((cy_1 - y_1y_3 - y_2) + u_2) \\ \dot{e}_3 = d_1z_1 + \frac{1}{2}z_2z_3 + \frac{1}{20}z_4 - ((y_1y_2 - by_3) + u_3) \end{cases} \quad (8-3-13)$$

Choosing Lyapunov function as:

$$V = \frac{1}{2}(e_1^2 + e_2^2 + e_3^2) \quad (8-3-14)$$

Its time derivative is:

$$\begin{aligned}
\dot{V} &= e_1 \dot{e}_1 + e_2 \dot{e}_2 + e_3 \dot{e}_3 \\
&= e_1(-z_2 z_3 + a_1 z_1 - (a(y_2 - y_1) + u_1)) \\
&\quad + e_2\left(\frac{1}{3} z_1 z_2 + c_1 z_3 - ((c y_1 - y_1 y_3 - y_2) + u_2)\right) \\
&\quad + e_3\left(d_1 z_1 + \frac{1}{2} z_2 z_3 + \frac{1}{20} z_4 - ((y_1 y_2 - b y_3) + u_3)\right)
\end{aligned} \tag{8-3-15}$$

We divide Eq. (8-3-15) into three parts as follows:

Assume  $V = \frac{1}{2}(e_1^2 + e_2^2 + e_3^2) = V_1 + V_2 + V_3$ , then  $\dot{V} = e_1 \dot{e}_1 + e_2 \dot{e}_2 + e_3 \dot{e}_3 = \dot{V}_1 + \dot{V}_2 + \dot{V}_3$ ,

where  $V_1 = \frac{1}{2}e_1^2$ ,  $V_2 = \frac{1}{2}e_2^2$  and  $V_3 = \frac{1}{2}e_3^2$ .

$$\text{Part 1: } \dot{V}_1 = e_1 \dot{e}_1 = e_1(-z_2 z_3 + a_1 z_1 - (a(y_2 - y_1) + u_1))$$

$$\text{Part 2: } \dot{V}_2 = e_2 \dot{e}_2 = e_2\left(\frac{1}{3} z_1 z_2 + c_1 z_3 - ((c y_1 - y_1 y_3 - y_2) + u_2)\right)$$

$$\text{Part 3: } \dot{V}_3 = e_3 \dot{e}_3 = e_3\left(d_1 z_1 + \frac{1}{2} z_2 z_3 + \frac{1}{20} z_4 - ((y_1 y_2 - b y_3) + u_3)\right)$$

Part 1:

FLCC in *Part 1* can be obtained via the fuzzy rules in Table 8-1 and Table 8-2 as follows and the maxima value and minima value of  $\dot{e}_1$  (without any controller) can be observed in time history of error derivatives drawn in Fig 8-4. We choose  $f_4$  to be the upper bound value and  $g_4$  to be the lower bound value of  $\dot{e}_1$  (without any controller), they are satisfied with  $f_4 < \dot{e}_1$  (without any controller)  $< g_4$  and  $f_4, g_4$  are all constants.

*Rule 1: if  $e_1$  is P, then  $\dot{e}_1$  is N and we take  $u_{11} = f_4$*

*Rule 2: if  $e_1$  is N, then  $\dot{e}_1$  is P and we take  $u_{12} = g_4$*

*Rule 3: if  $e_1$  is Z, then  $\dot{e}_1$  is Z and we take  $u_{13} = 0 = e_1$*

where  $f_4 = -g_4 = \text{constant} = 2000$  and we choose  $u_{13} = 0 = e_1$  when  $e_1$  approaches to zero.

We take *Rule 1~3* in Part 1,  $\dot{V}_1 = e_1 \dot{e}_1$ , for explaining:

*Rule 1: if  $e_1$  is P, then  $\dot{e}_1$  is N and we take  $u_{11} = f_4$ .*

$$\dot{V}_1 = e_1 \dot{e}_1 = e_1(-x_2 x_3 + a_1 x_1 - a(y_2 - y_1) - f_4)$$

where  $e_1 > 0$  and  $(-z_2 z_3 + a_1 z_1 - a(y_2 - y_1) - f_4) = (\dot{e}_1(\text{without controller}) - f_4) < 0$ .

Therefore,  $\dot{V}_1 = e_1 \dot{e}_1 = e_1(-z_2 z_3 + a_1 z_1 - a(y_2 - y_1) - f_4) < 0$  and is going to approach asymptotically stable.

*Rule 2: if  $e_1$  is N, then  $\dot{e}_1$  is P and we take  $u_{12} = g_4$*

$$\dot{V}_1 = e_1 \dot{e}_1 = e_1(-x_2 x_3 + a_1 x_1 - a(y_2 - y_1) - g_4)$$

where  $e_1 < 0$  and  $(-x_2 x_3 + a_1 x_1 - a(y_2 - y_1) - g_4) = (\dot{e}_1(\text{without controller}) - g_4) > 0$ .

Therefore,  $\dot{V}_1 = e_1 \dot{e}_1 = e_1(-x_2 x_3 + a_1 x_1 - a(y_2 - y_1) - g_4) < 0$  and is going to approach asymptotically stable.

*Rule 3: if  $e_1$  is Z, then  $\dot{e}_1$  is Z and we take  $u_{13} = 0 = e_1$*

$$\dot{V}_1 = e_1 \dot{e}_1 = e_1(-x_2 x_3 + a_1 x_1 - a(y_2 - y_1) - e_1)$$

where  $e_1 = 0$  and we don't need any controller now. Therefore,  $\dot{V}_1 = e_1 \dot{e}_1 = 0$  and achieve asymptotically stable.

As a results, FLCC in *Part 1* can be obtained from *Rule 1, 2 and 3*:

$$u_1 = \frac{\mu_P \times u_{11} + \mu_N \times u_{12} + \mu_Z \times u_{13}}{\mu_P + \mu_N + \mu_Z} \quad (8-3-16)$$

*Part 2:*

FLCC in *Part 2* can be obtained via the fuzzy rules in Table 8-1 and Table 8-2 as follows and the maxima value and minima value of  $\dot{e}_2$  (without any controller) can be observed in time history of error derivatives drawn in Fig 8-4. We choose  $f_5$  to be the upper bound value and  $g_5$  to be the lower bound value of  $\dot{e}_2$  (without any controller), they are satisfied with  $f_5 < \dot{e}_2(\text{without any controller}) < g_5$  and  $f_5, g_5$  are all constants.

*Rule 1: if  $e_2$  is P, then  $\dot{e}_2$  is N and  $u_{21} = f_5$*

*Rule 2: if  $e_2$  is N, then  $\dot{e}_2$  is P and  $u_{22} = g_5$*

*Rule 3: if  $e_2$  is Z, then  $\dot{e}_2$  is Z and  $u_{23} = 0 = e_2$*

where  $f_5 = -g_5 = \text{constant} = 1000$  and we choose  $u_{23} = 0 = e_2$  when  $e_2$  approaches to zero.



The process of FLCC designing is the same as *Part 1*, as a results, FLCC in *Part 2* can be obtained from *Rule 1,2 and 3* and are going to take  $\dot{V}_2 = e_2 \dot{e}_2 < 0$  :

$$u_2 = \frac{\mu_P \times u_{21} + \mu_N \times u_{22} + \mu_Z \times u_{23}}{\mu_P + \mu_N + \mu_Z} \quad (8-3-17)$$

*Part 3:*

FLCC in *Part 3* can be obtained via the fuzzy rules in Table 8-1 and Table 8-2 as follows and the maxima value and minima value of  $\dot{e}_3$  (without any controller) can be observed in time history of error derivatives drawn in Fig 8-4. We choose  $f_6$  to be the upper bound value and  $g_6$  to be the lower bound value of  $\dot{e}_3$  (without any controller), they are satisfied with  $f_6 < \dot{e}_3$  (without any controller)  $< g_6$  and  $f_6, g_6$  are all constants.

*Rule 1: if  $e_3$  is P, then  $\dot{e}_3$  is N and  $u_{31} = f_6$*

*Rule 2: if  $e_3$  is N, then  $\dot{e}_3$  is P and  $u_{32} = g_6$*

*Rule 3: if  $e_3$  is Z, then  $\dot{e}_3$  is Z and  $u_{33} = 0 = e_3$*

where  $f_3 = -g_3 = \text{constant} = 2000$  and we choose  $u_{33} = 0 = e_3$  when  $e_3$  approaches to zero.

The process of FLCC designing is the same as *Part 1*, as a results, FLCC in *Part 3* can be obtained from *Rule 1,2 and 3* and are going to take  $\dot{V}_3 = e_3 \dot{e}_3 < 0$  :

$$u_3 = \frac{\mu_P \times u_{31} + \mu_N \times u_{32} + \mu_Z \times u_{33}}{\mu_P + \mu_N + \mu_Z} \quad (8-3-18)$$

FLCC are proposed in Eq. (8-3-16), (8-3-17) and (8-3-18) and are going to take  $\dot{V}_1 = e_1 \dot{e}_1 < 0$  ,  $\dot{V}_2 = e_2 \dot{e}_2 < 0$  and  $\dot{V}_3 = e_3 \dot{e}_3 < 0$  separately. Hence, we have  $\dot{V} = \dot{V}_1 + \dot{V}_2 + \dot{V}_3 < 0$ . It is clear that all of the rules in our FLC can lead the Lyapunov function to approach asymptotically stable and the simulation results are shown in Figs. 8-9 and 8-10.

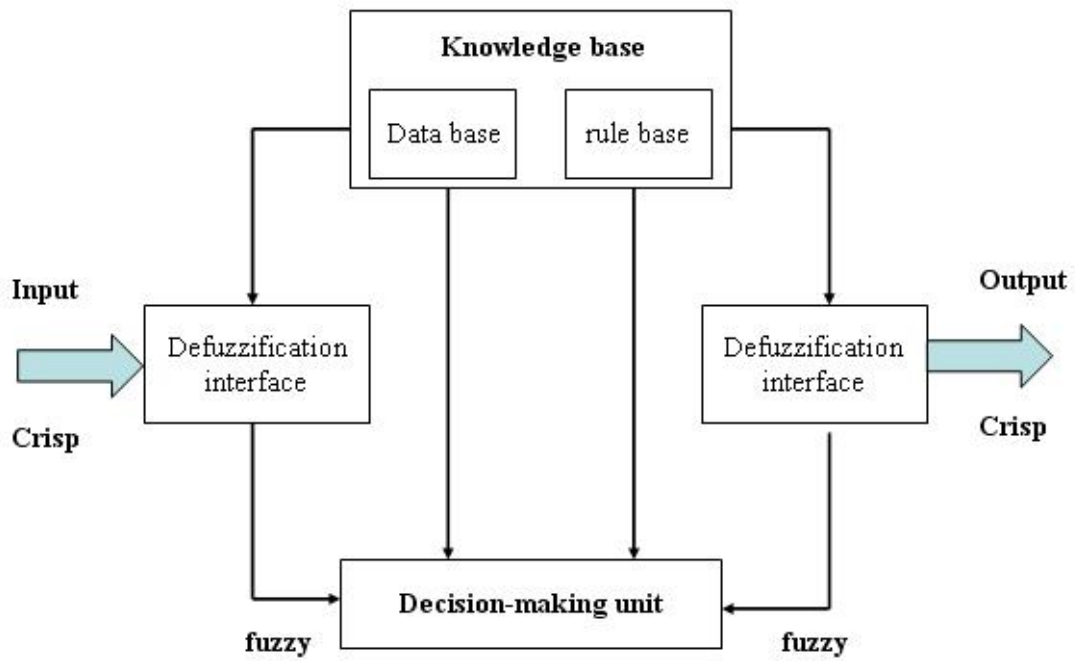


Fig.8-1. The configuration of fuzzy logic controller.

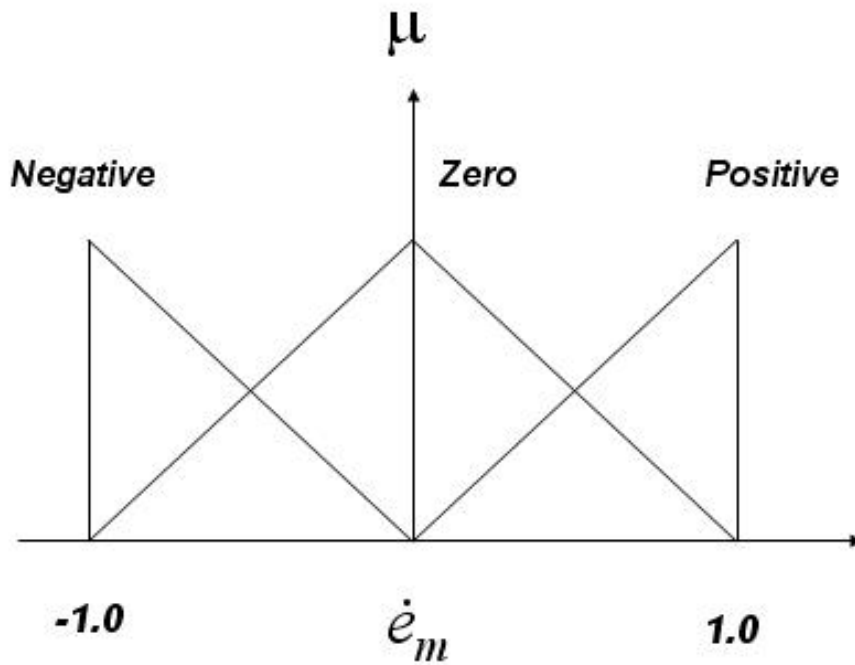


Fig. 8-2. Membership function.

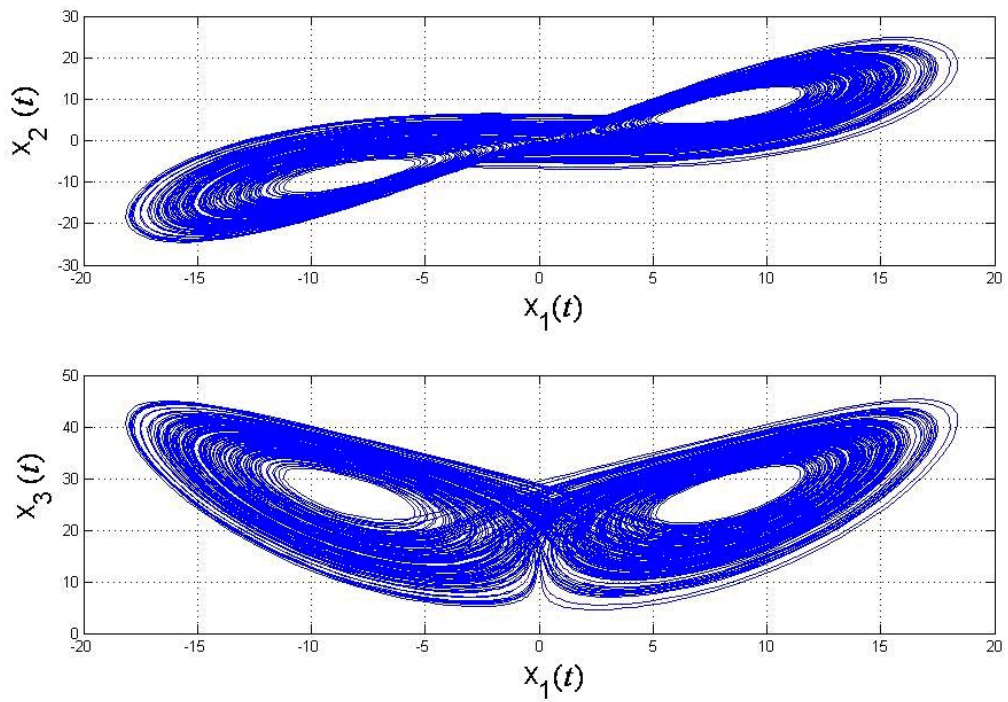


Fig. 8-3. Projections of phase portrait of chaotic Lorenz system with  $a=10$ ,  $b=8/3$  and

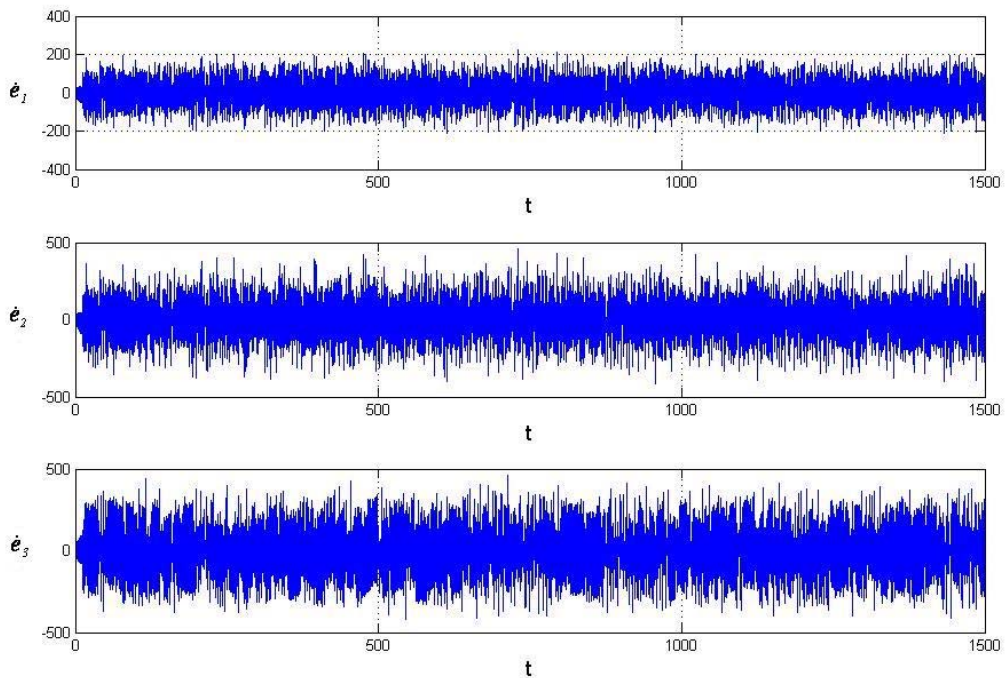


Fig. 8-4. Time histories of error derivatives for master and slave Lorenz chaotic systems without controllers.

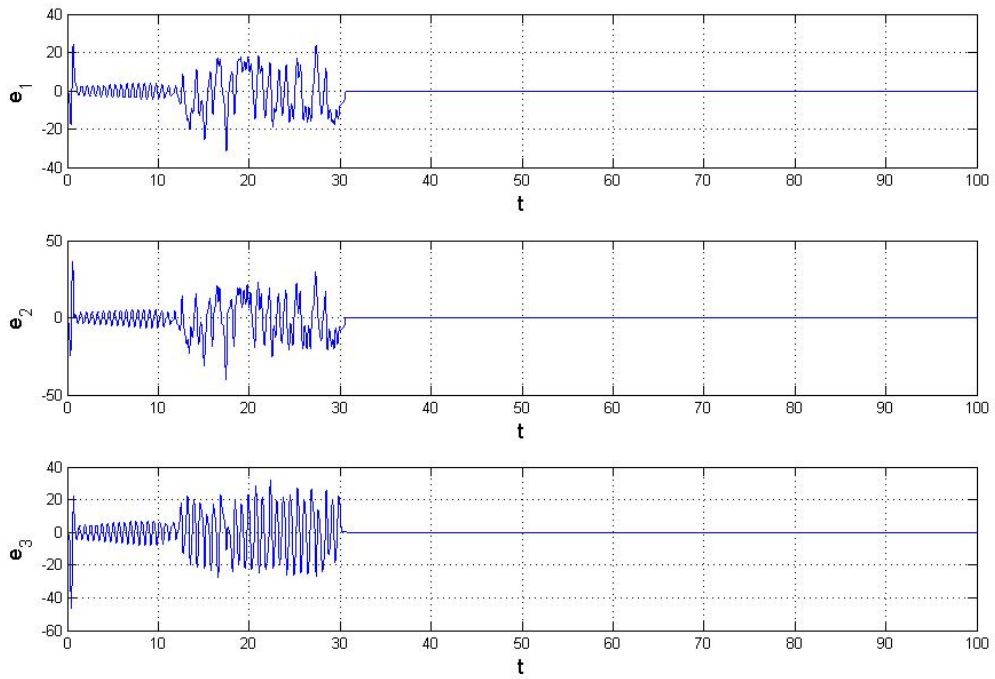


Fig. 8-5 Time histories of errors for Example 1- the FLCC is coming into after 30s.

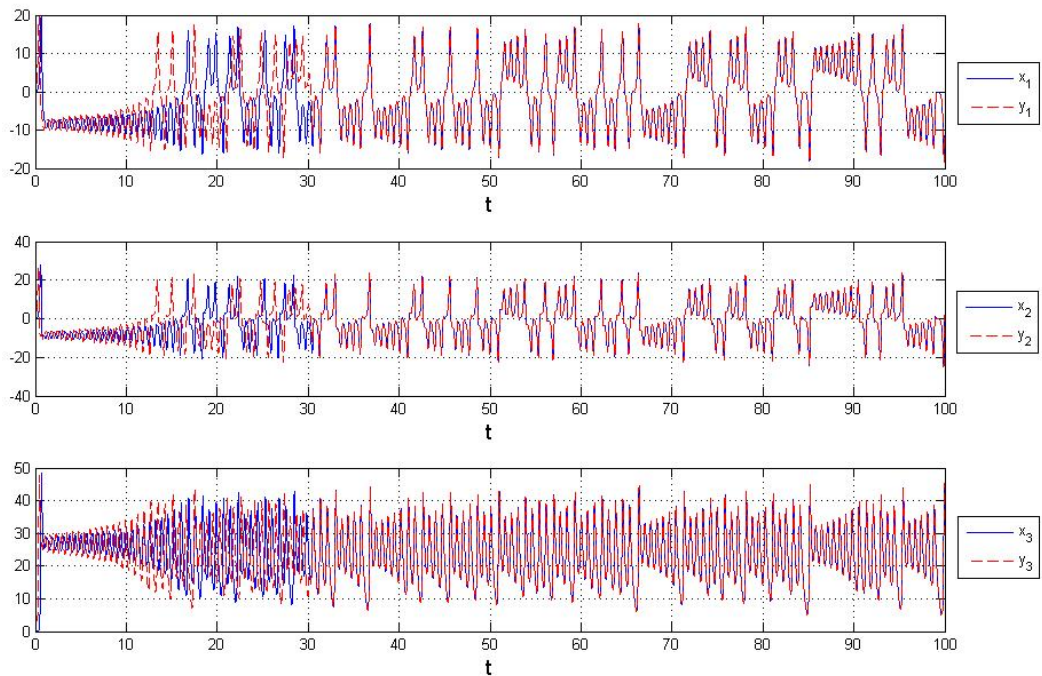


Fig. 8-6. Time histories of states for Example 1- the FLCC is coming into after 30s.

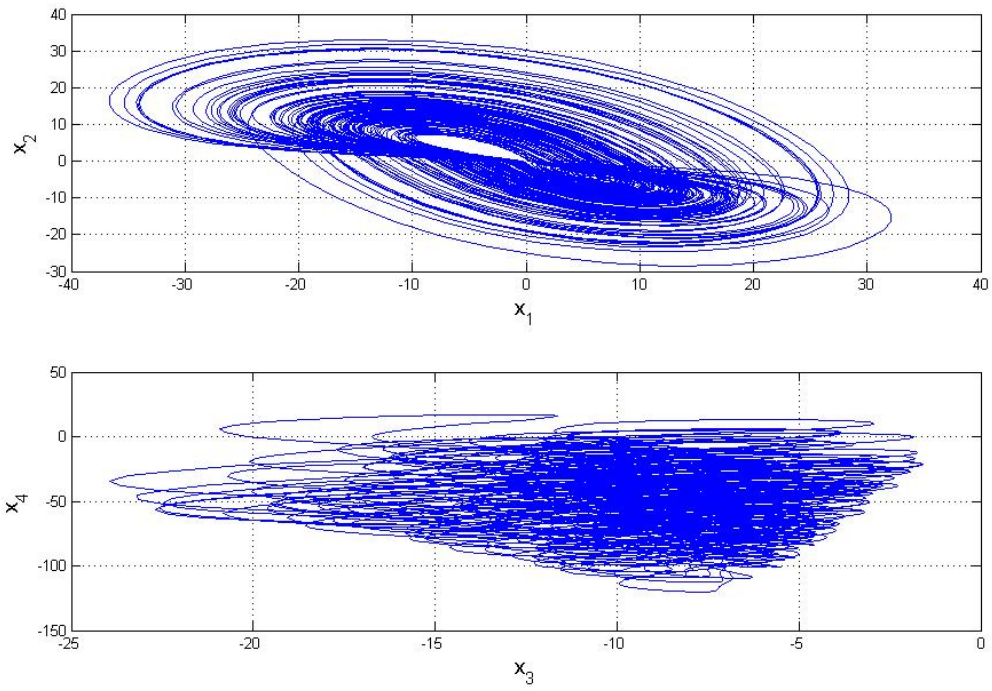


Fig. 8-7. Projections of phase portrait of chaotic Chen-Lee system.

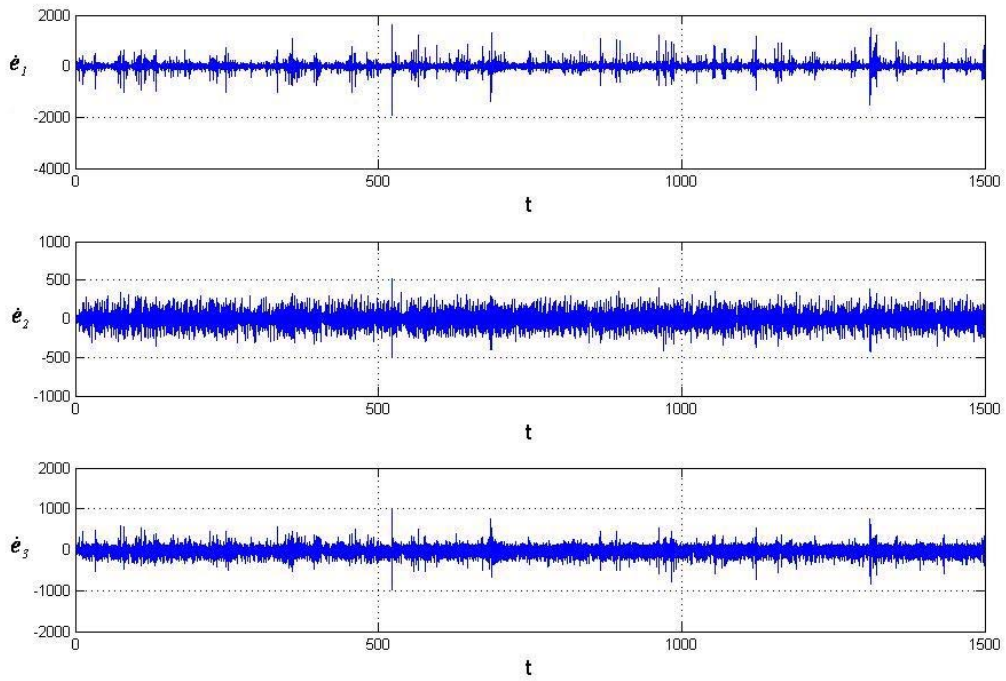


Fig. 8-8. Time histories of error derivatives for master and slave chaotic systems without controllers.

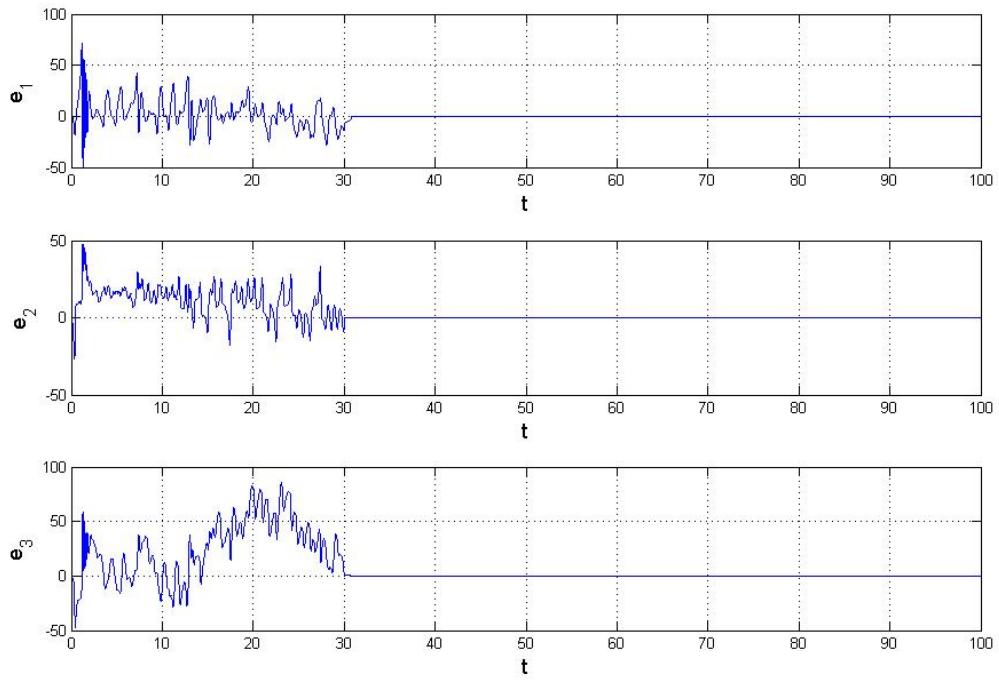


Fig. 8-9. Time histories of errors for Example 2- the FLCC is coming into after 30s.

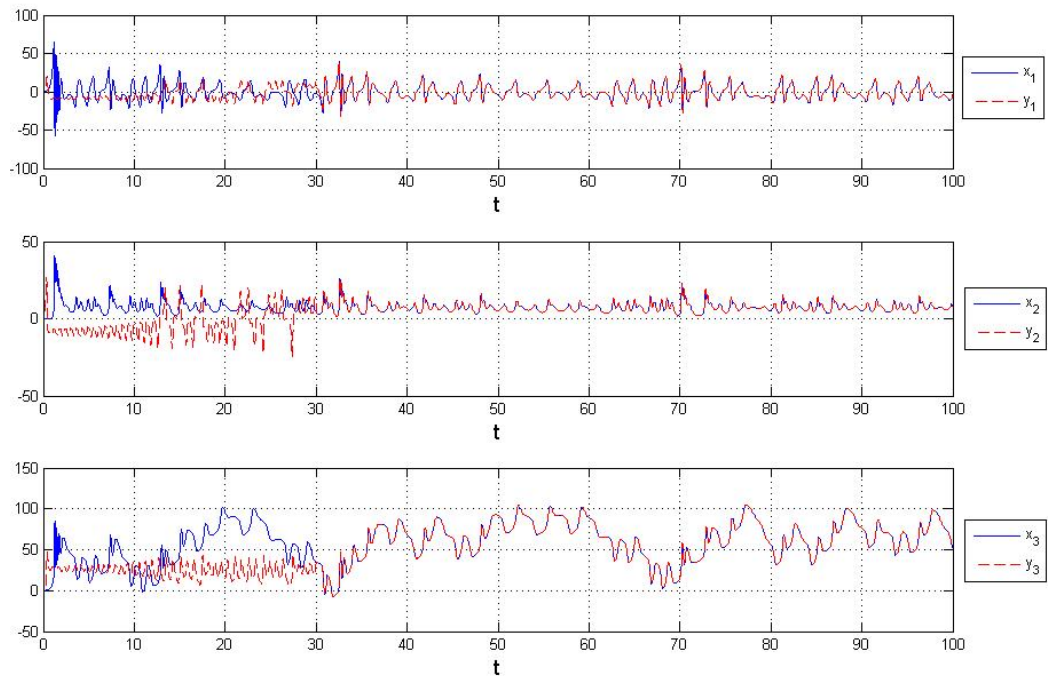


Fig. 8-10. Time histories of states for Example 2- the FLCC is coming into after 30s.

# Chapter 9

## Conclusions

In this thesis, hyperchaos of new chaotic systems with three positive Lyapunov exponents, *Yin-Yang* chaos, new fuzzy model to simulate the complicated chaotic behaviors via only two linear subsystems, new fuzzy logic controllers, generalized chaos synchronization via GYC partial region stability theory and pragmatical asymptotically stability theorem are presented.

In Chapter 2, 7 Tables and 14 Figs are proposed to investigate the *Yin-Yang* chaos of the Lorenz system. This topic, *Yin-Yang* chaos, explores another half battle field for chaos study, may have epoch-making significance in the future.

In Chapter 3, the autonomous Mathieu-van der pol autonomous system with four state variables can exhibit hyperchaos with three positive Lyapunov exponents have been investigated in phase portraits, power spectrum, parameter diagrams and Lyapunov exponents.

In Chapter 4 and 5, a new strategy by using GYC partial region stability theory is proposed to achieve chaos control and generalized synchronization. Via using the GYC partial region stability theory, the new Lyapunov function used is a simple linear homogeneous function of states and the lower order controllers are much more simple and introduce less simulation error. The new chaotic Mathieu-van der Pol system and new chaotic Mathieu-Duffing system system are used as simulation examples which confirm the scheme effectively.

In Chapter 6, a new strategy, pragmatical asymptotically stability theorem via GYC partial region stability theory, are proposed to achieve adaptive *Yin-Yang* synchronization of *Yin* chaos and *Yang* chaos. Via comparison of numerical simulation results listed in Table 6-1 and 6-2, it is very obvious that there is high efficiency in

adaptive synchronization when using our new strategy.

In Chapter 7, two totally different and complicated chaotic systems, Quantum-CNN system and Qi system is successfully and efficiently simulated and synchronized via the new fuzzy model. Through the new idea, not only a complicated nonlinear system can be linearized to a simple form – linear coupling of only two linear subsystems and the numbers of fuzzy rules can be reduced from  $2^N$  to  $2 \times N$ , but also the idea of PDC and LMI-based method can be applied to synchronize two totally different fuzzy systems. The asymptotical stability of the error dynamic systems can be achieved with only two feedback gains in the fuzzy controllers.

In Chapter 8, a simplest controller – fuzzy logic constant controller (FLCC) is introduced. Based on Lyapunov direct method and the upper bound and lower bound of the error derivatives, we construct the fuzzy rules and the simplest corresponding constant controllers. Complicated and nonlinear controllers would no longer appear and are replaced with simple and constant controllers through our new strategy. Simulation results in synchronization show that FLCC is effective enough and give very satisfactory results. Through this new approach, not only all cases in chaos synchronization or control can be achieved, but also the implement or experimental application of chaos synchronization could be attained much more easily.



## References

- [1]. A. Arnéodo, F. Argoul, J. Elezgaray and P. Richetti, “Homoclinic chaos in chemical systems”, *Physica D: Nonlinear Phenomena* 62 (1993) 134-169.
- [2]. H. Li, B. Zhang, Z. Li, W. A. Halang and G. Chen, “Controlling DC–DC converters by chaos-based pulse width modulation to reduce EMI”, *Chaos, Solitons & Fractals* 42 (2009) 1378-1387.
- [3]. X. P. Yan and Y. D. Chu, “Stability and bifurcation analysis for a delayed Lotka–Volterra predator–prey system”, *Journal of Computational and Applied Mathematics* 196 (2006) 198-210.
- [4]. D. Ning, J. a. Lu and X. Han, “Dual synchronization based on two different chaotic systems: Lorenz systems and Rössler systems”, *Journal of Computational and Applied Mathematics* 206 (2007) 1046-1050.
- [5]. F. J. Muzzio and M. Liu, “Chemical reactions in chaotic flows”, *The Chemical Engineering Journal and the Biochemical Engineering Journal* 64 (1996) 117-127.
- [6]. K. Igeta and T. Ogawa, “Information dissipation in quantum-chaotic systems: Computational view and measurement induction”, *Chaos, Solitons & Fractals* 5 (1995) 1365-1379.
- [7]. E. N. Lorenz, “Deterministic non-periodic flows”, *J. Atmos.* 20 (1963) 130.
- [8]. L. A. Sanchez, “Convergence to equilibria in the Lorenz system via monotone methods”, *Journal of Differential Equations* 217 (2005) 341-362.
- [9]. R. Barrio and S. Serrano, “A three-parametric study of the Lorenz model”, *Physica D: Nonlinear Phenomena* 229 (2007) 43-51.
- [10]. M. Cox Stephen, “The transition to chaos in an asymmetric perturbation of the Lorenz system”, *Phys Lett A* 144 (1990) 325-332.
- [11]. Y. Liu and L.C. Barbosa, “Periodic locking in coupled Lorenz systems”, *Phys Lett A* 197 (1995) 13-21.
- [12]. C. C. Chen, C. H. Tsai and C. C. Fu, “Rich dynamics in self-interacting Lorenz systems” *Phys Lett A* 194 (1994) 265-279.
- [13]. A.S. Elwakil and A.M. Soliman, “A family of Wien-type oscillators modified for chaos”, *Int. J. Circuit Theory & Applications* 25 (1997) 561-579.

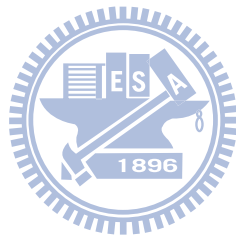
- [14].A. A. Martynyuk and Y. A. Martynyuk-Chernienko, “Stability analysis of quasilinear uncertain dynamical systems”, *Nonlinear Analysis: Real World Applications* 9 (2008) 1090-1102.
- [15].S. T. Ariaratnam and W. C. Xie, “Almost-sure stochastic stability of coupled non-linear oscillators”, *Int. J. Non-Linear Mechanics* 29 (1994) 197–204.
- [16].Y. Ji and Q. Bi, “Dynamical analysis of a compound oscillator with initial phase difference”, *Nonlinear Analysis: Real World Applications* 9 (2008) 1261-1268.
- [17].Z. M. Ge and T. N. LIN, “Chaos, chaos control and synchronization of electro-mechanical gyrostat system”, *Chaos, Solitons and Fractals* 259 (2003) 585-603.
- [18].Z. M. Ge and W. Y. Leu, “Anti-Control of Chaos of Two-degrees-of- Freedom Louderspeaker System and Chaos Synchronization of Different Order Systems”, *Chaos, Solitons and Fractals* 20 (2004) 503-521.
- [19].Z. M. Ge and Y. S. Chen, “Synchronization of Unidirectional Coupled Chaotic Systems via Partial Stability”, *Chaos, Solitons and Fractals* 21 (2004) 101-111.
- [20].A. Alasty and R. Shabani, “Chaotic motions and fractal basin boundaries in spring-pendulum system”, *Nonlinear Analysis: Real World Applications* 7 (2006) 81-95.
- [21].T. Kapitaniak, K. E. Thylwe, I. Cohen and J. Wojewoda, “Chaos-hyperchaos transition”, *Chaos, Solitons & Fractals* 5 (1995) 2003-2011.
- [22].H. Haken, “At least one Lyapunov exponent vanishes if the trajectory of an attractor does not contain a fixed point”, *Physics Letters A* 94 (1983) 71-72.
- [23].R. Riganti and M. G. Zavattaro, “Transition to hyperchaos in the dynamics of a nonlinear vibration absorber”, *Mathematical and Computer Modelling* 22 (1995) 55-61.
- [24].S. Yanchuk and T. Kapitaniak, ”Chaos–hyperchaos transition in coupled Rössler systems”, *Physics Letters A* 290 (2001) 139-144.
- [25].T. Kapitaniak, “Transition to hyperchaos in chaotically forced coupled oscillators”, *Phys Rev E*, 47 (1993) R2978.
- [26].A. Namajunas, A. Tamasevicius, “Simple RC chaotic oscillator”, *Electronics Letters* 32 (1996) 945-946.
- [27].T. S. Parker, L. O. Chua, *Practical numerical algorithms for chaotic systems*, Springer, New York 1989.
- [28].A. Parlitz, T. Kocarev and H. Preckel, “Encoding messages using chaotic

- synchronization”, *Physical Review E* 53 (1996) 4351-4361.
- [29]. T. Matsumoto, L.O. Chua, K. Kobayashi, “Hyperchaos: Laboratory experiment and numerical”, confirmation, *IEEE Trans. Circuits & Syst.-I* 33 (1986) 1143-1147.
- [30]. A. S. Elwakil and M. P. Kennedy, “Inductorless hyperchaos generator”, *Microelectronics Journal* 30 (1999) 739-743.
- [31]. T. Saito, “A simple hyperchaos generator including one ideal diode, *IEICE Trans. Fundamentals*”, E75-A (1992) 294-298.
- [32]. G.Q. Zhong, F. Ayrom, “Periodicity and chaos in Chua’s circuit”, *IEEE Trans. Circuits & Syst.-I* 32 (1985) 501-505.
- [33]. S. M. Chang, M. C. Li and W. W. Lin, “Asymptotic synchronization of modified logistic hyper-chaotic systems and its applications”, *Nonlinear Analysis: Real World Applications* 10 (2009) 869-880.
- [34]. G. Chen and X. Dong, *From Chaos to Order*, World Scientific, New Jersey 1998.
- [35]. I. B. Cohen, *Revolution in Science*, Six printing, The Belknap Press of Harvard University Press, Cambridge, Massachusetts, pp.467, 1985, 1994.
- [36]. W. Ott and J. A. Yorke, “When Lyapunov exponents fail to exist”, *Phys Rev E* 78 (2008) 3755-3763.
- [37]. Z. M. Ge and C. H. Yang, “Hyperchaos of four state autonomous system with three positive Lyapunov exponents”, *Physics Letters A* 373(3) (2009) 349-353.
- [38]. E. G. Awad and A. S. Al-Ruzaiza, “Chaos and adaptive control in two prey, one predator system with nonlinear feedback”, *Chaos, Solitons & Fractals*, 34 (2007) 443-453.
- [39]. Z. M. Ge and Y. T. Wong “Chaos in Integral and Fractional Order Double Mackey-Glass Systems”, *Mathematical Methods, Physical Models and Simulation in Science & Technology* (2006).
- [40]. Z. M. Ge, Y. T. Wong and S. Y. Li, “Temporary Lag and Anticipated Synchronization and Anti-synchronization of Uncoupled Time-delayed Chaotic Systems”, *Journal of Sound and Vibration* 318(1-2) (2008) 267-278.
- [41]. Y. G. Zu, Z. H. Zhao, J. H. Yu and F. J. Yang, *Non-linear Ecological Modelling*, Beijing: Science Press; 2004.
- [42]. B. Mukhopadhyay and R. Bhattacharyya, “Analysis of a virus-immune system model with two distinct delays”, *Nonlinear Studies* 15 (2008) 37-50.

- [43].Z. M. Ge, C. W. Yao and H. K. Chen, “Stability on Partial Region in Dynamics”, Journal of Chinese Society of Mechanical Engineer, 15(2) (1994) 140-148.
- [44].Z. M. Ge, and H. K. Chen, “Three Asymptotical Stability Theorems on Partial Region with Applications”, Japanese Journal of Applied Physics, 37 (1998) 2762.
- [45].P. Q. Tong, “Adaptive control of chaos”, Journal of Physics 44 (1995) 169-176.
- [46].X. Wu, Z. H. Guan and Z. Wu, “Adaptive synchronization between two different hyperchaotic systems”, Nonlinear Analysis: Theory, Methods & Applications 68 (2008) 1346-1351.
- [47].A. El-Gohary and A. S. Al-Ruzaiza, “Chaos and adaptive control in two prey, one predator system with nonlinear feedback”, Chaos, Solitons & Fractals, 34 (2007) 443-453.
- [48].J. H. Kim, C. W. Park, K. Euntai and P. Mignon, “Fuzzy adaptive synchronization of uncertain chaotic systems”, Physics Letters A 334 (2005) 295-305.
- [49].Wei Ding and Maoan Han, “Synchronization of delayed fuzzy cellular neural networks based on adaptive control”, Physics Letters A 372(26) (2008) 4674-4681.
- [50].Hassan Salarieh and Mohammad Shahrokhi, “Adaptive synchronization of two different chaotic systems with time varying unknown parameters”, Chaos, Solitons & Fractals 37(1) (2008) 125-136.
- [51].A. Lazzouni Sihem, Samuel Bowong, F.M. Moukam Kakmeni and Brahim Cherki, “An adaptive feedback control for chaos synchronization of nonlinear systems with different order”, Communications in Nonlinear Science and Numerical Simulation 12(4) (2007) 568-583.
- [52].Xiaoyun Chen and Jianfeng Lu, “Adaptive synchronization of different chaotic systems with fully unknown parameters”, Physics Letters A 364(2) (2007) 123-128.
- [53].Z. M. Ge and C. H. Yang, “Pragmatical generalized synchronization of chaotic systems with uncertain parameters by adaptive control”, Physica D: Nonlinear Phenomena 231(2) (2007) 87-94.
- [54].Z. M. Ge, C. H. Li, S. Y. Li and C. M. Chang, “Chaos Synchronization of Double Duffing Systems with Parameters Excited by a Chaotic Signal”, Journal of Sound and Vibration 317 (3-5) (2008) 449-455.
- [55].H. T. Yau, “Chaos synchronization of two uncertain chaotic nonlinear gyros

- using fuzzy sliding mode control”, *Mechanical Systems and Signal Processing* 22 (2008) 408-418.
- [56]. W. Junwei, X. Xiaohua, Z. Meichun and Z. Yanbin, “Fuzzy stability and synchronization of hyperchaos systems”, *Chaos, Solitons & Fractals* 35 (2008) 922-930.
- [57]. Y. W. Wang, Z. H. Guan and O. Hua, Wang, “Impulsive synchronization for Takagi–Sugeno fuzzy model and its application to continuous chaotic system”, *Physics Letters A* 339 (2005) 325-332.
- [58]. J. H. Kim, C. W. Park, K. Euntai and P. Mignon, “Fuzzy adaptive synchronization of uncertain chaotic systems”, *Physics Letters A* 334 (2005) 295-305.
- [59]. L. A. Zadeh, “Fuzzy logic”, *IEEE Comput.* 21 (1988) 83-93.
- [60]. K. Tanaka, M. Sugeno, ”Stability analysis and design of fuzzy control systems”, *Fuzzy Set Systems* 45 (1992) 135-156.
- [61]. Y. W. Wang, Z. H. Guan and H. O. Wang, “LMI-based fuzzy stability and synchronization of Chen’s system”, *Physics Letters A* 320 (2003) 154–159.
- [62]. H. Zhang, X. Liao and J. Yu, “Fuzzy modeling and synchronization of hyperchaotic systems”, *Chaos, Solitons & Fractals* 26(3) (2005) 835-843.
- [63]. J. Wang, X. Xiong, M. Zhao and Y. Zhang, “Fuzzy stability and synchronization of hyperchaos systems”, *Chaos, Solitons & Fractals* 35(5) (2008) 922-930.
- [64]. L. A. Zadeh, “Fuzzy logic”, *IEEE Comput.* 21 (1988) 83-93.
- [65]. A. Shahraz, R. Bozorgmehry Boozarjomehry, “A fuzzy sliding mode control approach for nonlinear chemical processes”, *Control Engineering Practice* 17 (2009) 541-550.
- [66]. C. Y. Chen, T. H. S. Li, Y. C. Yeh, “EP-based kinematic control and adaptive fuzzy sliding-mode dynamic control for wheeled mobile robots”, *Information Sciences* 179 (2009) 180-195.
- [67]. Y. W. Wang, Z. H. Guan and H. O. Wang, “LMI-based fuzzy stability and synchronization of Chen’s system”, *Physics Letters A* 320 (2003) 154–159.
- [68]. G. Li, A. Khajepour, “Robust control of a hydraulically driven flexible arm using backstepping technique”, *Journal of Sound and Vibration* 280 (2005) 759-775.
- [69]. T. H. S. Li, C. L. Kuo, N. R. Guo, “Design of an EP-based fuzzy sliding-mode control for a magnetic ball suspension system”, *Chaos, Solitons & Fractals* 33 (2007) 1523-1531.

[70].H. Yau and C S. Shieh, “Chaos synchronization using fuzzy logic controller”,  
Nonlinear Analysis: Real World Applications 9 (2008) 1800-1810.



## Paper List

- \*1. **Shih-Yu Li** and Zheng-Ming Ge, “A Novel Study of Parity and Attractor in the Time Reversed Lorentz System”, *Physics Letter A*, 373(44) Oct. (2009) 4053-4059. (SCI, Impact Factor: 2.174)
- \*2. Zheng-Ming Ge and **Shih-Yu Li**, “Chaos Control of New Mathieu-Van der Pol Systems with New Mathieu -Duffing Systems as Functional System by GYC Partial Region Stability Theory”, *Nonlinear Analysis: Theory, Methods, and Applications*, 71(9) Nov. (2009) 4047-4059. (SCI, Impact Factor: 1.295)
- \*3. Zheng-Ming Ge and **Shih-Yu Li**, “Fuzzy Modeling and Synchronization of Chaotic Two-Cells Quantum Cellular Neural Networks Nano System via A Novel Fuzzy Model” accepted by *Journal of Computational and Theoretical Nanoscience* 2009. (SCI, Impact Factor: 1.256)
- \*4. Zheng-Ming Ge and **Shih-Yu Li** “Fuzzy Modeling and Synchronization of Two Totally Different Chaotic Systems via Novel Fuzzy Model” submitted to *IEEE Transactions on Fuzzy Systems*. (SCI, Impact Factor: 3.624)
- \*5. Zheng-Ming Ge and **Shih-Yu Li**, “Yang and Yin Parameters in the Lorenz System” submitted to *Applied Physics Letters*. (SCI, Impact Factor: 3.726).
- \*6. Zheng-Ming Ge and **Shih-Yu Li** “Generating Tri-Chaos Attractors with Three Positive Lyapunov Exponents in New Four Order System via Linear Coupling” submitted to *Nonlinear Dynamics*. (SCI, Impact Factor: 1.295)
- \*7. Zheng-Ming Ge and **Shih-Yu Li** “Chaos Generalized Synchronization of New Mathieu-Van der Pol Systems with New Duffing-Van der Pol systems as Functional system by GYC Partial Region Stability Theory” submitted to. (SCI, Impact Factor: 0.545)
- \*8. Zheng-Ming Ge and **Shih-Yu Li** “Chaotic Motion in *Yin* Lorenz System and Its

- Adaptive P-N Synchronization by Pragmatical Asymptotically Stability Theorem”  
submitted to Journal of Sound and Vibration. (SCI, Impact Factor: 1.065)
- \*9. Zheng-Ming Ge and **Shih-Yu Li** “Generalized Synchronization of Chaotic Systems with Different Orders by Fuzzy Logic Constant Controller” submitted to Expert Systems with Application. (SCI, Impact Factor: 2.596)
- \*10. Zheng-Ming Ge and **Shih-Yu Li** “Chaos control of New Mathieu-Van der Pol Systems by Fuzzy Logic Constant Controllers” submitted to Applied Soft Computing. (SCI, Impact Factor: 1.909)
- \*11. Zheng-Ming Ge and **Shih-Yu Li** and Hsien-Keng Chen “Chaotic Motions in the Real Fuzzy Electronic Circuits” submitted to Applied Mathematical Modelling. (SCI, Impact Factor: 0.931)
12. Zheng-Ming Ge and **Shih-Yu Li** “Pragmatical Adaptive Synchronization of Different Orders Chaotic Systems with All Uncertain Parameters via Nonlinear Control” submitted to Mathematical Methods in the Applied Sciences. (SCI, Impact Factor: 0.707)
13. Zheng-Ming Ge and **Shih-Yu Li** “Chaos Generalized Synchronization of fuzzy chaotic systems by GYC Partial Region Stability Theory” submitted to Journal of the franklin institute. (SCI, Impact Factor: 0.616)
14. Zheng-Ming Ge and **Shih-Yu Li** “Adaptive Synchronization of Two Different Fuzzy Chaotic Systems with Different number of fuzzy Rules by Pragmatical Asymptotically Stability Theorem” submitted to Information Sciences. (SCI, Impact Factor: 3.095)
15. Zheng-Ming Ge and **Shih-Yu Li** “Pragmatical Fuzzy Adaptive synchronization of Time Reversed Lorenz System via Ge-Yao-Chen Partial Region Stability Theorem” submitted to Information Sciences. (SCI, Impact Factor: 3.095)
16. Zheng-Ming Ge, Yu-Ting Wong and **Shih-Yu Li** “Temporary Lag and Anticipated



- Synchronization and Anti-synchronization of Uncoupled Time-delayed” Journal of Sound and Vibration 318 (1-2) (2008) 267-278. (SCI, Impact Factor: 1.024)
17. Zheng-Ming Ge, Shoh-Chung Li, **Shih-Yu Li** and Ching-Ming Chang “Pragmatical Adaptive Chaos Control from Double Van der Pol System to Double Duffing System” Applied Mathematics and Computation 203 (2) (2008) 513-522. (SCI, Impact Factor: 0.821)
18. Zheng-Ming Ge, Chien-Hao Li, **Shih-Yu Li** and Ching Ming Chang, “Chaos Synchronization of Double Duffing Systems with Parameters Excited by a Chaotic Signal”, Journal of Sound and Vibration 317 (3-5) (2008) 449-455. (SCI, Impact Factor: 1.024)
19. Zheng-Ming Ge, C-Y Chiang, Ching Ming Chang and **Shih-Yu Li** “Chaos control and anticontrol of tachometer system by Ge-Yao-Chen partial region stability theory”, Proceedings of the Institution of Mechanical Engineers. Part C, Journal of Mechanical Engineering Science (2009). (SCI, Impact Factor: 0.212)
20. Zheng-Ming Ge, Chun-Yen Ho, **Shih-Yu Li** and Ching Ming Chang “Chaos control of new Ikeda–Lorenz systems by GYC partial region stability theory” accepted by Mathematical Methods in the Applied Sciences 2009. (SCI, Impact Factor: 0.594)
21. Cheng-Hsiung Yang, Zheng-Ming Ge, Ching-Ming Chang, **Shih-Yu Li**, “Chaos synchronization and chaos control of quantum-CNN chaotic system by variable structure control and impulse control”, Nonlinear Analysis: Real World Applications (2009). (SCI, Impact Factor: 1.232)

\* 為以博士論文內容撰寫者